# Envases activos basados en el anclaje covalente reversible de compuestos antimicrobianos en quitosano
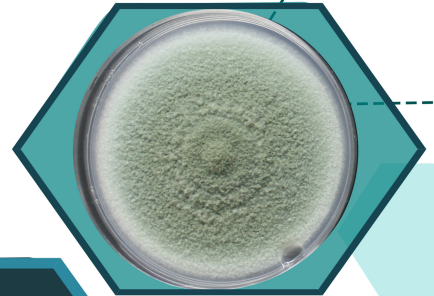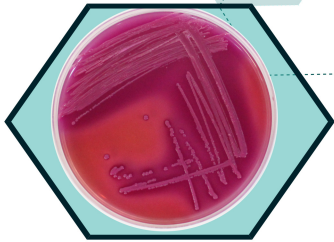
## Raquel Heras Mozos

UNIVERSITAT POLITÈCNICA DE VALÈNCIA

CSIC
CONSEJO SUPERIOR DE INVESTIGACIONES CIENTÍFICAS

Directores:
Dra. Pilar Hernández Muñoz
Dr. Rafael Gavara Clemente

Valencia, Septiembre 2022

# Envases activos basados en el anclaje covalente reversible de compuestos antimicrobianos en quitosano

TESIS DOCTORAL

# Envases activos basados en el anclaje covalente reversible de compuestos antimicrobianos en quitosano

# Raquel Heras Mozos

Directores:

**Dra. Pilar Hernández Muñoz**

**Dr. Rafael Gavara Clemente**

Tutor:

**Dr. Rafael Gavara Clemente**

Valencia, Septiembre de 2022

**Dra. Pilar Hernández Muñoz**, Científica Titular del Instituto de Agroquímica y Tecnología de los Alimentos del Consejo Superior de Investigaciones Científicas,

**Dr. Rafael Gavara Clemente**, Profesor de Investigación del Instituto de Agroquímica y Tecnología de los Alimentos del Consejo Superior de Investigaciones Científicas,

Hacen constar que:

La memoria titulada "**Envases activos basados en el anclaje covalente reversible de compuestos antimicrobianos en quitosano**" que presenta **Dª Raquel Heras Mozos,** para optar al grado de Doctor por la Universidad Politécnica de Valencia, ha sido realizada en el **Instituto de Agroquímica y Tecnología de Alimentos** (IATA-CSIC) bajo su dirección y que reúne las condiciones para ser defendida por su autora.

Paterna-Valencia, septiembre de 2022.

Firmado: Dra. Pilar Hernández Muñoz     Dr. Rafael Gavara Clemente

*A mi familia*

# Agradecimientos

La tesis doctoral es más que formación académica y profesional, conlleva a su vez un crecimiento personal del que forma parte mucha gente. Durante estos años muchas personas me han acompañado en este largo trayecto y sin ellos no hubiera sido posible.

En primer lugar, quiero dar las gracias a mis directores de tesis por ofrecerme la posibilidad de realizar esta tesis doctoral en su grupo de investigación y por todas las oportunidades que me han brindado a lo largo de estos años para crecer profesional y personalmente.

A *Pilar,* mi más sincero agradecimiento por toda la ayuda prestada y por compartir sus conocimientos conmigo sobre el quitosano y esas reacciones que han completado esta tesis. Gracias por tu dedicación y a tus magníficas correcciones. A *Rafa,* gracias por siempre estar disponible para resolver esas "pequeñas dudas" con las que acudía a tu despacho. Gracias por el apoyo académico y experimental con los equipos del laboratorio, y por darme la oportunidad de haber participado en tus clases.

Gracias a *Rebeca Hernández* y a todo su grupo de Polímeros Nanoestructurados y Geles del Instituto de Ciencia y Tecnología de Polímeros, por acogerme durante mi breve estancia en plena pandemia y por toda la ayuda brindada para caracterizar el material.

Gracias a *Laura H*. y *Gracia* porque desde que inicié esta aventura han sido un pilar fundamental en su desarrollo. Gracias por vuestras enseñanzas y consejos que tan útiles son siempre. Gracias por las charlas de ciencia sobre polímeros, envases y micro y por las charlas de pasillo no tan científicas. Y, sobre todo, gracias por vuestro apoyo personal en los momentos de más flaqueza.

Gracias a mis compañeras de tesis, con ellas he compartido esta experiencia doctoral. Gracias por ser las mejores compañeras y amigas de este maravilloso viaje. Gracias a *Laura S*. y *Patricia* que han sido todo un apoyo, con ellas cualquier desafío se lleva mejor.

# Resumen

La presente Tesis Doctoral plantea el desarrollo de sistemas antimicrobianos basados en el anclaje covalente reversible de aldehídos de origen natural con actividad antimicrobiana en películas de quitosano para su aplicación en el envasado de alimentos.

En primer lugar, se desarrolló un protocolo para la formación de bases de Schiff o iminas de diferentes aldehídos en películas de quitosano. Estas iminas son producto de la condensación de los grupos amino primarios del quitosano con los grupos carbonilo del aldehído. El anclaje de dichos aldehídos, en su mayoría de elevada volatilidad, permite su estabilización a largo plazo en estructuras poliméricas, facilitando su manejo. Las iminas son hidrolizables, y dicha hidrolisis está favorecida a pH < 5, por lo que la naturaleza reversible del enlace ofrece un mecanismo para controlar la liberación del antimicrobiano. Previamente a la incorporación de estos compuestos en las películas de quitosano, se evaluó la capacidad antimicrobiana de los aldehídos frente a diversos microorganismos patógenos y alterantes de alimentos. Se caracterizó el enlace imina mediante técnicas espectroscópicas y se cuantificó la incorporación del aldehído a la película de quitosano mediante análisis elemental. Adicionalmente otras propiedades funcionales del material fueron evaluadas, como propiedades térmicas, ópticas o de absorción de agua, verificando la modificación del polímero.

En segundo lugar, se evaluó la reversibilidad del enlace imina o base de Schiff por el contacto con soluciones acuosas de diferente acidez. La respuesta al pH de las películas permitió determinar la mayor estabilidad del enlace imina a pH neutros, mientras que a pH ácidos resultó más hidrolizable, permitiendo así una mayor liberación del aldehído anclado.

Las películas activas desarrolladas mostraron una buena respuesta antimicrobiana contra *Botrytis cinerea* y *Penicillium expansum*, especialmente al someterlas a una solución de pH ácido. La respuesta antimicrobiana de las películas se debió exclusivamente a la liberación del aldehído al espacio de cabeza tras la hidrólisis de la imina.

## | *Resumen*

La estructura química de los aldehídos tuvo un impacto significativo en la formación de iminas y en las propiedades de la película, así como en su reversibilidad. Así, la presencia del doble enlace ($C^{\alpha}=C^{\beta}$) en aldehídos α,β-insaturados podría generar otro tipo de enlaces como la adición de Michael, permitiendo obtener matrices entrecruzadas y más estables que sus análogos saturados. El grado de entrecruzamiento y propiedades de estas películas puede ser modulado por el pH del medio empleado en su síntesis.

Para la aplicación tecnológica de las películas antimicrobianas de quitosano con los volátiles anclados reversiblemente, se trabajó con productos de postcosecha frescos o mínimamente procesados. Se empleó la respuesta al pH de las películas siguiendo diferentes estrategias. Por una parte, el sistema se incorporó en el envasado de moras frescas, para ello, se diseñó un envase de doble fondo donde depositar las películas junto con el medio activador a pH ácido. La solución se añadió en el momento del envasado de la fruta, y permitió hidrolizar el enlace imina y liberar el aldehído al espacio de cabeza donde ejerció su función. Se redujo satisfactoriamente el crecimiento de hongos sobre la superficie de la fruta, aumentando el tiempo de vida útil de las moras envasadas de 3 a 12 días.

Por otra parte, se envasó piña fresca cortada empleando el mismo diseño del envase, de forma que el jugo ácido exudado por la piña durante su almacenamiento favoreció la hidrólisis de la imina. Las películas activas mejoraron la calidad y redujeron la carga microbiana habitual de la piña, observando una reducción notable respecto al control a partir del día 9.

Por último, la actividad antimicrobiana de las películas activas se evaluó en un alimento líquido refrigerado, concretamente en un zumo de frutas ligeramente ácido e inoculado con *E. coli*. La acidez del zumo provocó la liberación del aldehído al medio inhibiendo el crecimiento del patógeno.

Las películas de quitosano con los aldehídos anclados presentaron respuesta al pH, mostrando una mayor capacidad antimicrobiana al ser sometidas a pH ácido, y pudiendo emplearse en el diseño de envases activos antimicrobianos.

# Resum

Aquesta Tesi Doctoral planteja el desenvolupament de sistemes antimicrobians basats en l'ancoratge covalent reversible d'aldehids d'origen natural amb activitat antimicrobiana en pel·lícules de quitosà per aplicar-les a l'envasament d'aliments.

En primer lloc, es va desenvolupar un protocol per a la formació de bases de Schiff o imines de diferents aldehids en pel·lícules de quitosà. Aquestes imines són el producte de la addició nucleòfila dels grups amino del quitosà al carbonil de l'aldehid que s'ancorarà. L'ancoratge d'aquests aldehids, majoritàriament d'elevada volatilitat, permet la seva estabilització a llarg termini en estructures polimèriques, facilitant-ne el seu maneig. Les imines són hidrolitzables, i aquesta hidròlisi està afavorida a pH < 5, per la qual cosa la naturalesa reversible de l'enllaç ofereix un mecanisme per controlar l'alliberament de l'antimicrobià. Prèviament a la incorporació d'aquests compostos a les pel·lícules de quitosà, es va avaluar la capacitat antimicrobiana dels aldehids davant de diversos microorganismes patògens i alterants d'aliments. Es va caracteritzar l'enllaç imina mitjançant tècniques espectroscòpiques i es va quantificar la incorporació de l'aldehid a la pel·lícula de quitosà mitjançant anàlisi elemental. Addicionalment, altres propietats funcionals del material van ser avaluades, com a propietats tèrmiques, òptiques o d'absorció d'aigua, verificant la modificació del polímer.

En segon lloc, es va avaluar la reversibilitat de l'enllaç imina o base de Schiff pel contacte amb solucions aquoses de diferent acidesa. La resposta al pH de les pel·lícules va permetre determinar la major estabilitat de l'enllaç imina a pH neutres, mentre que a pH àcids va resultar més hidrolitzable, permetent així un alliberament més gran de l'aldehid ancorat.

Les pel·lícules actives desenvolupades van mostrar una bona resposta antimicrobiana contra *Botrytis cinerea* i *Penicillium expansum*, especialment en sotmetre-les a una solució de pH àcid. La resposta antimicrobiana de les pel·lícules es va deure exclusivament a l'alliberament de l'aldehid a l'espai de cap després de la hidròlisi de la imina.

L'estructura química dels aldehids va tenir un impacte significatiu en la formació d'imines i en les propietats de la pel·lícula, així com en la reversibilitat. Així, la presència del doble enllaç ($C^\alpha = C^\beta$) en aldehids $\alpha,\beta$-insaturats podria generar un altre tipus d'enllaços com l'addició de Michael, permetent obtenir matrius entrecreuades i més estables que els seus anàlegs saturats. El grau d'entrecreuament i propietats d'aquestes pel·lícules pot ser modulat pel pH del medi emprat a la síntesi.

Per a l'aplicació tecnològica de les pel·lícules antimicrobianes de quitosà amb els volàtils ancorats reversiblement, es va treballar amb productes de postcollita frescos o mínimament processats. Es va emprar la resposta al pH de les pel·lícules seguint diferents estratègies. D'una banda, el sistema es va incorporar a l'envasat de móres fresques, per això es va dissenyar un envàs de doble fons on dipositar les pel·lícules juntament amb el medi activador a pH àcid. La solució es va afegir en el moment de l'envasament de la fruita, i va permetre hidrolitzar l'enllaç imina i alliberar l'aldehid a l'espai de cap on va exercir la seva funció. Es va reduir satisfactòriament el creixement de fongs sobre la superfície de la fruita, augmentant el temps de vida útil de les móres envasades de 3 a 12 dies.

D'altra banda, es va envasar pinya fresca tallada emprant el mateix disseny de l'envàs, de manera que el suc àcid exsudat per la pinya durant el seu emmagatzematge va afavorir la hidròlisi de la imina. Les pel·lícules actives van millorar la qualitat i van reduir la càrrega microbiana habitual de la pinya, observant una reducció notable respecte al control a partir del dia 9.

Per acabar, l'activitat antimicrobiana de les pel·lícules actives es va avaluar en un aliment líquid refrigerat, concretament en un suc de fruites lleugerament àcid i inoculat amb *E. coli*. L'acidesa del suc va provocar l'alliberament de l'aldehid al medi inhibint el creixement del patogen.

Les pel·lícules de quitosà amb els aldehids ancorats van presentar resposta al pH, mostrant una major capacitat antimicrobiana en ser sotmeses a pH àcid, i podent emprar-se en el disseny d'envasos actius antimicrobians.

# Abstract

This Doctoral Thesis proposes the development of antimicrobial systems based on the reversible covalent anchoring of naturally occurring aldehydes with antimicrobial activity in chitosan films for their application in food packaging.

First, a protocol for the formation of Schiff bases or imines of different aldehydes on chitosan films was developed. These imines are the product of the condensation of the primary amino groups of chitosan with the carbonyl groups of the aldehyde. The immobilization of these aldehydes, most of which are highly volatile, allows their long-term stabilisation in polymeric structures, facilitating their handling. The imines are hydrolysable, and its hydrolysis is favoured at pH < 5, so the reversible nature of the bond provides a mechanism to control the antimicrobial release. Prior to the incorporation of these compounds into chitosan films, the antimicrobial capacity of aldehydes was evaluated against various pathogenic and food spoilage microorganisms. The formed imine bond was characterised by spectroscopic techniques and the incorporation of the aldehyde into the chitosan film was quantified by elemental analysis. Additionally, other functional properties were evaluated, such as thermal, optical and water absorption properties, verifying the modification of the polymer.

Secondly, the reversibility of the imine bond or Schiff's base was evaluated by contact with aqueous solutions of different acidity. The pH response of the films allowed determining the higher stability of the imine bond at neutral pH, while at acidic pH it was more hydrolysable, leading a higher release of the anchored aldehyde

The developed active films showed a good antimicrobial response against *Botrytis cinerea* and *Penicillium expansum*, especially when subjected to an acidic pH solution. The antimicrobial response of the films was exclusively due to the aldehyde released into the headspace after imine hydrolysis.

The chemical structure of the aldehydes had a significant impact on imine formation and film properties, as well as on their reversibility. Thus, the presence of the double bond ($C^\alpha = C^\beta$) in $\alpha,\beta$-unsaturated aldehydes could generate other types of bonds such as Michael addition,

allowing cross-linked polymer, which are more stable than their saturated analogues. The degree of cross-linking and properties of these films can be modulated by the pH of the medium used in their synthesis.

For the technological application of chitosan antimicrobial films with reversibly grafted volatiles, fresh or minimally processed post-harvest products were used. The pH response of the films was used following different strategies. On the one hand, the system was incorporated in the packaging of fresh blackberries, for this purpose, a double-bottom package was designed to deposit the films together with the activating medium at acid pH. The solution was added at the time of fruit packaging and allowed the imine bond to be hydrolysed subsequently the aldehyde release into the headspace where it exerted its function. Fungal growth on the fruit surface was successfully reduced, increasing the shelf life of the packed blackberries from 3 to 12 days.

Moreover, fresh cut pineapple was packaged using the same packaging design, so that the exuded juice by the pineapple during storage favoured the imine hydrolysis. The active films improved the quality and reduced the usual microbial load of the pineapple, with a noticeable reduction compared to the control from day 9 onwards. Finally, the antimicrobial activity of the active films was evaluated in a refrigerated liquid food, specifically in a slightly acidic fruit juice inoculated with *E. coli*. The acidity of the juice resulted in the release of aldehyde into the medium inhibiting the growth of the pathogen.

The aldehyde immobilization in chitosan films were pH-responsive, showing a higher antimicrobial capacity when subjected to acidic pH, which can be used in the design of antimicrobial active packaging.

# Prólogo

Esta Tesis Doctoral está estructurada en siete apartados: introducción, objetivos, justificación y esquema de la tesis, capítulos, discusión general, conclusiones y anexos.

El apartado de **Introducción** presenta el contexto general en el que se desarrolla esta Tesis, describiendo los aspectos fundamentales sobre envasado activo y los agentes implicados en el desarrollo de los mismos, compuestos activos antimicrobianos y biopolímeros, así como los diferentes métodos de incorporación, destacando la inmovilización covalente reversible de aldehídos volátiles en quitosano. En la sección **Objetivos,** se expone el objetivo general y los diferentes objetivos específicos asociados a la Tesis Doctoral. A continuación, en la sección **Justificación y esquema de la tesis** se expone un breve esquema y descripción de los capítulos y los artículos que lo conforman. La siguiente sección, **Capítulos**, está constituida por dos capítulos que engloban las publicaciones científicas originadas de esta investigación. Estos están estructurados a su vez en seis apartados, incluyendo resumen, introducción, materiales y métodos, resultados y discusión, conclusión y referencias. En la sección, **Discusión general**, se examinan e integran los resultados de cada apartado, resaltando aquellos resultados más relevantes. También se presentan las **Conclusiones** más relevantes obtenidas de la investigación. Y finalmente, se incluye una sección de **Anexos**, con una tabla bibliográfica y las publicaciones que han tenido lugar durante el desarrollo de esta Tesis Doctoral.

# Índice de contenidos

# 1. INTRODUCCIÓN

La pérdida y el desperdicio de alimentos se han convertido en un problema de gran preocupación para la población. Alrededor de un tercio de los alimentos destinados para consumo humano se desechan anualmente, lo que constituye alrededor de 1300 millones de toneladas cada año [1]. La pérdida y el desperdicio de alimentos puede ocurrir a lo largo de toda cadena alimentaria, incluyendo la producción, transporte, procesamiento y almacenamiento del producto [2]. El 40% de las pérdidas de alimentos en países desarrollados se producen durante la venta y en la etapa de consumo, mientras que en países en vías de desarrollo se producen en niveles de postcosecha y procesamiento [1]. Aunque la relación entre la vida útil y el desperdicio de alimentos no es directa, gran parte del desperdicio de los alimentos está relacionada con la corta vida útil de los productos frescos [3].

Por tanto, uno de los objetivos de la industria alimentaria es reducir el desperdicio de alimentos con el fin de reducir los costes de producción y aumentar la eficiencia del sistema, incrementando la seguridad y calidad alimentaria y promoviendo un sistema medioambiental más sostenible [4]. Esto también se enmarca dentro de los Objetivos de Desarrollo Sostenible (ODS) para el 2030 marcados por Naciones Unidas, cuyo objetivo es una producción y consumo más sostenible [5].

El deterioro de los alimentos se puede producir por cambios físicos, químicos y microbiológicos. Los alimentos frescos son muy perecederos y se deterioran rápidamente. Entre ellos destacan las frutas y hortalizas que suponen más del 30% de los desechos alimentarios [6]. Entre los factores de deterioro de los alimentos, la contaminación microbiológica producida por bacterias, hongos, levaduras o virus es un factor predominante. Se estima que alrededor de un 50% de las pérdidas de frutas y verduras están asociadas al desarrollo de enfermedades postcosecha [7]. Además, la presencia de microorganismos patógenos, puede suponer un riesgo para la salud del consumidor [8].

Para evitar el daño y disminuir la pérdida de alimentos, se desarrollan nuevas tecnologías que permitan alargar la vida útil de los productos, que engloban tanto técnicas de conservación como mejoras de las tecnologías de envasado y almacenamiento [9]. El desarrollo de estas técnicas se traduce a su vez en un suministro continuo de alimentos nutritivos, saludables y seguros en todo el mundo. Estas

técnicas van desde la salazón, secado, fermentaciones, hasta técnicas más sofisticadas como las altas presiones o la pasteurización [10]. En esta línea, el envasado juega un importante rol en la cadena alimentaria, permitiendo cubrir la demanda del consumidor con productos seguros y con un tiempo de vida útil adecuado. Todo ello permite reducir los desechos alimentarios o las posibles contaminaciones alimentarias que puedan ocurrir [3]. La utilización de envases permite una mejora de la distribución, venta, calidad y seguridad del alimento envasado. Además, muchos de los procesos de preparación y preservación de la industria alimentaria dependen de un envasado efectivo, por ejemplo, enlatado, pasteurizado, envasado aséptico o envasado en atmósfera modificada [11,12].

Los envases alimentarios tradicionales son fundamentales para la preservación y conservación del alimento. Las principales funciones del envase son contener, proteger y facilitar su distribución. Además, presenta otras funciones, como desarrollo de productos de conveniencia y facilita información al consumidor [13]. Además, proporciona una barrera entre el alimento y el entorno, ya que previene del deterioro producido por agentes externos e internos (daños físicos, oxidativos, humedad, contaminaciones químicas o biológicas) [3].

Existe una extensa variedad de materiales para el envasado de alimentos que permite responder a los requerimientos específicos para cada producto envasado. Entre ellos destacan los materiales plásticos, por su amplia versatilidad, formas y funciones. Alrededor del 40% de los plásticos son utilizados como envases para alimentos [14]. Los polímeros sintéticos de origen petroquímico presentan propiedades que los hacen idóneos para su uso en el envasado de alimentos, entre éstas están las propiedades térmicas, mecánicas y propiedades barrera, y además presentan un bajo coste y una buena procesabilidad [15]. Sin embargo, su amplia versatilidad y ventajosas propiedades se ven contrarrestadas por el persistente impacto negativo en el medio ambiente al final de su vida útil, puesto que estos no son biodegradables y suponen un grave problema medioambiental. En un intento de cambiar las oportunidades del mercado, la industria del envasado ha dado lugar a la sucesión de numerosos nichos de mercado, entre los que destaca el incremento de uso de biopolímeros derivados de fuentes renovables [16]. Estos pueden ser obtenidos a partir de la revalorización

de subproductos de la industria alimentaria o residuos industriales, conllevando a la conservación de los recursos naturales. Además, permite dirigir la producción hacia una economía circular [17].

Los cambios emergentes en la industria alimentaria y el aumento de la preocupación por el medio ambiente, así como los cambios en las preferencias del consumidor por productos más naturales y sostenibles, acoplado a la expansión y globalización del sector alimentario, hace que se promuevan cambios en la industria del envasado. En este contexto, la tecnología del envasado activo permite aumentar el tiempo de vida útil de los alimentos, contribuyendo al aumento de la seguridad y calidad del alimento, y presenta un gran potencial para minimizar la pérdida de alimentos causada por el crecimiento de microorganismos patógenos.

## 1.1. Envasado activo

El envasado activo va más allá de las funciones del envase convencional o pasivo, ya que posee la capacidad de interaccionar con el producto o con el entorno. El sistema generado entre alimento-envase-entorno permite aumentar el tiempo de vida útil mejorando la calidad y seguridad del producto envasado (**Figura 1**). Los envases activos están diseñados para emitir o captar sustancias del alimento o su entorno que pueden promover el deterioro del producto [18]. Estos sistemas constituyen un grupo amplio con diversas funcionalidades, las cuales dependen de su aplicación. Entre los diferentes tipos de envases activos, se encuentran los absorbedores de humedad u oxígeno, reguladores de etileno o dióxido de carbono, absorbedores de compuestos indeseados o los liberadores de compuestos antimicrobianos o antioxidantes [19].

El desarrollo de un envase activo suele responder a la necesidad de conservar un producto específico, por lo que depende directamente de las propiedades fisicoquímicas del alimento envasado, además se requiere conocer qué factores deterioran el alimento para diseñar un envase funcional específico.

**Figura 1.** Envase activo y su efecto en el envasado de alimentos.

El diseño de envases activos supone un desafío para la industria del envasado, ya que, aunque presenta ciertas desventajas frente al uso de un envase tradicional, proporciona significativas ventajas, las cuales pueden contribuir a la reducción de desechos alimentarios y a mejorar la calidad y seguridad de los alimentos (**Tabla 1**). Además, otros factores socio-económicos y tecnológicos podrían influir en el desarrollo de estos envases avanzados y que van desde el productor del material activo hasta el consumidor [20].

La comercialización de envases activos comenzó hace más de tres décadas en Japón, Estados Unidos y Australia, donde la normativa es más flexible que en Europa [21]. Actualmente, se prevé que el mercado mundial de los envases activos e inteligentes crezca alrededor de un 9.8% durante el período de 2022 – 2027 [22].

**Tabla 1**. Ventajas y desventajas del uso de envases activos.

| Desventajas | Ventajas |
|---|---|
| Más caro que el envase tradicional | Controla las condiciones internas del envase, manteniendo la calidad del producto |
| Las sustancias activas liberadas intencionadamente pueden modificar las propiedades organolépticas del producto | Permite extender el tiempo de vida útil del producto |
| Requiere un mayor conocimiento y concienciación del consumidor | Mejora la seguridad microbiológica del alimento |
| La presencia de elementos extraños en el envase podría tener un impacto negativo en la intención de compra del consumidor | Puede reducir el uso de conservantes en el alimento |
| | Mayor sostenibilidad debido a la reducción de desechos alimentarios |

En Europa, la aplicación de materiales activos para el envasado de alimentos se encuentra regulado por el Reglamento de la Unión Europea (UE) 450/2009 [23], además debe de cumplir la legislación específica relativa a los materiales en contacto con el alimento establecidos en el Reglamento UE 1935/2004 [24]. El reglamento para la comercialización de envases activos en contacto con alimentos establece requisitos relativos a su función y su composición e incorpora restricciones asociadas al etiquetado y a las sustancias incorporadas, las cuales deben de ser previamente autorizadas por la Autoridad Europea de Seguridad Alimentaria (EFSA) para usarse en los materiales activos. A su vez, si el agente activo es liberado intencionadamente al interior del envase, la migración del compuesto no debe incluirse en la evaluación de la migración global [21], pero debe de cumplir con el Reglamento UE 1333/2008 sobre aditivos alimentarios [25]. Puesto que la liberación intencionada del compuesto activo puede entrar en contacto con el alimento, requiere de un etiquetado seguro y correcto de acuerdo con la legislación alimentaria relativa al etiquetado de alimentos establecido en la norma de UE 1169/2011 [26].

Entre los diferentes tipos de envases activos, destacan los envases antimicrobianos. Estos actúan inhibiendo o retardando el crecimiento de microorganismos e incrementando la seguridad y calidad del alimento.

## 1.2. Envasado activo antimicrobiano

La incorporación de compuestos antimicrobianos al material de envasado permite diseñar envases activos que aumentan el tiempo de vida útil del alimento gracias a la liberación de estos compuestos en el interior del envase.

Los productos frescos (carne, pescado, productos lácteos, frutas y verduras) pueden ser objeto de frecuentes contaminaciones microbiológicas. Según la EFSA en 2020 se reportaron 3.086 brotes asociados a alimentos que supusieron 20.017 casos en humanos, principalmente causados por *Salmonella*, *Campylobacter, Escherichia coli* y *Listeria monocytogenes* [27]. En frutas y hortalizas el crecimiento de hongos fitopatógenos como *Penicillium* spp. y *Botrytis cinerea* producen pérdidas significativas de alimentos a lo largo de toda la cadena alimentaria [28]. A su vez, los hongos pueden ser productores de micotoxinas, como la patulina producida por *Penicillium expansum*, y pueden suponer un grave riesgo para la salud del consumidor [29]. Por tanto, el uso de envasado activo antimicrobiano resulta una tecnología interesante que permite reducir o evitar estos problemas microbiológicos.

Los envases activos antimicrobianos tienen como objetivo aumentar la seguridad alimentaria frente a microorganismos concretos. Su actividad se produce bien por la liberación del compuesto en el espacio de cabeza del envase o por contacto directo con el alimento. La adición de estos compuestos a la matriz polimérica resulta más efectiva que la incorporación directa en el alimento, ya que puede promover una liberación controlada del activo en la superficie del alimento, donde suele ser más necesario. El diseño de envases activos antimicrobianos requiere de un complejo estudio que incluye evaluar no solo las características del alimento, sino también del microrganismo patógeno o alterante que afecta al producto, así como de la incorporación y liberación del compuesto activo durante el envasado [30].

### 1.2.1. Compuestos activos antimicrobianos para el envasado activo de alimentos

La incorporación de un agente activo a la matriz polimérica puede mejorar la actividad biológica del mismo, y dota al polímero de nuevas funcionalidades. Entre los diferentes agentes antimicrobianos se incluyen compuestos de naturaleza muy diversa como son: bacteriocinas, enzimas, ácidos orgánicos y sales, metales, polímeros, péptidos, extractos de plantas, aceites esenciales o sus compuestos mayoritarios [31].

Entre ellos, destacan los compuestos volátiles procedentes de extractos naturales de plantas o aceites esenciales. Estos son una mezcla de compuestos naturales extraídos de diferentes partes de las plantas, frutas o especias. La composición química de los aceites esenciales es muy variable y depende de la parte de la planta, factores genéticos, climáticos, geográficos, condiciones temporales, momento de la recolecta o de las técnicas de extracción. Están compuestos por diversas moléculas de diferente naturaleza química, incluyendo ésteres, cetonas, ácidos, aminas, alcoholes y aldehídos [32]. Estos compuestos suelen ser de carácter lipófilo, con elevada volatilidad y de bajo peso molecular, además, poseen un aroma característico. Entre sus propiedades biológicas destaca una reconocida actividad antimicrobiana contra diferentes patógenos alimentarios [33,34]. La mayoría de estas moléculas son habitualmente utilizadas como aditivos en la industria alimentaria [35], ya que algunos se encuentran clasificados como compuestos generalmente reconocidos como seguros (GRAS). Solamente los aditivos alimentarios autorizados y considerados seguros para su consumo pueden ser incorporados a los materiales poliméricos para el desarrollo de envases activos antimicrobianos, puesto que se puede producir la migración deliberada hacia el producto envasado.

Los compuestos activos antimicrobianos utilizados en esta Tesis Doctoral fueron aldehídos de origen natural.

#### 1.2.1.1. Aldehídos volátiles naturales

Los aldehídos naturales forman parte de los aceites esenciales y extractos de plantas, por lo que existen en la naturaleza y muchos de ellos son utilizados como aromatizantes en la industria alimentaria. Son compuestos de bajo peso molecular y se caracterizan por ser altamente

volátiles. Presentan ciertas propiedades biológicas, destacando su actividad antimicrobiana contra hongos y bacterias [36–39].

El mecanismo de acción de estos compuestos no está claro, y depende de la estructura química y propiedades de cada aldehído. Se cree que su actividad antimicrobiana pueda estar relacionada con su lipofilicidad. Los aldehídos pueden difundir a través de la membrana plasmática de las células por su afinidad con los componentes que la constituyen (ácidos grasos, polisacáridos y fosfolípidos), causando cambios en la permeabilidad celular e irrumpiendo su normal funcionamiento [40–42]. Además, los aldehídos α,β-insaturados, en el interior de las células, pueden reaccionar con moléculas de importancia biológica como proteínas, amino ácidos o las cadenas de ADN [43,44].

Las propiedades físico-químicas, estructura, actividad antimicrobiana de algunos de los aldehídos empleados en esta Tesis Doctoral se revisan en el **Anexo A**.

### 1.2.2. Biopolímeros para el envasado activo de alimentos

En la actualidad, hay un creciente interés en buscar alternativas sostenibles a los envases plásticos derivados del petróleo, por materiales renovables, biodegradables y más sostenibles con el medio ambiente. Anualmente, en Europa se generan unos 25.8 millones de toneladas de residuos plásticos, de los cuales, solo alrededor de un 30% se reciclan. Los desechos plásticos que acaban en ecosistemas, como el marino, son de gran preocupación, ya que cada año entre 5 y 13 millones de toneladas de plástico acaban en el océano, lo que representa un 80% de la basura marina. De estos, se estima que entre 150.000 y 500.000 toneladas de plástico proceden de la Unión Europea [45]. Además del problema medioambiental que supone la acumulación de grandes cantidades de plástico en los ecosistemas, estos residuos pueden degradarse generando microplásticos, los cuales pueden incorporarse a la cadena trófica y suponen un riesgo para la salud [46]. Esto ha fomentado que el sector del plástico y embalaje y la industria alimentaria apueste por buscar alternativas sostenibles como el uso de polímeros procedentes de fuentes naturales. A su vez, se encuentra en consonancia con los ODS para 2030 centrados en la reducción de la contaminación provocada por los plásticos derivados del petróleo y no degradables y por un consumo más sostenible. La Unión Europea ha

establecido una estrategia de economía circular para plásticos, con el objetivo de proteger al medioambiente de la contaminación del plástico en los diferentes ecosistemas, apostando por la innovación en materiales biodegradables, la reducción del consumo de plásticos de un solo uso y reforzando el uso de reciclado de plásticos convencionales [45].

La producción global de biopolímeros en 2020 se estima que alcanzó los 2.1 millones de toneladas, de las cuales un 47% fue destinado a la industria del envasado, sin embargo, sigue estando muy por debajo del plástico convencional [47]. En la **Figura 2** se muestra un esquema de los polímeros obtenidos a partir de biomasa, entendiéndose ésta como materia orgánica procedente de residuos, desechos o procesos de origen biológico.



**Figura 2.** Clasificación de polímeros procedentes de la biomasa.

Los recursos biomásicos son muy diversos, y dan lugar a un gran grupo heterogéneo de polímeros biobasados. Algunos biopolímeros pueden obtenerse a partir de la revalorización de desechos y excedentes de la industria alimentaria permitiendo reaprovechar y aportar alto valor añadido a los desechos de estas industrias [16].

Además, los polímeros pueden clasificarse según su origen y su degradabilidad, tal y como se muestra en la **Figura 3**. Los biopolímeros se caracterizan por ser materiales biodegradables. Sin embargo, no todos los materiales biodegradables tienen que ser procedentes de la

biomasa. La biodegradabilidad de los materiales no depende de su origen, sino de su estructura química [48].



**Biodegradable**

Almidón
Celulosa
Quitosano
Alginato
Gelatina
Zeina
PLA
PHA

Policaprolactona (PCL)
Polivinil alcohol (PVOH)
Succinato de polibutileno (PBS)

Bio-Polietileno (PE)
Bio-Polipropileno (PP)
Bio-Poliamida (PA)

Poliestireno (PS)
Polietileno (PE)
Cloruro de polivinilo (PVC)
Tereftalato de polietileno (PET)
etc.

**Bio-basado**

**Petro-químico**
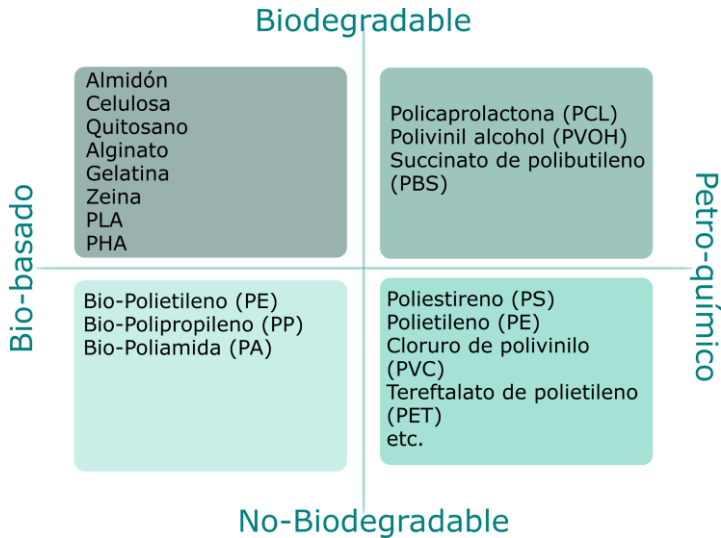
**No-Biodegradable**

**Figura 3.** Clasificación de polímeros en función de su origen y degradabilidad (adaptado de [16]).

El interés por el uso de biopolímeros se ha incrementado por las ventajas que presenta, ya que suelen ser biocompatibles, biodegradables, compostables y pueden ser obtenidos de fuentes renovables procedentes del reaprovechamiento de desechos agroalimentarios. Sin embargo, requieren de una evaluación del impacto medioambiental para asegurar una producción sostenible, ya que su extracción y purificación puede requerir energía, agua y puede generar efluentes contaminados que podría suponer un importante problema medioambiental [49], por lo que se han de diseñar técnicas eficientes para su obtención. Además, se ha de tener en cuenta el uso del terreno cultivable dedicado a la producción de biopolímeros [50]. Otros factores que se han de considerar, en el uso de biopolímeros para el envasado de alimentos, está relacionado con las propiedades físico-químicas y mecánicas que presentan. Los materiales obtenidos a partir de biomasa, principalmente proteínas y polisacáridos suelen ser muy hidrófilos, lo que causa que muchas de sus propiedades se vean influidas por la humedad, como las propiedades barrera a los gases o

las propiedades mecánicas [51,52]. Además, sus débiles propiedades térmicas dificultan el procesado con técnicas industriales habituales como termo-formado, extrusión o inyección. Estas propiedades pueden mejorarse por adición de compuestos o por la mezcla con otros polímeros [53–56].

Sin embargo, la capacidad de formación de películas de muchos de estos biopolímeros, los hace idóneos para su uso como recubrimientos y películas en el envasado de alimentos. Además, son excelentes materiales portadores de compuestos volátiles activos, gracias a su estructura y propiedades barrera, ya que son capaces de retener los volátiles favoreciendo la liberación cuando son expuestos a entornos húmedos, gracias a la plastificación de su estructura en presencia de alta humedad. Diferentes materiales biopoliméricos han sido utilizados como sistemas para transportar, encapsular y liberar compuestos bioactivos con el objetivo de otorgarle nuevas funcionalidades biológicas como propiedades antimicrobianas o antioxidantes [47,57].

Por tanto, la producción de envases activos antimicrobianos basados en el uso de biopolímeros resulta una alternativa prometedora para aumentar la seguridad y calidad del alimento, reducir el desperdicio y la pérdida de alimentos, así como, implantar un enfoque circular, en la que residuos de la industria agroalimentaria pueden ser reaprovechados [17,45] para la obtención no solo de biopolímeros, sino también de compuestos bioactivos.

Entre los diferentes biopolímeros obtenidos de la biomasa, destaca la quitina, que es el segundo polisacárido más abundante en la naturaleza después de la celulosa.

### 1.2.2.1. Quitosano

El quitosano es un aminopolisacárido lineal catiónico formado por unidades de *D*-glucosamina (GlcN) y *N*-acetil-*D*-glucosamina (GlcNAc) unidas mediante enlaces β-(1,4)-glicosídicos. Es un derivado parcialmente desacetilado de la quitina, se encuentra presente en diversas fuentes renovables, principalmente en exoesqueletos de crustáceos, aunque también se puede extraer de otros invertebrados, como insectos y hongos [58]. La quitina junto con el colágeno y la gelatina puede obtenerse de la revalorización de residuos de la industria

del marisco [17,49,59]. El proceso de obtención del quitosano comúnmente utilizado es la desacetilación alcalina a altas temperaturas de la quitina, el cual se muestra en la **Figura 4**. Aunque se han reportado otros métodos, como procesos enzimáticos para su extracción y desacetilación [60].
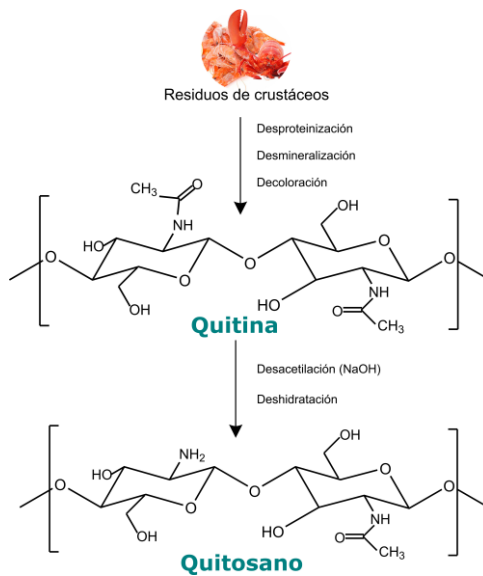


**Figura 4.** Metodología de extracción de quitina y quitosano.

La desacetilación de la quitina mejora la solubilidad del polisacárido en el medio, ya que mientras que la quitina es insoluble en agua, el quitosano puede disolverse en soluciones acuosas ácidas. Un aumento del grado de desacetilación de la quitina no solo implica un aumento de la solubilidad, sino que mejora la actividad biológica del quitosano, así como sus propiedades y aplicaciones. Por tanto, las características del quitosano se encuentran estrechamente relacionadas con su peso molecular, grado de desacetilación y distribución de los grupos acetilo [60,61], e incluso por el origen del quitosano y el ácido orgánico con el que se solubiliza [62]. Por tanto, el quitosano no se identifica como una sustancia única, sino que se ha de considerar como una familia de compuestos que presentan diferentes propiedades en función de su peso molecular (50 – 2000 kDa) y su grado de desacetilación (40 – 98%) [63].

La estructura química del quitosano ha permitido un gran número de modificaciones, lo que posibilita la obtención de nuevos derivados que mejoran sus propiedades, o bien le otorgan nuevas funciones biológicas [64]. Como se muestra en la **Figura 5**, el quitosano está formado por un anillo glicosídico y dotado de tres tipos de grupos funcionales, un grupo amino (NH$_2$) en el C-2, y dos grupos hidroxilo (OH), un grupo secundario en la posición C-3 y otro primario en la posición C-6. La presencia de estos grupos reactivos hace que sea fácilmente modificable y expande sus potenciales aplicaciones. La mayoría de las modificaciones se han centrado en la derivatización del grupo amino en el C-2 y en el grupo hidroxilo en el C-6 [64–66].
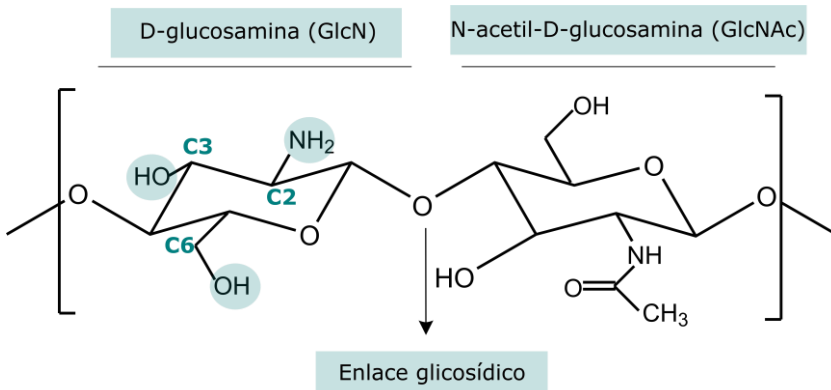


**Figura 5.** Estructura de química del quitosano.

El quitosano ha sido definido como un biopolímero biodegradable, biocompatible, no tóxico, comestible y con buena capacidad filmogénica [67]. Además, la presencia de los grupos amino a lo largo de la cadena polimérica, le confiere una actividad quelante y antimicrobiana [68]. Pueden obtenerse en diversas estructuras, como películas, recubrimientos, fibras, esponjas, partículas y nano-partículas, sistemas multicapa e hidrogeles [61]. Debido a su versatilidad y sus ventajosas propiedades, el quitosano y sus derivados han sido aplicados en diversas áreas: biomedicina, agroquímica, farmacia así como en el envasado de alimentos [58,68–70].

En esta línea, su actividad antimicrobiana intrínseca contra una amplia variedad de patógenos, ha sido objeto de estudio en numerosas

investigaciones en el área del envasado activo [71,72]. Su efectividad normalmente se relaciona con la naturaleza catiónica del quitosano, asociada a su grupo amino en C-2. Sin embargo, su actividad depende a su vez de otros parámetros; intrínsecos, como el grado de desacetilación, peso molecular, distribución de grupos amino a lo largo de la cadena polimérica y de factores extrínsecos, como el tipo de microorganismo, pH y temperatura del medio [73].

El quitosano exhibe unas propiedades que lo hacen un buen candidato para su aplicación en la industria alimentaria. Presenta una elevada barrera a los gases, sin embargo, ésta se ve afectada por la humedad, lo que limita su uso directo en el envasado de alimentos. Además, posee unas pobres propiedades termoplásticas, lo que restringe su aplicación en la industria. Por lo que se suele aplicar en combinación con otros polímeros [36,74].

Adicionalmente, el quitosano ha despertado mucho interés como vehículo para incorporar y liberar compuestos activos, mejorando sus propiedades antimicrobianas. Para el desarrollo de esta Tesis Doctoral se ha seleccionado el quitosano como matriz portadora de compuestos volátiles.

## 1.3. Incorporación de compuestos volátiles en matrices de quitosano

El quitosano puede utilizarse como portador y liberador de diversos compuestos bioactivos, y se ha empleado previamente para el desarrollo de materiales activos para el envasado de alimentos [75].

Se pueden aplicar diferentes enfoques en el diseño de envases activos antimicrobianos. En este sentido, el agente activo puede ser incorporado en almohadillas o bolsas depositadas en el interior del envase, en un recubrimiento sobre la superficie de otro polímero, mediante inmovilización a la superficie del material o incorporándolo directamente en el material de envasado [76]. Las películas de quitosano que incorporan compuestos activos son fácilmente obtenidas por la técnica de extensión y evaporación del disolvente o *casting*, donde el compuesto activo se añade directamente en la solución formadora de la película o film. Sin embargo, se han explorado otros métodos como la pulverización, electrospinning, encapsulación, emulsión, inmersión, ensamblaje capa a capa, extrusión o inmovilización covalente o iónica [77]. Todos estos sistemas permiten

la incorporación de compuestos antimicrobianos para la obtención de biopolímeros activos para su posterior aplicación en el envasado de alimentos (**Figura 6**).
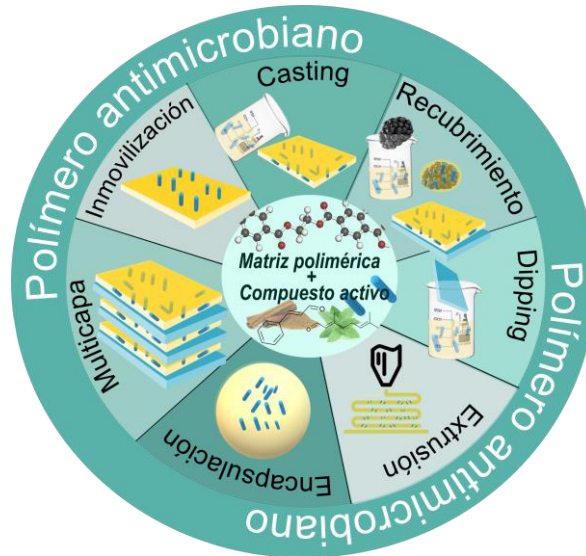


**Figura 6.** Esquema de los diferentes tipos de incorporación de activos en matrices poliméricas.

El uso de aldehídos antimicrobianos en el envasado activo de alimentos supone un gran reto, ya que la mayoría de estos compuestos son principalmente hidrofóbicos, lo que puede dificultar su incorporación en matrices más hidrofílicas, como es el caso de biopolímeros, como el quitosano. A su vez, son moléculas altamente volátiles e inestables, y pueden producirse mermas durante el procesamiento y/o durante el almacenamiento del polímero [78,79], lo cual puede afectar directamente a su eficacia antimicrobiana.

En este sentido, diferentes estrategias, como la encapsulación, han sido desarrolladas para estabilizar y neutralizar la volatilidad de los compuestos activos, así como para controlar su liberación durante el envasado [80,81].

La liberación del compuesto al interior del envase o al alimento, depende de múltiples factores, entre ellos, el método de incorporación del activo, el espesor del material, afinidad del compuesto por la matriz

polimérica y temperatura. Además, otras condiciones ambientales pueden inducir cambios estructurales en el polímero modificando la migración de los volátiles al espacio de cabeza, como la humedad relativa o por efecto del pH [82–84]. Esto permite un mayor control del proceso de liberación del compuesto activo durante el envasado. Concretamente, el quitosano posee una naturaleza hidrofílica que permite atrapar eficientemente bioactivos en su matriz, los cuales pueden difundir rápidamente en condiciones de elevada humedad debido a la plastificación de su estructura. Adicionalmente, posee otro mecanismo de liberación debido a su naturaleza policatiónica, que permite a este biopolímero responder a cambios del pH como resultado de la protonación y desprotonación de los grupos amino, lo que ha incrementado su uso como matriz polimérica portadora de moléculas activas [85]. Siguiendo esta línea, un enfoque más sofisticado para estabilizar el compuesto volátil y controlar su liberación en quitosano, es mediante su inmovilización a los grupos reactivos del quitosano a través de la formación de enlaces covalentes reversibles (ECR). Estos enlaces reversibles pueden ser hidrolizados de forma controlada bajo ciertos estímulos externos, provocando la migración del volátil cuando sea necesario (**Figura 7**).

Esta tecnología basada en la inmovilización de aldehídos al quitosano mediante ECR provee al polímero de un mecanismo más preciso para controlar la liberación de los compuestos anclados, obteniendo polímeros de respuesta a estímulo.
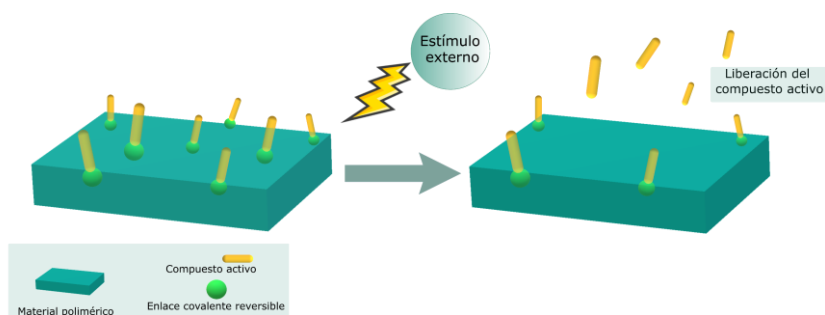


**Figura 7.** Anclaje covalente reversible de compuestos activos en matrices poliméricas.

## 1.4. Química covalente reversible para el anclaje de compuestos activos

Las reacciones covalentes reversibles basadas en la química *click* se han convertido en una herramienta prometedora para un gran número de aplicaciones en la ciencia de materiales, debido a su simplicidad, selectividad, eficiencia y el empleo de diferentes grupos funcionales [86]. La química *click* es un concepto novedoso de síntesis orgánica que implica la conjugación selectiva de dos o más moléculas con diversas funcionalidades, y que tienen lugar en tiempos de reacción cortos, con condiciones suaves y con excelentes rendimientos [87]. Comúnmente, la química covalente reversible ha sido empleada para crear sofisticadas estructuras supramoleculares con características dinámicas [88–90]. Pueden otorgar a los polímeros novedosas propiedades como capacidad de respuesta a estímulos, degradación controlada y propiedades autorreparantes [91,92]. Además del diseño de nuevos materiales, el uso de ECR puede ser empleado en la postfuncionalización del polímero. Con esta estrategia se pueden modificar los polímeros inmovilizando de forma covalente reversible moléculas en su superficie o a lo largo de la cadena polimérica, ampliando sus aplicaciones tecnológicas [93]. En este sentido, su uso permite el desarrollo de polímeros de respuesta a estímulo, que consisten en la inmovilización de sustituyentes dinámicos a lo largo de la cadena del polímero, cuya liberación y acción es desencadenada bajo estímulos externos que promueven la hidrólisis del enlace.

En general, el uso de la química covalente reversible permite mejorar la estabilidad del material polimérico, o de los compuestos que se inmovilizan a lo largo de su estructura. Los ECR son un tipo de enlaces covalentes que responden a estímulos específicos y suponen una ventaja fundamental sobre los enlaces covalentes comunes. Principalmente por su naturaleza reversible que permite la hidrólisis controlada del enlace cuando son sometidos a ciertos estímulos (temperatura, luz, pH, etc), mientras que se mantienen estables en ausencia de éstos [91], pudiendo dotar a los materiales poliméricos de la capacidad de respuesta a estímulos específicos (**Figura 8**).
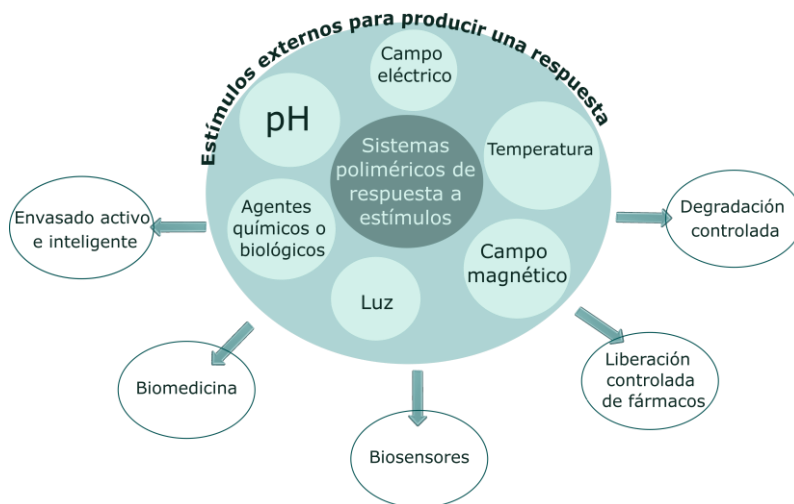
**Figura 8.** Estímulos potenciales para desencadenar la respuesta en matrices poliméricas y sus posibles aplicaciones.

Esta tecnología ofrece posibilidades sin precedentes para la innovación de la ciencia de los materiales y polímeros en muy diversos campos, especialmente en aplicaciones de liberación controlada de compuestos activos, aromas y fármacos [94–97].

Entre los diferentes tipos de enlaces covalentes reversibles destacan los enlaces iminas o bases de Schiff [94]. Estas bases de Schiff son un importante grupo de reacciones en química *click*.

El enlace imina o base de Schiff es un grupo funcional que posee un doble enlace carbono-nitrógeno ($R_1$-N=CH-$R_2$), resultado de una reacción de condensación entre un grupo amino primario ($R_1$-$NH_2$) y un grupo carbonilo ($R_2$-CHO) procedente de un aldehído o cetona, con la pérdida de una molécula de agua [98].

La formación de la imina ocurre en dos etapas; el mecanismo de la reacción se inicia mediante el ataque nucleófilo (cede los electrones) del grupo amino sobre el grupo carbonilo de un aldehído, grupo electrófilo, el cual forma un intermediario inestable denominado carbinolamina. La carbinolamina se transforma en una imina (C=N) mediante la pérdida de una molécula de agua, siendo la velocidad de este último paso dependiente del pH [99].

Respecto a su reversibilidad, la sensibilidad de la imina o bases de Schiff a cambios del pH es la principal característica de respuesta a

estímulos de esta estructura. Por tanto, los enlaces imina se hidrolizan fácilmente en contacto con agua, especialmente a pH ácidos [100].

En este contexto, el quitosano resulta un buen candidato para la formación de bases de Schiff o iminas, puesto que presenta numerosos grupos amino primarios en las unidades de glucosamina distribuidos a lo largo de su cadena polimérica, por lo que no necesita modificación para anclar de forma covalente grupos carbonilos como los aldehídos. El esquema de inmovilización de aldehídos en el grupo amino primario del quitosano mediante la función imina, así como su reversibilidad, se muestra en la **Figura 9**.
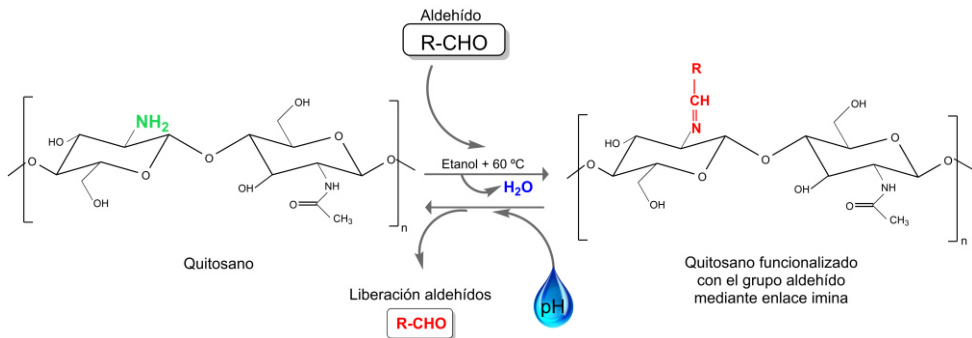


**Figura 9.** Formación de iminas o bases de Schiff en quitosano.

La formación de estos enlaces puede estar influenciada por la estructura química de los sustratos [101], además, las iminas pueden obtenerse fácilmente en condiciones suaves de temperatura y con solventes respetuosos con el medio ambiente, obteniendo altos ratios de conversión [102]. Habitualmente, la modificación de los grupos amino del quitosano se lleva a cabo en la solución formadora de film, en la cual se inmovilizan las moléculas de aldehídos [103,104]. Sin embargo, en esta Tesis Doctoral, se ha realizado la postfuncionalización del quitosano en estado sólido, anclándose covalentemente sobre una película preformada de quitosano.

La formación de bases de Schiff puede ser empleada para dotar al material de nuevas funciones [105] entre las que destaca su uso como portador y liberador de compuestos activos anclados.

### 1.4.1. Aplicaciones de la química covalente reversible como liberador de compuestos activos

El uso de enlaces imina reversibles para la liberación de compuestos activos mediante la aplicación de estímulos externos ha sido ampliamente explorada en diferentes áreas de estudio y empleando diversos polímeros [106–111]. Se ha demostrado el potencial de estas estructuras dinámicas para la liberación de los compuestos anclados, los cuales han empleado diferentes estrategias para promover la hidrólisis de la imina, y por consiguiente la liberación del bioactivo al entorno. Por ejemplo, el entorno ligeramente ácido del tejido tumoral ha sido utilizado como desencadenante de la liberación de fármacos anclados [112,113], la acción de los jugos gástricos también se ha aplicado para promover la hidrólisis de la imina [114], o bien se ha fomentado por la liberación de bioactivos desencadenada por la producción de ácidos orgánicos por parte de microorganismos [108,109].

El enfoque de la química covalente reversible y la formación de iminas en quitosano resulta muy atractivo para el diseño de biopolímeros portadores de activos de liberación controlada por estímulos externos, tanto por la presencia de grupos reactivos como por sus propiedades intrínsecas. Sin embargo, solo unos pocos estudios han explorado la liberación del compuesto anclado al quitosano cuya reversibilidad es promovida por contacto con soluciones acuosas ácidas [104,115]. Además, su uso en el envasado de alimentos ha sido escasamente explorado [116]. Su incorporación en el diseño de envases activos antimicrobianos podría resultar una tecnología novedosa, ya que permite estabilizar compuestos antimicrobianos volátiles anclados covalentemente, facilitando su manipulación y permitiendo controlar su liberación cuando sea necesario.

En esta línea, un nuevo concepto de envasado está siendo desarrollado, y puede resultar de interés para la aplicación de películas basadas en el anclaje reversible de bioactivos, y es el denominado envasado de respuesta a estímulo o *responsive packaging*. Sin embargo, el uso de materiales de respuesta a estímulo para el envasado alimentario se ha focalizado en el diseño de envases inteligentes [117] y su aplicación en envases antimicrobianos es limitada. Es evidente, que la aplicación de este tipo de sistemas puede resultar interesante para el envasado activo de alimentos ya que asegura una liberación del

compuesto a demanda, mientras que en ausencia de estímulo permanece estable en el material. En la **Figura 10**, se muestra un esquema de las estrategias, ventajas y desventajas de aplicación de los polímeros antimicrobianos de respuesta a estímulos en el diseño de envases activo de alimentos.

En esta Tesis Doctoral, se explora el enfoque de los ECR para inmovilizar compuestos altamente volátiles sobre películas de quitosano con el objetivo de desarrollar materiales activos antimicrobianos cuya liberación responde a cambios de pH.

**Figura 10.** Aplicación de compuestos volátiles naturales en el campo del envasado activo de alimentos: ventajas y desventajas.

## 1.5. Referencias bibliográficas

1. FAO *Food loss and food waste: Causes and solutions*; 2011; ISBN 9781788975391.

2. Priefer, C.; Jörissen, J.; Bräutigam, K.R. Food waste prevention in Europe - A cause-driven approach to identify the most relevant leverage points for action. *Resour. Conserv. Recycl.* **2016**, *109*, 155–165, doi:10.1016/j.resconrec.2016.03.004.

3. Guillard, V.; Gaucel, S.; Fornaciari, C.; Angellier-Coussy, H.; Buche, P.; Gontard, N. The next generation of sustainable food packaging to preserve our environment in a circular economy context. *Front. Nutr.* **2018**, *5*, 1–13, doi:10.3389/fnut.2018.00121.

4. FAO *The State of Food and Agriculture: moving forward on food loss and waste reduction*; 2019; ISBN 9781315764788.

5. UN Transforming Our World: the 2030 Agenda for Sustainable Development Available online (2022, June 04): https://sdgs.un.org/2030agenda.

6. Onwude, D.I.; Chen, G.; Eke-Emezie, N.; Kabutey, A.; Khaled, A.Y.; Sturm, B. Recent advances in reducing food losses in the supply chain of fresh agricultural produce. *Processes* **2020**, *8*, 1–31, doi:10.3390/pr8111431.

7. Porat, R.; Lichter, A.; Terry, L.A.; Harker, R.; Buzby, J. Postharvest losses of fruit and vegetables during retail and in consumers' homes: Quantifications, causes, and means of prevention. *Postharvest Biol. Technol.* **2018**, *139*, 135–149, doi:10.1016/j.postharvbio.2017.11.019.

8. Aiyedun, S.O.; Onarinde, B.A.; Swainson, M.; Dixon, R.A. Foodborne outbreaks of microbial infection from fresh produce in Europe and North America: a systematic review of data from this millennium. *Int. J. Food Sci. Technol.* **2021**, *56*, 2215–2223, doi:10.1111/ijfs.14884.

9. Ciccullo, F.; Cagliano, R.; Bartezzaghi, G.; Perego, A. Implementing the circular economy paradigm in the agri-food supply chain: The role of food waste prevention technologies. *Resour. Conserv. Recycl.* **2021**, *164*, 105114, doi:10.1016/j.resconrec.2020.105114.

10. Mustapha, A.; Lee, J.H. Food preservation and safety. In *Microbial Control and Food Preservation: Theory and Practice*; Juneja, V.K., Dwivedi, H.P., Sofos, J.N., Eds.; Springer New York: New York, NY, 2017; pp. 1–15 ISBN 978-1-4939-7556-3.

11. Ahvenainen, R. *Novel food packaging techniques*; Elsevier, 2003;

12. Wilson, M.D.; Stanley, R.A.; Eyles, A.; Ross, T. Innovative processes and technologies for modified atmosphere packaging of fresh and fresh-cut fruits and vegetables. *Crit. Rev. Food Sci. Nutr.* **2019**, *59*, 411–422, doi:10.1080/10408398.2017.1375892.

13. Wohner, B.; Pauer, E.; Heinrich, V.; Tacker, M. Packaging-related food losses and waste: An overview of drivers and issues. *Sustain.* **2019**, *11*, doi:10.3390/su11010264.

14. Matthews, C.; Moran, F.; Jaiswal, A.K. A review on European Union's strategy for plastics in a circular economy and its impact on food safety. *J. Clean. Prod.* **2021**, *283*, 125263, doi:10.1016/j.jclepro.2020.125263.

15.     Sangroniz, A.; Zhu, J.B.; Tang, X.; Etxeberria, A.; Chen, E.Y.X.; Sardon, H. Packaging materials with desired mechanical and barrier properties and full chemical recyclability. *Nat. Commun.* **2019**, *10*, 1–7, doi:10.1038/s41467-019-11525-x.

16.     Geueke, B. Dossier - Bioplastics as food contact materials. *Food Packag. Forum* **2014**, 1–8, doi:10.5281/zenodo.33517.

17.     de la Caba, K.; Guerrero, P.; Trung, T.S.; Cruz-Romero, M.; Kerry, J.P.; Fluhr, J.; Maurer, M.; Kruijssen, F.; Albalat, A.; Bunting, S.; et al. From seafood waste to active seafood packaging: An emerging opportunity of the circular economy. *J. Clean. Prod.* **2019**, *208*, 86–98, doi:10.1016/j.jclepro.2018.09.164.

18.     Yildirim, S.; Röcker, B.; Pettersen, M.K.; Nilsen-Nygaard, J.; Ayhan, Z.; Rutkaite, R.; Radusin, T.; Suminska, P.; Marcos, B.; Coma, V. Active packaging applications for food. *Compr. Rev. Food Sci. Food Saf.* **2018**, *17*, 165–199, doi:10.1111/1541-4337.12322.

19.     Wyrwa, J.; Barska, A. Innovations in the food packaging market: active packaging. *Eur. Food Res. Technol.* **2017**, *243*, 1681–1692, doi:10.1007/s00217-017-2878-2.

20.     Tiekstra, S.; Dopico-Parada, A.; Koivula, H.; Lathi, J.; Buntinx, M. Holistic approach to a successful market implementation of active and intelligent food packaging. *Foods* **2021**, *10*, doi:10.3390/foods10020465 Academic.

21.     Drago, E.; Campardelli, R.; Pettinato, M.; Perego, P. Innovations in smart packaging concepts for food: An extensive review. *Foods* **2020**, *9*, doi:10.3390/foods9111628.

22.     Future Market Insights, F. Active, smart and intelligent packaging market snapshot - 2022 – 2027 Available online (2022, March 30): https://www.futuremarketinsights.com/reports/active-smart-and-intelligent-packaging-market.

23.     EC Regulation (EC) No 450/2009 of the European Parliament and of the Council of 29 May 2009 on active and intelligent materials and articles intended to come into contact with food. *Off. J. Eur. Union.* **2009**.

24.     EC Regulation (EC) No 1935/2004 of the European Parliament and of the council of 27 October 2004 on materials and articles intended to come into contact with food and repealing Directives 80/590/EEC and 89/109/EEC. *Off. J. Eur. Union.* **2004**.

25.     EC Regulation (EC) No 1333/2008 of the European Parliament and of the Council of 16 December 2008 on food additives. *Off. J. Eur. Union.* **2008**.

26.     EC Regulation (EC) No 1169/2011 of the European Parliament and of the Council of 25 October 2011 on the provision of food information to consumers, amending Regulations (EC) Nº 1924/2006 and (EC) Nº 1925/2006 of the European Parliament. *Off. J. Eur. Union*. **2011**.

27.     EFSA The European Union One Health 2020 Zoonoses Report. *EFSA J.* **2021**, *19*, doi:10.2903/j.efsa.2021.6971.

28.     Davies, C.R.; Wohlgemuth, F.; Young, T.; Violet, J.; Dickinson, M.; Sanders, J.W.; Vallieres, C.; Avery, S. V. Evolving challenges and strategies for fungal

control in the food supply chain. *Fungal Biol. Rev.* **2021**, *36*, 15–26, doi:10.1016/j.fbr.2021.01.003.

29.  Agriopoulou, S.; Stamatelopoulou, E.; Varzakas, T. Advances in occurrence, importance, and mycotoxin control strategies: Prevention and detoxification in foods. *Foods* **2020**, *86*, 137.

30.  Gavara, R. *Practical guide to antimicrobial active packaging*; Smithers Pira, 2015; ISBN 1910242101.

31.  Benbettaïeb, N.; Debeaufort, F.; Karbowiak, T. Bioactive edible films for food applications: mechanisms of antimicrobial and antioxidant activity. *Crit. Rev. Food Sci. Nutr.* **2019**, *59*, 3431–3455, doi:10.1080/10408398.2018.1494132.

32.  Falleh, H.; Ben Jemaa, M.; Saada, M.; Ksouri, R. Essential oils: A promising eco-friendly food preservative. *Food Chem.* **2020**, *330*, 127268, doi:10.1016/j.foodchem.2020.127268.

33.  Burt, S.A. *Antibacterial activity of essential oils : potential applications in food*; 2004; Vol. 94; ISBN 9789039346617.

34.  Taghavi, T.; Kim, C.; Rahemi, A. Role of natural volatiles and essential oils in extending shelf life and controlling postharvest microorganisms of small fruits. *Microorganisms* **2018**, *6*, 104, doi:10.3390/microorganisms6040104.

35.  Bampidis, V.; Azimonti, G.; Bastos, M. de L.; Christensen, H.; Kouba, M.; Kos Durjava, M.; López-Alonso, M.; López Puente, S.; Marcon, F.; Mayo, B.; et al. Safety and efficacy of 26 compounds belonging to chemical group 3 (α,β-unsaturated straight-chain and branched-chain aliphatic primary alcohols, aldehydes, acids and esters) when used as flavourings for all animal species and categories. *EFSA J.* **2019**, *17*, doi:10.2903/j.efsa.2019.5654.

36.  Wang, H.; Qian, J.; Ding, F. Emerging chitosan-based films for food packaging applications. *J. Agric. Food Chem.* **2018**, *66*, 395–413, doi:10.1021/acs.jafc.7b04528.

37.  Kawacka, I.; Olejnik-Schmidt, A.; Schmidt, M.; Sip, A. Natural plant-derived chemical compounds as *Listeria monocytogenes* inhibitors in vitro and in food model systems. *Pathogens* **2021**, *10*, 1–36, doi:10.3390/pathogens10010012.

38.  Friedman, M.; Henika, P.R.; Mandrell, R.E. Antibacterial activities of phenolic benzaldehydes and benzoic acids against *Campylobacter jejuni, Escherichia coli, Listeria monocytogenes,* and *Salmonella enterica*. *J. Food Prot.* **2003**, *66*, 1811–1821, doi:10.4315/0362-028X-66.10.1811.

39.  Taguchi, T.; Kozutsumi, D.; Nakamura, R.; Sato, Y.; Ishihara, A.; Nakajima, H. Effects of aliphatic aldehydes on the growth and patulin production of *Penicillium expansum* in apple juice. *Biosci. Biotechnol. Biochem.* **2013**, *77*, 138–144, doi:10.1271/bbb.120629.

40.  Cai, R.; Hu, M.; Zhang, Y.; Niu, C.; Yue, T.; Yuan, Y.; Wang, Z. Antifungal activity and mechanism of citral, limonene and eugenol against *Zygosaccharomyces rouxii*. *Lwt* **2019**, *106*, 50–56, doi:10.1016/j.lwt.2019.02.059.

41.  Zhang, J.; Tian, H.; Sun, H.; Wang, X. Antifungal activity of Trans-2-Hexenal against *Penicillium cyclopium* by a membrane damage mechanism. *J. Food Biochem.* **2017**, *41*, 1–9, doi:10.1111/jfbc.12289.

42.     Wang, Y.; Feng, K.; Yang, H.; Yuan, Y.; Yue, T. Antifungal mechanism of cinnamaldehyde and citral combination against: *Penicillium expansum* based on FT-IR fingerprint, plasma membrane, oxidative stress and volatile profile. *RSC Adv.* **2018**, *8*, 5806–5815, doi:10.1039/c7ra12191a.

43.     Friedman, M. Chemistry, Antimicrobial mechanisms, and antibiotic activities of cinnamaldehyde against pathogenic bacteria in animal feeds and human foods. *J. Agric. Food Chem.* **2017**, *65*, 10406–10423, doi:10.1021/acs.jafc.7b04344.

44.     Lopachin, R.M.; Gavin, T. Molecular mechanisms of aldehyde toxicity: A chemical perspective. *Chem. Res. Toxicol.* **2014**, *27*, 1081–1091, doi:10.1021/tx5001046.

45.     EC A European strategy for plastics in a circular economy. **2018**, *28*.

46.     Ivar Do Sul, J.A.; Costa, M.F. The present and future of microplastic pollution in the marine environment. *Environ. Pollut.* **2014**, *185*, 352–364, doi:10.1016/j.envpol.2013.10.036.

47.     Barone, A.S.; Matheus, J.R.V.; de Souza, T.S.P.; Moreira, R.F.A.; Fai, A.E.C. Green-based active packaging: Opportunities beyond COVID-19, food applications, and perspectives in circular economy—A brief review. *Compr. Rev. Food Sci. Food Saf.* **2021**, *20*, 4881–4905, doi:10.1111/1541-4337.12812.

48.     Siracusa, V.; Rocculi, P.; Romani, S.; Rosa, M.D. Biodegradable polymers for food packaging: a review. *Trends Food Sci. Technol.* **2008**, *19*, 634–643, doi:10.1016/j.tifs.2008.07.003.

49.     Muñoz, I.; Rodríguez, C.; Gillet, D.; M. Moerschbacher, B. Life cycle assessment of chitosan production in India and Europe. *Int. J. Life Cycle Assess.* **2018**, *23*, 1151–1160, doi:10.1007/s11367-017-1290-2.

50.     European Bioplastics Report - bioplastic marked data 2017. *Bioplastics Mark. data 2017, Glob. Prod. Capacit. bioplastics 2017-2022* **2017**, 1–7.

51.     Cisneros-Zevallos, L.; Krochta, J.M. Whey protein coatings for fresh fruits and relative humidity effects. *JFS Food Eng. Phys. Prop.* **2003**, *68*, 176–181, doi:10.1111/j.1365-2621.2003.tb14136.x

52.     Aguirre-Loredo, R.Y.; Rodríguez-Hernández, A.I.; Morales-Sánchez, E.; Gómez-Aldapa, C.A.; Velazquez, G. Effect of equilibrium moisture content on barrier, mechanical and thermal properties of chitosan films. *Food Chem.* **2016**, *196*, 560–566, doi:10.1016/j.foodchem.2015.09.065.

53.     Benbettaïeb, N.; Kurek, M.; Bornaz, S.; Debeaufort, F. Barrier, structural and mechanical properties of bovine gelatin-chitosan blend films related to biopolymer interactions. *J. Sci. Food Agric.* **2014**, *94*, 2409–2419, doi:10.1002/jsfa.6570.

54.     Tarique, J.; Sapuan, S.M.; Khalina, A. Effect of glycerol plasticizer loading on the physical, mechanical, thermal, and barrier properties of arrowroot (*Maranta arundinacea*) starch biopolymers. *Sci. Rep.* **2021**, *11*, 1–17, doi:10.1038/s41598-021-93094-y.

55.     Grande, R.; Pessan, L.A.; Carvalho, A.J.F. Thermoplastic blends of chitosan: A method for the preparation of high thermally stable blends with polyesters.

*Carbohydr. Polym.* **2018**, *191*, 44–52, doi:10.1016/j.carbpol.2018.02.087.

56. Balaguer, M.P.; Gómez-Estaca, J.; Gavara, R.; Hernandez-Munoz, P. Biochemical properties of bioplastics made from wheat gliadins cross-linked with cinnamaldehyde. *J. Agric. Food Chem.* **2011**, *59*, 13212–13220, doi:10.1021/jf203055s.

57. Talón, E.; Trifkovic, K.T.; Nedovic, V.A.; Bugarski, B.M.; Vargas, M.; Chiralt, A.; González-Martínez, C. Antioxidant edible films based on chitosan and starch containing polyphenols from thyme extracts. *Carbohydr. Polym.* **2017**, *157*, 1153–1161, doi:10.1016/j.carbpol.2016.10.080.

58. Philibert, T.; Lee, B.H.; Fabien, N. Current status and new perspectives on chitin and chitosan as functional biopolymers. *Appl. Biochem. Biotechnol.* **2017**, *181*, 1314–1337, doi:10.1007/s12010-016-2286-2.

59. Santos, V.P.; Marques, N.S.S.; Maia, P.C.S.V.; de Lima, M.A.B.; Franco, L. de O.; de Campos-Takaki, G.M. Seafood waste as attractive source of chitin and chitosan production and their applications. *Int. J. Mol. Sci.* **2020**, *21*, 1–17, doi:10.3390/ijms21124290.

60. Younes, I.; Rinaudo, M. Chitin and chitosan preparation from marine sources. Structure, properties and applications. *Mar. Drugs* **2015**, *13*, 1133–1174, doi:10.3390/md13031133.

61. Lizardi-Mendoza, J.; Argüelles Monal, W.M.; Goycoolea Valencia, F.M. Chemical characteristics and functional properties of chitosan. In *Chitosan in the Preservation of Agricultural Commodities*; Elsevier Inc., 2016; pp. 3–31 ISBN 9780128027356.

62. Park, S.Y.; Marsh, K.S.; Rhim, J.W. Characteristics of different molecular weight chitosan films affected by the type of organic solvents. *J. FOOD Sci.* **2002**, *67*, 16–19, doi:10.1111/j.1365-2621.2002.tb11382.x.

63. Cazón, P.; Vázquez, M. Applications of chitosan as food packaging materials BT - Sustainable Agriculture Reviews 36: Chitin and chitosan: Applications in food, agriculture, pharmacy, medicine and wastewater treatment. In; Crini, G., Lichtfouse, E., Eds.; Springer International Publishing: Cham, 2019; pp. 81–123 ISBN 978-3-030-16581-9.

64. Boeriu, C.G.; van den Broek, L.A.M. Chemical and enzymatic modification of chitosan to produce new functional materials with improved properties. *Chitin and Chitosan* 2019, 245–258.

65. Brasselet, C.; Pierre, G.; Dubessay, P.; Dols-Lafargue, M.; Coulon, J.; Maupeu, J.; Vallet-Courbin, A.; de Baynast, H.; Doco, T.; Michaud, P.; et al. Modification of chitosan for the generation of functional derivatives. *Appl. Sci.* **2019**, *9*, doi:10.3390/app9071321.

66. Wang, W.; Xue, C.; Mao, X. Chitosan: Structural modificatin, biological activity and application. *Int. J. Biol. Macromol.* **2020**, *164*, 4532–4546, doi:10.1016/j.ijbiomac.2020.09.042.

67. Rinaudo, M. Chitin and chitosan: Properties and applications. *Prog. Polym. Sci.* **2006**, *31*, 603–632, doi:10.1016/j.progpolymsci.2006.06.001.

68. Bakshi, P.S.; Selvakumar, D.; Kadirvelu, K.; Kumar, N.S. Chitosan as an environment friendly biomaterial – a review on recent modifications and

applications. *Int. J. Biol. Macromol.* **2020**, *150*, 1072–1083, doi:10.1016/J.IJBIOMAC.2019.10.113.

69.    Muxika, A.; Etxabide, A.; Uranga, J.; Guerrero, P.; de la Caba, K. Chitosan as a bioactive polymer: Processing, properties and applications. *Int. J. Biol. Macromol.* **2017**, *105*, 1358–1368, doi:10.1016/j.ijbiomac.2017.07.087.

70.    Higueras, L.; López-Carballo, G.; Hernández-Muñoz, P.; Gavara, R.; Rollini, M. Development of a novel antimicrobial film based on chitosan with LAE (ethyl-N$^\alpha$-dodecanoyl-L-arginate) and its application to fresh chicken. *Int. J. Food Microbiol.* **2013**, *165*, 339–345, doi:10.1016/j.ijfoodmicro.2013.06.003.

71.    Souza, V.G.L.; Pires, J.R.A.; Rodrigues, C.; Coelhoso, I.M.; Fernando, A.L. Chitosan composites in packaging industry-current trends and future challenges. *Polymers (Basel).* **2020**, *12*, 1–16, doi:10.3390/polym12020417.

72.    Dutta, P.K.; Tripathi, S.; Mehrotra, G.K.; Dutta, J. Perspectives for chitosan based antimicrobial films in food applications. *Food Chem.* **2009**, *114*, 1173–1182, doi:10.1016/j.foodchem.2008.11.047.

73.    Li, J.; Zhuang, S. Antibacterial activity of chitosan and its derivatives and their interaction mechanism with bacteria: Current state and perspectives. *Eur. Polym. J.* **2020**, *138*, 109984, doi:10.1016/j.eurpolymj.2020.109984.

74.    Van Den Broek, L.A.M.; Knoop, R.J.I.; Kappen, F.H.J.; Boeriu, C.G. Chitosan films and blends for packaging material. *Carbohydr. Polym.* **2015**, *116*, 237–242, doi:10.1016/j.carbpol.2014.07.039.

75.    Flórez, M.; Guerra-Rodríguez, E.; Cazón, P.; Vázquez, M. Chitosan for food packaging: Recent advances in active and intelligent films. *Food Hydrocoll.* **2022**, *124*, doi:10.1016/j.foodhyd.2021.107328.

76.    Almasi, H.; Jahanbakhsh Oskouie, M.; Saleh, A. A review on techniques utilized for design of controlled release food active packaging. *Crit. Rev. Food Sci. Nutr.* **2020**, *0*, 1–21, doi:10.1080/10408398.2020.1783199.

77.    Zhang, X.; Ismail, B.B.; Cheng, H.; Jin, T.Z.; Qian, M.; Arabi, S.A.; Liu, D.; Guo, M. Emerging chitosan-essential oil films and coatings for food preservation - A review of advances and applications. *Carbohydr. Polym.* **2021**, *273*, 118616, doi:10.1016/j.carbpol.2021.118616.

78.    Suppakul, P.; Sonneveld, K.; Bigger, S.W.; Miltz, J. Loss of AM additives from antimicrobial films during storage. *J. Food Eng.* **2011**, *105*, 270–276, doi:10.1016/j.jfoodeng.2011.02.031.

79.    Wicochea-Rodríguez, J.D.; Chalier, P.; Ruiz, T.; Gastaldi, E. Active food packaging based on biopolymers and aroma compounds: How to design and control the release. *Front. Chem.* **2019**, *7*, 1–16, doi:10.3389/fchem.2019.00398.

80.    Sanahuja, A.B.; García, A.V. New trends in the use of volatile compounds in food packaging. *Polymers (Basel).* **2021**, *13*, doi:10.3390/polym13071053.

81.    Zaitoon, A.; Luo, X.; Lim, L.T. Triggered and controlled release of active gaseous/volatile compounds for active packaging applications of agri-food products: A review. *Compr. Rev. Food Sci. Food Saf.* **2022**, *21*, 541–579, doi:10.1111/1541-4337.12874.

82.    Cerisuelo, J.P.; Alonso, J.; Aucejo, S.; Gavara, R.; Hernández-Muñoz, P.

Modifications induced by the addition of a nanoclay in the functional and active properties of an EVOH film containing carvacrol for food packaging. *J. Memb. Sci.* **2012**, *423–424*, 247–256, doi:10.1016/j.memsci.2012.08.021.

83. Kocak, G.; Tuncer, C.; Bütün, V. PH-Responsive polymers. *Polym. Chem.* **2017**, *8*, 144–176, doi:10.1039/c6py01872f.

84. Mascheroni, E.; Fuenmayor, C.A.; Cosio, M.S.; Silvestro, G. Di; Piergiovanni, L.; Mannino, S.; Schiraldi, A. Encapsulation of volatiles in nanofibrous polysaccharide membranes for humidity-triggered release. *Carbohydr. Polym.* **2013**, *98*, 17–25, doi:10.1016/j.carbpol.2013.04.068.

85. Carreira, A.S.; Gonçalves, F.A.M.M.; Mendonça, P. V.; Gil, M.H.; Coelho, J.F.J. Temperature and pH responsive polymers based on chitosan: Applications and new graft copolymerization strategies based on living radical polymerization. *Carbohydr. Polym.* **2010**, *80*, 618–630, doi:10.1016/j.carbpol.2009.12.047.

86. Xi, W.; Scott, T.F.; Kloxin, C.J.; Bowman, C.N. Click chemistry in materials science. *Adv. Funct. Mater.* **2014**, *24*, 2572–2590, doi:10.1002/adfm.201302847.

87. Gupta, S.; Ameta, C.; Ameta, R.; Punjabi, P.B. *Click chemistry: A tool for green chemical organic synthesis*; Elsevier Inc., 2020; ISBN 9780128195390.

88. Busseron, E.; Ruff, Y.; Moulin, E.; Giuseppone, N. Supramolecular self-assemblies as functional nanomaterials. *Nanoscale* **2013**, *5*, 7098–7140, doi:10.1039/c3nr02176a.

89. Lehn, J.-M. Dynamers: dynamic molecular and supramolecular polymers. *Prog. Polym. Sci.* **2005**, *30*, 814–831, doi:10.1016/j.progpolymsci.2005.06.002.

90. Meguellat, K.; Ladame, S. Reversible covalent chemistries compatible with the principles of constitutional dynamic chemistry: New Reactions to Create More Diversity. *Top. Curr. Chem.* **2012**, *322*, 291–314, doi:10.1007/128_2011_277.

91. Zhang, Z.P.; Rong, M.Z.; Zhang, M.Q. Polymer engineering based on reversible covalent chemistry: A promising innovative pathway towards new materials and new functionalities. *Prog. Polym. Sci.* **2018**, *80*, 39–93, doi:10.1016/j.progpolymsci.2018.03.002.

92. Fukuda, K.; Shimoda, M.; Sukegawa, M.; Nobori, T.; Lehn, J.-M. Doubly degradable dynamers: dynamic covalent polymers based on reversible imine connections and biodegradable polyester units. *Green Chem.* **2012**, *14*, 2907, doi:10.1039/c2gc35875a.

93. García, F.; Smulders, M.M.J. Dynamic covalent polymers. *J. Polym. Sci. Part A Polym. Chem.* **2016**, *54*, 3551–3577, doi:10.1002/pola.28260.

94. Huang, S.; Kong, X.; Xiong, Y.; Zhang, X.; Chen, H.; Jiang, W.; Niu, Y.; Xu, W.; Ren, C. An overview of dynamic covalent bonds in polymer material and their applications. *Eur. Polym. J.* **2020**, *141*, 110094, doi:10.1016/j.eurpolymj.2020.110094.

95. Ulrich, S. Growing prospects of dynamic covalent chemistry in delivery applications. *Acc. Chem. Res.* **2019**, doi:10.1021/acs.accounts.8b00591.

96.    Tchakalova, V.; Lutz, E.; Lamboley, S.; Moulin, E.; Benczédi, D.; Giuseppone, N.; Herrmann, A. Design of stimuli-responsive dynamic covalent delivery systems for volatile compounds (Part 2): Fragrance-releasing cleavable surfactants in functional perfumery applications. *Chem. - A Eur. J.* **2021**, *27*, 13468–13476, doi:10.1002/chem.202102051.

97.    Guaresti, O.; García–Astrain, C.; Palomares, T.; Alonso–Varona, A.; Eceiza, A.; Gabilondo, N. Synthesis and characterization of a biocompatible chitosan–based hydrogel cross–linked via 'click' chemistry for controlled drug release. *Int. J. Biol. Macromol.* **2017**, *102*, 1–9, doi:10.1016/J.IJBIOMAC.2017.04.003.

98.    Zhang, Z.; He, C.; Chen, X. Hydrogels based on pH-responsive reversible carbon-nitrogen double-bond linkages for biomedical applications. *Mater. Chem. Front.* **2018**, *2*, 1765–1778, doi:10.1039/c8qm00317c.

99.    Ciaccia, M.; Di Stefano, S. Mechanisms of imine exchange reactions in organic solvents. *Org. Biomol. Chem.* **2015**, *13*, 646–654, doi:10.1039/c4ob02110j.

100.   Xin, Y.; Yuan, J. Schiff's base as a stimuli-responsive linker in polymer chemistry. *Polym. Chem.* **2012**, *3*, 3045–3055, doi:10.1039/c2py20290e.

101.   Godoy-Alcántar, C.; Yatsimirsky, A.K.; Lehn, J.M. Structure-stability correlations for imine formation in aqueous solution. *J. Phys. Org. Chem.* **2005**, *18*, 979–985, doi:10.1002/poc.941.

102.   Dekamin, M.G.; Azimoshan, M.; Ramezani, L. Chitosan: A highly efficient renewable and recoverable bio-polymer catalyst for the expeditious synthesis of α-amino nitriles and imines under mild conditions. *Green Chem.* **2013**, *15*, 811–820, doi:10.1039/c3gc36901c.

103.   Marin, L.; Ailincai, D.; Mares, M.; Paslaru, E.; Cristea, M.; Nica, V.; Simionescu, B.C. Imino-chitosan biopolymeric films. Obtaining, self-assembling, surface and antimicrobial properties. *Carbohydr. Polym.* **2015**, *117*, 762–770, doi:10.1016/j.carbpol.2014.10.050.

104.   Fadida, T.; Selilat-Weiss, A.; Poverenov, E. N-hexylimine-chitosan, a biodegradable and covalently stabilized source of volatile, antimicrobial hexanal. Next generation controlled-release system. *Food Hydrocoll.* **2015**, *48*, 213–219, doi:10.1016/j.foodhyd.2015.02.033.

105.   Antony, R.; Arun, T.; Manickam, S.T.D. A review on applications of chitosan-based Schiff bases. *Int. J. Biol. Macromol.* **2019**, *129*, 615–633, doi:10.1016/j.ijbiomac.2019.02.047.

106.   Xu, J.; Liu, Y.; Hsu, S. Hydrogels based on Schiff base linkages for biomedical applications. *Molecules* **2019**, *24*, 1–21.

107.   Bao, J.; Zhang, H.; Zhao, X.; Deng, J. Biomass polymeric microspheres containing aldehyde groups: Immobilizing and controlled-releasing amino acids as green metal corrosion inhibitor. *Chem. Eng. J.* **2018**, *341*, 146–156, doi:10.1016/j.cej.2018.02.047.

108.   Li, M.; Wang, H.; Chen, X.; Jin, S.; Chen, W.; Meng, Y.; Liu, Y.; Guo, Y.; Jiang, W.; Xu, X.; et al. Chemical grafting of antibiotics into multilayer films through Schiff base reaction for self-defensive response to bacterial infections.

*Chem. Eng. J.* **2020**, *382*, doi:10.1016/j.cej.2019.122973.

109. Neqal, M.; Fernandez, J.; Coma, V.; Gauthier, M.; Héroguez, V. pH-Triggered release of an antifungal agent from polyglycidol-based nanoparticles against fuel fungus *H. resinae*. *J. Colloid Interface Sci.* **2018**, *526*, 135–144, doi:10.1016/j.jcis.2018.03.106.

110. Shi, C.; Jash, A.; Lim, L.T. Activated release of hexanal and salicylaldehyde from imidazolidine precursors encapsulated in electrospun ethylcellulose-poly(ethylene oxide) fibers. *SN Appl. Sci.* **2021**, *3*, 1–13, doi:10.1007/s42452-021-04372-3.

111. Zhai, Y.; Zhou, X.; Zhang, Z.; Zhang, L.; Wang, D.; Wang, X.; Sun, W. Design, synthesis, and characterization of Schiff base bond-linked pH-responsive doxorubicin prodrug based on functionalized mPEG-PCL for targeted cancer therapy. *Polymers (Basel).* **2018**, *10*, doi:10.3390/polym10101127.

112. Tao, Y.; Liu, S.; Zhang, Y.; Chi, Z.; Xu, J. A pH-responsive polymer based on dynamic imine bonds as a drug delivery material with pseudo target release behavior. *Polym. Chem.* **2018**, *9*, 878–884, doi:10.1039/c7py02108a.

113. Park, W.; Park, S.J.; Shin, H.; Na, K. Acidic tumor pH-responsive nanophotomedicine for targeted photodynamic cancer therapy. *J. Nanomater.* **2016**, *2016*, doi:10.1155/2016/3739723.

114. Chen, H.; Zhao, R.; Hu, J.; Wei, Z.; Mcclements, D.J.; Liu, S.; Li, B.; Li, Y. One-step dynamic imine chemistry for preparation of chitosan-stabilized emulsions using a natural aldehyde: acid trigger mechanism and regulation and gastric delivery. *J. Agric. Food Chem.* **2020**, *68*, 5412–5425, doi:10.1021/acs.jafc.9b08301.

115. Chabbi, J.; Aqil, A.; Katir, N.; Vertruyen, B.; Jerôme, C.; Lahcini, M.; El Kadib, A. Aldehyde-conjugated chitosan-graphene oxide glucodynamers: Ternary cooperative assembly and controlled chemical release. *Carbohydr. Polym.* **2020**, *230*, doi:10.1016/j.carbpol.2019.115634.

116. Higueras, L.; López-Carballo, G.; Gavara, R.; Hernández-Muñoz, P. Reversible covalent immobilization of cinnamaldehyde on chitosan films via Schiff base formation and their application in active food packaging. *Food Bioprocess Technol.* **2015**, *8*, 526–538, doi:10.1007/s11947-014-1421-8.

117. Brockgreitens, J.; Abbas, A. Responsive food packaging: Recent progress and technological prospects. *Compr. Rev. Food Sci. Food Saf.* **2016**, *15*, 3–15, doi:10.1111/1541-4337.12174.

# 2. OBJETIVOS

El **objetivo principal** de esta Tesis Doctoral es desarrollar y caracterizar polímeros funcionales antimicrobianos basados en la inmovilización covalente reversible de compuestos activos naturales en películas de quitosano para su posterior aplicación en envases alimentarios, con el propósito de aumentar la seguridad y vida útil de alimentos postcosecha frescos y mínimamente procesados.

Para lograr este objetivo principal se plantearon los siguientes **objetivos específicos**:

1. Elección de compuestos volátiles y no volátiles de origen natural y estudio de su actividad antimicrobiana *in vitro* frente a patógenos y alterantes alimentarios.

2. Desarrollo de películas activas de quitosano con los compuestos activos que presentan mayor actividad antimicrobiana. Para ello, se inmovilizan aldehídos de origen natural sobre las películas preformadas de quitosano a través de la formación de enlaces imina o bases de Schiff.

3. Caracterización espectroscópica de las bases de Schiff y estudio de las propiedades funcionales más relevantes de las películas desarrolladas.

4. Evaluación del efecto del pH sobre la reversibilidad de las bases de Schiff.

5. Estudio *in vitro* de las propiedades antimicrobianas de las películas desarrolladas cuando son sometidas a diferentes pH.

6. Incorporación de las películas desarrolladas en el diseño de envases activos antimicrobianos y estudio de su efectividad en alimentos modelo.

# 3. JUSTIFICACIÓN Y ESQUEMA DE TESIS

El objetivo principal de esta Tesis ha sido explorar el uso de la química covalente reversible para desarrollar y caracterizar películas biopoliméricas con compuestos antimicrobianos anclados de forma reversible. Para ello, se seleccionó el quitosano, un biopolímero procedente de la revalorización de residuos de la industria del marisco, disponible, biodegradable y no tóxico cuya elevada presencia de grupos amino lo hace idóneo para ser modificado químicamente a través de la formación de un enlace imina o base de Schiff. La inmovilización de aldehídos de origen natural al quitosano mediante el enfoque de la química covalente reversible permite generar polímeros activos antimicrobianos que responden a estímulos externos, ya que estos enlaces pueden ser revertidos bajo condiciones específicas y liberar el compuesto anclado. Así, la naturaleza reversible del enlace permite controlar la liberación del compuesto anclado. El enlace puede ser hidrolizado por cambios en el pH del entorno, mientras que en ausencia de éstos permanecen estables. Las películas de quitosano con los aldehídos inmovilizados se aplicaron en el envasado activo de alimentos sólidos, liberándose al espacio de cabeza, y en alimentos líquidos, liberándose directamente al alimento, donde ejercieron su función.

El trabajo realizado para lograr este objetivo se presenta dividido en dos capítulos que corresponden al desarrollo y caracterización de los polímeros activos, y a la aplicación en alimentos, respectivamente.

## Capítulo I. Desarrollo de películas de quitosano que incorporan compuestos antimicrobianos mediante el anclaje covalente reversible

Este primer capítulo consta de tres artículos científicos. En el primer artículo "**Dynamic covalent chemistry of imines for the development of stimuli-responsive chitosan films as carriers of sustainable antifungal volatiles**" se han desarrollado películas antimicrobianas de quitosano a las que han anclado aldehídos de origen natural, mediante el uso de la química covalente reversible. Entre los diferentes tipos de enlaces reversibles, se ha empleado la formación de iminas o bases de Schiff para la inmovilización de volátiles

antimicrobianos a las películas de quitosano. Se ha estudiado el efecto de diferentes aldehídos en la formación del enlace imina incluyendo compuestos α,β-insaturados y sus análogos saturados, con estructuras aromáticas y lineales, siendo estos cinamaldehído, hidrocinamaldehído, citral y citronellal. Se ha caracterizado el enlace formado entre el grupo amino primario del quitosano y el aldehído mediante técnicas espectroscópicas y se ha calculado el porcentaje de aldehído incorporado a la matriz polimérica mediante análisis elemental. Adicionalmente, se han caracterizado las propiedades térmicas, ópticas y otras propiedades funcionales de las películas desarrolladas, como la sorción de agua.

Posteriormente, se ha evaluado la reversibilidad del enlace imina entre el grupo carbonilo de los aldehídos y el grupo amino del quitosano. Para ello, las películas activas se han puesto en contacto con soluciones acuosas de diferente pH, determinándose cambios en el porcentaje de aldehído retenido mediante análisis elemental y modificaciones en el espectro de infrarrojos de las películas. Finalmente, se ha evaluado el potencial antimicrobiano de las películas desarrolladas cuando son sometidas a diferentes pH contra dos hongos, *Penicillium expansum* y *Botrytis cinerea.*

En el siguiente artículo científico "**Chitosan films as responsive sustained release systems of naturally occurring antimicrobial compounds**", se ha continuado explorando el efecto de diferentes estructuras químicas en la modificación y reversibilidad de la base de Schiff sobre las películas de quitosano. Además, se ha profundizado en el estudio de la reversibilidad del enlace imina mediante cromatografía de gases. Para ello, se ha cuantificado el aldehído liberado al espacio de cabeza tras sumergir las películas en soluciones acuosas con diferente pH, evidenciando la susceptibilidad de este enlace por efecto del pH ácido.

En estos estudios se ha observado que los aldehídos α,β-insaturados, citral y cinamaldehído, actúan como entrecruzantes de la matriz polimérica. Se ha determinado que el pH de la reacción de Schiff entre estos aldehídos y las películas de quitosano resulta un factor clave para modular el entrecruzamiento de la película, permitiendo obtener materiales con diferentes propiedades. Esto se recoge en el artículo científico "**Dual functionality of citral and cinnamaldehyde as**

**crosslinking agents and active components of dynamic antifungal imine-chitosan films**". En este artículo, se ha explorado el efecto de entrecruzamiento de las películas de quitosano cuando son reaccionadas con los aldehídos α,β-insaturados, citral y cinamaldehído, modificando el pH de la reacción de Schiff (2, 5 y 7). El enlace imina ha sido caracterizado mediante técnicas espectroscópicas, y se han evaluado algunas propiedades funcionales de las películas obtenidas dependiendo del pH del medio en la síntesis de las bases de Schiff.

Finalmente, se ha analizado el efecto del entrecruzamiento en la reversibilidad del enlace imina. Para ello, se ha cuantificado la liberación del aldehído y su capacidad antifúngica cuando son sometidas a soluciones acuosas con diferentes pH.

## Capítulo II. Aplicación tecnológica de películas antimicrobianas que responden a estímulos externos en el envasado de alimentos

La propuesta de esta última parte se centra en la aplicación tecnológica de las películas antimicrobianas desarrolladas en el envasado activo de productos postcosecha y productos frescos mínimamente procesados. Este capítulo se ha dividido en dos partes, la primera parte se ha basado en la liberación del aldehído anclado reversiblemente al espacio de cabeza del envase, mientras que la segunda parte se ha orientado a su migración directa al alimento, donde ejerce su actividad antimicrobiana.

La primera parte del capítulo dedicada al envasado activo de productos poscosecha incluye dos artículos científicos. Para su desarrollo se ha diseñado un envase de doble fondo donde las películas de quitosano con el aldehído inmovilizado se separan del alimento, evitando el contacto directo entre ellos. La liberación del aldehído en el interior del envase se desencadena tras poner en contacto las películas activas con una solución acuosa ácida, la cual promueve la hidrólisis del enlace imina y por tanto la liberación del volátil. En el primer estudio "**Development of antifungal biopolymers based on dynamic imines as responsive release systems for the postharvest preservation of blackberry fruit**" se centra en el envasado de moras, un producto fresco altamente susceptible al crecimiento de hongos como *Penicillium* spp. o *Botrytis cinerea.* La liberación del aldehído al espacio de cabeza se desencadena por la adición de un activador, una

solución acuosa ácida añadida en el momento del envasado de la fruta. Un segundo estudio, se centra en el aprovechamiento del exudado de la piña fresca cortada para desencadenar la hidrólisis de la imina, y por tanto la liberación del agente activo al espacio de cabeza del envase durante el almacenamiento del producto, con el objetivo de alargar su tiempo de vida útil. Este estudio se recoge en el artículo "**Responsive packaging for extending the shelf-life of refrigerated fresh-cut pineapple**".

La segunda parte del capítulo, compuesta por el artículo "**pH modulates antibacterial activity of hydroxybenzaldehyde derivatives immobilized in chitosan films via reversible Schiff bases and their application to preserve freshly-squeezed juice**" está enfocada a su aplicación directa en un alimento líquido, el aldehído es liberado del enlace imina directamente en el producto. Para ello, se ha evaluado el potencial antimicrobiano de aldehídos aromáticos frente a *Escherichia coli* en medio líquido. Se ha comparado la inmovilización de distintos hidroxibenzaldehídos en la matriz de quitosano. Se seleccionaron aquellos compuestos activos que presentaron un mayor porcentaje de incorporación a las películas de quitosano y una mayor actividad antimicrobiana para determinar su liberación en simulantes alimentarios. Posteriormente, se evaluó su efectividad en un alimento real, aplicando las películas de quitosano modificadas en un zumo de frutas natural inoculado artificialmente con *Escherichia coli*.

# 4. CAPÍTULOS

# CAPÍTULO I.

# Desarrollo de películas de quitosano que incorporan compuestos antimicrobianos mediante el anclaje covalente reversible

## Artículo 1

**Dynamic covalent chemistry of imines for the development of stimuli-responsive chitosan films as carriers of sustainable antifungal volatiles**

## Artículo 2

**Chitosan films as pH-responsive sustained release systems of naturally occurring antifungal volatile compounds**

## Artículo 3

**Dual functionality of citral and cinnamaldehyde as crosslinking agents and active components of dynamic antifungal imine-chitosan films**

# Artículo 1

**Dynamic covalent chemistry of imines for the development of stimuli-responsive chitosan films as carriers of sustainable antifungal volatiles**

Raquel Heras-Mozos[a], Rebeca Hernández[b], Rafael Gavara[a], Pilar Hernández-Muñoz[a]

[a] Instituto de Agroquímica y Tecnología de Alimentos (IATA-CSIC), Av, Agustín Escardino, 7, 46980, Paterna, Valencia, Spain.

[b] Instituto de Ciencia y Tecnología de Polímeros (ICTP-CSIC), C/Juan de la Cierva, 3, 28006, Madrid, Spain.

*Food Hydrocolloids* (2022), 125, 107326

**ABSTRACT**

The aim of this work was to develop pH-responsive antifungal chitosan (CS) films based on the reversible bonding of the naturally occurring volatile aldehydes: cinnamaldehyde (CN), citral (CT) and their saturated derivatives hydrocinnamaldehyde (HC) and citronellal (CO) that have antifungal properties. Acid-catalysed bonds were created by condensation of the carbonyl functional group of aldehydes with amino groups in CS films to yield imines which was confirmed by Attenuated Total Reflectance – Fourier Transform Infrared Spectroscopy (ATR-FTIR) and $^{13}$C solid-state nuclear magnetic resonance ($^{13}$C-NMR).

α,β-unsaturated CN and CT were more reactive than their derivatives, reaching around 60% degree of substitution of aldehydes to chitosan films compared to 25% for HC and CO. Imines created with α,β-unsaturated aldehydes and aromatic HC remained quite stable at neutral pH. With regard to the hydrolysis of imines at pH 4, around 35% of anchored α,β-unsaturated aldehydes were lost, this value being 80% for HC whereas 100% of CO was lost after the first week of film immersion in buffered solution. The differences in the extent of hydrolysis of imine bonds depended on both the pH of the aqueous medium and also the chemical structure of the aldehyde.

Curiously, it was observed α,β-unsaturated aldehydes exerted crosslinking effects on CS films since they did not disintegrate in water at pH 3. The crosslinking mechanism is discussed in the text. The antifungal activities of the developed films were tested against *Penicillium expansum* and *Botrytis cinerea* by the micro-atmosphere method using a double Petri dish system. Mould growth was completely inhibited by CN-imine-CS films activated at pH 4.

**Keywords:** Reversible imines, pH, α,β-unsaturated aldehydes, chitosan, antifungal films.

## 1. Introduction

The use of polymers for the sustained release of antimicrobial molecules have a huge range of technological applications, being textile, agrochemical, pharmaceutical and food packaging industries high demanding areas of these materials. Commonly, these kind of antimicrobial polymers are based on monolithic delivery systems where the active molecule is uniformly distributed in the carrier. In these systems the release mechanism relies on the diffusion of the active through the polymer matrix to reach the surface of the device and its delivery to the surrounding media. These diffusion-controlling devices can have certain drawbacks such as fast release of the active molecule to the media which is not appropriate for many applications. Moreover, crystallization of the active on the surface of the device due to lack of compatibility with the polymer and the solvent when it is prepared in liquid media, or phase separation could alter the release increasing burst effect when is not desirable [1] the effect of molecular weight of the active on the diffusion is other aspect to be considered [2].

Stimuli-responsive supramolecular assemblies based on polymers are a revealing alternative to conventional diffusion-controlled polymer systems for the delivery of actives. The distinctive characteristic of these structures is that they are sensitive to changes in the environment which trigger the breakage of molecular associations. Therefore, physical and/or chemical modifications in the structure, and as a consequence, the release of the active molecule via one or more different mechanisms depends on the polymer chemical structure and its assembly (liposomes, micelles and others) and if they are forming or integrated in a gel, particle or film [1].

The use of dynamic covalent chemistry (DCvC) in the field of the delivery of bioactives is relatively new. Reversible covalent bonds allow the design of adaptive and dynamic self-assembled supramolecular structures employing more stable and robust bonds than non-covalent interactions. These structures have the capability of falling apart in response to physico-chemical changes in the medium which provokes the reversibility of the covalent bond and the release of the bioactive [3–5]. Reversible covalent bonds are also being employed in polymeric conjugates to deliver bioactive molecules, in that the active molecule is covalently attached to the polymer, thus, its release

is chemically controlled. This technique does not present some of the drawbacks of monolithic systems, allowing a high load and enhanced solubilisation of the active, higher stability in the formulation, and greater control on the release [6].

Depending on the nature of the covalent bond, one or several external stimuli triggers the cleavage of the bond restoring the activity of the bioactive. Biodegradable or hydrolysable bonds have commonly been used for the link of the bioactive to the polymer chain. Currently, the use of dynamic covalent chemistry in the delivery of actives has introduced new ways of linking the molecule to the polymer via formation of reversible covalent bonds including condensation and addition reactions, disulphide exchange reactions, and boronic ester chemistry [7–9].

Polymeric conjugates that employ smart linkers based on dynamic covalent bonds are being mostly explored with therapeutic purposes [10–14]. However, in other areas such as agrochemistry little work has been done until now [15,16] and it is even unexplored in active food packaging, hence, these areas should be benefited of DCvC. The rationale for employing DCvC is to create smart controlled release formulations more effective and sustainable than the currently used. Within this context, the employment of biodegradable polymers from renewable sources for the design of smart conjugates based on reversible covalent bonds that are sensitive to light, humidity, temperature, enzyme activity, pH is very attractive and of great potential for the development of novel sustained release systems with improved specific targeting [17,18].

In this framework, the objective of the present work has been the application of the concept "dynamic covalent chemistry" for the design of smart molecule-polymer conjugates to be employed as films for responsive antifungal food packaging. For that, chitosan in the form of film was used as a static skeleton and dynamic chain substituents were created using the primary amino groups for the linking of naturally occurring aldehydes with probed antifungal properties via the synthesis of Schiff bases and thus, the replacement of primary amino groups of chitosan by imine bonds. The aldehydes anchored were, an acyclic α,β-unsaturated aldehyde, citral (CT, 3,7-dimethyl-2,6-octadienal), the derivative citronellal (CO, 3,7-Dimethyl-6-octenal), and an aromatic

α,β-unsaturated aldehyde, cinnamaldehyde (CN, 3-phenyl-2-propenal) and the derivative hydrocinnamaldehyde (HC, 3-phenylpropanal). All of them are approved for use in food-related applications. Schiff bases synthesized from chitosan films and bioactive aldehydes were characterized. Moreover, the antifungal activity of the films developed which was triggered by the acidic hydrolysis of the formed imine bond and consequent release of the grafted volatile aldehyde was studied *in vitro.* Common food spoilage fungi *Penicillium expansum* and *Botrytis cinerea* were chosen for the antifungal assay. The effect of the pH on the hydrolysis of the imine bond and antifungal activity of the film was also studied.

## 2. Materials and methods

### 2.1. Materials

Low molecular weight chitosan with a degree of deacetylation of 75-85%, phosphorus pentoxide, citral (CT), citronellal (CO), cinnamaldehyde (CN), hydrocinnamaldehyde (HC) and acetic acid glacial were supplied by Sigma-Aldrich (Barcelona-Spain). Sodium hydroxide, hydrochloric acid 37% and ethanol 96% (v/v) were purchased from Scharlab (Barcelona, Spain). Buffer medium pH 3, pH 4 and pH 7 were prepared with citric acid and disodium phosphate supplied by Sigma-Aldrich (Barcelona-Spain). *Penicillium expansum* and *Botrytis cinerea* were supplied by the Spanish Type Culture Collection (CECT 2278, CECT 2100). Milli-Q water was obtained from Milli-Q Plus purification system (Millipore, Molsheim, France).

### 2.2. Synthesis of imine-chitosan films

#### 2.2.1. Preparation of chitosan films

A chitosan solution was prepared dissolving 1.5 g of chitosan in 100 ml of 0.5% (v/v) acetic acid aqueous solution under stirring for 1 hour at 50 °C, after that, it was filtered with a cheesecloth to eliminate impurities. Then, the chitosan solution was film casted on polystyrene plates and dried at 37 °C for 24 h and 30-40% relative humidity. Chitosan films were peeled from the trays, and the resulting average thickness was of $35 \pm 5$ μm which was measured with a digital Mitutoyo micrometer (Metrotec, San Sebastian, Spain). Then, they were cut into 2 x 2 cm samples and neutralized with 0.1 M sodium hydroxide for 24

h. After neutralization, the films were washed with distilled water and dried at 37 °C. The dry chitosan films (CS) were stored in glass desiccators until usage.

### 2.2.2. *Schiff Base formation between aldehydes and CS films*

Citral (CT), citronellal (CO), cinnamaldehyde (CN) and hydrocinnamaldehyde (HC) were covalently linked to neutralized chitosan film through Schiff base formation at the solid/liquid interface via solvent method using ethanol 96% (v/v) as the reaction medium. Each aldehyde was added in a 2:1 (CS film:CHO aldehyde) weight ratio. Neutralized chitosan films were immersed in an Erlenmeyer containing 75 ml ethanol 96% (v/v) and 4 g of the solubilized aldehyde and then it was placed in a shaking bath at 60 °C for 24 h. After that time, the films were washed to remove the excess of aldehyde which was no anchored to the film by immersing and shaking them three times in ethanol 96% *(*v/v*)* for 24 h at 60 °C. Thus, imine-chitosan films were obtained with citral (CSCT), citronellal (CSCO), cinnamaldehyde (CSCN) and hydrocinnamaldehyde (CSHC). Finally, reacted chitosan films were dried and stored in a glass desiccator with $P_2O_5$ prior use.

## 2.3. Spectroscopic characterization of Schiff base formation between aldehydes and chitosan films

Formation of carbon–nitrogen double bond (C=N) between primary amino groups of 2-amino-2-deoxy-d-glucopyranose (*GlcN*) units of chitosan and aldehydes was evaluated by Attenuated Total Reflectance – Fourier Transform Infrared Spectroscopy (ATR-FTIR) and solid state nuclear magnetic resonance ($^{13}$C NMR). The degree of substitution (DS, %) of aldehydes to chitosan was quantified by elemental analysis.

### 2.3.1. *ATR-FTIR*

Formation of the IR band of imine group in neutralized chitosan films was recorded with a Bruker Tensor 27 FTIR spectrometer (Bruker Española S.A., Barcelona, Spain). Spectrum was obtained by accumulation of at least 32 scans per test with a resolution of 4 cm$^{-1}$ in the range of 4.000 to 600 cm$^{-1}$. Results were analysed in triplicate and treated with the OPUS v. 5.0 software.

### 2.3.2. Solid state nuclear magnetic resonance NMR

A ^{13}C NMR spectrometer Brucker DSX 400 spectrometer operating at resonance frequencies of 399.53 and 100.47 MHz for ^{1}H and ^{13}C, respectively was employed for the acquisition of solid state ^{13}C NMR spectra. The ^{13}C CP/MAS spectra were measured with a 3.9-s 90° pulse, a 3-s pulse delay time, an acquisition time of 30 ms, and 2000 scans. All NMR spectra were taken at 300 K with the use of broadband proton decoupling and a normal cross-polarization pulse sequence. An MAS rate of 7.0 kHz was used to eliminate resonance broadening due to the anisotropy of chemical shift tensors.

### 2.4. Quantification of aldehydes attached to the films by elemental analysis

Elemental analysis (EA) of the films was obtained with a FlashSmart elemental analyser (Thermo Fisher Scientific, Waltham, MA, USA). The degree of substitution (DS, %) of aldehydes to chitosan was calculated by determining the C/N ratio of control and modified films [19]. Elemental composition also was used to estimate the degree of acetylation (DA, %) of neutralized chitosan films according to a previous reported methodology [20]. Samples were analysed in triplicate.

### 2.5. Stability of synthetized Schiff bases at different pH

Hydrolysis of the imine bond formed between primary amino groups of chitosan films and each aldehyde was evaluated at neutral and acid pH. For this purpose, imine-chitosan films were placed in glass vials containing buffer solutions at pH 7 and 4 for 7 days at 23 °C. To study the reversibility of the imine bond, the films were analysed ATR-FTIR and elemental analysis as described in previous section.

### 2.6. Thermogravimetric analysis (TGA) of imine-chitosan films

Thermogravimetric analysis of the films was carried out with a thermal analyser TGA Q5000 v.3.17 (TA Instruments, USA). Control and modified films were placed in a volatile pan. And submitted to the operating conditions of a maximum temperature of 500 °C and a heating rate of 10 °C/min. Thermograms of films were analysed with TA Instruments Universal Analysis 2000 v4.5A software.

## 2.7. Functional properties of imine-chitosan films

### 2.7.1. Optical properties

The apparent opacity of the films was determined as the area under the absorption curve (Au × nm) in the UV-visible wavelengths (190-800 nm), the spectra were recorded with an Agilent 8453 UV-visible spectrophotometer (Agilent, Barcelona, Spain). The colour coordinates of the films were measured with a CR-300 Minolta Chroma meter® (Minolta Camera Co. Ltd., Osaka, Japan). Films were placed on a white plate and the results expressed in accordance with the CIELAB colour space with reference to illuminant D65 and a visual angle of 10, being L* the lightness, C* the chroma or saturation index and h° the hue angle.

### 2.7.2. Water uptake

The water uptake or swelling of the films was evaluated by immersing the pre-weighted dry films in aqueous solution buffered at several pH (3, 4 and 7) at 23 °C. At predefined time intervals, films were removed from water, wiped off with a paper towel and immediately weighed (wet weight, $w_w$), then, films were dried to constant weight ($w_d$). This action was repeated on time until constant weight. The percentage of water uptake ($\Delta W$) was obtained with the equation:

$$\Delta W \ (\%) = \frac{w_w - w_d}{w_d} \cdot 100$$

## 2.8. Microbiological studies

The *in vitro* antifungal properties of the modified films against *P. expansum* and *B. cinerea* was evaluated at pH 7 and 4. First, the antifungal properties of the aldehydes used to synthetize Schiff bases was evaluated.

### 2.8.1. Antifungal activity of aldehydes employed for the formation of Schiff Bases

The effectiveness of aldehydes (CT, CO, CN and HC) was carried out by determining the minimum inhibitory concentration (MIC) and minimum fungicidal concentration (MFC) against *P. expansum* and *B. cinerea*. For that, the MIC was considered as the smallest volume of

active compound that causes at least a 50% fungal growth reduction at 7 days of incubation respect to control sample. The MFC was defined as the smallest volume of active agent that produced a complete inhibition of fungal growth after 10 days of incubation. MIC and MFC were expressed as volume (µL) of active compound per $cm^3$ of air in the plate above the agar culture medium, according with previous studies [21–23].

The fungal strains were grown on potato dextrose agar (PDA) at 26 °C for 7 days. Conidial suspension was collected by addition of sterile peptone water with Tween 80 (0.05% v/v) and then scraping the surface with a digralsky handle. One mL of conidial suspension was transferred to sterile tube and serial dilutions were made until to obtain $10^6$ spores/mL. The Neubauer improved method (Bright-Line Hematocytometer Hausser Scientific, Horshan PA) was used to determinate spore concentration.

Antifungal assay was taken place in Petri dishes (90 mm) containing with 15 mL of PDA (potato dextrose agar) which were inoculated at three equidistant points with 3 µL of the fungal suspension. Subsequently, volumes of 1, 2.5, 5, 7.5 and 10 µL of each aldehyde were added on 50 mm of sterile paper disk and placed on the lid of Petri plate and sealed with Parafilm ®. Finally, to obtain the volume of active necessary to reach the MIC and MFC was adjusted increasing or decreasing 0.5 µL of each aldehyde.

Control without aldehyde was also prepared. All the plates were incubated at 26 °C for 10 days and the antifungal effect was evaluated over time by measuring the diameter of colony. The experiments were carried out in triplicate.

### 2.8.2. Antifungal response of imine-chitosan films
The antifungal response of the modified films was tested at neutral and acid pH against *P. expansum* and *B. cinerea*. In order to promote the release of the aldehydes in the Petri plate headspace, a double plate system was developed (**Figure 1**). For that, 0.3 g of each film were placed in an empty Petri dish having a diameter of 90 mm and 15 mm of height, together with a Petri dish of 58 mm of diameter and a height of 10 mm with PDA medium inoculated with 3 µL of the fungal suspension containing $10^6$ spores/mL without lid. After that, around 10

mL of pH 7 or pH 4 buffered solution were poured on films. Then, the lid of 90 mm Petri dish was placed and sealed with Parafilm®. Control samples with neutralized chitosan films and without film were also prepared. The plates were incubated at 26 °C for 10 days and fungal growth was monitored by measuring the fungal colony diameter at 3, 5, 7 and 10 days and the growth inhibition percentage was calculated. The experiments were carried out in triplicate.
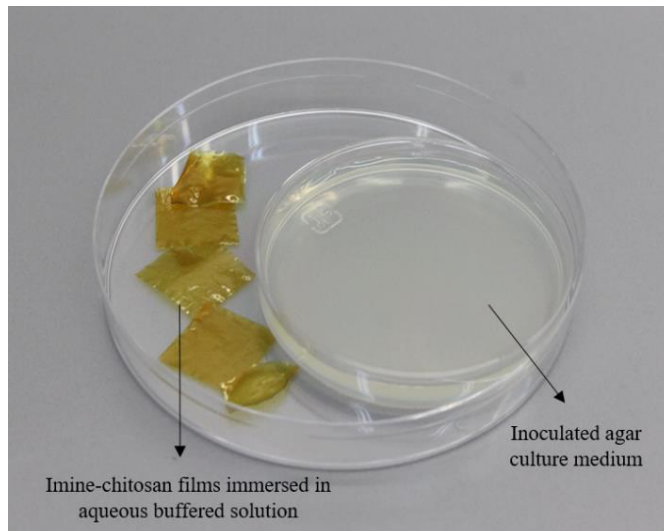


**Figure 1.** Double Petri dish system to test antifungal activity of imine-chitosan films.

*2.9. Statistical analysis*

All the tests were conducted at least in triplicate and represented as the average ± standard deviation. Statistical analysis of the results was performed with SPSS® computer program, v.24 (SPSS commercial software, SPSS Inc., Chicago, IL). Results were analysed applying a one-way analysis of variance (ANOVA). Means were separated using the Tukey *b* test with a level of significance of $P \leq 0.05$.

## 3. Results and discussion

*3.1. Spectroscopic characterization of Schiff base formation between aldehydes and chitosan films*

Neutralized CS films were modified through formation of Schiff bases with naturally occurring aldehydes. Schematic chemical reaction to form imine bond is represented in **Figure 2**. ATR-FTIR was used to examine the formation of imine bonds (C=N) produced by the nucleophilic addition of aldehydes to primary amino groups of 2-amino-2-deoxy-d-glucopyranose (*GlcN*) units of chitosan in the form of film.
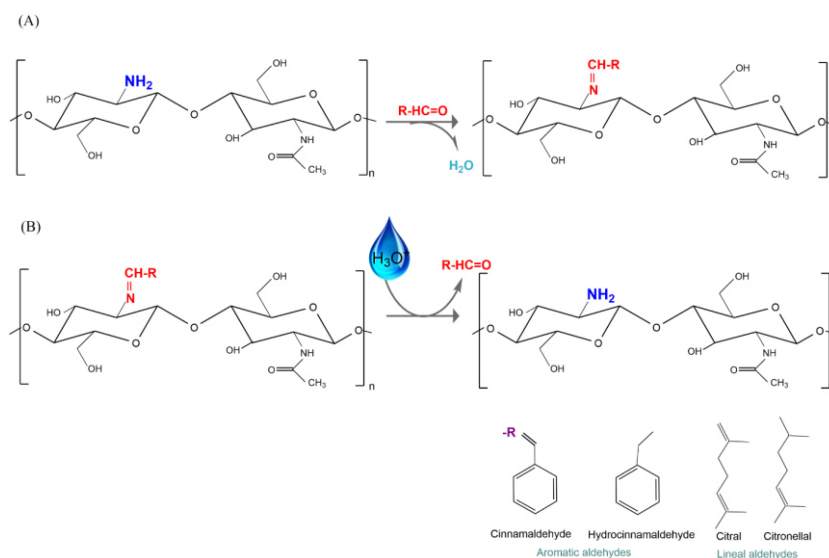


**Figure 2.** Schemes showing A) formation of imine bond through acid-catalysed condensation of carbonyl from aldehyde and primary amine group of chitosan, and B) acid-catalysed hydrolysis of imine bond and subsequent release of aldehyde.

The IR spectra of neutralized chitosan films and imine-chitosan films are represented in **Figure 3A** (aromatic aldehydes) and **3B** (lineal aldehydes). The spectrum of chitosan (CS) shows two characteristic bands of partially deacetylated chitosan, one appears at 1648 cm$^{-1}$ and it is assigned to the C=O stretching of amide I, whereas the N-H bending of the primary amine appears at 1589 cm$^{-1}$ (amide II) [24]. In films reacted with aldehydes, a strong absorption band appears between

1631 and 1659 cm$^{-1}$ depending on the aldehyde, and it is attributed to the C=N stretching of imines or Schiff base [25]. Moreover, the absorption band corresponding to –NH$_2$ suffered a considerable intensity decrease after formation of the imine, which indicates that aldehydes reacted with primary amino groups of chitosan.

It is important to note that no evidence of absorption bands attributed to C=O stretching bands of free aldehydes located at 1740-1720 cm$^{-1}$ for saturated aliphatic aldehydes, and at 1710-1685 cm$^{-1}$ for unsaturated aldehydes were observed for any of the modified chitosan films. This indicates that the washing steps carried out after reaction of the chitosan with aldehydes are effective to eliminate unreacted molecules. In reacted films with cinnamaldehyde (CSCN) and hydrocinnamaldehyde (CSHC) it can be clearly observed the presence of two bands between 690 and 750 cm$^{-1}$ attributed to the C-H stretching of the aromatic aldehydes.

The absorption band attributed to C=N vibration depends largely on the aldehyde employed to form the Schiff base with chitosan [26]. When lineal aldehydes were employed, the C=N vibration has been reported to appear at a higher wavenumber compared to that corresponding to the reaction with aromatic aldehydes [27]. Imine band at 1633 cm$^{-1}$ and 1638 cm$^{-1}$ has been reported in literature when chitosan Schiff base was synthesized with cinnamaldehyde [28,29]. In the present work, imine band appeared at 1632 cm$^{-1}$ for CSCN, and at 1634 cm$^{-1}$ for CSHC. Schiff bases formed from citral (CSCT) and citronellal (CSCO) showed peaks at wavenumbers higher than that for aromatic aldehydes, that is, at 1640 cm$^{-1}$ and 1659 cm$^{-1}$, respectively. The imine absorption band corresponding to imine formation because of reaction between CT and chitosan has been reported at 1648 cm$^{-1}$ [30].
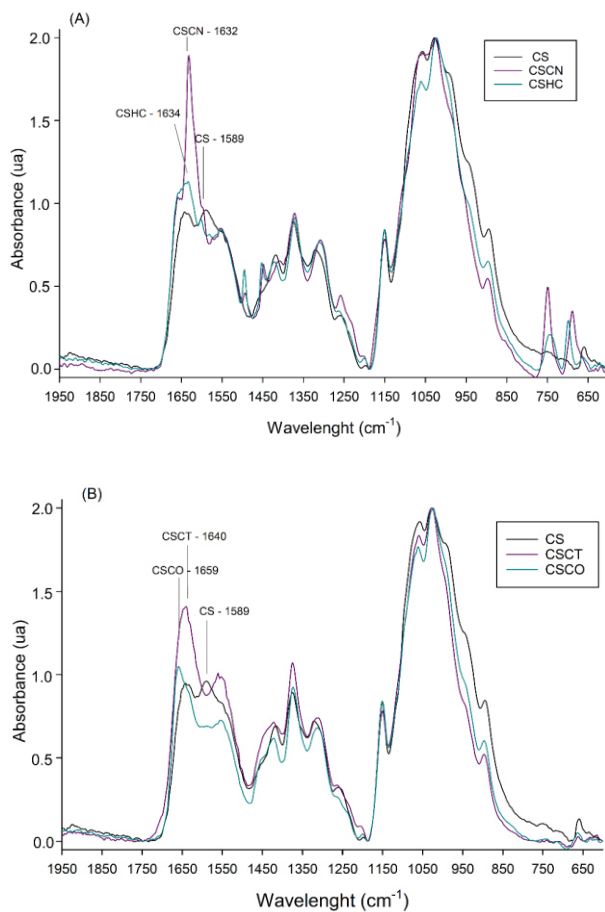
**Figure 3.** ATR-FTIR spectra of chitosan and imine-chitosan films after attaching cinnamaldehyde (CSCN) and hydrocinnamaldehyde (CSHC) (A) and citral (CSCT) and citronellal (CSCO) (B).

3.2. *Quantification of aldehydes attached to chitosan films*

The amount of aldehyde attached to chitosan films was given as the degree of substitution (in percentage) of free amino groups of chitosan film by using the C/N relationships described in experimental section. Previously, the deacetylation degree of neutralized CS films was evaluated, being around 79.9% and in accordance with the value given by the commercial supplier. **Table 1** shows substitution degree of imine-chitosan films and after being subjected at hydrolysis step. That high value implies a large amount of free primary amino groups susceptible to conversion into imines. The DS varied with the aldehyde grafted, CSCT and CSCN presented a high degree of substitution, 65.8 ± 1.2 and 73.3 ± 1.4, respectively; similar values were observed in cinnamaldehyde [28] and citral [31]. However, the DS when employed saturated analogous aldehydes was much lower, 27.3 ± 0.6 and 34.1 ± 0.1 for CSCO and CSHC, respectively. It was also noticeable that the DS was slightly higher for saturated or unsaturated aldehydes wearing benzene ring, that is, for HC compared to CO, and for CN compared to CT.

The conversion degree of primary amino groups into imines is associated to several parameters, among them, the reactivity of the aldehyde which is closely related to its chemical structure. Based on computational and experimental approaches, the reactivity of several aldehydes has been predicted according to the electrophilicity index which combines chemical hardness and chemical potential parameters, reporting cinnamaldehyde being more reactive than citral [32], which is in accordance with the results.

**Table 1.** Substitution degree (%) of imine-chitosan films before and after immersion in buffered aqueous medium at pH 7 and 4 at 23 °C for 1, 7 and 14 days.

| Films | DS (%) | $DS_{pH\ 7}$ (%) | | | $DS_{pH\ 4}$ (%) | | |
|---|---|---|---|---|---|---|---|
| | | Day 1 | Day 7 | Day 14 | Day 1 | Day 7 | Day 14 |
| CSCT | $57.1 \pm 1.1^{cD}$ | $52.3 \pm 1.0^{cC}$ | $50.9 \pm 0.7^{cC}$ | $46.3 \pm 1.57^{cB}$ | $37.1 \pm 0.8^{cA}$ | $37.4 \pm 1.4^{bA}$ | $38.5 \pm 2.0^{bA}$ |
| CSCO | $23.7 \pm 0.5^{aD}$ | $15.5 \pm 0.8^{aC}$ | $9.8 \pm 1.3^{aB}$ | $11.1 \pm 0.5^{aB}$ | $1.5 \pm 0.6^{aA}$ | - | - |
| CSCN | $63.6 \pm 1.2^{dE}$ | $61.3 \pm 1.0^{dDE}$ | $59.6 \pm 0.7^{dD}$ | $62.3 \pm 1.9^{dDE}$ | $43.0 \pm 1.5^{dC}$ | $36.5 \pm 1.2^{bA}$ | $40.3 \pm 0.7^{bB}$ |
| CSHC | $29.6 \pm 0.1^{bD}$ | $27.1 \pm 0.2^{bCD}$ | $24.5 \pm 0.2^{bC}$ | $25.8 \pm 2.8^{bC}$ | $14.7 \pm 0.9^{bB}$ | $8.2 \pm 1.0^{aA}$ | $6.2 \pm 0.5^{aA}$ |

Different superscript letters in the same row[(A-E)] and column[(a-d)] indicate a statistically significant difference (P≤ 0.05).

Since α,β-unsaturated aldehydes can undergo nucleophilic direct 1,2-addition reaction at the carbonyl carbon atom, or 1,4-addition at the β-carbon atom also called Michael addition, there is a competition between both nucleophilic additions that depends on diverse variables. Thus, α,β-unsaturated CN and CT are susceptible of imine formation and Michael addition of primary amino groups of chitosan [33]. In fact, CN has previously been reported as a bifunctional reactive molecule capable of reacting forming a Schiff base and a Michael adduct [34].

**Figure 4** shows a schematic representation of the possible reactions of CN and CT with chitosan through condensation of carbonyls with pendant amino groups and formation of imines or Schiff bases (I) and the conjugated addition of chitosan amino groups to ethylenic double bonds of aldehydes and formation of Michael adducts (II). In excess of amino groups, a mixed product can be found (III) as previously reported for glutaraldehyde reacting with primary amino groups of proteins [35]. Pendant aldehyde groups of structure II could condensate in aldols (IV). Besides Schiff base formation between aldehydes and chitosan, the possibility of Michael addition of amino groups of chitosan to ethylenic double bond of α,β-unsaturated aldehydes could explain the greater DS of primary amino groups of chitosan found when is treated with CN and CT compared with HC and CO, respectively.

In order to shed further light on the mechanism of reaction between the α,β-unsaturated CN and CT and chitosan, solid-state $^{13}$C NMR CP-MAS spectra were carried out for samples CSCN and CSCT, and the results are shown in **Figure 5**. $^{13}$C NMR spectra of neutralized chitosan films is added for comparison. According with the results of other authors [36], **Figure 5a** shows the resonance peaks corresponding to the *D*-glucosamine units of chitosan are located at 174 ppm (C=O), 105 ppm (C1), 82 ppm (C4), 75 ppm (C5, C3), 61(C6), 58.0 (C2) and 23 ppm (CH$_3$). **Figure 5b** depicts the solid-state $^{13}$C NMR CP-MAS spectrum corresponding to sample CSCN which showed the peaks for C=C and benzene ring at 120.0-140.0 ppm; the imine (C=N) signal appeared at 145 ppm which confirmed the formation of a Schiff base through reaction of the aldehyde group of the CN and the chitosan amine group as previously described [37].
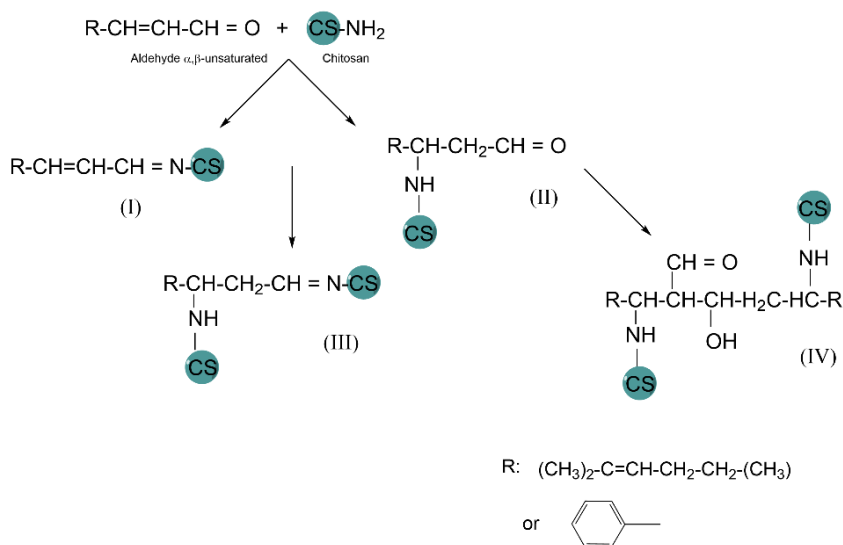
**Figure 4**. Schematic representation of possible reactions of α,β-unsaturated aldehydes cinnamaldehyde and citral with primary amino groups of chitosan.

The solid-state $^{13}$C NMR CP-MAS spectrum of CSCT films in **Figure 5c** showed the appearance of new bands in the region 20-40 ppm attributed to the hydrocarbon chain of CT; the peaks in the region at 120.0-140.0 ppm corresponds to the double linked carbon atoms of CT; moreover, a small intensity signal located at 155 ppm can be assigned to the imine bond (C=N).

For spectra corresponding to chitosan modified films, the decrease of intensity of the resonance peak located at 58 ppm assigned to the amine group linked to C2 in chitosan further confirmed the successful grafting of CT and CN to the chitosan backbone. Interestingly, imine-chitosan samples show the appearance of a resonance band at 165 ppm that could be ascribed to non-reacted carbonyl carbons from CN and CT. These results suggest that in the case of CT and CN, part of the molecules react with chitosan to yield Michael adducts. It is hypothesized that aldehyde groups can further react with other amino groups in neighbouring chitosan segments or between them forming aldols and giving rise to crosslinking points [35,38].
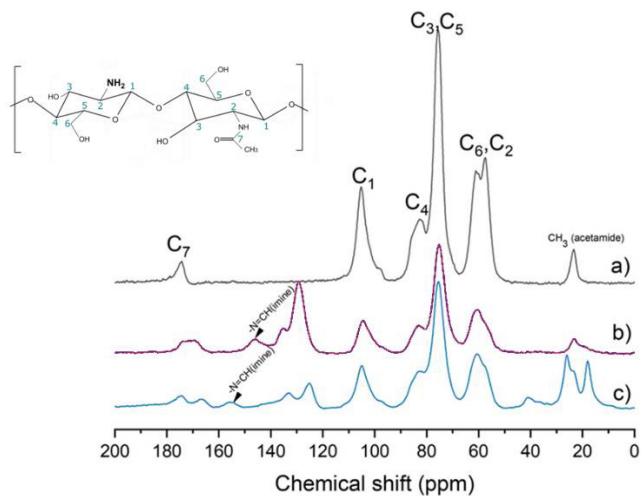
**Figure 5.** Solid state $^{13}$C NMR spectra corresponding to a) chitosan, and imine-chitosan films grafted with b) cinnamaldehyde and c) citral.

### 3.3. Stability of synthetized Schiff bases in aqueous media at different pH

The stability of the imine bonds formed between chitosan film and citral (CSCT), cinnamaldehyde (CSCN) and their saturated homologues, citronellal (CSCO) and hydrocinnamaldehyde (CSHC) was evaluated by placing the modified films in aqueous buffered solution at pH 7, and 4 at 23 °C for two weeks. ATR-FTIR and elemental analysis were again employed, this time to study the stability of the imine bond.

**Figures 6A and 6B** show the ATR-FTIR spectra of CSHC and CSCN, respectively, before and after contact with water at neutral and acidic pH for two weeks. The absorption band corresponding to the imine bond obtained by condensation of primary amino groups of chitosan with HC suffered a slight decrease after immersion of the imine-chitosan films into buffered aqueous solution at pH 7. Moreover, after water treatment, and regarding the spectrum of CSHC films, the intensity of the bands characteristic of the aromatic ring of HC which appeared at 745 cm$^{-1}$ and 698 cm$^{-1}$ experienced a decrease.

However, when films were exposed at pH 4 the spectra of chitosan films modified with saturated aldehydes suffered considerable modifications, the imine absorption band practically disappeared, and a new band appears at 1562 cm$^{-1}$ as can be seen in **Figure 6**, which corresponds to the protonated amino group of chitosan [24].
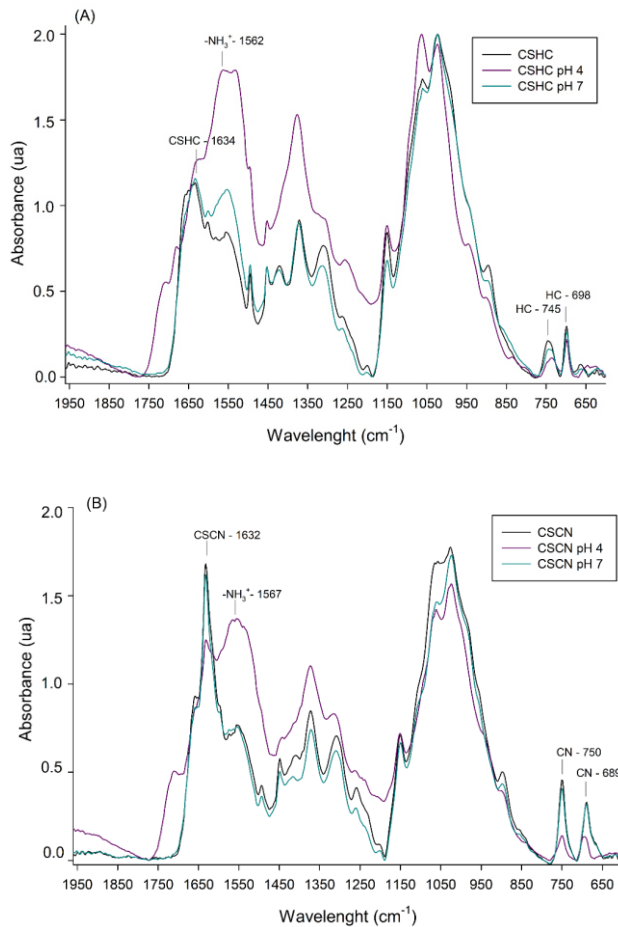


**Figure 6.** ATR-FTIR spectra of (A) imine-chitosan films grafted with hydrocinnamaldehyde (HC) and (B) cinnamaldehyde (CN), before and after treatment at pH 4 and 7 at 23 °C for one week.

The hydrolysis of imine bonds in imine-chitosan films and consequently the release of the aldehyde covalently linked was monitored by elemental analysis determining C/N ratio of films immersed in neutral and acidic aqueous buffered solution at 23 °C for two weeks at days 1, 7, and 14. The results given as percentage of degree of substitution (% DS) are displayed in **Table 1**. A decrease in % DS reflects the hydrolysis of imine bond and release of the aldehyde attached to the film. It is noticeable that the stability of the synthetized Schiff bases depended on the pH of the aqueous solution. Moreover, the extent of the hydrolysis of the imine bond also depended on the aldehyde used for the synthesis. Hydrolysis of imines synthetized with saturated aldehydes HC and CO have different behaviour at pH 7; whereas hydrolysis of imine bonds created with HC achieved 13%, this value increased to 47% for imines synthetized with CO. Related to grafted $\alpha,\beta$-unsaturated aldehydes CN and CT, the imine bond remained quite stable after two weeks of immersion in buffered solution at pH 7, and only 19% of CT was hydrolysed whereas imine bonds created with CN remained stable. Schiff bases created from $\alpha,\beta$-unsaturated aldehydes are more stable to hydrolysis due to the resonance stabilization through conjugation with the $\alpha, \beta$-carbon-carbon double bond. The results point to imines formed from aromatic aldehydes CN and HC remain more stable at neutral pH than those obtained from CT and CO, respectively. Hydrolysis of imine bond in films immersed in buffered solution at pH 4 increased considerably; almost complete released of CO was observed after 24 h as depicted in **Table 1**, whereas HC was liberated gradually until reaching a DS of 6% after two weeks. With regard to imine bond formed with $\alpha,\beta$-unsaturated aldehydes, the extent of the hydrolysis reached around 35% for CT and CN. Therefore, the results obtained by elemental analysis are in accordance with the ATR-FTIR observations. As discussed above, CN and CT are heterobifunctional molecules and together with Schiff base formation through amine-carbonyl condensation reaction, they are susceptible to Michael addition of primary amino groups of chitosan to the carbon-carbon double bond of the aldehyde. This fact would explain the lower variation in DS obtained for $\alpha,\beta$-unsaturated aldehydes after immersion in acid pH compared with saturated homologues.

The current results are in line with studies reported in the bibliography regarding how the hydrolysis of the imine bond is affected by the environmental pH, and the chemical structure of the amine and the aldehyde. Thus, studies carried out on the hydrolysis of imine bonds formed from alkylated sodium alginate and gentamicin sulphate have reported much faster release at pH 5.5 than at pH 7.4 [39]. In this line, the hydrolysis of imine bond and release of biocide dodecylamine from functionalized polynorbornene-g-polyglycidol particles has been studied [40], the authors reported no release of the biocide at pH 7 whereas the extent of the release was determined to be 26 and 41% at pH 6 and 5, respectively, after 24 h. Bao et al. [41] studied the hydrolysis of imines from polymeric microspheres containing aldehyde groups and amino acids inhibitors of corrosion and found that under acidic conditions (pH 1.5-5) almost all the amount of amines were released, whereas at pH 7 only 30% was liberated and at pH $\geq$ 9, imine bonds remained stable. pH-sensitive aryl imine derivatives were synthetized with differing aromatic substituents and substitution patterns and then, the derivatives were imine-linked at the C3 of a N-substituted isatin cytotoxin [42], for all the derivatives, the imine bond was stable at physiological pH and was readily cleaved at pH 4.5, the rate of hydrolysis of the imine moiety depended on the aromatic substituent and substitution pattern. The hydrolysis of Schiff bases formed from pyridoxal-5'-phosphate and different amino acids and amines has been studied [43], concluding that the absence of ionic groups in the surroundings of imine bond can increase the stability of the Schiff base, the authors also found that the type of amino acid residue also affected the hydrolysis constant, Schiff base with bulky nonpolar groups as in leucine and isoleucine are more stable than when the substituents are just hydrogen as in glycine.

The pH-dependent imine grafting of aminated drugs to functionalized polymers with aromatic aldehydes has also been reported [44–46].

*3.4. Functional properties of imine-chitosan films*

The effect of covalently attaching aldehydes to chitosan films was studied on some functional properties of them which are relevant for the final application of the created carriers, such as their appearance and swelling behaviour at different pH.

*3.3.1. Optical properties of imine-chitosan films*

Untreated chitosan films were transparent and homogeneous to the naked eye, whereas films treated with α, β-unsaturated aldehydes, cinnamaldehyde (CSCN) and citral (CSCT), developed yellow-orange colour compared to the control, and those films modified with hydrocinnamaldehyde (CSHC) and citronellal (CSCO) had similar appearance to the control. **Table 2** shows the colour parameters: lightness, hue and Chroma of control films and those treated with aldehydes. Control films possessed high lightness indicating great transparency, lightly pale yellow according with the hue, and very low chromaticity. Films reacted with saturated aldehydes hydrocinnamaldehyde and citronellal did not change their colour coordinates considerably which corroborates the visual inspection. Schiff base formed with α,β-unsaturated aldehydes cinnamaldehyde and citral imparted to the films a saturated orange-yellow colour as shown by their Chroma (80.4 and 69.7, respectively, vs 7.6 of CS film) and hue (89.2° and 84°, respectively vs 102.7° of CS film). Although for most of the time a yellow/pale-yellow colour is indicative of Schiff base formation, colour development depends on the nature of the amine and carbonyl group, as it is observed in the present study.

Previous studies have reported coloured Schiff base for chitosan films and hydrogels with citral, cinnamaldehyde, vanillin and salicylaldehyde but not for benzaldehyde [26,28,30]. The Schiff bases formed with CN and CT possesses a conjugated imine and olefin chromophores contributing to the colour development of the films. The apparent opacity of the resulting films also was calculated from the UV-Visible spectra and data are displayed in **Table 2**. Films of chitosan were transparent and absorbed light in the UV region more than in the visible (VIS) region (226.6 vs 33). This trend was maintained for the modified films; opacity values in the VIS region for control films and CSCO and CSHC were similar whereas opacity of the films greatly

increased after imine formation in CSCN and CSCT. These results are in accordance with the films colour parameters. In the UV region, greater opacity values were obtained for all the modified films compared to control chitosan films, however, the greatest opacity values were obtained for CSCN and CSCT films and the lowest value was for CSCO films.

**Table 2.** Optical properties of chitosan and imine-chitosan films modified with aldehydes.

| Films | L* | C* | h (°) | Opacity (Au x nm) | |
|---|---|---|---|---|---|
| | | | | UV (190-399nm) | VIS (400-800nm) |
| CS | 93.3 ± 0.6[d] | 7.6 ± 0.5[b] | 102.7 ± 0.3[c] | 226.6 ± 11.8[a] | 33.0 ± 3.2[a] |
| CSCT | 72.7 ± 0.5[a] | 69.7 ±0.7[d] | 84.0 ± 0.7[a] | 796.07 ± 10.5[d] | 165.4 ± 7.8[c] |
| CSCO | 90.8 ± 0.8[c] | 5.6 ± 0.3[a] | 103.5 ± 0.3[c] | 342.8 ± 10.0[b] | 46.1 ± 12.0[ab] |
| CSCN | 76.6 ± 0.9[b] | 80.4 ± 1.4[e] | 89.2 ± 0.1[b] | 809.1 ± 3.14[d] | 217.9 ± 6.4[d] |
| CSHC | 89.7 ± 0.5[c] | 15.5 ± 0.9[c] | 103.4 ± 0.1[c] | 573.1 ± 4.0[c] | 61.0 ± 7.8[b] |

Different letters in the same column indicate a statistically significant difference (P ≤ 0.05).

### 3.3.2. Water uptake of imine-chitosan films at several pH

Chitosan is a natural hydrophilic polysaccharide with hydroxyl and amino functional groups for water retention. In addition, water solubility and swelling degree of films depends on the degree of deacetylation and the pH of the aqueous solution [47]. Water uptake (%) of chitosan films and those modified through covalent grafting of hydrophobic aldehydes was investigated at pH 7 and 4 and the results are shown in **Figure 7**. In general terms, all the films reached swelling constant weight in less than 240 min and the films immersed at pH 4 present higher water uptake ratios compared to films measured at pH 7. Chitosan polymer has a pKa around 6.5, thus, at pH values lower than 6.5, primary amino groups in the polymer backbone have the ability to be protonated into ammonium form increasing the swelling of chitosan films.

At pH 4, the water uptake ratios found for the CSCO and CSHC films are similar to those found for unmodified chitosan films measured at the same pH (around 250%). This could be related to the high

hydrolysis of imine bonds occurring at pH 4 that leaves primary amino groups of chitosan free again to retain water molecules.

Water uptake values were slightly but significantly lower for chitosan films grafted with α, β-unsaturated aldehydes (around 200%), this can be attributed to the fact that part of aldehydes CT and CN react with chitosan amine groups through Michael addition giving rise to non-hydrolysable –C-N bonds. Moreover, formation of aldols between pendant carbonyl groups of aldehydes previously inserted in chitosan through Michael addition could also occur as proposed in **Figure 4**. This might give rise to crosslinking points that would explain the lower uptakes values found for these samples. At pH 7, imine groups cannot be hydrolysed, therefore, grafting of hydrophobic aldehydes to free amino groups of chitosan films significantly decreased water uptake of modified chitosan films with respect to unmodified chitosan films.
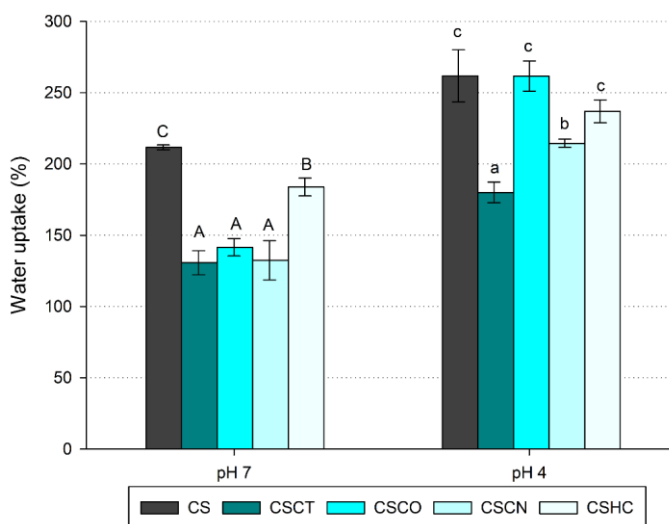


**Figure 7.** Effect of pH on water uptake (%) of chitosan and imine-chitosan films immersed in buffered aqueous solution at pH 7 and 4 at 23 °C. Bars with same letters in lower (a-c) and capital (A-C) in samples treated at pH 4 and pH 7, respectively, are not significantly different ($P \leq 0.05$).

Water uptake of films was monitored at pH 3 as a function of time and the results are shown in **Figure 8** and the statistical analysis of the results of the results is displayed in **Table 3**. Disintegration and final dissolution of unmodified CS films was observed after 15 min and the final swelling degree was 1206.4 ± 68.7% (g of water/100 g of film). Similarly, films grafted with citronellal, CSCO, lost their structural integrity after 15 min being the water uptake 1340.3 ± 90.9%. CSHC films swelled up to 1931.2 ± 163.6% and dissolved after 30 min. The higher water uptake of CSHC with respect to CSCO could be expected since, despite the fact that HC is less hydrophobic than CO, the degree of substitution achieved with HC was higher (29%), and hydrolysis of imine bonds was not as rapid as in the case of films grafted with CO.
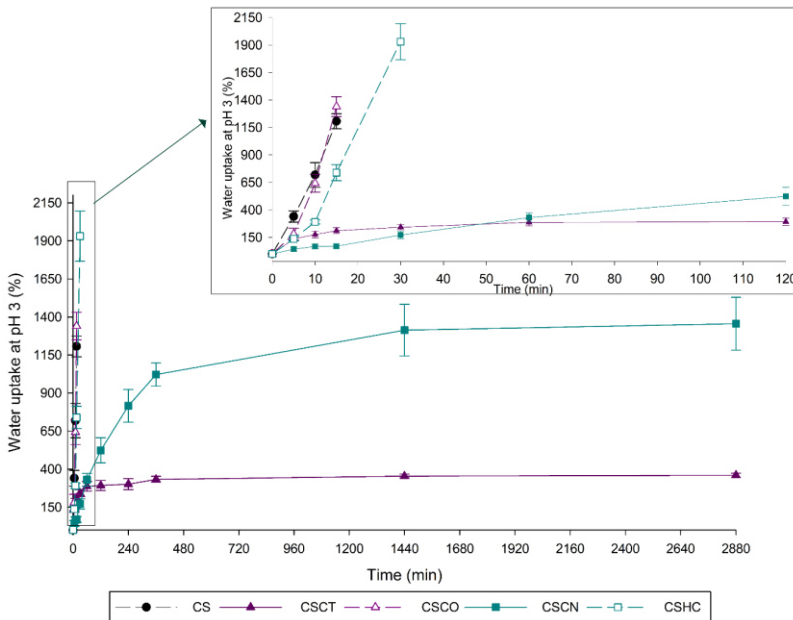


**Figure 8.** Water uptake (%) as a function of time of chitosan and imine-chitosan films immersed in buffered aqueous solution at pH 3 and measured at 23 °C for 48 h. The insert shows swelling behaviour at pH 3 of imine-chitosan films for the first 2 h.

It is important to point out that during the first 5 min, the water uptake of CSCO and CSHC films were lower than the corresponding to the unmodified chitosan film. However, after 10 minutes, the water uptake of the samples CSCO was similar to that corresponding to the unmodified chitosan film. Although CO can confer some hydrophobicity to the chitosan film, the low degree of substitution achieved (23%) and the rapid reversibility of imine bond observed in films grafted with CO can explain this behaviour.

Films modified with α,β-unsaturated aldehydes did not lose their structural integrity after being immersed for 48 h in an aqueous solution at pH 3. CSCT films reached constant weight after 6 h with a water uptake amount of $332.6 \pm 19.6$ (g of water/ 100 g of film) whereas CSCN films reached it after 24 h having a water uptake of $1313.7 \pm 169.5$ (g of water/ 100 g of film). CSCN films swelled less than CSCT films during the first 30 minutes; after that time, they surpassed water uptake of CSCT films. CN is more reactive than CT which gives rise to chitosan films with a higher degree of attached aldehydes by imine formation and Michael adducts slowing down water uptake, meanwhile its lower hydrophobicity compared to CT could increase water retention capacity of the films.

### 3.4. Thermogravimetric analysis (TGA) of imine-chitosan films

The covalent attachment of aldehydes on the surface of chitosan films was studied by thermal analysis. TGA and first derivate (DTG) curves of neutralized chitosan films, and imine-chitosan films are depicted in **Figure 9**. All the curves showed several thermal events. The first thermal event occurred in the temperature range 25-150 °C and is associated with the loss of residual water present in the films; the weight loss in the first stage was slightly higher for unmodified chitosan (5.2%) whereas for modified films weight loss was around 3.5%. The second thermal event corresponds to the main stage of degradation; for chitosan films it was observed a rapid loss of weight between 200 and 350 °C and a subsequent change in the slope of the thermogram curve, suggesting a lower rate of decomposition, films suffered a considerable loss of weight of around 59% and attributed to deacetylation, depolymerization of the polymer and decomposition and elimination of volatile products.

**Table 3.** Water mass increase (%) of imine-chitosan films at pH 3 until reach mass equilibrium or until its fully dissolved (-).

| | Water uptake at pH 3 (%) | | | | | | | | |
|---|---|---|---|---|---|---|---|---|---|
| | Time (min) | | | | | | | | |
| Films | 5 | 10 | 15 | 30 | 60 | 120 | 360 | 1440 | 2880 |
| CS | $340\pm51^{cA}$ | $719\pm113^{cB}$ | $1206\pm69^{cC}$ | - | - | - | - | - | - |
| CSCT | $136\pm21^{bA}$ | $177\pm31^{aAB}$ | $211\pm27^{aBC}$ | $242\pm24^{aC}$ | $288\pm32^{aD}$ | $301\pm36^{aD}$ | $333\pm20^{aDE}$ | $354\pm13^{aE}$ | $361\pm13^{aE}$ |
| CSCO | $181\pm53^{bA}$ | $643\pm81^{cB}$ | $1341\pm91^{cC}$ | - | - | - | - | - | - |
| CSCN | $43\pm19^{aA}$ | $67\pm20^{aA}$ | $70\pm20^{aA}$ | $172\pm34^{aA}$ | $331\pm42^{aB}$ | $524\pm83^{bC}$ | $916\pm77^{bD}$ | $1314\pm170^{bE}$ | $1356\pm174^{bE}$ |
| CSHC | $165\pm57^{bA}$ | $387\pm171^{bB}$ | $842\pm227^{bC}$ | $1932\pm164^{bD}$ | - | - | - | - | - |

[a-c] Different letters in the same column indicate a statistically significant difference (P ≤ 0.05).

[A-E] Different letters in the same line indicate a statistically significant difference (P ≤ 0.05).

For chitosan derivatives, the onset temperature of degradation was around 175 °C, and at 350 °C a change in the slope of the TGA curve suggested a second process slower than the previous one that finished at 500 °C, that event was roughly observed in chitosan films.
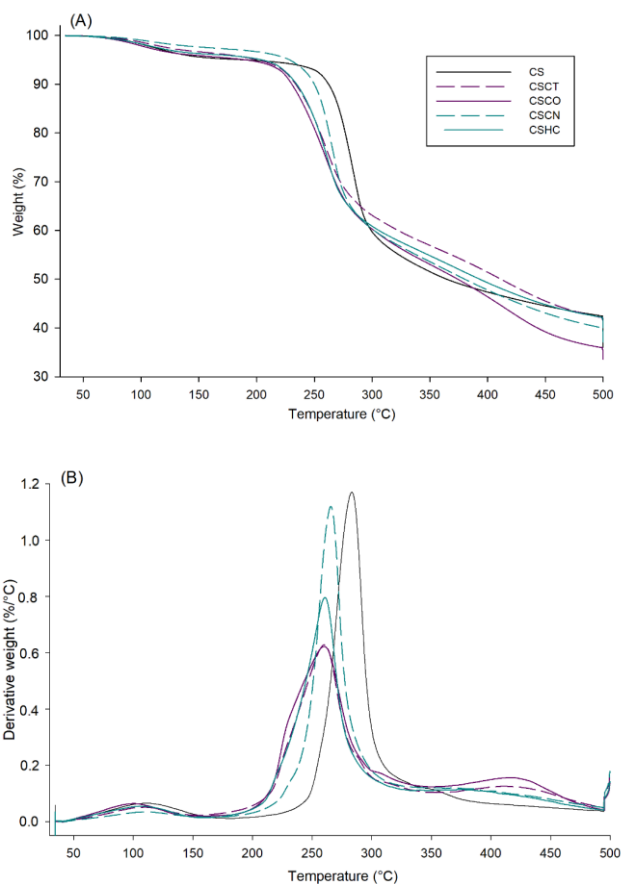


**Figure 9.** TG (A) and DTG (B) curves for chitosan and imine-chitosan films at a heating rate of 10 °C/min.

The weight loss of derivatives was around 41% in the range 175-350 °C, and between 350 °C and 500 °C a second weight loss of around 15% took placed. In this second event, it can be observed from DTG curves that the maximum loss weight rate was at 283 °C in chitosan films whereas films grafted with aldehydes resulted in a less thermal stable material having a first and main degradation temperature at around 260 °C. A decrease in thermal stability of Schiff bases obtained

by reaction of chitosan with aldehydes has previously been reported by other authors [48]. It can be appreciated in DTG curves of chitosan derivatives that in the main stage of degradation there is a broad minimum peak with the maximum loss weight rate at 420 °C associated with the change in the slope of the TGA curve and being more evident for CSCT and CSCO film. It can also be observed a small shoulder in DTG of chitosan film with maximum degradation rate at 350 °C. These degradation processes could be associated with the release of $CH_3COOH$ from acetylated amino groups of chitosan as reported by using TGA coupled on-line with FTIR [49] and with degradation of imines and released of the aldehyde in the derivatives.

The third stage of degradation of chitosan and its derivatives was not completely recorded in the current study but has been reported to longer from 500 until 800 °C with a systemic mass loss and further degradation of chitosan being reduced to a graphite like structure.

## 3.5. Microbiological studies
### 3.5.1. Antifungal activity of aldehydes used for the formation of Schiff bases

Prior to test the effectiveness of the imine-chitosan films against *P. expansum* and *B. cinerea,* the antifungal properties of the aldehydes attached to chitosan was evaluated in vapour phase. All the aldehydes showed a considerable antifungal activity against the moulds based on the MIC and MFC values which are displayed in **Table 4**.

The increasing order of antifungal activity against *P. expansum* was CO < CT < HC < CN and in the order CO < HC < CT < CN against *B. cinerea*. The α, β-unsaturated aldehydes showed a greater antifungal activity compared to their saturated derivatives against these moulds. This effect was also noticed in other studies with cinnamaldehyde and hydrocinnamaldehyde [50], *trans*-2-hexenal and hexanal [21], *trans*-2-nonenal and nonanal [51] and others ketones and alcohols [52]. In addition, citral and cinnamaldehyde have been reported to be more effective than citronellal against *Aspergillus flavus*, *A. carbonarius* and *P. viridicatum* [22]. In general, conjugated double bond present in α, β-unsaturated aldehydes provides to carbonyl group high electrophilic properties, which makes these compounds more reactive to nucleophilic attack, being good electron acceptors. The antifungal

inhibitory mechanism of α, β-unsaturated aldehydes could be related to electronic characteristics and the ability for reacting with SH groups of proteins and amino groups of the microorganism [53,54]. When comparing α, β-unsaturated cinnamaldehyde and citral, Kurita et al. [53] reported greater antimicrobial activity against diverse fungi for the former.

Observing MIC and MFC results in **Table 4**, it looks like the benzene ring in the structure of cinnamaldehyde and hydrocinnamaldehyde provides an increased activity respect to lineal aldehydes citral and citronellal.

**Table 4.** MIC and MFC (μL/cm³of air) of grafted aldehydes assayed in vapour phase against *P. expanusm* and *B. cinerea.*

| | *P. expansum* | | *B. cinerea* | |
|---|---|---|---|---|
| | MIC | MFC | MIC | MFC |
| **Aldehydes** | (μL/cm³) | (μL/cm³) | (μL/cm³) | (μL/cm³) |
| CT | 0.094 | 0.188 | 0.063 | 0.125 |
| CO | 0.313 | 0.938 | 0.250 | 0.625 |
| CN | 0.025 | 0.063 | 0.031 | 0.188 |
| HC | 0.069 | 0.150 | 0.094 | 0.250 |

In general, the antifungal activity of the aldehydes used in this work was considerable and this has been demonstrated in the pass against diverse fungal strains: citronellal [55,56], citral [54,57], cinnamaldehyde [58–60] and hydrocinnamaldehyde [46,61]. Neri et al. [21] also reported a great antifungal activity against *P. expansum* of several compound such as citral, *trans*-2-hexenal, *trans*-cinnamaldehyde and carvacrol.

### 3.5.2. Antifungal response of imine-chitosan films

The growth of *P. expansum* and *B. cinerea* was evaluated by microatmosphere generated in double plate system in the presence of 0.3 g of imine-chitosan films subjected at pH 7 and 4. No direct contact took place between films and culture medium; hence antifungal activity was only caused by the aldehyde released in the headspace of the Petri

dish system (see **Figure 1**). No differences in the fungal colony growth were observed between control with untreated chitosan and control without film, so there only are reporting data of control without chitosan film in both strains. **Figure 10** shows the effectiveness of imine-chitosan films immersed in aqueous buffered solution at pH 7 and 4 against *P. expansum* (**Figures 10A** and **10B**) and *B. cinerea* (**Figures 10C & 10D**) as percentage of inhibition of fungal colony respect to control through 10 days of incubation at 26 °C. Statistical analysis of the results is displayed in **Table 5.**
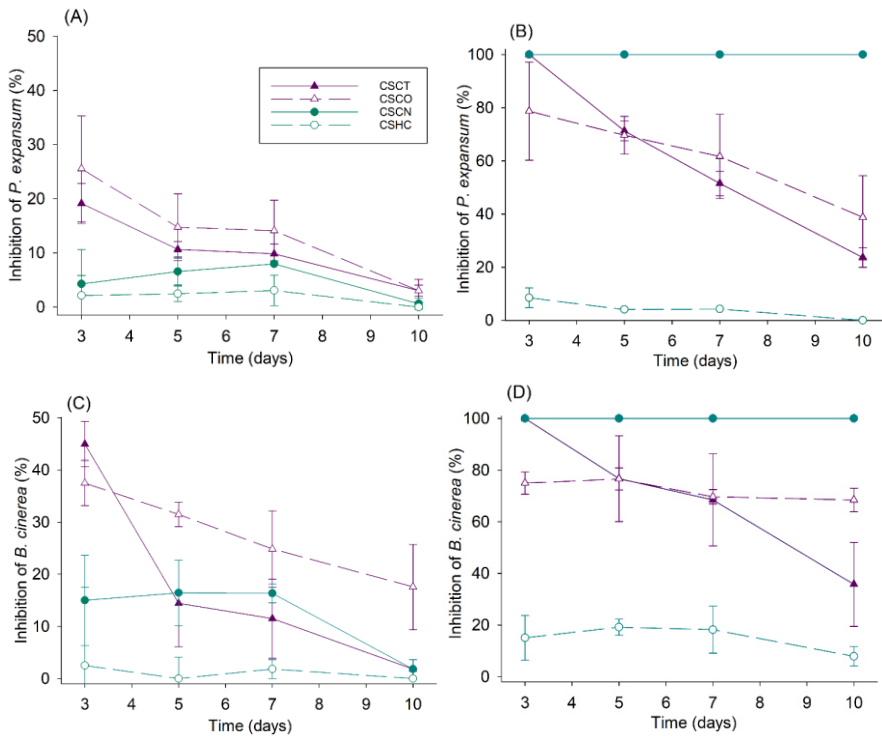


**Figure 10.** Inhibition of fungal colony growth by imine-chitosan films against *P. expansum* at pH 7 (A) and pH 4 (B) and against *B. cinerea* at pH 7 (C) and pH 4 (D) at 26 °C for 10 days.

Regarding the effect of the pH of imine hydrolysis and its effectiveness on the growth of both microorganisms, it is noticeable a greater inhibition when imine-chitosan films were subjected at acidic pH, revealing the effect of the pH over the hydrolysis of the imine bond and the release of the volatile.

**Table 5.** Antifungal inhibition of imine-chitosan films subjected at pH 4 and pH 7 against *Penicillium expansum* and *Botrytis cinerea* for 10 days at 26 °C.

| Inhibition of *P. expansum* colony (%) at pH 7 | | | |
|---|---|---|---|
| **Films** | **Day 3** | **Day 5** | **Day 7** | **Day 10** |
| CSCT | $19.1 \pm 3.7^b$ | $10.7 \pm 1.4^{ab}$ | $9.8 \pm 1.8^b$ | $3.0 \pm 2.1^a$ |
| CSCO | $25.5 \pm 9.8^b$ | $14.8 \pm 6.2^b$ | $14.1 \pm 5.6^{ab}$ | $3 \pm 1.1^a$ |
| CSCN | $4.3 \pm 6.4^a$ | $6.6 \pm 2.5^{ab}$ | $8.0 \pm 0.0^{ab}$ | $0.6 \pm 1.1^a$ |
| CSHC | $2.1 \pm 3.7^a$ | $2.5 \pm 1.4^a$ | $3.1 \pm 2.8^a$ | $0^a$ |
| **Inhibition of *P. expansum* colony (%) at pH 4** | | | |
| | **Day 3** | **Day 5** | **Day 7** | **Day 10** |
| CSCT | $100^b$ | $71.3 \pm 3.8^b$ | $51.5 \pm 4.6^b$ | $23.6 \pm 3.6^b$ |
| CSCO | $78.7 \pm 18.4^b$ | $69.7 \pm 7.1^b$ | $62 \pm 15.9^b$ | $38.8 \pm 15.7^b$ |
| CSCN | $100^b$ | $100^c$ | $100^c$ | $100^c$ |
| CSHC | $8.5 \pm 3.7^a$ | $4.1 \pm 0.1^a$ | $4.3 \pm 0.0^a$ | $0^a$ |
| **Inhibition of *B. cinerea* colony (%) at pH 7** | | | |
| | **Day 3** | **Day 5** | **Day 7** | **Day 10** |
| CSCT | $45 \pm 4.3^b$ | $14.4 \pm 8.3^b$ | $11.5 \pm 7.6^{ab}$ | $1.8 \pm 2.1^a$ |
| CSCO | $37.5 \pm 4.3^b$ | $31.5 \pm 2.4^c$ | $24.9 \pm 7.3^b$ | $17.6 \pm 8.2^b$ |
| CSCN | $15 \pm 8.7^a$ | $16.4 \pm 6.3^b$ | $16.4 \pm 1.8^b$ | $1.8 \pm 1.8^a$ |
| CSHC | $2.5 \pm 15.0^a$ | $0 \pm 4.1^a$ | $1.8 \pm 1.8^a$ | $0^a$ |
| **Inhibition of *B. cinerea* colony (%) at pH 4** | | | |
| | **Day 3** | **Day 5** | **Day 7** | **Day 10** |
| CSCT | $100^c$ | $76.7 \pm 16.6^b$ | $68.5 \pm 17.8^b$ | $35.8 \pm 16.3^c$ |
| CSCO | $75 \pm 4.3^b$ | $76.7 \pm 4.3^b$ | $69.7 \pm 2.8^b$ | $68.5 \pm 4.6^b$ |
| CSCN | $100^c$ | $100^c$ | $100^c$ | $100^d$ |
| CSHC | $15 \pm 8.7^a$ | $19.2 \pm 3.1^a$ | $18.2 \pm 9.1^a$ | $7.9 \pm 3.8^a$ |

[a-d] Different letters in the same column indicate a statistically significant difference ($P \leq 0.05$).

The percentage of inhibition against *P. expansum* of imine-chitosan films subjected at pH 7 was below 20% (**Figure 10A**), having the highest percentages of inhibition films modified with citral (CSCT) and citronellal (CSCO). These results are in accordance with the results obtained by elemental analysis which showed that imines synthetized with CT and CO were less stable at pH 7. In **Figure 10C** it can be appreciated that the percentages of inhibition of CSCT and CSCO films at pH 7 were a little higher when were exposed to *B. cinerea* which is related with the greater sensitivity of this mould to these aldehydes.

When imine-chitosan films were subjected at pH 4 (**Figures 10B** and **10D**), chitosan grafted with cinnamaldehyde (CSCN) films inhibited the growth of both moulds through the ten days of incubation. Films of CSCT and CSCO subjected at pH 4 showed percentages of inhibition against *P. expansum* greater that 80% at the beginning of the storage but the percentage decrease to 50% after seven days and it was around 30% at the end of ten days. When CSCT and CSCO were assayed against *B. cinerea*, the greater sensitivity of *B. cinerea* to CT and CO compared with *P. expansum* was demonstrated since the percentage of inhibition of CSCO films subjected at pH 4 was around 80% through the ten days of storage period, whereas CSCT films completely inhibited the mould during the three first days of storage, however, this percentage was reduced to 40% after ten days. CT has greater antifungal activity than CO against the tested moulds possessing lower MIC and MFC values (**Table 3**), imine films synthetized with both aldehydes showed similar antimicrobial activity which is related to the greater hydrolysis and release of CO compared with CT; as already commented, CT can act as a crosslinker in the chitosan matrix since α,β-unsaturated aldehyde can also have 1,4 addition or Michael addition, thus, formation of C-N between aldehyde and chitosan limits the release of the aldehyde and thus, film effectivity. The crosslinking effect of CT also happens with CN, however, the antifungal effectivity of CSCN films is not limited due to great antifungal activity of CN and the films totally inhibited the moulds in the experiments carried out. It also should be mentioned the rapid degradation of CT at low pH [62]. Thus, when imine bond is hydrolysed and CT is released to the buffer medium, it is susceptible to acid catalysed cyclization and oxidative

degradation [63] and it could also imply a loss of antifungal activity of CSCT film.

With regard to imine films synthetized with hydrocinnamaldehyde (CSHC), they roughly showed antifungal activity even although the imine bond was almost totally hydrolysed at acid pH. Hydrocinnamdehyde presents antifungal activity against *P. expansum* and *B. cinerea*, showing lower MIC and MFC values than CT and CO against *P. expansum*, and lower MIC and MFC values than CO against *B. cinerea* (**Table 4**). Thus, the lack of activity of CSHC films could be related to the greater retention of HC in the buffered solution after hydrolysis of the imine bond. According to the literature, the amount of flavour compound release from a water matrix to the gaseous phase greatly depends on the hydrophobicity of the compound [64]. The hydrophobicity of a compound can be measured through its partition coefficient (P) between n-octanol and water, and it is given as log P [65]; for the aldehydes tested, log P followed the order HC (1.78) > CN (2.12) > CO (3.29) > CT (3.45). In view of the results, the greater affinity of HC by water could reduce its release to the headspace of the double Petri dish system reducing film effectivity.

**Figure 11** shows photographs *of P. expansum* and *B. cinerea* colonies after being subjected to imine-chitosan films for seven days of incubation at 26 °C. The pictures reveal fungal colonies were notably affected in both fungi, especially when the dynamic films carrying the aldehydes with greater activity (CN and CT) were activated in acidic medium.
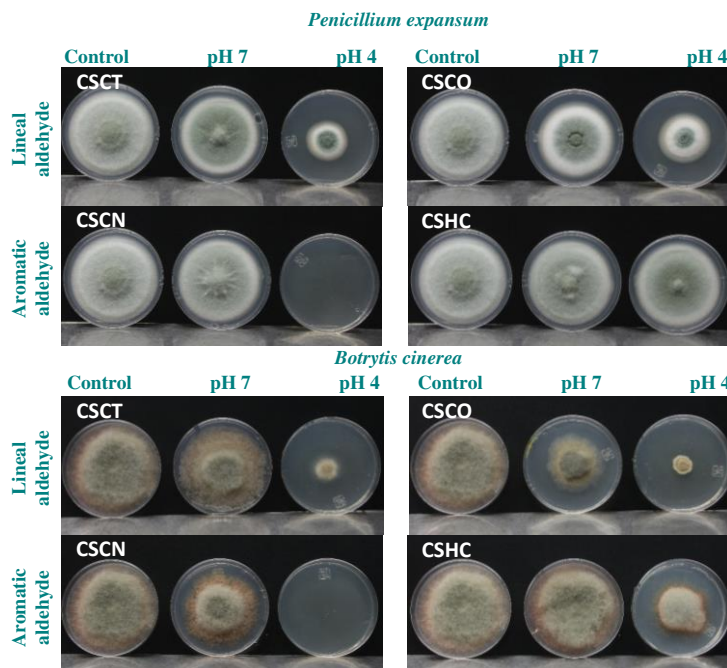
**Figure 11.** Antifungal activity of imine-chitosan films against *P. expansum* and *B. cinerea* after 7 days of incubation at 26 °C. The images show samples without films (control), and those treated with imine-chitosan films with covalently attached citral (CT), citronellal (CO), cinnamaldehyde (CN) and hydrocinnamaldehyde (HC) whose release was triggered at pH 7 and 4.

## 4. Conclusions

In this work the reversible covalent chemistry of imines has been successfully applied to the synthesis of pH-responsive antifungal films. These films were based on the chitosan polymer and naturally occurring aldehydes of different chemical structures possessing antifungal activity. Aldehydes were grafted on to the surface of the chitosan films by acid-catalysed condensation of carbonyls with amino groups forming imines. The stability of the synthesized imine bonds depends on the acidity of the aqueous medium and the chemical structure of the aldehyde. In general, imines formed from aromatic and α,β-unsaturated aldehydes remained quite stable at neutral pH whereas they were hydrolysed under acidic conditions. Swelling of the grafted films suggested that α,β-unsaturated aldehydes can also participate in Michel

addition with primary amino groups in chitosan resulting in crosslinking. The antifungal activity of dynamic films was tested *in vitro* against *P. expansum* and *B. cinerea*, two common fungi responsible for the spoilage or deterioration of fresh fruits and vegetables. All the films exhibited antifungal activity which was based on the hydrolysis of the imine bond in acid aqueous medium and the consequent release of the aldehyde. Antifungal activity was exerted by the aldehydes after imine bond hydrolysis, release to the aqueous medium and subsequent entry to the vapour phase and thus exposure to the mould. These data indicate that novel dynamic films could be of utility in the design of antimicrobial-responsive packaging to fight postharvest fungal spoilage.

## References

1. Priya James, H.; John, R.; Alex, A.; Anoop, K.R. Smart polymers for the controlled delivery of drugs – a concise overview. *Acta Pharm. Sin. B* **2014**, *4*, 120–127, doi:10.1016/j.apsb.2014.02.005.

2. Taepaiboon, P.; Rungsardthong, U.; Supaphol, P. Drug-loaded electrospun mats of Poly(Vinyl Alcohol) fibres and their release characteristics of four model drugs. *Nanotechnology* **2006**, *17*, 2317–2329, doi:10.1088/0957-4484/17/9/041.

3. Ulrich, S. Growing prospects of dynamic covalent chemistry in delivery applications. *Acc. Chem. Res.* **2019**, doi:10.1021/acs.accounts.8b00591.

4. Wu, X.; Busschaert, N.; Wells, N.J.; Jiang, Y.B.; Gale, P.A. Dynamic covalent transport of amino acids across lipid bilayers. *J. Am. Chem. Soc.* **2015**, *137*, 1476–1484, doi:10.1021/ja510063n.

5. Lehn, J.M. Dynamers: Dynamic molecular and dupramolecular polymers. *Prog. Polym. Sci.* **2005**, *30*, 814–831, doi:10.1016/j.progpolymsci.2005.06.002.

6. Larson, N.; Ghandehari, H. Polymeric conjugates for drug delivery. *Chem. Mater.* **2012**, *24*, 840–853, doi:10.1021/cm2031569.

7.  Jin, Y.; Yu, C.; Denman, R.J.; Zhang, W. Recent advances in dynamic covalent chemistry. *Chem. Soc. Rev.* **2013**, *42*, 6634–6654, doi:10.1039/c3cs60044k.

8.  Meguellat, K.; Ladame, S. Reversible covalent chemistries compatible with the principles of constitutional dynamic chemistry: New reactions to create more diversity. *Top. Curr. Chem.* **2012**, *322*, 291–314, doi:10.1007/128_2011_277.

9.  West, K.R.; Otto, S. Reversible Covalent Chemistry in Drug Delivery. *Curr. Drug Discov. Technol.* **2005**, *2*, 123–160, doi:https://doi.org/10.2174/1570163054866882.

10. Cobo, I.; Li, M.; Sumerlin, B.S.; Perrier, S. Smart Hybrid Materials by Conjugation of Responsive Polymers to Biomacromolecules. *Nat. Mater.* **2015**, *14*, 143–149, doi:10.1038/nmat4106.

11. Chang, M.; Zhang, F.; Wei, T.; Zuo, T.; Guan, Y.; Lin, G.; Shao, W. Smart linkers in polymer–drug conjugates for tumor-targeted delivery. *J. Drug Target.* **2016**, *24*, 475–491.

12. Seidi, F.; Jenjob, R.; Crespy, D. Designing smart polymer conjugates for controlled release of payloads. *Chem. Rev.* **2018**, *118*, 3965–4036, doi:10.1021/acs.chemrev.8b00006.

13. Zhang, W.; Jin, Y. *Dynamic Covalent Chemistry: Principles, reactions, and applications*; John Wiley & Sons Ltd., **2017**; ISBN 9781119075639.

14. Huang, W.; Wang, Y.; Huang, Z.; Wang, X.; Chen, L.; Zhang, Y.; Zhang, L. On-demand dissolvable self-Healing hydrogel based on carboxymethyl chitosan and cellulose nanocrystal for deep partial thickness burn wound healing. *ACS Appl. Mater. Interfaces* **2018**, *10*, 41076–41088, doi:10.1021/acsami.8b14526.

15. Atta, S.; Paul, A.; Banerjee, R.; Bera, M.; Ikbal, M.; Dhara, D.; Singh, N.D.P. Photoresponsive polymers based on a coumarin moiety for the controlled release of pesticide 2,4-D. *RSC Adv.* **2015**, *5*, 99968–99975, doi:10.1039/c5ra18944f.

16. Atta, S.; Bera, M.; Chattopadhyay, T.; Paul, A.; Ikbal, M.; Maiti, M.K.; Singh, N.D.P. Nano-pesticide formulation based on fluorescent organic photoresponsive nanoparticles: For controlled release of 2,4-D and real time monitoring of morphological changes induced by 2,4-D in plant systems. *RSC Adv.* **2015**, *5*, 86990–86996, doi:10.1039/c5ra17121k.

17. Jackson, A.W.; Fulton, D.A. Making Polymeric nanoparticles stimuli-responsive with dynamic covalent bonds. *Polym. Chem.* **2013**, *4*, 31–45, doi:10.1039/c2py20727c.

18. Wang, S.; Huang, P.; Chen, X. Stimuli-responsive programmed specific targeting in nanomedicine. *ACS Nano* **2016**, *10*, 2991–2994, doi:10.1021/acsnano.6b00870.

19. Inukai, Y.; Chinen, T.; Matsuda, T.; Kaida, Y.; Yasuda, S. Selective separation of germanium(IV) by 2,3-dihydroxypropyl chitosan resin. *Anal. Chim. Acta* **1998**, *371*, 187–193, doi:10.1016/S0003-2670(98)00313-4.

20. Kasaai, M.R.; Arul, J.; Chin, S.L.; Charlet, G. The use of intense femtosecond laser pulses for the fragmentation of chitosan. *J. Photochem. Photobiol. A Chem.* **1999**, *120*, 201–205, doi:10.1016/S1010-6030(98)00432-8.

21. Neri, F.; Mari, M.; Brigati, S. Control of *Penicillium expansum* by plant volatile compounds. *Plant Pathol.* **2006**, *55*, 100–105, doi:10.1111/j.1365-3059.2005.01312.x.

22. Wang, H.; Yang, Z.; Ying, G.; Yang, M.; Nian, Y.; Wei, F.; Kong, W. Antifungal evaluation of plant essential oils and their major components

against toxigenic fungi. *Ind. Crops Prod.* **2018**, *120*, 180–186, doi:10.1016/j.indcrop.2018.04.053.

23. Stinson, M.; Ezra, D.; Hess, W.M.; Sears, J.; Strobel, G. An endophytic G*liocladium* sp. of *Eucryphia cordifolia* producing selective volatile antimicrobial compounds. *Plant Sci.* **2003**, *165*, 913–922, doi:10.1016/S0168-9452(03)00299-1.

24. Mauricio-Sánchez, R.A.; Salazar, R.; Luna-Bárcenas, J.G.; Mendoza-Galván, A. FTIR spectroscopy studies on the spontaneous neutralization of chitosan ccetate films by moisture conditioning. *Vib. Spectrosc.* **2018**, *94*, 1–6, doi:10.1016/j.vibspec.2017.10.005.

25. Gavalyan, V.B. Synthesis and characterization of new chitosan-based Schiff base compounds. *Carbohydr. Polym.* **2016**, *145*, 37–47, doi:10.1016/j.carbpol.2016.02.076.

26. Marin, L.; Ailincai, D.; Mares, M.; Paslaru, E.; Cristea, M.; Nica, V.; Simionescu, B.C. Imino-chitosan biopolymeric films. Obtaining, self-assembling, surface and antimicrobial properties. *Carbohydr. Polym.* **2015**, *117*, 762–770, doi:10.1016/j.carbpol.2014.10.050.

27. Moore, G.K.; Roberts, G. a. F. Reactions of chitosan: 3. Preparation and reactivity of Schiff's base derivatives of chitosan. *Int. J. Biol. Macromol.* **1981**, *3*, 337–340, doi:10.1016/0141-8130(81)90053-2.

28. Higueras, L.; López-Carballo, G.; Gavara, R.; Hernández-Muñoz, P. Reversible covalent immobilization of cinnamaldehyde on chitosan films via Schiff base formation and their application in active food packaging. *Food Bioprocess Technol.* **2015**, *8*, 526–538, doi:10.1007/s11947-014-1421-8.

29. Marin, L.; Moraru, S.; Popescu, M.C.; Nicolescu, A.; Zgardan, C.; Simionescu, B.C.; Barboiu, M. Out-of-water constitutional self-organization of chitosan-cinnamaldehyde dynagels. *Chem. - A Eur. J.* **2014**, *20*, 4814–4821, doi:10.1002/chem.201304714.

30. Jin, X.; Wang, J.; Bai, J. Synthesis and antimicrobial activity of the Schiff base from chitosan and citral. *Carbohydr. Res.* **2009**, *344*, 825–829, doi:10.1016/j.carres.2009.01.022.

31. Marin, L.; Simionescu, B.; Barboiu, M. Imino-chitosan biodynamers. *Chem. Commun.* **2012**, *48*, 8778, doi:10.1039/c2cc34337a.

32. Chen, J.Y.; Jiang, H.; Chen, S.J.; Cullen, C.; Sabbir Ahmed, C.M.; Lin, Y.H. Characterization of electrophilicity and oxidative potential of atmospheric carbonyls. *Environ. Sci. Process. Impacts* **2019**, *21*, 856–866, doi:10.1039/c9em00033j.

33. Balaguer, M.P.; Gómez-Estaca, J.; Gavara, R.; Hernandez-Munoz, P. Biochemical properties of bioplastics made from wheat gliadins cross-linked with cinnamaldehyde. *J. Agric. Food Chem.* **2011**, *59*, 13212–13220, doi:10.1021/jf203055s.

34. Autelitano, A.; Minassi, A.; Pagani, A.; Taglialatela-Scafati, O.; Appendino, G. The reaction of cinnamaldehyde and cinnam(o)Yl derivatives with thiols. *Acta Pharm. Sin. B* **2017**, *7*, 523–526, doi:10.1016/j.apsb.2017.06.005.

35. Migneault, I.; Dartiguenave, C.; Bertrand, M.J.; Waldron, K.C. Glutaraldehyde: Behavior in aqueous solution, reaction with proteins, and application to enzyme crosslinking. *Biotechniques* **2004**, *37*, 790–802, doi:10.2144/04375rv01.

36. Demetgül, C.; Beyazit, N. Synthesis, characterization and antioxidant activity of chitosan-chromone derivatives. *Carbohydr. Polym.* **2018**, *181*, 812–817, doi:10.1016/j.carbpol.2017.11.074.

37.   Chauhan, D.S.; Mazumder, M.A.J.; Quraishi, M.A.; Ansari, K.R. Chitosan-cinnamaldehyde Schiff base: A bioinspired macromolecule as corrosion inhibitor for oil and gas industry. *Int. J. Biol. Macromol.* **2020**, *158*, 127–138, doi:10.1016/j.ijbiomac.2020.04.200.

38.   Kildeeva, N.R.; Perminov, P.A.; Vladimirov, L. V.; Novikov, V. V.; Mikhailov, S.N. About mechanism of chitosan cross-linking with glutaraldehyde. *Russ. J. Bioorganic Chem.* **2009**, *35*, 360–369, doi:10.1134/S106816200903011X.

39.   Li, M.; Wang, H.; Chen, X.; Jin, S.; Chen, W.; Meng, Y.; Liu, Y.; Guo, Y.; Jiang, W.; Xu, X.; et al. Chemical grafting of antibiotics into multilayer films through Schiff base reaction for self-defensive response to bacterial infections. *Chem. Eng. J.* **2020**, *382*, doi:10.1016/j.cej.2019.122973.

40.   Neqal, M.; Fernandez, J.; Coma, V.; Gauthier, M.; Héroguez, V. PH-Triggered Release of an Antifungal agent from polyglycidol-based nanoparticles against fuel fungus *H. Resinae*. *J. Colloid Interface Sci.* **2018**, *526*, 135–144, doi:10.1016/j.jcis.2018.03.106.

41.   Bao, J.; Zhang, H.; Zhao, X.; Deng, J. Biomass polymeric microspheres containing aldehyde groups: Immobilizing and controlled-releasing amino acids as green metal corrosion inhibitor. *Chem. Eng. J.* **2018**, *341*, 146–156, idoi:10.1016/j.cej.2018.02.047.

42.   Matesic, L.; Locke, J.M.; Vine, K.L.; Ranson, M.; Bremner, J.B.; Skropeta, D. Synthesis and hydrolytic evaluation of acid-labile imine-linked cytotoxic isatin model systems. *Bioorganic Med. Chem.* **2011**, *19*, 1771–1778, doi:10.1016/j.bmc.2011.01.015.

43.   Vázquez, M.A.; Muñoz, F.; Donoso, J.; García Blanco, F. Stability of schiff bases of amino acids and pyridoxal-5′-phosphate. *Amino Acids* **1992**, *3*, 81–94, doi:10.1007/BF00806010.

44.   Sedlák, M.; Pravda, M.; Staud, F.; Kubicová, L.; Týčová, K.; Ventura, K. Synthesis of pH-sensitive amphotericin B-poly(ethylene glycol) conjugates and study of their controlled release *in vitro*. *Bioorganic Med. Chem.* **2007**, *15*, 4069–4076, doi:10.1016/j.bmc.2007.03.083.

45.   Park, W.; Park, S.J.; Shin, H.; Na, K. Acidic tumor pH-responsive nanophotomedicine for targeted photodynamic cancer therapy. *J. Nanomater.* **2016**, *2016*, doi:https://doi.org/10.1155/2016/3739723.

46.   Zhai, Y.; Zhou, X.; Zhang, Z.; Zhang, L.; Wang, D.; Wang, X.; Sun, W. Design, synthesis, and characterization of Schiff base bond-linked pH-responsive doxorubicin prodrug based on functionalized MPEG-PCL for targeted cancer therapy. *Polymers (Basel).* **2018**, *10*, doi:10.3390/polym10101127.

47.   Cho, Y.W.; Jang, J.; Park, C.R.; Ko, S.W. Preparation and solubility in acid and water of partially deacetylated chitins. *Biomacromolecules* **2000**, *1*, 609–614, doi:10.1021/bm000036j.

48.   Hassan, M.A.; Omer, A.M.; Abbas, E.; Baset, W.M.A.; Tamer, T.M. Preparation, physicochemical characterization and antimicrobial activities of novel two phenolic chitosan Schiff base derivatives. *Sci. Rep.* **2018**, *8*, 1–14, doi:10.1038/s41598-018-29650-w.

49.   Corazzari, I.; Nisticò, R.; Turci, F.; Faga, M.G.; Franzoso, F.; Tabasso, S.; Magnacca, G. Advanced physico-chemical characterization of chitosan by means of TGA coupled on-line with FTIR and GCMS: Thermal degradation and water adsorption capacity. *Polym. Degrad. Stab.* **2015**, *112*, 1–9, doi:10.1016/j.polymdegradstab.2014.12.006.

50.   Wang, S.Y.; Chen, P.F.; Chang, S.T. Antifungal activities of essential oils and

their constituents from indigenous Cinnamon (*Cinnamomum osmophloeum*) leaves against wood decay fungi. *Bioresour. Technol.* **2005**, *96*, 813–818, doi:10.1016/j.biortech.2004.07.010.

51.  Hamilton-Kemp, T.R.; McCracken, C.T.; Loughrin, J.H.; Andersen, R.A.; Hildebrand, D.F. Effects of some natural volatile compounds on the pathogenic fungi *Alternaria alternata* and *Botrytis cinerea*. *J. Chem. Ecol.* **1992**, *18*, 1083–1091, doi:10.1007/BF00980064.

52.  Andersen, R.A.; Hamilton-Kemp, T.R.; Hildebrand, D.F.; McCracken, C.T.; Collins, R.W.; Fleming, P.D. Structure-antifungal activity relationships among volatile C6 and C9 aliphatic aldehydes, ketones, and alcohols. *J. Agric. Food Chem.* **1994**, *42*, 1563–1568, doi:10.1021/jf00043a033.

53.  Kurita, N.; Miyaji, M.; Kurane, R.; Takahara, Y.; Ichimura, K. Antifungal activity and molecular orbital energies of aldehyde compounds from oils of higher plants. *Agric. Biol. Chem.* **1979**, *43*, 2365–2371, doi:10.1271/bbb1961.43.2365.

54.  Ramos-Nino, M.E.; Ramirez-Rodriguez, C.A.; Clifford, M.N.; Adams, M.R. QSARs for the effect of benzaldehydes on foodborne bacteria and the role of sulfhydryl groups as targets of their antibacterial activity. *J. Appl. Microbiol.* **1998**, *84*, 207–212, doi:10.1046/j.1365-2672.1998.00324.x.

55.  Aguiar, R.W.D.S.; Ootani, M.A.; Ascencio, S.D.; Ferreira, T.P.S.; Santos, M.M.D.; Santos, G.R.D. Fumigant antifungal activity of *Corymbia citriodora* and *Cymbopogon nardus* essential oils and citronellal against three fungal species. *Sci. World J.* **2014**, *2014*, doi:10.1155/2014/492138.

56.  Wu, Y.; OuYang, Q.; Tao, N. Plasma membrane damage contributes to antifungal activity of citronellal against *Penicillium digitatum*. *J. Food Sci. Technol.* **2016**, *53*, 3853–3858, doi:10.1007/s13197-016-2358-x.

57.  Tao, N.; OuYang, Q.; Jia, L. Citral inhibits mycelial growth of *Penicillium italicum* by a membrane damage mechanism. *Food Control* **2014**, *41*, 116–121, doi:10.1016/j.foodcont.2014.01.010.

58.  Balaguer, M.P.; Lopez-Carballo, G.; Catala, R.; Gavara, R.; Hernandez-Munoz, P. Antifungal properties of gliadin films incorporating cinnamaldehyde and application in active food packaging of bread and cheese spread foodstuffs. *Int. J. Food Microbiol.* **2013**, *166*, 369–377, doi:10.1016/j.ijfoodmicro.2013.08.012.

59.  Xie, X.M.; Fang, J.R.; Xu, Y. Study of antifungal effect of cinnamaldehyde and citral on *Aspergillus flavus*. *Food Sci.* **2004**, *25*, 32–34, doi:10.3321/j.issn:1002-6630.2004.09.002.

60.  López, P.; Sánchez, C.; Batlle, R.; Nerín, C. Vapor-phase activities of cinnamon, thyme, and oregano essential oils and key constituents against foodborne microorganisms. *J. Agric. Food Chem.* **2007**, *55*, 4348–4356, doi:10.1021/jf063295u.

61.  Venturini, M.E.; Blanco, D.; Oria, R. *In vitro* antifungal activity of several antimicrobial compounds against *Penicillium expansum*. *J. Food Prot.* **2002**, *65*, 834–839, doi:10.4315/0362-028X-65.5.834.

62.  Kimura, K.; Iwata, I.; Nishimura, H. Relationship between acid-catalyzed cyclization of citral and deterioration of lemon flavor. *Agric. Biol. Chem.* **1982**, *46*, 1387–1389, doi:10.1271/bbb1961.46.1387.

63.  Kimura, K.; Iwata, I.; Nishimura, H.; Mizutani, J. Deterioration mechansim of lemon flavor. 2. Formation mechanism of off-odor substances arising from citral. *J. Agric. Food Chem.* **1983**, *31*, 801–804, doi:10.1021/jf00118a030.

64.  Philippe, E.; Seuvre, A.M.; Colas, B.; Langendorff, V.; Schippa, C.; Voilley, A. Behavior of flavor compounds in model food systems: A thermodynamic

study. *J. Agric. Food Chem.* **2003**, *51*, 1393–1398, doi:10.1021/jf020862e.

65.      Leo, A.J.; Hansch, C. Role of hydrophobic effects in mechanistic QSAR. *Perspect. Drug Discov. Des.* **1999**, *17*, 1–25.

# Artículo 2

**Chitosan films as pH-responsive sustained release systems of naturally occurring antifungal volatile compounds**

Raquel Heras-Mozos, Rafael Gavara, Pilar Hernández-Muñoz

Instituto de Agroquímica y Tecnología de Alimentos (IATA-CSIC),

Av, Agustín Escardino, 7, 46980, Paterna, Valencia, Spain.

*Carbohydrate Polymers* (2022), 283, 119137

**ABSTRACT**

Reversible imine bonds have been used as a strategy to develop pH-dependent antifungal systems based on grafting benzaldehyde and citral onto the surface of chitosan films. Formation of imine bonds was confirmed by ATR-FTIR and XPS. Aldehyde unit incorporation respect to glucosamine units of chitosan polymer was estimated by elemental analysis. The rate and extent of imine bond hydrolysis depended on the pH of the media and the chemical structure of the aldehyde. The release of the aldehydes was monitored by gas chromatography observing acidic media favours the release. Imine bond obtained from benzaldehyde was more prone to be hydrolysed than citral. Chitosan films grafted with benzaldehyde and triggered at acidic pH controlled *in vitro* growth of common fruit and vegetable spoilage and pathogenic fungi. The films developed could be applied in the design of food packages intended to prevent postharvest fungal spoilage.

**Keywords:** Reversible imines, hydrolysis, pH-sensitive, antifungal aldehydes, chitosan films

## 1. Introduction

Polymers based on dynamers offer new possibilities in polymer chemistry to create functional materials with unique properties. In this framework, the concept of component exchange in reversible polymers allows the development of polymers consisting of a static molecular skeleton decorated with dynamic chain substituents attached through reversible covalent bonds that can be decorporated under an external trigger. These polymers can be formed as films or coatings giving rise to materials with new functions [1,2].

In general, reversible covalent bonds present greater strength and their reversibility is more controllable than that in reversible connections based on non-covalent interactions. These features make those bonds very attractive for the creation of new functional materials with controlled release properties which action is triggered by external stimuli. Among dynamic covalent bonds, Schiff bases are imines formed by the condensation reaction of a carbonyl group with a primary amino group giving rise to an imine bond (C=N). Schiff bases are greatly spread in chemistry and are commonly used for protecting functional groups in organic synthesis or to create coordination compounds. Moreover, they are easy to perform, requiring mild conditions for synthesis with short reaction times, which meets the criteria of "Click Chemistry" [3]. Hydrolytic cleavage of C=N bonds is favoured at acid pH, therefore, it makes Schiff base sensitive to pH, giving rise to the possibility of using Schiff base structure to create stimuli-responsive systems [4].

Chitosan is a biopolymer obtained by deacetylation of chitin, which forms part of various natural structures, such as the shell of crustaceans and insects. Chitosan has a linear structure consisting of β-(1-4)-d-glucosamine and *N*-acetyl-*d*-glucosamine, arranged randomly along the chain [5]. Chitosan has been highly studied during more than 20 years as biopolymer to carry and release active molecules of diverse interest in different scientific and industrial fields such as pharmacy, medicine, agriculture, heath care, textile and food industry [6–9]. Chitosan has a great potential to be used for creating stimuli-responsive polymer-aldehyde conjugates based on imines since it has primary amine groups that can be used to reversibly attach active biomolecules having carbonyl groups.

Recently, a few researchers have employed the reversibility of imines to create aldehyde-chitosan conjugates with antimicrobial properties. Marin et al. [10] and Demitri et al. [11] developed aldehyde-imino-chitosan conjugates in a homogeneous solution of chitosan, they cast the solution into films studying their antimicrobial properties. Chabbi et al. [12] also synthetized aldehyde-chitosan conjugates in homogeneous liquid media and were beyond studying the release of the aldehydes in buffered water.

In this work, the reversibility of the imine bond has been employed to obtain antifungal stimuli-responsive chitosan films. For that, naturally-occurring aldehydes with antifungal properties were grafted on the surface of chitosan films at the solid/liquid interface. Next, the antifungal effectivity of the films based on the reversibility of the bond and release of the aldehyde has been studied with the aim to apply the films in active food packaging.

Therefore, the aim of this work has been the design of responsive films that allow the smart release of antifungal volatiles previously anchored to a biopolymeric surface through reversible imine bonds. For that, two naturally occurring volatile aldehydes with proved antifungal activity were chosen, that is, an α, β-unsaturated aldehyde, 3,7-dimethyl-2,6-octadienal (citral, CT) and an aromatic aldehyde, benzaldehyde (BZ), both of them are approved by the FAO/WHO Expert Committee on Food Additives (*JECFA*) for use as food flavouring agents and are generally recognized as safe (GRAS). Chitosan in the form of neutralized film was chosen as the backbone polymer. A novel methodology based on the grafting of aldehydes to the surface of chitosan films via imine synthesis is described, and the synthetized new bonds characterized. The pH-responsive hydrolysis of the imine-bonds and release of the aldehyde from the films has been studied and monitored by gas chromatography. Finally, the antifungal activity of the films was proved *in vitro* against *Penicillium expansum* and *Botrytis cinerea*, being both of them common fungi causing postharvest infection of fruits.

## 2. Hypothesis

Click chemistry is a powerful tool for developing functional and reactive polymeric materials. Imine click (condensation) chemistry can be employed for the reversible grafting of active carbonyls to polymeric structures containing primary amine groups. Antifungal volatile aldehydes can be stabilized in chitosan films through the formation of imines. Films could release them when necessary upon triggering by one or more environmental stimuli. Based on that, stimuli-responsive imine-chitosan films which antifungal properties are based on the reversibility of imine bonds and the subsequent release of the active aldehyde could be developed for the preservation of packaged fresh produce that can respond to microbiological deterioration. This approach could open up a new area of research on the delivery of actives for the preservation of foods by means of responsive packaging.

## 3. Materials and methods

### 3.1. Materials

Low molecular weight chitosan (LMW) was employed with a molecular weight of 50–190 kDa and a degree of deacetylation of 75-85% as provided by Sigma-Aldrich (Barcelona, Spain). Sodium hydroxide, hydrochloric acid 37%, acetic acid, ethanol 96% (*v/v*), citral and benzaldehyde were also purchased from Sigma-Aldrich (Barcelona, Spain). Buffer medium at pH 4 and 7 were prepared with citric acid and disodium phosphate supplied by Sigma-Aldrich (Barcelona-Spain). Water was obtained from a Milli-Q Plus purification system (Millipore, Molsheim, France). Potato dextrose agar (PDA) was purchased from Scharlau (Scharlab S.L., Barcelona, Spain). The strain of *Penicillium expansum* (CECT 2278) and *Botrytis cinerea* (CECT 2100), were supplied by the Spanish Type Culture Collection (CECT, Valencia, Spain).

### 3.2. Formation of chitosan films and synthesis of Schiff bases

Chitosan films were obtained dissolving 1.5 g of LMW chitosan in 100 mL of 0.5% acetic acid aqueous solution at 50 °C under stirring until complete dissolution. After that, the solution was filtered to eliminate impurities. Chitosan acetate solution was spread on polystyrene plates and dried at 37 °C for 24 h. Chitosan acetate films

with a thickness of 35 ± 5 µm were neutralized with 0.1 M sodium hydroxide solution for 24 h. The films were washed with distilled water and dried at 37 °C. After that, neutralized chitosan films (nt-CS) were covalently grafted with benzaldehyde (BZ) and citral (CT) in a single step process at the solid/liquid interface (film/aldehyde) using ethanol as solvent medium. A scheme of the reaction is shown in **Figure 1**. For this purpose, a 250 mL flask was charged with 75 mL of ethanol 96% (*v/v*) and 4 g of BZ or CT, 2 g of chitosan in the form of films were incorporated and hydrochloric acid was added as catalyst. The flask was placed in a shaking bath at 60 °C for 24 h. Then, chitosan films were removed from the reaction medium and washed with ethanol 96% (*v/v*) in a shaking bath at 60 °C to removed unreacted aldehyde for 24 h. A control without anchored aldehydes was also carried out. For that, nt-CS film was submitted to the grafting reaction medium without aldehydes and it is referred as reacted chitosan films (CS). Finally, control and grafted chitosan films were dried and stored in a desiccator with $P_2O_5$ prior to characterization.
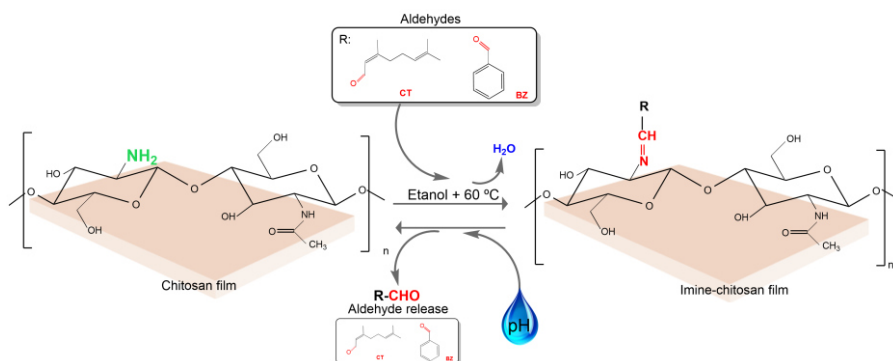


**Figure 1.** Schematic reaction of imine bond formation between carbonyl groups of aldehydes and primary amino groups of chitosan.

### 3.3. Characterization of modified chitosan films by Schiff base

Imine-bonds formed in chitosan films were characterized by ATR-FTIR analysis using a Bruker Tensor 27 FTIR spectrometer (Bruker Española S.A., Barcelona, Spain). The resolution was 4 $cm^{-1}$ in the range of 4000 to 600 $cm^{-1}$ and 32 scans were recorded per test. X-ray

photoelectron spectra of sample surfaces were recorded using a Thermo Scientifics K-alpha compact XPS with a monochromatic Al KAlfa X-ray source (1486.6 eV). Spectra were acquired using a pass energy of 20 eV and 0.1 eV energy steps. Data were analysed and deconvoluted with Avantage software. X-ray diffraction (XRD) patterns were obtained using a D8 Advance diffractometer (Bruker Inc., Germany). The XRD patterns were obtained in a diffraction angle (2θ) range from 3° to 40°.

Some functional properties of chitosan films grafted with aldehydes such as optical, swelling, water contact angle, surface morphology and thermal properties were studied. Optical properties were determined through CIELAB colour coordinates using a CR-300 Minolta Chroma meter® (Minolta Camera Co. Ltd., Osaka, Japan), and apparent opacity of the films measured as the area under the absorption curve (Au × nm) in the UV-visible wavelengths (190-800 nm). The spectra were recorded with an Agilent 8453 UV-visible spectrophotometer (Agilent, Barcelona, Spain).

Swelling of the films in water buffered at pH 3, 4 and 7 at 23 °C was described by water uptake (WU) and surface area increase (SA): WU or SA (%) = [(Ms- Mf)/Mf] x 100, where Ms is the mass or area of the film in the swollen state at equilibrium and Mf is the mass or area of this film after drying to constant weight in $P_2O_5$. Samples were analysed in triplicate and the results given as average value ± standard deviation.

Contact angle (CA) was measured using an OCA 15EC goniometer (DataPhysics Instruments HmbH, Filderstadt, Germany). A 2 µL water droplet was dispensed onto the film surface, and the drop image was recorded for 2 min. The CA at 60 and 120 s was estimated by using the SCA20 embedded software module.

Thermogravimetric Analysis (TGA) was employed to test the thermal stability of the films after grafting, using a Q5000 v.3.17 (TA Instruments, USA). A film sample of 10 mg was placed in an aluminium pan and heated from room temperature to 500 °C at 10 °C/min under a nitrogen atmosphere.

### 3.4. Quantification of aldehydes grafted to the films.

The incorporation of aldehydes to chitosan films, measured as degree of substitution (DS, %), was estimated with the C/N ratio by using a CHN elemental analyser (CE Instruments EA 1110, Thermo Fisher Scientific, Waltham, MA, USA). The degree of deacetylation (DD), expressed as free glucosamine units per N atom unit of nt-CS films was also evaluated by elemental analysis. DD and DS were calculated according to previous studies [13–15]. DS was defined as the percentage of incorporated aldehydes respect to glucosamine units of chitosan films. For that, it was assumed that the free amino groups present in the matrix, determined by DD, could be susceptible to modification. The DS (%) was calculated as follows:

$$DS\ (\%) = \frac{((C/N)_{grafted} - (C/N)_{control})}{n}/DD$$

where (C/N) $_{grafted}$ is the C/N ratio of the imine-chitosan films and (C/N) $_{control}$ is the ratio of control reacted CS films, while "n" refers to the number of carbons of the incorporated compound. Additionally, the DS of imine-chitosan films was also calculated after film immersion in neutral (pH 7) and acid solution (pH 4) for 7 days at 23 °C. To calculate DS, it was used the C/N ratio of imine-chitosan films after hydrolysis and the C/N ratio of control reacted CS films subjected to the same hydrolytic treatment.

### 3.5. Evaluation of pH-responsive release of aldehydes from imine-chitosan films

#### 3.5.1. Static and dynamic release

The effect of the pH on triggering the hydrolysis of formed C=N bonds and the release of the volatiles anchored to the film to the surrounding atmosphere, was studied by gas chromatography (GC). A static and a dynamic assay were carried out to study the release of the volatiles (**Figure 2**). In the static assay, 0.5 g of CSBZ or CSCT film was immersed in 10 mL of buffered solution (pH 4 or 7) previously placed in a 250 mL glass jar which was hermetically closed with a twist-off cap having an inserted septum for sampling the volatile release to

the headspace of the closed jar. Sampling was carried out with a 500 µl gas syringe at days 1, 3 and 7 and the volatile analysed by GC.

For the dynamic assay, 0.25 g of CSBZ films were placed in the jars, but in this case the caps were equipped with two septa to allow a 15 mL/min nitrogen flux streams enter and flows up the jar. Prior to enter the jar, the nitrogen flux was bubbled in distilled water to provide it with a high humidity content. The concentration of aldehyde in the flux that flows up the jar was monitored by GC, taking samples with a 500 µl gas syringe at different time intervals. The temperature of the assays was carried out at 23 °C.
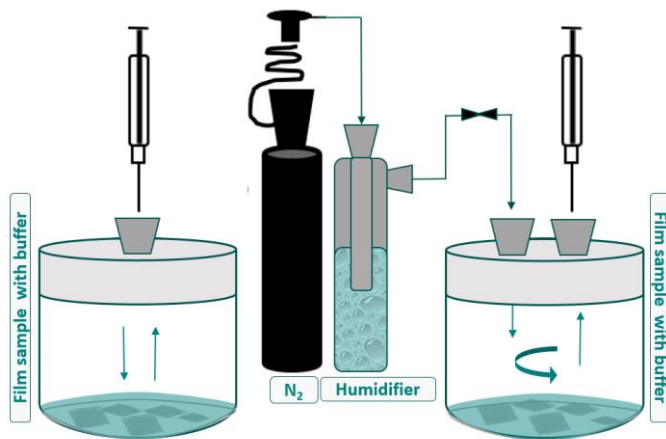


**Figure 2.** Scheme of the GC assays for characterization of aldehyde release at several pH in static (A) and dynamic (B) headspace sampling.

### 3.5.2. Gas chromatography analysis

The collected samples from the headspace of the jars were injected manually in the inlet of a gas chromatograph 6850 Series II Network GC System (Agilent Technologies, Palo Alto, CA, USA) equipped with a flame ionization detector (FID) and a Restek RTX1 capillary column (30 m x 0.53 x 5 µm) with a flow rate of 14.6 mL/min using helium as carrier gas. Chromatographic conditions were as follow: 220 °C of temperature in the injector and FID, splitless injection and temperature of oven was from 35 to 220 °C. A calibration curve was previously obtained by injecting known amounts of citral and benzaldehyde. All analyses were carried out in triplicate.

*3.6. Antifungal assays*

*3.6.1. In vitro antifungal activity of aldehydes*

The fungal strains were grown and maintained on PDA in plastic Petri dishes (9 cm diameter) for 7 days at 26 °C. A conidial suspension of $10^6$ spores/mL of each fungal strain were prepared by washing the fungi colonies surface of with sterile peptone water containing 0.05% (*v/v*) of Tween 80 and spore concentration was adjusted using the improved Neubauer method (Bright-Line Hemacytometer, Hausser Scientific, Horsham, PA).

The antifungal activity of aldehydes was evaluated by the micro-atmosphere method in petri dish with 15 mL of sterile PDA. For that, the minimum fungicidal concentration (MFC) of the aldehydes were determined. MFC has been defined as the amount of volatile, as volume, per plate that completely inhibits the fungal growth after 10 days of incubation. The test was carried out inoculating the petri dishes with 3 µL of conidial solution in three equidistant points. Different volumes of each aldehyde were added to 50 mm of sterile paper filter discs and placed on the lid of a Petri dish. The plates were sealed with Parafilm® to decrease the volatile agent loss and incubated at 26 °C for 10 days. Controls were prepared without aldehyde and the test were carried out in triplicate.

*3.6.2. In vitro antifungal activity of imine-chitosan films*

The antifungal response of imine-chitosan films was tested against the above fungal strains, and evaluated at different pHs. The assay was performed employing two Petri dishes of different diameter. One Petri dish with a diameter of 6 cm, filled with PDA medium and inoculated with 3 µL of the spore solution, was placed into an empty petri dish of 9 cm of diameter, then, 0.1 g of film was placed in the largest Petri dish. The films were covered with 5 mL of buffer solution at different pH (7 and 4) to trigger the hydrolysis of the imine bond, and the release of the antifungal aldehyde to the headspace of the system. Two controls, one without films and another with a CS films were used. Samples were incubated at 26 °C for 7 days and plates were inspected for fungal growth after 3, 5 and 7 days of incubation. All experiments were performed in triplicate.

## 4. Results and Discussion

### 4.1. Appearance of chitosan films

Chitosan acetate films suffered shrinkage and became brittle when were neutralized with NaOH. This fact has previously been reported by other authors [16]; when neutralized chitosan films were subjected to ethanol as reaction medium, they became more brittle but they did not shrink, and their dimensional stability remained constant when compared with neutralized films without being subjected to ethanol reaction medium. The films obtained after reaction with aldehydes and also the control were homogeneous and without cracks or discontinuities. CSCT films were coloured.

### 4.2. Characterization of imine-chitosan films

FTIR spectra of CS control and imine-CS films are shown in **Figure 3**. The spectra have been maximized at 1025 cm$^{-1}$, a characteristic peak of polysaccharide structure of chitosan. An overlapping and wide broadband due to O-H and N-H vibrations appear in the range of 3600 to 2600 cm$^{-1}$. Also, a clear peak appears at 2918 and 2874 cm$^{-1}$ which is due to C-H stretching vibration of chitosan. In the IR spectrum of CS, the peaks at 1644 and 1582 cm$^{-1}$ are attributed to the amide I and -$NH_2$ bending, respectively [17]. In addition, characteristic absorption bands of chitosan appeared at 1151, 1025 and 895 cm$^{-1}$, which are associated to the glycosidic ring characteristic of chitosan saccharide structure [18]. After aldehyde immobilization a sharp novel peak was observed at 1645 and 1639 cm$^{-1}$ in CSCT and CSBZ films, respectively, which can be attributed to Schiff base (-CH=N-) formation [19], whereas a change was observed in the band of -$NH_2$ at 1582 cm$^{-1}$ in both films due to its involvement in -CH=N- formation. The overlapping of absorption band of imine bond and amide group, around 1640 cm$^{-1}$ makes difficult the identification of each peak. However, an increase in the relative intensities of imine band was observed using 1025 cm$^{-1}$ as a reference peak respect to amide of CS films ($I_{1644}/I_{1025}$: 0.44 for CS, $I_{1639}/I_{1025}$: 0.70 for CSBZ and $I_{1645}/I_{1025}$: 0.66 for CSCT).
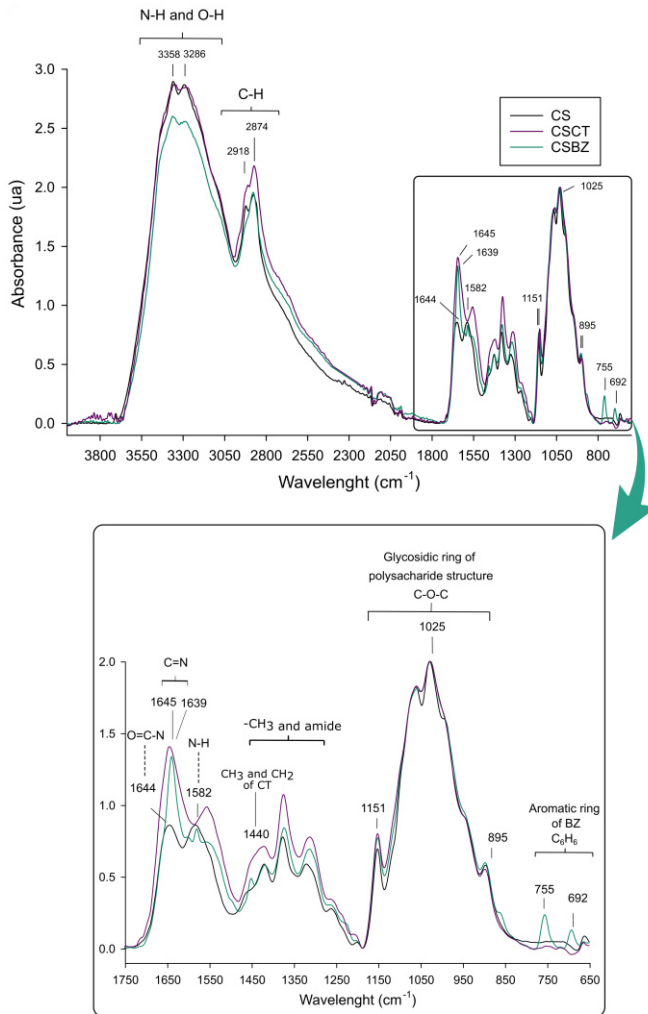
**Figure 3.** ATR-FTIR spectra of untreated chitosan films (CS) and after modification with benzaldehyde (CSBZ) and citral (CSCT) in the range of 4000-600 cm$^{-1}$. Zoom in the range of 1750-600 cm$^{-1}$.

**Figure 4** shows the spectra of free aldehydes, reacted CS control and films grafted with aldehydes. The peak associated to aldehyde group (-CH=O) was not observed in the spectra of CSCT and CSBZ films, which implies there is no unreacted aldehyde in the modified film after the washing step. Characteristics peaks of BZ can be observed in CSBZ films at 755 and 692 cm$^{-1}$ corresponding to the aromatic ring of

benzaldehyde [18]. In CSCT films, a new peak at 1440 cm$^{-1}$ appears as a shoulder due to the aliphatic chain of citral.
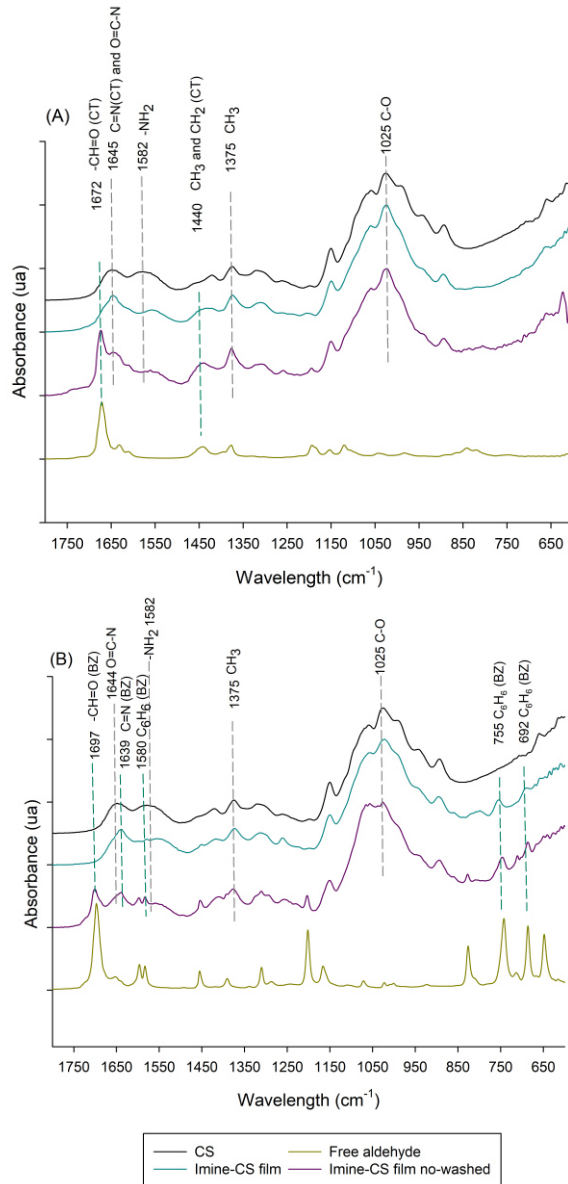


**Figure 4.** FTIR spectra of control CS film, free aldehyde, and imine-chitosan before and after washing step. (A) Spectra for citral and citral-chitosan films. (B) Spectra for benzaldehyde and benzaldehyde-chitosan films.

The spectra of control CS before and after being submitted to reaction conditions are depicted in **Figure 5** without appreciating any change in the peaks due to the reaction processing parameters.
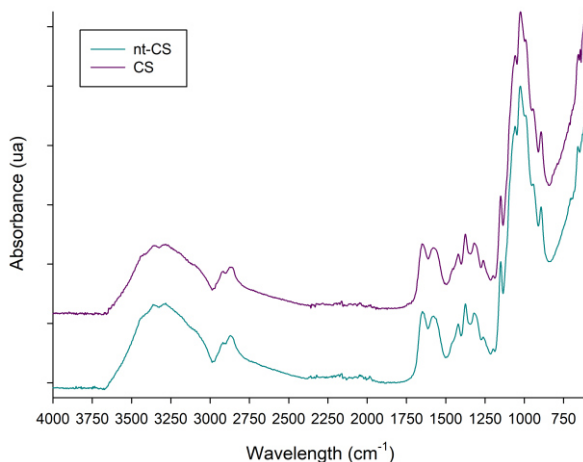


**Figure 5.** FTIR spectra of neutralized chitosan film (nt-CS) and the same one (CS) after being subjected to the reaction medium.

XPS spectroscopy was used to confirm the formation at the surface of CS films of imine bonds by condensation of aldehydes with amine groups of chitosan. For that, the N1s spectra of CS, CSCT and CSBZ were deconvoluted and depicted in **Figure 6**. XPS elemental composition of the films is displayed in **Table 1**. The deconvoluted N1s envelope for CS films shows three peaks, the one appearing at 399.4 eV is characteristic of $-NH_2$ species and reveals a great amount of amino groups at the surface of the films [20]. The peak appearing at 400.4 eV is ascribed to -NH- species and associated to acetamide groups (O=CH-NH-) present in partially deacetylated chitosan. The calculated acetylation degree of chitosan used in this study was around 21%, being in the range provided by the supplier (25-15%), which implies a large number of non-acetylated amino groups as observed above. The third and minor peak at 402.2 eV corresponds to residual protonated nitrogen species [21], and represents $-NH_3^+$ groups that were not neutralized during the treatment of CS films with NaOH. After grafting CT and BZ onto the surfaced of CS films, the deconvoluted N1s spectrum showed

a decrease in the peak at 399.4 eV and the appearance of a new peak at 398.8 eV which is attributed to the formation of imine bonds (-CH=N-) [22]. After the attachment of aldehydes, the peak at 402.2 eV corresponding to $N^+$ species suffered an increase which can be related to protonated imine linkages [23], due to the reaction medium was acidified.
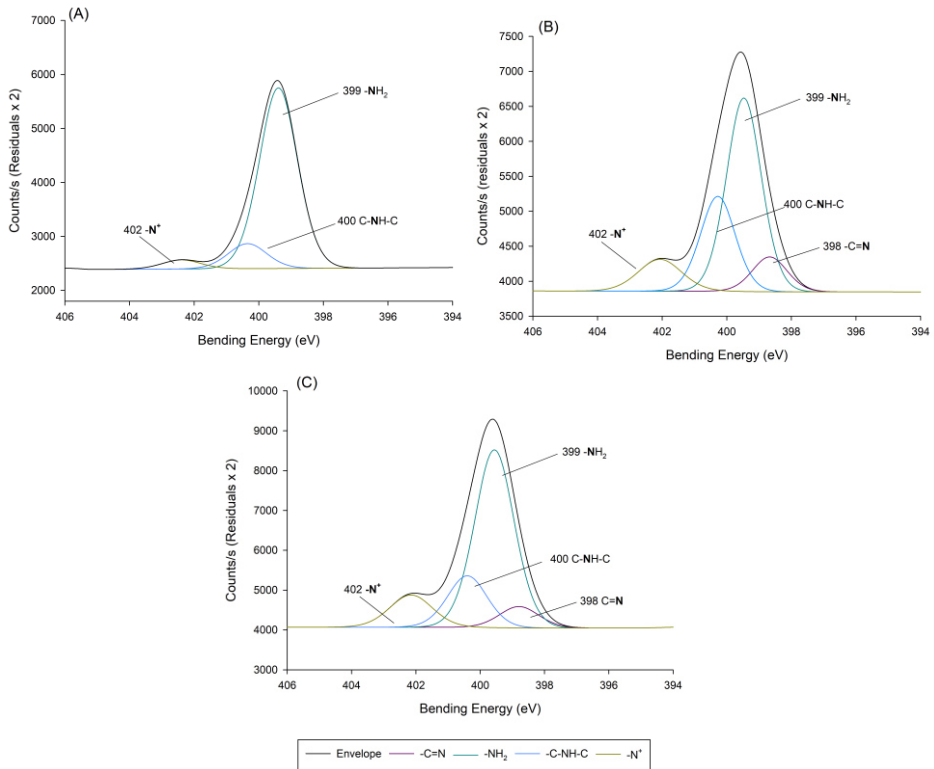


**Figure 6.** XPS N1s spectra of control chitosan films (A) and after modification with citral (B) and benzaldehyde (C).

**Table 1.** XPS elemental composition of control chitosan and imine-chitosan films.

| Film | C (%) | N (%) | O (%) | C/N |
|------|-------|-------|-------|------|
| CS   | 64.3  | 6.1   | 29.7  | 10.6 |
| CSCT | 67.5  | 3.9   | 28.5  | 17.1 |
| CSBZ | 65.5  | 5.3   | 29.2  | 12.3 |

Diffractograms of control neutralized CS films after the reaction step and those modified with BZ and CT are represented in **Figure 7**. Films grafted with BZ and CT showed a strong reflection at $2\theta = 6°$ for CSBZ films and at a lower degree for CSCT film. Similar reflection peaks were described by Zong et al. [24] for acyl chitosans synthetized in pyridine/chloroform reaction medium. The authors suggested a new type of ordering structure for the new strong reflection peaks. They hypothesised a structure with the side chains being interdigitated with each other forming a layered structure and the main chitosan polymer chains extended.
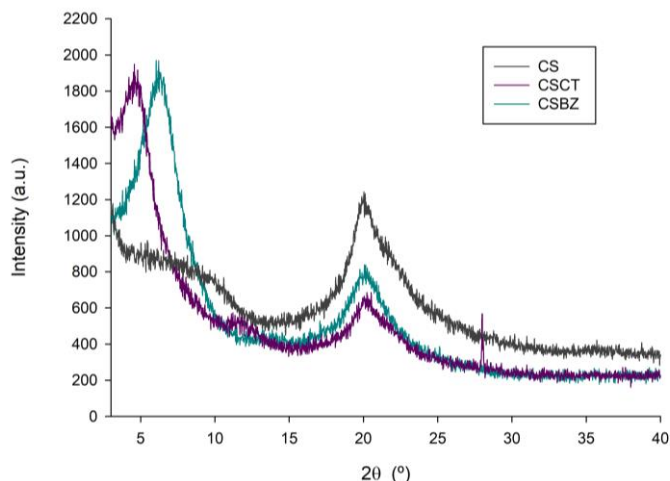


**Figure 7.** XRD patterns of chitosan films grafted with citral and benzaldehyde.

Optical properties of unreacted and reacted control films, and CSCT and CSBZ films including the colour parameters lightness, hue and Chroma and opacity values are displayed in **Table 2**. In general, films were transparent and homogeneous to the naked eye. Chemical processing of control chitosan films did not affect to its transparency and colour properties. However, optical properties were affected after grafting aldehydes. Chitosan films increased their opacity and developed yellow-orange colour after grafting of CT.

Previous studies in the bibliography have reported coloured Schiff base for chitosan films and hydrogels with $\alpha,\beta$-unsaturated aldehydes [25]. Schiff base formed with CT possesses a conjugated imine and olefin chromophores contributing to the colour development of the films. Films grafted with BZ did not develop any colour neither increased their transparency. However, opacity values in the UV region (190-399 nm) increased for CS films after grafting.

Water uptake (WU) and surface area (SA) of neutralized, and reacted chitosan control films (nt-CS and CS, respectively) and films grafted with CT and BZ were evaluated after immersion in buffered solutions at pH 7 and 4 at 23 °C (**Table 3**).

Neutralized chitosan films absorbed a considerable amount of water at pH 7 due to the presence in its structure of hydroxyl and amine groups. After the chemical reaction step in ethanol without aldehydes, the films maintained dimensional stability and swelling properties. When chitosan films were grafted with CT and BZ the water absorbed was reduced markedly due to the hydrophobic character of the aldehydes attached. Since chitosan is a cationic polymer with a pK of 6.5, the protonation of chitosan amino groups at pH 4 increased the amount of water absorbed by all the films. Swelling of CSCT films was lower than that for CSBZ films due to the higher lipophilicity conferred by CT [26].

**Table 2.** Optical properties of chitosan and imine-chitosan films.

| Films | L*(D65) | C*(D65) | $h^o$ (D65) | Opacity (A x nm) | |
|---|---|---|---|---|---|
| | | | | UV (190-399 nm) | VISIBLE (400-800 nm) |
| nt-CS | 94.9 ± 1.1[c] | 4.7 ± 1.1[a] | 102.8 ± 0.5[a] | 209 ± 6.2[a] | 30.1 ± 2.2[a] |
| CS | 95.9 ± 0.1[c] | 5.6 ± 0.6[a] | 104.6 ± 0.5[b] | 225.3 ± 11.6[a] | 33 ±3.2[a] |
| CSCT | 72.7 ± 0.5[a] | 69.7 ± 0.7[c] | 84 ± 0.7[a] | 796.1 ± 10.5[c] | 165.4 ± 7.8[b] |
| CSBZ | 89.9 ± 1.2[b] | 8.3 ± 0.5[b] | 103.2 ± 0.2[b] | 537.6 ± 9.1[b] | 41.1 ± 5.4[a] |

[a-d] Different superscript letters in the same column indicate a statistically significant difference ($P \leq 0.05$)

**Table 3.** Water uptake (WU) and surface area (SA) of controls and grafted films subjected at pH 4 and 7 for 24 h at 23 °C.

| Films | WU (%) | | SA (%) | |
|---|---|---|---|---|
| | pH 4 | pH 7 | pH 4 | pH 7 |
| nt-CS | $297.9 \pm 19.7^d$ | $258.6 \pm 10^d$ | $126.5 \pm 12^b$ | $114.6 \pm 14.0^b$ |
| CS | $267.9 \pm 8.4^c$ | $236.9 \pm 6.2^c$ | $126.5 \pm 9.3^b$ | $105.8 \pm 8.9^b$ |
| CSCT | $180.4 \pm 6.3^a$ | $134.9 \pm 9.6^a$ | $94.6 \pm 6.5^a$ | $20.2 \pm 7.3^a$ |
| CSBZ | $219.9 \pm 9.3^b$ | $174.9 \pm 6.5^b$ | $101.5 \pm 8.7^a$ | $36.8 \pm 8.6^a$ |

[a-d] Different letters in the same column indicate a statistically significant difference. Results are based on a one-way analysis of variance (ANOVA) using the Tukey *b* test with a level of P ≤0.05.

CSCT films immersed in aqueous solution buffered at pH 7 and 4 reached swelling equilibrium before 24 h, CSBZ film immersed at pH 7 showed the same behaviour. After 7 days of immersion in aqueous buffered solutions at pH 4 and 7 the films maintained their dimensional stability. When films were tested at pH 3 (**Figure 8**), CS films dissolve after 15 min of immersion in the buffer, whereas CSBZ films dissolved after 30 min. CSCT films kept stable and swell but not dissolved, reaching swelling equilibrium after 2 h of immersion. The stability of the films at pH 3 could be due to the crosslinking properties of CT in an excess of amino groups [27]. That is, films could be crosslinked due to 1,2 and 1,4 additions of amino groups of CS to the same molecule of CT. CSCT films reached swelling equilibrium after 2 h of immersion in the buffer, retaining around 320% of water. Regarding the dimensional stability of the films in buffered media and measured as surface area increase, it was considerably reduced after grafting aldehydes as can be seen in **Table 3**, being these reductions higher at pH 7 and for films modified with CT.
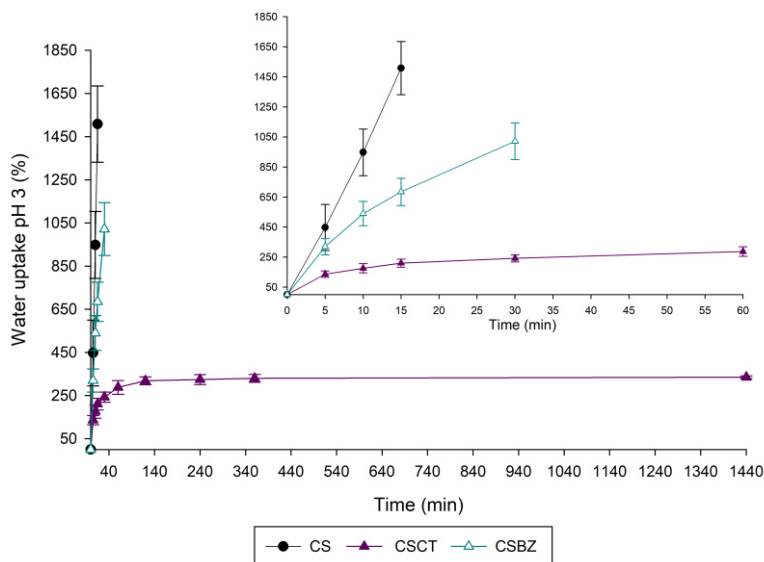
**Figure 8.** Swelling behaviour of chitosan and imine-chitosan films with citral (CSCT) and benzaldehyde (CSBZ) immersed in buffered aqueous solution at pH 3 and 23 °C.

Contact angle measurements provide information about the hydrophobicity of film surface. Chitosan is a hydrophilic polymer and grafting of hydrophobic aldehydes is expected to produce some modification to the film surface wettability. Contact angle (CA) at 60 and 120 s for reacted control chitosan films and films modified with CT and BZ is depicted in **Table 4**. Contact angle of all the films were < 90° which is typical of hydrophilic surfaces; CA of a solid surface is expected to increase when is modified with hydrophobic compounds, however contact angle for CSBZ was similar to reacted control chitosan film at 60 s, whereas CA of CSCT film was slightly lower. The CA value for reacted control chitosan films is around ten units lower than the values found in the in the bibliography for chitosan acetate films neutralized with NaOH [28,29]. The wettability of a solid surface is affected by its chemical structure and roughness, and according to Wenzel, (1936) CA tends to decrease with roughness for hydrophilic surfaces. Chemical processing of the films in ethanol could increase roughness of the films as reported by Nosal et al. [31]. It was observed

that CA of reacted control CS film at 120 s decreased to lower values than those obtained for CSCT and CSBZ films after this time. The greater resistance to deformation and disappearance of the water droplet into grafted films could be consequence of grafting hydrophobic aldehydes.

**Table 4.** Contact angle with water of control chitosan film (CS) and modified film with citral (CSCT) and benzaldehyde (CSBZ) for 60 and 120s.

| Films | Contact angle ($^0$) | |
|---|---|---|
| | $CA_{60}$ | $CA_{120}$ |
| CS | $82.7 \pm 1.1^b$ | $65.3 \pm 3.3^a$ |
| CSCT | $77.9 \pm 1.1^a$ | $74.1 \pm 1.2^b$ |
| CSBZ | $82.5 \pm 1.5^b$ | $77.4 \pm 1.1^b$ |

[a-b] Different superscript letters in the same column indicate a statistically significant difference.

TGA analyses were carried out to study the effect of grafting BZ and CT on the thermal stability of CS films in the range of temperatures of 25-500 °C (**Figure 9**). The thermal parameters extracted from the thermograms are displayed in **Table 5**. Imine-chitosan films had a similar degradation pattern than chitosan films. Grafted films suffered a first thermal event in the same temperature range than CS films with a mass loss of aprox. 3-4% which was slightly lower than for CS films, and it can be due to the grafted aldehydes confers some hydrophobicity to the films. The second and most important thermal even happened in the same range of temperatures for films grafted with BZ (200-350 °C), but the maximum rate of decomposition occurred at a lower temperature of 277 °C, and films lost weight more slowly. Several authors have also reported this thermal behaviour for Schiff bases of aldehydes and chitosan [32,33]. A similar behaviour was observed when CT was grafted to CS films but the maximum rate of decomposition occurred at 260 °C in the range 175-350 °C.
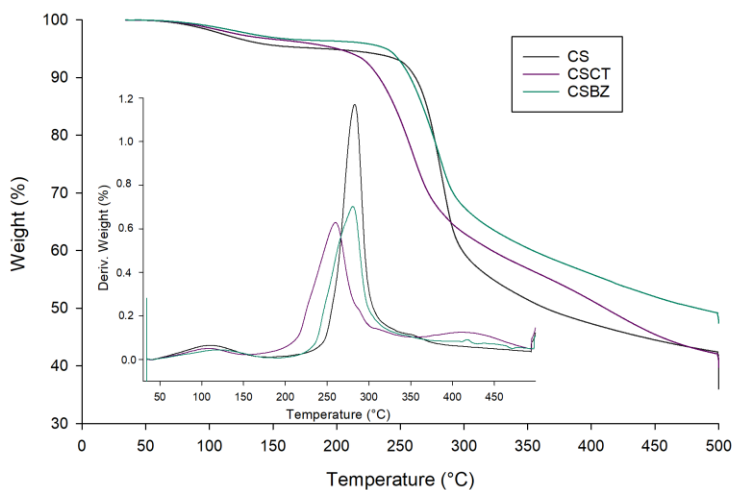
**Figure 9.** TG/DTG curves of chitosan films, and after covalent grafting with citral and benzaldehyde.

It is well known that aromatic structures are more stable to thermal degradation than aliphatic double bonds which could explain differences in the degradation temperature of modified films. However, it is difficult to compare their thermal stability since they also have a different degree of substitution. An additional degradation process appears as a broad minimum peak in the high temperature side of the main peak for functionalized films, with the maximum loss weight rate at 420 °C and being more evident for films.

**Table 5.** Thermal parameters for chitosan and imine-chitosan films.

| Film | First stage | | | Second stage | | |
|---|---|---|---|---|---|---|
| | Temperature range (°C) | $T_{max}$ (°C) | Weight loss (%) | Temperature range (°C) | $T_{max}$ (°C) | Weight loss (%) |
| CS | 25-175 | 110.2 | 5.2 | 200-500 | 283 | 52.6 |
| CSCT | 25-150 | 106.1 | 3.7 | 175-350 | 260 | 38.1 |
| CSBZ | 25-175 | 112 | 3.7 | 200-350 | 277 | 39.2 |

*4.3. Quantification of aldehydes grafted to chitosan films.*

The amount of CT and BZ covalently attached to chitosan films was given as the degree of substitution (DS, %) of the aldehydes to chitosan films by using the C/N relationships described in experimental section and obtained through elemental analysis, the data are displayed in **Table 6**. In the same table also appears these data for CS, CSCT and CSBZ films after being subjected to hydrolysis at pH 7 and 4 for seven days at 23 °C.

The substitution of aldehydes to unreacted chitosan films was confirmed by the increases in the atomic ratios of carbon to nitrogen of CSCT films (10.0) and CSBZ films (7.9), compared with those of CS films (5.5). Regarding the degree of substitution (DS) of CT and BZ to chitosan films, the content of CT and BZ reached values of 57% and 43%, respectively, these data are in accordance with the spectroscopic observations revealing grafting of aldehydes to chitosan through imine bonds. The higher values found for CT can be explained because this aldehyde is an α,β-unsaturated carbonyl and thus, highly reactive with nucleophiles, moreover, besides forming adducts through 1,2 carbonyl addition, they can also undergo 1,4-conjugate addition, commonly known as Michael addition [34].

DS values decreased after subjecting imine-chitosan films to different pH treatments. The hydrolysis of imine bond was limited at pH 7, obtaining DS reductions of 16.8 and 7.4% in CSBZ and CSCT films, respectively. These values were higher for imine-chitosan films triggered at pH 4. The DS value of CSBZ films was reduced from 43.4 to 1.6%, and from 56.2 to 37.1% for CSCT films. These results are in agreement with other studies reporting the greater stability of imine bonds at neutral pH [35,36].

The higher decreased of DS values for CSBZ (96%) compared with CSCT films (34%) can be due to the formation of Michael adducts between CT and CS that cannot be hydrolysed as imine bonds.

In a media with a high amount of primary amine groups as chitosan films, α, β-unsaturated aldehydes can experience 1,2 and 1,4 addition of amino groups of chitosan to the same molecule, exerting a crosslinking effect that is supported by the low hydrolysis degree of CSCT film and its stability and low swelling at pH 3.

Furthermore, imine bonds created from CT are more stable to hydrolysis due to the resonance stabilization through conjugation with the α,β-carbon-carbon double bond. In this line, Chen et al. [37] reported that α,β-unsaturated aldehydes citral and cinnamaldehyde, anchored to chitosan emulsions were more stable and less hydrolysable at several pH than citronellal, a saturated terpene, or vanillin, an aromatic compound.

**Table 6.** Elemental analysis and degree of substitution (DS) of neutralized chitosan films (nt-CS), reacted chitosan films without aldehydes (CS) and those modified with benzaldehyde and citral (CSBZ and CSCT) before and after immersion in buffered aqueous medium at pH 7 and pH 4 for one week at 23 °C.

| Films | N (%) | C (%) | H (%) | C/N | DS (%) |
|---|---|---|---|---|---|
| nt-CS | 7.8 ± 0.2[g] | 43 ± 1.5[b] | 7.5 ± 0.7[cd] | 5.5 ± 0.3[a] | - |
| CS | 7.7 ± 0.1[g] | 43.6 ± 0.1[bc] | 7 ± 0.0[bc] | 5.7 ± 0.0[a] | - |
| CSCT | 5.4 ± 0.1[b] | 53.7 ± 0.2[f] | 7.7 ± 0.1[d] | 10 ± 0.1[e] | 57.2 ± 1.3[e] |
| CSBZ | 6.4 ± 0.0[e] | 50.6 ± 0.4[e] | 6.5 ± 0.1[a] | 7.9 ± 0.0[c] | 43.4 ± 0.3[c] |
| CS pH7 | 6.6 ± 0.0[f] | 38 ± 0.6[a] | 6.8 ± 0.1[ab] | 5.7 ± 0.1[a] | - |
| CSCT pH7 | 5.7 ± 0.1[c] | 54.3 ± 0.2[f] | 7.7 ± 0.1[d] | 9.6 ± 0.2[d] | 49.1 ± 2.3[d] |
| CSBZ pH7 | 6.2 ± 0.1[d] | 47.5 ± 0.2[d] | 6.5 ± 0.1[a] | 7.7 ± 0.1[c] | 35.2 ± 1.0[b] |
| CS pH4 | 5.2 ± 0.0[b] | 37.1 ± 0.2[a] | 6.5 ± 0.0[a] | 7.1 ± 0.0[b] | - |
| CSCT pH4 | 4.5 ± 0.1[a] | 45 ± 0.2[c] | 7.1 ± 0.0[bc] | 9.9 ± 0.1[e] | 36.2 ± 1[b] |
| CSBZ pH4 | 5.3 ± 0.0[b] | 38.2 ± 0.1[a] | 6.6 ± 0.1[ab] | 7.2 ± 0.0[b] | 1.6 ± 0.4[a] |

Different letters in the same column indicate a statistically significant difference. Results are based on a one-way analysis of variance (ANOVA) using the Tukey *b* test with a level of $P \leq 0.05$.

### 4.4. pH-responsive release of aldehydes from imine-chitosan films.

The amount of aldehyde that reached the headspace of the static jars after immersing CSBZ and CSCT films in aqueous solution at neutral or acidic pH is depicted in **Figure 10A** and **10B**, respectively. After seven days, the maximum concentration of CT in the headspace of the jar was 38 and 13 ng/mL·$g_{film}$, when films were immersed at pH 4 and pH 7, respectively. While the release of benzaldehyde reached 414 ng/mL·$g_{film}$ at pH 4, and 203 ng/mL·$g_{film}$ at pH 7. The concentration of BZ in the headspace of the static jar was much higher when imine-

chitosan films were immersed in buffered aqueous solution at pH 4 which evidences that the reversibility of the imine bond is favoured in acidic media. Hydrolysis of Schiff base carrying BZ is also more prone to be hydrolysed that when carrying CT as commented above. Thus, these results are in accordance with those obtained determining the DS of the films after being exposed to acidic and neutral pH for one week, and finding that a greater amount of each aldehyde in the headspace of the jar is related to higher reductions of DS. Moreover, the concentration of each aldehyde in the headspace of the jar is also influenced by the vapour pressure of each volatile and its solubility in the aqueous phase where is firstly release before reaching the gas phase. In this regard, BZ has a greater vapour pressure than CT (1.270 and 0.091mm Hg at 25 °C, respectively), whereas the maximum concentration of BZ and CT in the vapour phase was calculated in the current study at 23 °C, being 5643.9 ± 8.8 ng/mL and 1173.5 ± 8.5 ng/mL, respectively.

Related to the retention of the aldehyde in the aqueous solution, the partition coefficient at equilibrium between n-octanol and water (log P) of CT is higher than for BZ being expected to be less retained in the aqueous phase. Previous studies have reported that the chemical structure of the aldehyde may affect the stability of the Schiff base structure. Chen et al. [37] reported chitosan Schiff bases of α,β-unsaturated aldehydes citral and cinnamaldehyde are more stable and less hydrolysable at several pH than the saturated terpene citronellal, and the aromatic compound vanillin.

The dynamic assay was only carried out with CSBZ films at pH 7 and 4. When working in a dynamic system, a flow of an inert gas is introduced and the volatile does not accumulate in the headspace, and the film releases volatile into the air until exhausted.

The dynamic approach allows to monitor the kinetics of volatile release from the film. In the system used for the assay, equilibrium between the different phases is not reached and the BZ released to the headspace of the jar is continuously removed by the $N_2$ flux passing through the container.
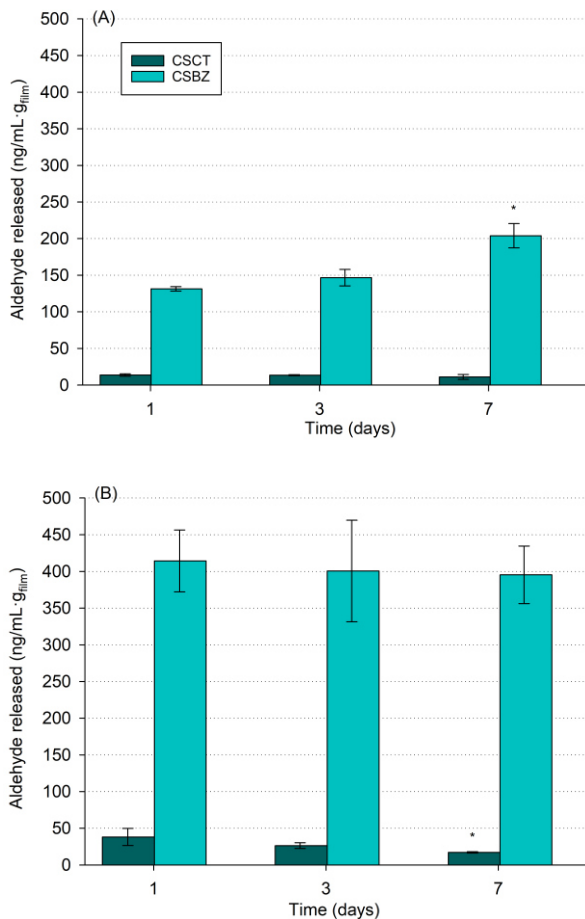
**Figure 10.** Aldehyde released from imine-chitosan films triggered at pH 7 (A) and 4 (B) measured in a static assay for 7 days at 23 °C. Bars with * indicate significant differences between different times for each film.

Samples of 500 µL were collected from the headspace of the jar for 144 h and the concentration of BZ over time (mg/h·$g_{film}$) is displayed in **Figure 11**. The maximum amount of BZ found in the headspace of the jar was reached after 2 h of triggering the films with buffered solutions at pH 4 and 7. Then, concentration of BZ began to decrease progressively, being more accused when the hydrolysis occurred at pH 4.
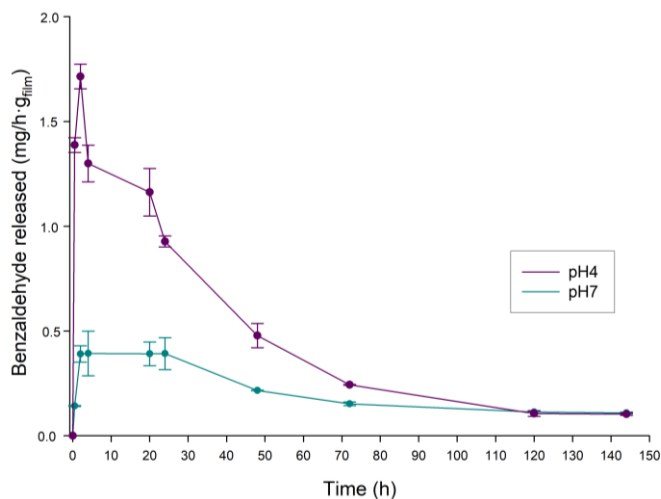
**Figure 11.** Release of benzaldehyde triggered at pH 4 and 7 from imine-chitosan films and measured in a dynamic assay carried out for 144 h at 23 °C with a constant $N_2$ flux of 15 mL/min.

After 120 h the amount of BZ reached similar values at both pHs. The total amount of BZ released from the films has been depicted in **Figure 12**, where it can be clearly observed that when the hydrolysis occurred in acid media, BZ was released in a greater extent and more rapidly.
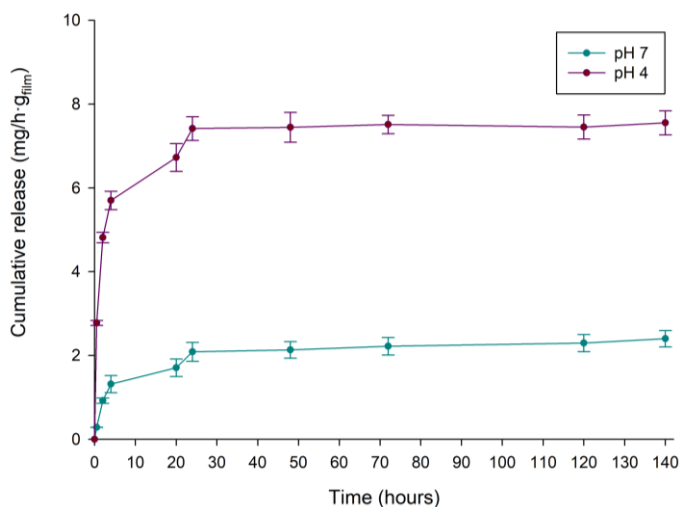


**Figure 12.** Benzaldehyde release of 0.25 g of film subjected at pH 4 and pH 7 at 23 °C for 140 h.

## 4.5. Antifungal assays

### 4.5.1. Antifungal activity of citral and benzaldehyde in vapour phase

The MFC of aldehydes against both mould was determined in vapour phase. *B. cinerea* resulted more sensitive than *P. expansum* to the aldehydes tested, MFC of 10 µL CT/plate and 7.50 µL BZ/plate were necessary to exhert a fungicidal effect on *B. cinerea*, whereas these concentrations were of 15 µL CT/plate and 10 µL BZ/plate for *P. expansum*. In view of the data, benzaldehyde presented greater antifungal activity against the tested fungi which has been attributed to the presence of the aromatic ring in its structure [38]. The antifungal activity of both aldehydes has previously reported by other authors [39,40].

### 4.5.2. Antifungal activity of imine-chitosan films

The antifungal activity of CSCT and CSBZ films was tested *in vitro* against the above fungi using the double Petri dish system described in material & methods section. Then, the mould was exposed to the micro-atmosphere created by the aldehyde released from the triggering aqueous buffered medium (pH 7 and 4) were the film previously was placed. No difference between control and control with unmodified chitosan films was observed, and hence only the values of control without films were reported.

**Table 7** shows the antifungal effect of imine-chitosan films triggered at different pH and was measured as the evolution of mould colony diameter for 7 days at 26 °C. Total growth inhibition against *P. expansum* and *B. cinerea* was achieved with CSBZ films subjected at pH 4, but its activity was limited when were immersed at pH 7. No fungicidal activity was observed for CSCT films even when triggered at pH 4, although in this case, a slight inhibition of the growth could be observed and was more noticeable at the third day of storage.

**Table 7.** Diameter of *P. expansum* and *B. cinerea* colony when subjected to imine-chitosan films grafted with benzaldehyde and citral triggered at pH 4 and 7.

| Films | pH | Diameter of *P. expansum* colony (cm) | | |
|---|---|---|---|---|
| | | Day 3 | Day 5 | Day 7 |
| Control | - | 2.3 ± 0.1[c] | 5.1 ± 0.1[b] | 5.4 ± 0.1[b] |
| CSCT | 7 | 2.1 ± 0.1[c] | 4.8 ± 0.1[b] | 5.1 ± 0.1[b] |
| | 4 | 1.4 ± 0.1[a] | 4.3 ± 0.6[a] | 4.8 ± 0.3[a] |
| CSBZ | 7 | 1.6 ± 0.1[b] | 4.2 ± 0.1[a] | 4.8 ± 0.1[a] |
| | 4 | - | - | - |
| | | Diameter of *B. cinerea* colony (cm) | | |
| | pH | Day 3 | Day 5 | Day 7 |
| Control | - | 3.4 ± 0.1[c] | 5.5 ± 0.1[b] | 5.5 ± 0[b] |
| CSCT | 7 | 2.2 ± 0.2[b] | 5.4 ± 0.1[b] | 5.5 ± 0.1[b] |
| | 4 | 0.7 ± 0.1[a] | 4.2 ± 0.4[a] | 4.3 ± 0.8[a] |
| CSBZ | 7 | 0.7 ± 0.1[a] | 4.3 ± 0.1[a] | 4.8 ± 0.1[ab] |
| | 4 | - | - | - |

Different letters in the same column indicate a statistically significant difference. Results are based on a one-way analysis of variance (ANOVA) using the Tukey *b* test with a level of P ≤0.05.

Morphological changes can be appreciated in the colonies growth in the presence of the films after seven days of incubation (**Figure 13**), and it is explainable because even for low amounts of aldehyde released from the films they caused damage in the cell membranes and reduction in sporulation [40], showing colony colourless and lack of density of the mycelia. These results are in accordance with those obtained by elemental analysis and GC, which showed that certain amount of aldehyde is released even at neutral pH although not enough to kill the fungi assayed. The acidic environment promoted a higher release of the volatile through the hydrolysis of the imine bond. Thus, CSBZ showed the highest release and the greater antifungal inhibition.

Encapsulation of essential oils or their active components within a polymer matrix formed as a film has been the usual protocol to prepare antimicrobial films for active food packaging applications [41]. Previous studies report the incorporation of volatiles with antifungal properties found in essential oils such as citral in other polymer films such as soy protein isolates [42] and ethylene-vinyl alcohol (EVOH) [43]. Commonly, these kind of antimicrobial polymer films are based

on monolithic delivery systems where the active molecule is uniformly distributed in the polymer matrix used as a carrier. The release mechanism relies on the diffusion of the volatile through the polymer matrix to reach the surface of the film and its release to the surrounding media. However, this methodology has several drawbacks specially when working with volatile compunds.
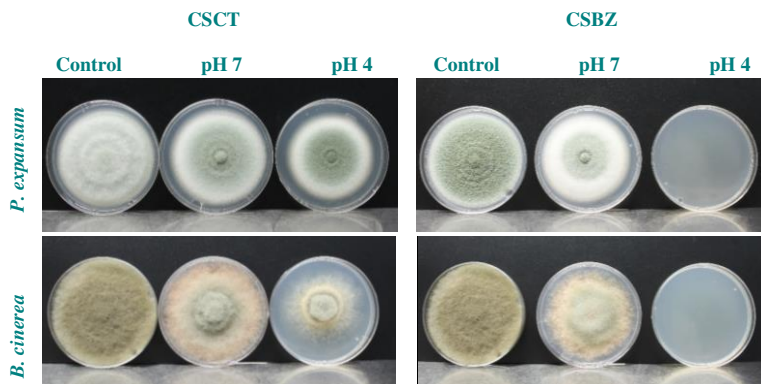


**Figure 13.** Photographs showing the antifungal effect against *Penicillium expansum* and *Botrytis cinerea* of imine-chitosan films when triggered at pH 7 and 4. Images were taken after 7 days of fungi incubation at 26 °C.

Major difficulties relies on fixing labile molecules in the polymer matrix for an indefinite time and the lack of a reliable triggering mechanism. The antimicrobial films designed in this work stabilize the active in the film by reversible covalent bonds avoiding its evaporation previous to be used in food packaging applications, and an external stimulus is required for triggering its release to the headspace of the package.

It is worthy to point out that recent studies have evaluated the potential of imine bonds as pH-responsive sustained released systems of active compounds [12,35,36,44]. However, the use of reversible covalent bonds intended for active food packaging applications is practically unexplored. According to the results obtained in this work, reversible grafting of aldehydes on chitosan films allows the development of more efficient antimicrobial films and could be applied in the design of responsive antimicrobial food packaging.

## 5. Conclusions

Dynamic covalent chemistry based on the reversibility of imine bonds has been employed to develop pH-sensitive antifungal imine-chitosan films. Volatile aldehydes with proven antifungal activity and different chemical structure, BZ and CT, have been covalently grafted onto chitosan films through imine bond formation. Subsequently, the hydrolysis of the imine bond, and the release of the aldehydes have been studied at different pH. Finally, imine-chitosan films were assayed for antifungal activity. The extent of imine bond formation depended on the chemical structure and reactivity of the aldehyde, whereas its hydrolysis also depended on it, together with the pH of the media. Moreover, α,β-unsaturated aldehydes can undergo other reactions such as Michael addition limiting the release of the molecule.

Graft films with biomolecules which may be released under external stimuli is an example of the potential of reversible covalent bonds to be used as a strategy to generate pH-responsive sustained release systems for multiple purposes, including their use to prevent fungal growth which has been the purpose of this work. The developed pH-sensitive films allow that the antifungal volatile compound remains covalently anchored to the film until its released is required and triggered by acidic pH.

## References

1.      Liu, Y.; Lehn, J.M.; Hirsch, A.K.H. Molecular Biodynamers: Dynamic covalent analogues of biopolymers. *Acc. Chem. Res.* **2017**, *50*, 376–386, doi:10.1021/acs.accounts.6b00594.

2.      Lehn, J.-M. Dynamers: Dynamic molecular and supramolecular polymers. *Prog. Polym. Sci.* **2005**, *30*, 814–831, doi:10.1016/j.progpolymsci.2005.06.002.

3.      Kolb, H.C.; Finn, M.G.; Sharpless, K.B. Click chemistry: diveverse chemical

function from a few good reactions.Pdf. *Angew. Chemie - Int. Ed.* **2001**, *40*, 2004–2021, doi:10.1002/1521-3773(20010601)40:11<2004::AID-ANIE2004>3.3.CO;2-X.

4. Xin, Y.; Yuan, J. Schiff's base as a stimuli-responsive linker in polymer chemistry. *Polym. Chem.* **2012**, *3*, 3045–3055, doi:10.1039/c2py20290e.

5. Muxika, A.; Etxabide, A.; Uranga, J.; Guerrero, P.; de la Caba, K. Chitosan as a bioactive polymer: Processing, properties and applications. *Int. J. Biol. Macromol.* **2017**, *105*, 1358–1368, doi:10.1016/j.ijbiomac.2017.07.087.

6. Shi, W.; Ching, Y.C.; Chuah, C.H. Preparation of aerogel beads and microspheres based on chitosan and cellulose for drug delivery: A review. *Int. J. Biol. Macromol.* **2021**, *170*, 751–767, doi:10.1016/j.ijbiomac.2020.12.214.

7. Paul, W.; Sharma, C.P. Chitosan, a drug carrier for the 21* Century: A Review. *STP Pharma Sci.* **2000**, *10*, 5–22.

8. Qu, B.; Luo, Y. Chitosan-based hydrogel beads: Preparations, modifications and applications in food and agriculture sectors – A review. *Int. J. Biol. Macromol.* **2020**, *152*, 437–448, doi:10.1016/j.ijbiomac.2020.02.240.

9. França, D.; Medina, Â.F.; Messa, L.L.; Souza, C.F.; Faez, R. Chitosan spray-dried microcapsule and microsphere as fertilizer host for swellable − Controlled release materials. *Carbohydr. Polym.* **2018**, *196*, 47–55, doi:10.1016/j.carbpol.2018.05.014.

10. Marin, L.; Ailincai, D.; Mares, M.; Paslaru, E.; Cristea, M.; Nica, V.; Simionescu, B.C. Imino-chitosan biopolymeric films. Obtaining, self-assembling, surface and antimicrobial properties. *Carbohydr. Polym.* **2015**, *117*, 762–770, doi:10.1016/j.carbpol.2014.10.050.

11. Demitri, C.; De Benedictis, V.M.; Madaghiele, M.; Corcione, C.E.; Maffezzoli, A. Nanostructured active chitosan-based films for food packaging applications: Effect of graphene stacks on mechanical properties. *Meas. J. Int. Meas. Confed.* **2016**, *90*, 418–423, doi:10.1016/j.measurement.2016.05.012.

12. Chabbi, J.; Aqil, A.; Katir, N.; Vertruyen, B.; Jerôme, C.; Lahcini, M.; El Kadib, A. Aldehyde-conjugated chitosan-graphene oxide glucodynamers: ternary cooperative assembly and controlled chemical release. *Carbohydr. Polym.* **2020**, *230*, doi:10.1016/j.carbpol.2019.115634.

13. Kasaai, M.R.; Arul, J.; Chin, S.L.; Charlet, G. The use of intense femtosecond laser pulses for the fragmentation of chitosan. *J. Photochem. Photobiol. A Chem.* **1999**, *120*, 201–205, doi:10.1016/S1010-6030(98)00432-8.

14. Inukai, Y.; Chinen, T.; Matsuda, T.; Kaida, Y.; Yasuda, S. Selective separation of germanium(IV) by 2,3-Dihydroxypropyl chitosan resin. *Anal. Chim. Acta* **1998**, *371*, 187–193, doi:10.1016/S0003-2670(98)00313-4.

15. Takeshita, S.; Konishi, A.; Takebayashi, Y.; Yoda, S.; Otake, K. Aldehyde Approach to hydrophobic modification of chitosan aerogels. *Biomacromolecules* **2017**, *18*, 2172–2178, doi:10.1021/acs.biomac.7b00562.

16. Takara, E.A.; Marchese, J.; Ochoa, N.A. NaOH Treatment of chitosan films: Impact on macromolecular structure and film properties. *Carbohydr. Polym.* **2015**, *132*, 25–30, doi:10.1016/j.carbpol.2015.05.077.

17. Mauricio-Sánchez, R.A.; Salazar, R.; Luna-Bárcenas, J.G.; Mendoza-Galván,

A. FTIR Spectroscopy studies on the spontaneous neutralization of chitosan acetate films by moisture conditioning. *Vib. Spectrosc.* **2018**, *94*, 1–6, doi:10.1016/j.vibspec.2017.10.005.

18.    Barbosa, H.F.G.; Attjioui, M.; Leitão, A.; Moerschbacher, B.M.; Cavalheiro, É.T.G. Characterization, solubility and biological activity of amphihilic biopolymeric Schiff bases synthesized using chitosans. *Carbohydr. Polym.* **2019**, *220*, 1–11, doi:10.1016/j.carbpol.2019.05.037.

19.    Damiri, F.; Bachra, Y.; Bounacir, C.; Laaraibi, A.; Berrada, M. Synthesis and characterization of lyophilized chitosan-based hydrogels cross-linked with benzaldehyde for controlled drug release. *J. Chem.* **2020**, *2020*, doi:10.1155/2020/8747639.

20.    Wu, Y.; Fang, Q.; Yi, X.; Liu, G.; Li, R.W. Recovery of gold from hydrometallurgical leaching solution of electronic waste via spontaneous reduction by polyaniline. *Prog. Nat. Sci. Mater. Int.* **2017**, *27*, 514–519, doi:10.1016/j.pnsc.2017.06.009.

21.    Tree-Udom, T.; Wanichwecharungruang, S.P.; Seemork, J.; Arayachukeat, S. Fragrant chitosan nanospheres: Controlled release systems with physical and chemical barriers. *Carbohydr. Polym.* **2011**, *86*, 1602–1609, doi:10.1016/j.carbpol.2011.06.074.

22.    Kehrer, M.; Duchoslav, J.; Hinterreiter, A.; Cobet, M.; Mehic, A.; Stehrer, T.; Stifter, D. XPS Investigation on the reactivity of surface imine groups with TFAA. *Plasma Process. Polym.* **2019**, *16*, 1–8, doi:10.1002/ppap.201800160.

23.    Han, M.G.; Im, S.S. X-Ray Photoelectron spectroscopy study of electrically conducting polyaniline/polyimide blends. *Polymer (Guildf).* **2000**, *41*, 3253–3262, doi:10.1016/S0032-3861(99)00531-5.

24.    Zong, Z.; Kimura, Y.; Takahashi, M.; Yamane, H. Characterization of chemical and solid state structures of acylated chitosans. *Polymer (Guildf).* **2000**, *41*, 899–906, doi:10.1016/S0032-3861(99)00270-0.

25.    Jin, X.; Wang, J.; Bai, J. Synthesis and antimicrobial activity of the Schiff base from chitosan and citral. *Carbohydr. Res.* **2009**, *344*, 825–829, doi:10.1016/j.carres.2009.01.022.

26.    Philippe, E.; Seuvre, A.M.; Colas, B.; Langendorff, V.; Schippa, C.; Voilley, A. Behavior of flavor compounds in model food systems: A thermodynamic study. *J. Agric. Food Chem.* **2003**, *51*, 1393–1398, doi:10.1021/jf020862e.

27.    Migneault, I.; Dartiguenave, C.; Bertrand, M.J.; Waldron, K.C. Glutaraldehyde: behavior in aqueous solution, reaction with proteins, and application to enzyme crosslinking. *Biotechniques* **2004**, *37*, 790–802, doi:10.2144/04375rv01.

28.    Maraschin, T.G.; Correa, R. da S.; Rodrigues, L.F.; Balzarettid, N.M.; Galland, G.B.; Regina, N.; Basso, D.S.; Alegre, P.; Alegre, P.; Alegre, P.; et al. Chitosan nanocomposites with graphene-based filler 2. Experimental Section. **2018**, *22*, 1–10.

29.    Luo, Y.; Pan, X.; Ling, Y.; Wang, X.; Sun, R. Facile fabrication of chitosan active film with xylan via direct immersion. *Cellulose* **2014**, *21*, 1873–1883, doi:10.1007/s10570-013-0156-4.

30. Wenzel, R.N. Resistance of solid surfaces to wetting by water. *Ind. Eng. Chem.* **1936**, *28*, 988–994.

31. Nosal, W.H.; Thompson, D.W.; Yan, L.; Sarkar, S.; Subramanian, A.; Woollam, J.A. Infrared optical properties and AFM of spin-cast chitosan films chemically modified with 1,2 Epoxy-3-Phenoxy-Propane. *Colloids Surfaces B Biointerfaces* **2005**, *46*, 26–31, doi:10.1016/j.colsurfb.2005.08.006.

32. El Hamdaoui, L.; El Marouani, M.; El Bouchti, M.; Kifani-Sahban, F.; El Moussaouiti, M. Thermal stability, kinetic degradation and lifetime prediction of chitosan Schiff bases derived from aromatic aldehydes. *Chemistry Select* **2021**, *6*, 306–317, doi:10.1002/slct.202004071.

33. Estrela Dos Santos, J.; Dockal, E.R.; Cavalheiro, É.T.G. Thermal behavior of Schiff bases from chitosan. *J. Therm. Anal. Calorim.* **2005**, *79*, 243–248, doi:10.1007/s10973-005-0042-x.

34. Chen, J.Y.; Jiang, H.; Chen, S.J.; Cullen, C.; Sabbir Ahmed, C.M.; Lin, Y.H. Characterization of electrophilicity and oxidative potential of atmospheric carbonyls. *Environ. Sci. Process. Impacts* **2019**, *21*, 856–866, doi:10.1039/c9em00033j.

35. Bao, J.; Zhang, H.; Zhao, X.; Deng, J. Biomass polymeric microspheres containing aldehyde groups: Immobilizing and controlled-releasing amino acids as green metal corrosion inhibitor. *Chem. Eng. J.* **2018**, *341*, 146–156, doi:10.1016/j.cej.2018.02.047.

36. Li, M.; Wang, H.; Chen, X.; Jin, S.; Chen, W.; Meng, Y.; Liu, Y.; Guo, Y.; Jiang, W.; Xu, X.; et al. Chemical grafting of antibiotics into multilayer films through Schiff base reaction for self-defensive response to bacterial infections. *Chem. Eng. J.* **2020**, *382*, doi:10.1016/j.cej.2019.122973.

37. Chen, H.; Zhao, R.; Hu, J.; Wei, Z.; Mcclements, D.J.; Liu, S.; Li, B.; Li, Y. One-step dynamic imine chemistry for preparation of chitosan-stabilized emulsions using a natural aldehyde: Acid trigger mechanism and regulation and gastric delivery. *J. Agric. Food Chem.* **2020**, *68*, 5412–5425, doi:10.1021/acs.jafc.9b08301.

38. Fitzgerald, D.J.; Stratford, M.; Gasson, M.J.; Narbad, A. Structure-function analysis of the vanillin molecule and its antifungal properties. *J. Agric. Food Chem.* **2005**, *53*, 1769–1775, doi:10.1021/jf048575t.

39. Calvo, H.; Mendiara, I.; Arias, E.; Gracia, A.P.; Blanco, D.; Venturini, M.E. Antifungal activity of the volatile organic compounds produced by *Bacillus velezensis* strains against postharvest fungal pathogens. *Postharvest Biol. Technol.* **2020**, *166*, 111208, doi:10.1016/j.postharvbio.2020.111208.

40. Cai, R.; Hu, M.; Zhang, Y.; Niu, C.; Yue, T.; Yuan, Y.; Wang, Z. Antifungal activity and mechanism of citral, limonene and eugenol against *Zygosaccharomyces rouxii*. *Lwt* **2019**, *106*, 50–56, doi:10.1016/j.lwt.2019.02.059.

41. Varghese, S.A.; Siengchin, S.; Parameswaranpillai, J. Essential oils as antimicrobial agents in biopolymer-based food packaging - A comprehensive review. *Food Biosci.* **2020**, *38*, 100785, doi:10.1016/j.fbio.2020.100785.

42. González-Estrada, R.R.; Calderón-Santoyo, M.; Ragazzo-Sánchez, J.A.;

Peyron, S.; Chalier, P. Antimicrobial soy protein isolate-based films: Physical characterisation, active agent retention and antifungal properties against *Penicillium italicum*. *Int. J. Food Sci. Technol.* **2018**, *53*, 921–929, doi:10.1111/ijfs.13664.

43.     Muriel-Galet, V.; Cerisuelo, J.P.; López-Carballo, G.; Aucejo, S.; Gavara, R.; Hernández-Muñoz, P. Evaluation of EVOH-coated PP films with oregano essential oil and citral to improve the shelf-life of packaged salad. *Food Control* **2013**, *30*, 137–143, doi:10.1016/j.foodcont.2012.06.032.

44.     Neqal, M.; Fernandez, J.; Coma, V.; Gauthier, M.; Héroguez, V. pH-triggered telease of an antifungal agent from polyglycidol-based nanoparticles against fuel fungus *H. Resinae*. *J. Colloid Interface Sci.* **2018**, *526*, 135–144, doi:10.1016/j.jcis.2018.03.106.

# Artículo 3

**Dual functionality of citral and cinnamaldehyde as crosslinking agents and active components of dynamic antifungal imine-chitosan films**

Raquel Heras-Mozos, Rebeca Hernández[b], Rafael Gavara[a], Pilar Hernández-Muñoz[a]

[a] Instituto de Agroquímica y Tecnología de Alimentos (IATA-CSIC), Av, Agustín Escardino, 7, 46980, Paterna, Valencia, Spain.

[b] Instituto de Ciencia y Tecnología de Polímeros (ICTP-CSIC), C/Juan de la Cierva, 3, 28006, Madrid, Spain.

**ABSTRACT**

Cinnamaldehyde and citral were reversibly grafted to primary amino groups of chitosan film via covalent dynamic chemistry. These aldehydes can undergo to Schiff base and/or Michael addition, which can be modulated by pH of reaction. Different degree of polymerization of the biopolymer matrix was achieved when films were reacted at pH 2, 5 and 7. Modification of chitosan films was investigated by spectroscopic techniques and elemental analysis. The evaluation of swelling degree provided evidences of changes on cross-linking of chitosan films. In addition, the imine reversibility, and hence aldehyde release, was also affected by different cross-linking degree. Reversible covalent bond synthesized at pH 2 resulted in a high cross-linking structure, which showed a minor imine hydrolysis and a low water uptake, and hence a higher stability of films at acid pH, contrarily to observe when used pH 7 and 5. This study underlines the importance of pH on imine bond formation with α,β-unsaturated aldehyde to modulate the properties of chitosan active films based on reversible covalent chemistry.

**Keywords:** Chitosan, cross-linking, α,β-unsaturated aldehyde, water stability, reversible imines, pH-sensitive, biopolymer

## 1. Introduction

Essential oils (EOs) are aromatic volatile liquids extracted from different parts of the plants. Their aromatic and multiple biological properties confer them diverse technological uses in the food, cosmetic, agricultural and pharmaceutical industry [1–3]. Although the major application of EOs in the food industry is as flavouring agents, due to the antimicrobial and antioxidant properties of some of their components, the use of EOs as anti-spoilage agents has been widely investigated.

Trans-3-Phenyl-2-propenal (cinnamaldehyde, CN) and 3,7-dimethyl-2,6-octadienal (citral, CT) are major volatile components of the essential oils extracted from *Cinnamomum* spp. and *Cymbopogon citratus*, respectively. The activity of these aldehydes inhibiting microbial growth in postharvest products are well-reported in the literature [4,5]. Moreover, CN and CT are legally recognized as flavourings by the European Commission, and are generally accepted as safe (GRAS) for human health and environment by the United States Food and Drug Administration [6–8]. Legal recognition of these naturally-occurring volatile molecules facilitates their use as an alternative to chemical preservatives currently employed.

To date, most of the studies based on the application of EOs or their pure components are conducted spraying them directly on the food surface [9,10]. However, the way they are applied presents some limitations due to their high volatility and low stability being easily degraded by temperature, light and oxygen [11].

Another approach for their protection and application is based on their encapsulation in polymers, cyclodextrins or MOFs and the sustained release of these active volatile compounds [12–16]. However, in the afore mentioned systems, the release of the volatile molecules is activated by humidity and temperature, therefore they lack systems with a more sophisticated triggering mechanism to ensure the stability of bioactive volatiles during long-term storage time and until their use.

Recently our group has studied the reversible covalent grafting of volatile antifungal aldehydes from essential oils to the surface of chitosan films by means of the synthesis of imines [17]. Imine bond presents reversibility and stimulus responsiveness in such a way that it can break apart in mild acidic aqueous solution [18]. The antimicrobial properties of the synthetized films lied on the acid catalysed hydrolysis of the formed

imine bonds allowing the release of the volatiles from the film. Thus, the combination of reversibility and stimuli-responsiveness make imines greatly attractive in many research fields [18] including the release of active volatiles in different applications [19–23].

This novel approach of immobilizing molecules in chitosan films by means of reversible imines has some drawbacks when working with naturally occurring α, β-unsaturated aldehydes such as cinnamaldehyde (CN) and citral (CT). These molecules contain a double bond conjugated with a carbonyl group. The conjugated organic bonding system transmits the electrophilic character of the carbonyl carbon to the beta-carbon of the double bond; thus, besides 1,2-nucleophilic addition of primary amine groups of chitosan forming reversible imines, they are prone to undergo 1,4-nucleophilic or Michael addition. Since the covalent bond formed through Michael addition cannot be readily broken, the release of the aldehyde is hindered, and the antifungal responsiveness of the films is depleted [17]. In counterpart, 1,4 addition opens the possibility that, under specific reaction conditions, CN and CT are used as crosslinkers of chitosan structures. In this regard, an example of α,β-unsaturated aldehyde behaving as a crosslinker is acrolein. This small molecule is the strongest electrophile among all of the α,β-unsaturated aldehydes, and is capable to crosslink biological nucleophiles such as peptides, proteins and DNA without specific conditions due to its high reactivity. Acrolein is able to form Michael adducts with amines (β-substituted propanals, R-NH-CH2-CH2-CHO) which can participate in secondary cross-linking reactions; it can also form Schiff base cross-links (R-NH-CH2-CH2-CH=N-R) [24]. Acrolein has been proposed to crosslink insulin B chain forming aldimines with primary amine group of lysine and Michael adducts with secondary amine group of histidine [25]. However, acrolein cannot be used as a cross-linker for enhancing functional properties of biopolymer structures due to it is high toxic, carcinogenic, and mutagenic character [26]. Less toxic than acrolein, glyoxal and glutaraldehyde are frequently employed to improve functional properties of biomaterials. However, there is a need to find less toxic molecules that can work as cross-linkers of biological polymers [27]. In the pass, our group investigated the potential of CN as a natural cross-linker to improve the physical performance of cast wheat gliadin films. Cross-linking properties of CN were dependent on the pH of the reaction medium, with pH 2 as the optimum to obtain water resistant films [28].

Hence, the aim of this work has been to explore how the reactivity of CN and CT to nucleophilic addition of primary amine groups of chitosan films can be modulated by means of the acidity of the reaction media to achieve efficient responsive imine-chitosan films with desirable antifungal properties, and also to have a better knowledge of the performance of these molecules as cross-linkers of chitosan films to improve their stability in acid media.

## 2. Materials and methods

### 2.1. Materials

Sodium hydroxide (NaOH), hydrochloric acid 37% (HCl) and ethanol 96% (v/v) were provided by Scharlab (Barcelona, Spain). Both aldehydes, citral (CT) and cinnamaldehyde (CN), low molecular weight chitosan (75 - 85% deacetylation degree), acetic acid glacial, citric acid monohydrate and disodium phosphate to carry out buffer medium at pH 2, pH 3, pH 4 and pH 7 was purchased from Sigma-Aldrich (Barcelona-Spain). Milli-Q water was obtained by Milli-Q Plus purification system (Millipore, Molsheim, France). *Penicillium expansum* was supplied by the Spanish Type Culture Collection (CECT 2278). The culture medium for microorganism, Potato Dextrose Agar (PDA) was purchased from Scharlab (Barcelona, Spain).

### 2.2. Reaction of CN and CT with neutralized chitosan films

Chitosan films were obtained from 1.5% (*w/v*) polymer dissolved in 0.5% (*w/v*) acetic acid aqueous solution. The mixture was stirred vigorous at 50 °C until it was completely dissolved and then, the polymeric solution was filtered to eliminate impurities. After that, chitosan films were obtained using the solution casting method. The chitosan solution was poured in polystyrene plates (16 x 25 cm) and was dried at 37 °C for 24 h. The dried chitosan was peeled off the plate and the films with a thickness of 35 ± 5 μm were cut into 2 x 2 cm. After that, the films were neutralized by immersion in 0.1 M sodium hydroxide for 24 h. The neutralized films were dried at 37 °C and stored in desiccators until usage. Neutralized chitosan films were named CS.

Cinnamaldehyde (CN) and citral (CT) were reacted with CS in an Erlenmeyer with 75 mL of ethanol (96% (*v/v*)), 4 g of aldehyde and 2 g of neutralized chitosan film. The pH of the reaction medium was adjusted to

2, 5 and 7 using HCl (37%) and NaOH (2M). All reaction flask was placed in a shaking bath at 60 °C for 24 h. After that time, the excess of unreacted aldehyde was removed by washing with ethanol 96% (*v/v*) three times for 24 h at 60 °C.

The samples were coded as follows: CSCNX, and CSCTX films, meaning chitosan films treated with CN or CT, and X being the pH of the reaction (2, 5 or 7). In addition, a reaction of chitosan films without aldehydes was performed to obtain as a control films. The reacted control chitosan films were also obtained at pH 2, 5 and 7 (CS2, CS5 and CS7, respectively). The reacted chitosan films and those modified with aldehydes were dried and stored in a glass desiccator.

### 2.3. Effect of the acidity of the reaction medium on the grafting of CN and CT to chitosan films

The effect of the acidity of the reaction medium on the incorporation of aldehydes to chitosan films was quantitatively evaluated by elemental analysis. The synthesis of imine bonds (C=N) between carbonyl groups of aldehydes and primary amine groups of chitosan films was also qualitatively studied employing different spectroscopic techniques.

#### 2.3.1. Elemental analysis

The amount of aldehydes respect to glucosamine units of chitosan films was measured as degree of substitution (DS, %) according to Inukai et al. [29]. For that, the C/N ratio of the films was determined by using a CHN elemental analyser (CE Instruments EA 1110, Thermo Fisher Scientific, Waltham, MA, USA). The degree of deacetylation (DD) of chitosan, expressed as free glucosamine units per N atom unit of the polymer, was also evaluated by elemental analysis according to [30].

The DS (%) of modified chitosan films with CN and CT was calculated after synthesis. To have knowledge of the stability of imines to acid hydrolysis, DS was also evaluated for films that were immersed in aqueous solutions buffered at pH 4 and pH 2 at 23 °C after 7 and 14 days. Control chitosan films which were subjected to the reaction conditions without CN and CT carried on the same hydrolytic treatment and they were name r-CS films.

2.3.2. *Attenuated Total Reflectance-Fourier Transform Infrared (ATR-FTIR)*

Infrared spectra of the films were recorded using an FTIR spectrometer JASCO 4100 FTIR (Jasco, Easton, MD) equipped with a single reflection attenuated total reflectance (ATR) accessory (ZnSe crystal, PIKE Technologies, USA). Spectra were recorded in the wavenumber range from 4000 to 600 cm$^{-1}$ at 32 scans with the resolution of 4 cm$^{-1}$.

*2.4. Effect of the acidity of the reaction medium on the swelling properties of modified chitosan films*

The effect of the acidity of the reaction medium on the crosslinking capacity of CN and CT was evaluated indirectly evaluating the swelling of the films in buffered water at pH 7, 4 and 3 at 23 °C. The swelling was described as percentage of water uptake (WU) using the following equation:

$$WU\ (\%) = [(Ms - Mf)/Mf] \times 100$$

where Ms is the mass of the film in the swollen state at equilibrium and Mf is the mass of this film after drying to constant weight in $P_2O_5$. Samples were analyzed in triplicate and the results given as average value ± standard deviation.

*2.5. Effect of the reaction medium acidity on film pH-responsiveness for the release of aldehydes*

The effect of the acidity of the reaction medium on the capacity of the resulting films to release CN and CT when they were immersed in aqueous buffered solutions at pH 4 and 2 was evaluated. For that, a modified film specimen around 15-20 mg was placed in a 20 mL of glass vial and 5 mL of buffer medium was added. The vials were sealed with a crimp cap and septum to collect the samples. The samples were stored at 23 °C and aldehyde release was measured at 2 and 24, 48 and 72 h after contact between buffer and film.

The quantification of aldehyde released was determined by using a solid phase microextration (SPME) fibre coated with a DVB/CAR/PDMS (divinylbenzene/carboxen/polydimethylsiloxane) of 50/30 μm of thickness. The SPME fibre was exposed in the headspace of vial the with

the sample during 10 min at 23 °C, then the fibre was thermally desorbed in the gas chromatograph injector at 220 °C for 10 min.

The aldehyde release was analysed by gas chromatograph (GC) mod. 6850 Series II Network GC System (Agilent Technologies, Palo Alto, CA, USA). The GC was equipped with a flame ionisation detector (FID) and a Restek RTX1 capillary column (30 m length x 0.53 mm diameter x 5 μL thickness). Helium was used as carrier gas with a flow rate of 14.6 mL/min. The chromatograph method was programmed in splitless mode. Injector and detector temperature was set at 220 °C. The temperature program was from 75 to 220 °C, with an initial hold time of 2 min and a ramp of 15 °C/min until 120 °C, and then at 10 °C/min until reach 220 °C, with 5 min of hold temperature. A calibration curve was previously built by using different amount of aldehydes in buffer medium in the range between 0.05 and 8 mg of CT and 0.08 to 7 mg for CN, following the chromatographic conditions previously described. The results were expressed as $mg/g_{film}$.

## 2.6. Effect of the acidity of the reaction medium on in vitro antimicrobial pH-response of synthetized films

### 2.6.1. Microbial cultures

The microbial strain *P. expansum* was grown and maintained in PDA at 26 °C by sub-culturing every 7 days. To conduct the antifungal assay a conidial suspension of $10^6$ conidia/mL was obtained. For that, sterile peptone water with Tween 80 (0.05%) was spilled in the fungal surface of PDA plate and was dragged with the use of a digralsky handle. The suspension was transferred to sterile tube and several dilution was performed until obtain $10^6$ conidia/mL. The count was conducted with improved Neubauer chamber (Bright-Line Hemacytometer, Hausser Scientific, Horsham, PA, USA).

### 2.6.2. In vitro antimicrobial activity of free aldehydes

Prior to the evaluation of activity of the imine-chitosan films, citral (CT) and cinnamaldehdye (CN) were tested against *P. expansum*. Aldehyde effectiveness was evaluated by determining the minimum inhibitory concentration (MIC) and the minimum fungicidal concentration (MFC).

The effectiveness against fungi strain was tested as vapour phase by generation of micro-atmosphere inside of petri plate. For that, sterile PDA

plates were inoculated with 3 µL of fungal suspension of $10^6$ conidia/mL in three equidistant points of surface agar. Different doses of aldehydes were deposited on a sterile paper disk, which was glued to the lid of the plate. After that, the plates were closed and sealed with parafilm to reduce the volatile loss. Finally, the inoculated plates were incubated during 7 days at 26 °C. After the seventh day of incubation the colony growth was measured to determinate the MIC (mg/plate). Then, the paper disk was removed from the plate and were incubated 3 days more, and fungal growth was evaluated to determinate MFC. The parameters MIC and MFC were defined as minimal amount of volatile which inhibit fungal growth by at least 50% and 100% compared to control, respectively. Both parameters were expressed as amount of aldehyde (mg) dosed into each petri plate. Test were carried out in triplicate.

### 2.6.3. In vitro antimicrobial activity of modified chitosan films

Effectiveness of imine-chitosan films synthesised at different pH were evaluated against *P. expansum*. The imine-chitosan films were subjected at acid pH acting triggering of the imine bond and hence of the aldehyde release. Antifungal response of modified films against *P. expansum* was assessed in vapour phase according to previous studies [31]. For that, a double Petri plate system was performed with a large empty plate with a diameter of 90 mm and a small plate of 58 mm, which containing PDA culture medium. This plate was inoculated with 3 µL of conidia suspension previously obtained and was placed into large plate without lid. Around 0.1 g of imine-chitosan film were deposited in the free space of the large plate. Finally, 7 mL of buffer medium at pH 4 or 2 was poured on film, acting as trigger of imine bond hydrolysis. The plates were closed with the lid of the large plate and sealed with parafilm and were incubated for 10 days at 26 °C. Control samples without films were also monitored. The fungal colony growth was assessed during 3, 5, 7 and 10 days of storage by measuring colony diameter (cm) and inhibition percentage was calculated. Test were conducted in triplicate.

### 2.7. Data analyses

The experiments were carried out at least in triplicate and the obtained data were expressed as average ± standard deviation. The statistical analysis was conducted by one-way analysis of variance (ANOVA) using

the SPSS® Statistics computer program, version 27.0 (SPSS Inc., Chicago, IL, USA). Means were evaluated using the Tukey *b* test (P ≤ 0.05).

## 3. Results and discussion

The visual appearance of films is showed in **Figure 1**. To the naked eye, colourless and no discontinuities were observed in CS films after reaction without aldehyde. But, a colour change was found in CSCT and CSCN films in all pH of reaction. Different analyses were conducted to determine the effect of the acidity of the reaction media on modified chitosan films.
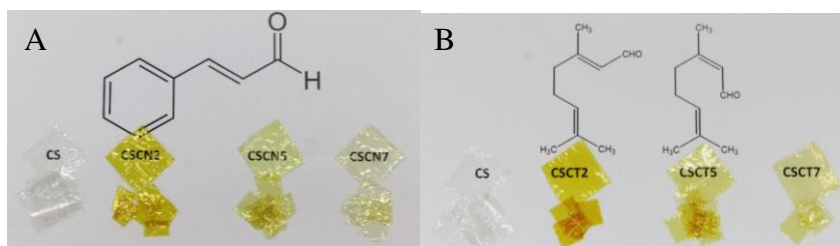


**Figure 1.** Visual appearance of chitosan and imine-chitosan film modified with cinnamaldehyde (A) and citral (B) synthesized at pH 2, 5 and 7.

### 3.1. Effect of the acidity of the reaction medium on the grafting of CN and CT to chitosan films

#### 3.1.1. Elemental analysis

The degree of substitution (DS, %) of anchored aldehydes to amino groups of CS film by imine linkage was quantified using elemental analysis. The DS of imine-CS films is given in **Table 1**. The data clearly showed a high efficiency of α,β-unsaturated aldehydes in amino group substitution, obtaining over 50% of DS after Schiff base reaction. The linear aldehyde, CT, resulted less efficient than CN, an aromatic aldehyde, showing ca. 50% and 70% of substitution, respectively. The imine bond formation is associated to the compound chemical structure, also with its reactivity or electrophilicity index [32]. In accordance with the results, a higher efficiency was also found for *trans*-2-cinnamaldehyde than for citral when they were reacted with amikacin disulfate salt [33]. The imine bond formation can occur at acidic, neutral or basic pH [34], however, a slightly acidity can promote a higher imination since too acidic pH may protonate

the amino groups and disable them from participating in the reaction [35,36]. However, in CSCT and CSCN the influence of catalysis at different pH was limited for the DS, as no major differences in DS were observed, reaching great substitution in all conditions. It could be observed that films synthetized at pH 5 there was a slight increase in the degree of substitution for both aldehydes, being 71 and 54% for CSCN5 and CSCT5, respectively.

The imine bond formed is labile to acid hydrolysis, hence, the reversibility of the reaction was evaluated at pH 4 and pH 2. The DS obtained after hydrolysis at pH 4 is also shown in **Table 1**. The imine-chitosan films reduced their DS after 7 and 14 days after contact with buffer at pH 4, nevertheless, those catalysed at pH 2 maintained a 25% substitution and did not reduce it after 14 days. However, imine-CS films at pH 5 and 7 showed an evolution of DS between days 7 and 14 of hydrolysis. This is an evidence that the imine bond formed at pH 5 and 7 is more reversible than those formed at acid pH. At acidic pH a cross-linked structure is formed, which is more robust and stable to hydrolysis. In fact, when films are immersed at pH 2 for 7 days, the DS of CSCN2 and CSCT2 was 25.8 and 24.3%, respectively. These values are similar to those obtained after 14 days at pH 4 for these films. This 25% is a percentage of the bond that are not reversed and that improve the resistance of the polymer structure.

**Table 1.** Substitution degree (DS, %) of imine-chitosan films with citral and cinnamaldehyde synthetized at pH 2, 5 and 7, and after immersion in buffer medium at pH 4 for 7 ($DS_{pH4}$ 7 d) and 14 days ($DS_{pH4}$ 14 d).

|  | pH $_{reaction}$ | DS (%) | $DS_{pH4}$ 7 d (%) | $DS_{pH4}$ 14 d (%) |
|---|---|---|---|---|
|  | 2 | $66.6 \pm 0.1^{cC}$ | $25.1 \pm 1.8^{cB}$ | $24.8 \pm 0.8^{dA}$ |
| CSCN | 5 | $70.9 \pm 0.3^{dC}$ | $21.2 \pm 1.7^{bcB}$ | $11.7 \pm 0.2^{bA}$ |
|  | 7 | $70.0 \pm 0.4^{dC}$ | $33.4 \pm 1.3^{dB}$ | $9.6 \pm 0.3^{aA}$ |
|  | 2 | $52.3 \pm 0.6^{aB}$ | $25.7 \pm 0.3^{cA}$ | $24.3 \pm 0.9^{dA}$ |
| CSCT | 5 | $54.5 \pm 1.0^{bC}$ | $17.4 \pm 0.2^{aB}$ | $13.9 \pm 0.2^{cA}$ |
|  | 7 | $51.9 \pm 0.2^{aB}$ | $17.4 \pm 4.5^{abA}$ | $13.5 \pm 0.2^{cA}$ |

Different superscript letters in the same row[(A-E)] and column[(a-d)] indicate a statistically significant difference ($P \leq 0.05$).

*3.1.2. ATR-FTIR analysis of Schiff base formation*

The functionalization of chitosan by aldehyde grafting was evaluated through spectroscopic analysis. FTIR spectra of chitosan, free aldehydes and those modified with cinnamaldehyde and citral at pH reaction 2, 5 and 7 are shown in **Figure 2A and 2B**, respectively. The infrared spectra of films were depicted in the range from 1800 to 600 cm$^{-1}$. In **Figure 3** the spectra of CS films subjected at same condition of reaction than those treated with cinnamaldehyde and citral are shown. The spectra of control films showed a band of amide I (-NH-CO-) and amine group (-NH$_2$) at 1644 and 1580 cm$^{-1}$, respectively. In addition, a distinctive bands are observed in the range of 1150 to 850 cm$^{-1}$, which are related with glycosidic structure of chitosan [37,38]. The successful anchoring of aldehydes to amino groups of CS was demonstrated by the increase in the intensity of the characteristic peaks of imine linkage (C=N) by comparing with spectra of untreated CS films. Thus, CSCN and CSCT films showed a significant increase in the band intensity at 1646 and 1632 cm$^{-1}$, respectively (**Figure 2A and 2B**).

Previous studies have also reported similar values of wavelength for imine bond appearance after chitosan modification, showing a new peak at 1634 cm$^{-1}$ with cinnamaldehyde [39] and 1645 cm$^{-1}$ in chitosan containing citral [40]. In the case of CSCT films, the imine band vibration is overlapped with characteristic amide I of chitosan, which is around 1645 cm$^{-1}$. However, an increase of relative intensity ($I_{peak/1025}$, %) of imine absorption band respect to 1025 cm$^{-1}$ peak of chitosan can be observed. Thus, relative intensity in control CS film for amide I ($I_{1645/1025}$) was 18%, whereas values of $I_{1644/1025}$ in CSCT spectra showed 25, 32 and 32% for CSCT2, CSCT5 and CSCT7, respectively. In the case of CSCN, an evident and sharp absorption band is found for imine peak for all condition, being the values of $I_{1632/1025}$ 43, 52 and 48% for CSCN2, CSCN5 and CSCN7, respectively. Furthermore, a modification of characteristic peak of amino group at 1580 cm$^{-1}$ is observed after reaction, mainly due to its involvement in the new forming bond along with aldehyde. In this regard, the band assigned to carboxyl group of aldehyde (-CH=O) is also not observed in the spectra after reaction due to imine formation, which is usually found around 1670 cm$^{-1}$ [33]. Moreover, other peaks related with aldehyde structure after reaction are observed, evidencing the aldehyde incorporation to polymer matrix. These peaks are clearly observed when

comparing the infrared spectra of imine-chitosan films with spectra of free aldehyde (**Figure 2**). In CSCT films, a shoulder appears at 1440 cm$^{-1}$, related to the aliphatic chain of the incorporated aldehyde [41]. For CSCN the characteristics band of aldehyde are more evident, thus, bands belonging to aromatic ring of aldehyde can be observed at 750 and 688 cm$^{-1}$ [42,43].
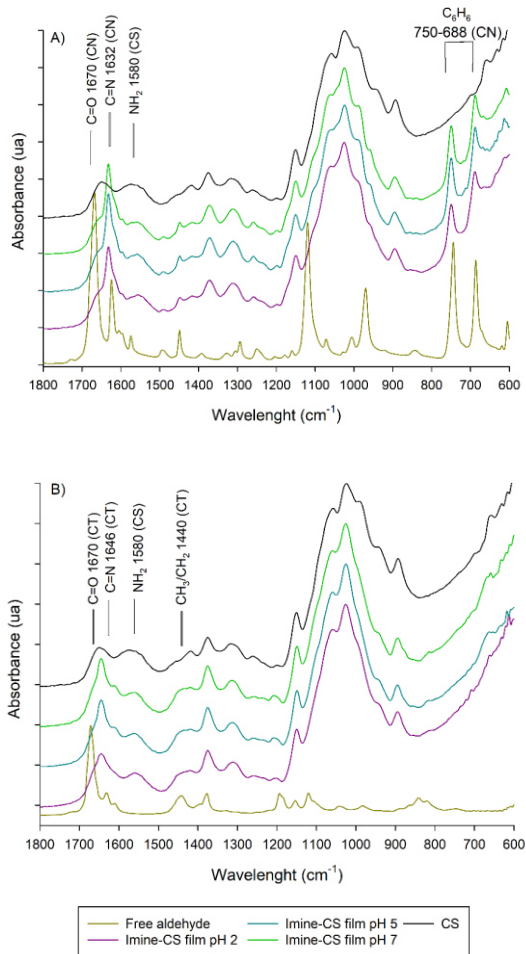


**Figure 2**. Infrared spectra of chitosan films and imine-chitosan films with citral and cinnamaldehyde synthetized at several pH.
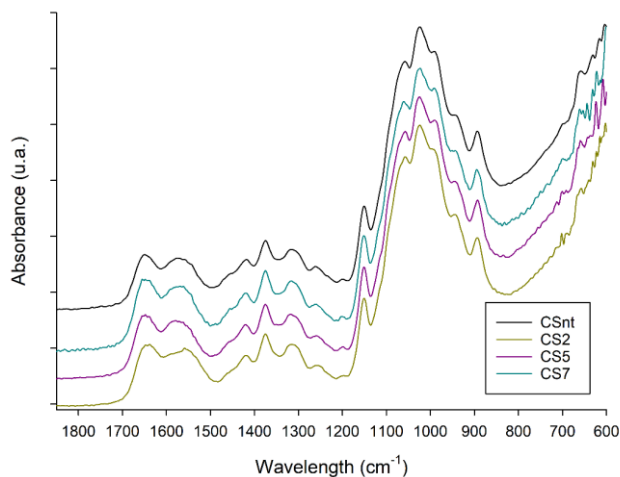
**Figure 3**. Infrared spectra of neutralized (CSnt) and reacted CS films at several pH (CS2, CS5 and CS7).

Regarding infrared spectra of imine-chitosan films formed at different pH of reaction, no major differences were observed between them. The functionalization of chitosan via nucleophilic addition to form imine bond, often require the presence of acid and mild conditions. Different pH can carry out the imination on the amino group [36,44]. According to these studies and obtained infrared spectra, the different pH-reaction (2, 5 and 7) showed similar modification and new imine linkage formation without difference in infrared spectra of films.

Previous studies observed that pH of reaction for the imination of biopolymer backbone by α,β-unsaturated aldehyde could have a crosslinking effect [28]. The proposed reactions between primary amino group of chitosan (-NH$_2$) and carboxyl group of aldehydes (-C=O) of unsaturated aldehydes are represented in **Figure 4**. The functionalization of CS with aldehydes occurs mainly by 1,2-addition (I) or Schiff base. Moreover, the α,β-unsaturated aldehydes have ability to form 1,4-addition (II) or Michael addition [45]. In addition, both type of condensation (III) could be taken place (**Figure 4**), generating a cross-linked chitosan matrix by double bonding of one aldehyde molecule to two different chains. This possible cross-linked structure could be caused by addition to amino groups of pendant aldehyde groups occurred during Michael addition or by

reaction with α,β-unsaturated bond to adjacent amino group from imine conjugate. The formation of Michael addition and/or Schiff base could be modulated with pH of the reaction media [28].

According to obtained data from FTIR analysis, the imine linkage was observed in all pH-reaction condition. However, it is difficult to determine the effect of pH on the type of bond with the data obtained from these analyses as spectra did not show any evidence about the formation of Michael addition. 1,2-addition or imine bond formation was clearly inferred by appearance of imine bond (C=N) around 1630-1640 cm$^{-1}$, but, a band related to aldehyde group (C=O) was not observed. The carboxyl group of aldehydes is, hence, involved in imine formation [46]. Conversely, the presence of 1,4-adition between aldehyde and primary amino group of chitosan (C-N) is hardly observable, due to overlapping of vibration of 1,4-addition (C-N) with chitosan bands. Michael addition bond was previously assigned around 1200 cm$^{-1}$ [47] and by the increase of band at 1580 cm$^{-1}$ [38,48], which is a characteristic band of amide II of chitosan. Michael addition adduct in chitosan polymer was performed by Guaresti [38], who assigned the intensity increase at 1584 cm$^{-1}$ to 1,4-addition band (C-N). In these sense, just the infrared spectrum of CSCT2 films showed an increase in amide II band, which could be related to 1,4-addition formation. Moreover, a shoulder appears around 1596 cm$^{-1}$ in all samples modified with cinnamaldehyde (CSCN) and 1612 cm$^{-1}$ for those with citral (CSCT) at pH 5 and pH 7, which could be related to conjugated C=C bond vibration [49]. Conversely, this peak is not observed in the CSCT2, which could be due to involvement of unsaturated C=C in Michael addition as is represented in **Figure 4** (III). Therefore, the complexity of the system required more thorough analysis to determine the effect of pH-reaction on imine-chitosan films.
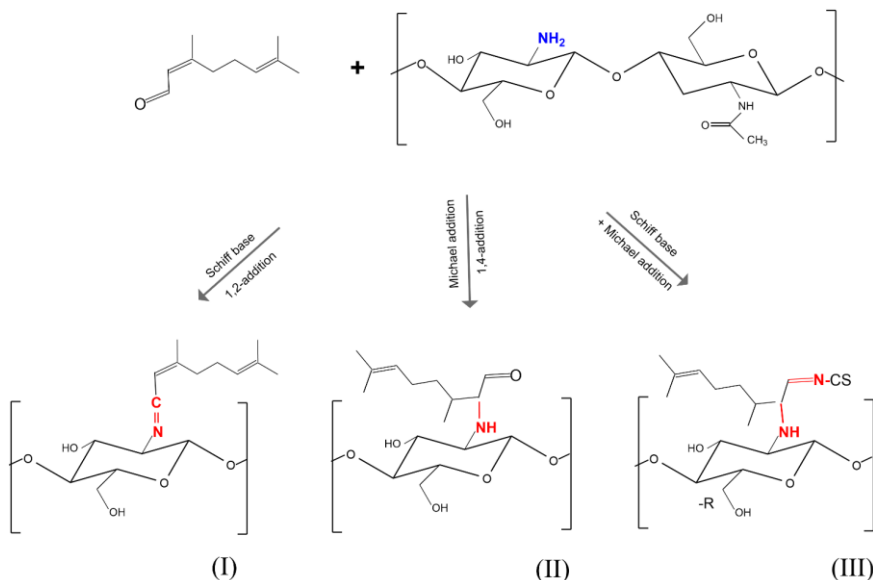
**Figure 4**. Possible reaction mechanism between primary amino groups of chitosan (NH$_2$) and carbonyl groups of α,β-unsaturated aldehyde, citral (C=O).

### 3.2. Effect of the acidity of the reaction medium on the swelling properties of modified chitosan films

To further investigate the influence of pH of reaction on the properties of the resulting imine-chitosan films, its stability under acid aqueous media was examined. The swelling degree (%) of films obtained after 24 h of immersion at pH 4 and 7 are shown in **Figure 5.** Chitosan is a biopolymer, which exhibit a great amount of amino and hydroxyl groups along backbone chain. Its hydrophilic nature favours the water entrance as revealed by the results in **Figure 5**, with a water absorption of 220 and 260% (w/w) at pH 7 and pH 4, respectively. Since no differences were found between the CS films reacted at the three pHs (CS2, 5 and 7), only data for CS2 are shown.

After Schiff base reaction, the formed covalent bond between aldehyde and primary amino group of chitosan contribute to the remarkably different of swelling ability respect to control. Swelling ability depends on the aldehyde structure and grafting degree, since anchored aldehydes are hydrophobic and could modify polymer water uptake of polymer. Moreover, the swelling behaviour modification can be indicative

of a crosslinking effect [38]. Thus, imine-chitosan films swelled in a limited manner, due to a reduction of the available amino groups in chitosan, since they are involved in the imine bond, and also due to the presence of hydrophobic molecules distributed across the polymeric structure.

Modified films immersed at pH 7 reduced its swelling degree respect to control sample, being around 110 – 130 % (w/w). Acid pH considerably increases swelling ability of films, when imine-chitosan films were immersed at pH 4 it was possible to observe differences in water uptake among films submitted to the diverse synthesis condition. These differences could be related to the degree of cross-linking as well as to the reversibility of the imine. When films are subjected at acid pH, imine bond could hydrolyse, releasing the aldehyde and setting free the amino groups that can be protonated and, subsequently, resulting in an increase of film swelling degree, being more evident for films at pH 5 and pH 7. The lower swelling degree observed in films reacted at pH 2 could be caused by a higher crosslinking.
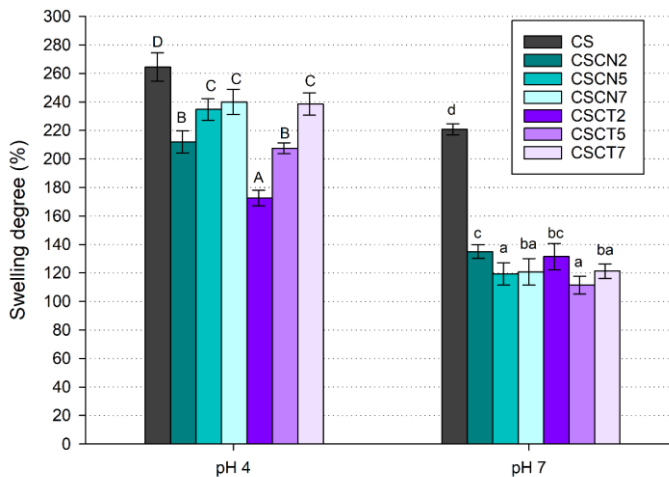


**Figure 5**. Swelling degree of chitosan and imine-chitosan film synthesized at several pH after immersion at pH 4 and pH 7 for 24 h. Bars with same letter in capital and lower in samples treated at pH 7 and 4, respectively, are not significantly different.

In this context, when films were immersed at pH 3, different behaviour were also observed and crosslinking behaviour of aldehydes was more evident. The swelling behaviour of CS and imine-CS films by immersion in pH 3 is shown in **Figure 6**. At pH 3, CS films absorbed rapidly a large amount of water, the amino groups were rapidly protonated, generating electrostatic repulsions of the polymer chains, and allowing more water uptake until it finally dissolved after 15 min of immersion with a swelling degree of 841%. The imine-chitosan films showed some hydrophobicity during first 15 min, but then greatly increased their water uptake until dissolved. The imine-chitosan films synthesized at pH 7, CSCN7 and CSCT7, were less resistant and dissolved after 60 min CSCN7 with a swelling of 502% and CSCT7 with 1400%. The CSCN5 reached an absorption of 947% and was also dissolved after 120 min, whereas CSCT5 maintained its structure for 24 h with a max. of 1970%, after which it fragmented and lost its structural integrity. In contrast, the CSCN2 and CSCT2 were stable and reached equilibrium after 24 and 4 h, respectively. CSCT2 reached 380%, whereas CSCN2 was 1558%. This results agree with data obtained from elemental analysis, which showed that imine-CS films at pH 2 presented anchored aldehyde not hydrolysable, enhancing stability of film structure when immersed in very acidic solutions. In accordance with results, there was a significant positive correlation between low swell degree with a high crosslinking effect of aldehyde [50] being imine-CS films catalysed at pH 2 more crosslinked than those at pH 5 and 7. Previous studies also reported improvement of of chitosan water stability in different aqueous solutions by crosslinking chitosan with a dialdehyde, glutaraldehyde [46], which allows different chitosan chains to be linked by the formation of two Schiff bases. Double cross-linked implying two different bond was also reported to obtain robust materials and modulate their properties; Michael addition and/or imine bond [51], or Diels-Alder reaction with imine bond [52]. Others authors also explored the use of natural-occurring aldehydes, as cinnamaldehyde, to improve water resistance films of proteins [28,53]. Although imine formation between aldehydes and primary amino group of chitosan can occur at acidic, neutral or basic pH [34], the obtained data revealed that there is a crosslinking effect of $\alpha,\beta$-unsaturated aldehydes when is synthetized at low pH. Therefore, reaction pH resulted fundamental to modulate functional properties of films. In this work, the structure proposed for films of

chitosan synthesized at pH 2 could be related to the scheme described in **Figure 4 (III)**, in which a crosslinking structure can be obtained by implying Schiff base and Michael-type bond between different  chitosan chains. The double cross-linked bond obtained in acid condition generated a robust and stable structure at acid pH, absorbing less water than those synthetized at pH 5 or 7.
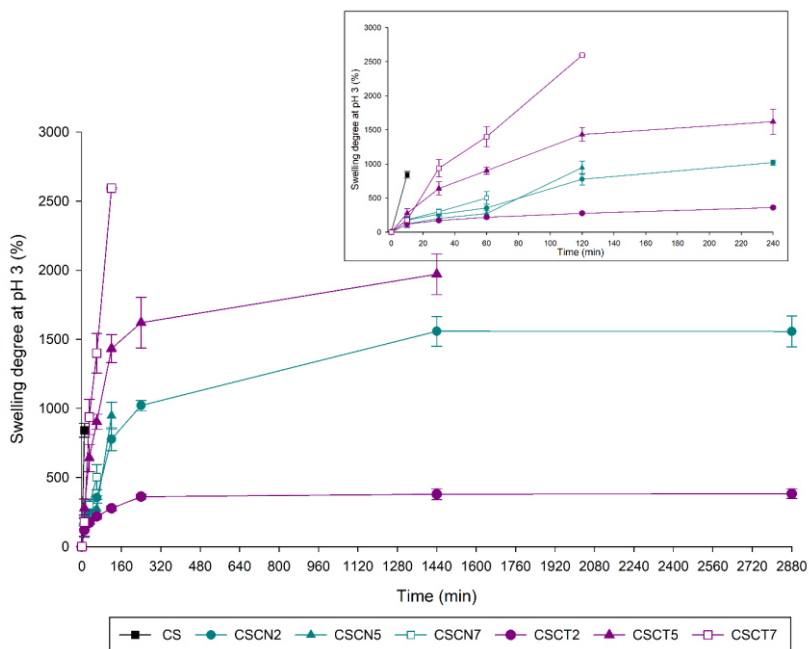


**Figure 6**. Swelling behaviour of chitosan and imine-chitosan film synthesized at several pH and immersed at pH 3 until equilibrium or dissolution.

### 3.3. Effect of the acidity of the reaction medium on film pH-responsiveness for the release of aldehydes

**Figure 7A** and **7B** shows the amount of released aldehyde (mg/$g_{film}$) from imine-CS films 2, 5 and 7 subjected at different medium (pH 2 and 4). Reversible nature of imine bond allows the release of the aldehyde to be modulated under certain stimuli. The reversible covalent bond is pH-sensitive, and so it is the release of volatile compounds which is triggered at acidic pH. In this line, great amounts of CT and CN were obtained in both acid conditions. Moreover, after 2 h of immersion, a significant

difference between the two pH values were observed. The data collected from the CN release at pH 4 showed that CSCN5 and CSCN7 needed ca. of 24 h for reach an equilibrium, while more than 48 h were needed to reach the maximum released in CSCN2. However, when CSCN2 was subjected at pH 2, the maximum concentration was obtained after 2 h. The rates of the imine hydrolysis, and hence aldehyde release was increased with decrease in pH. Therefore, the pH values varies the rate of imine hydrolysis, but similar amount of released aldehyde was reached [54].

The maximum amount of CN released from CSCN2 was the same for both pH of hydrolysis, but was first achieved at the acidest pH. However, CSCN5 and CSCN7, showed a higher release at pH 2 than pH 4. The enhanced release in these films could be due to other mechanisms besides imine reversibility, such as the disintegration of chitosan film in such an acidic medium.

**Figure 8** shows a scheme of how the proposed crosslinking could affect aldehyde release. The cross-linked chitosan generated when Schiff base reaction was catalysed at pH 2 maintained polymer structure, though less aldehyde was available to hydrolysis and hence release. In turn, this concept reinforces the data obtained from the swelling when films were immersed at acid pH solutions. These finds suggest that CSCN2 was more cross-linked than CSCN5 or 7, since this hypothesis is in agreement with lower aldehyde release, lower swelling degree and greater stability at acidic pH.

Similar to CSCN, films modified with CT catalyzed at pH 2, released less aldehyde than those catalyzed at pH 5 and 7. However, a drastic decrease of aldehyde was detected during the assay, being the most rapid at pH 2. The degradation of CT under acid aqueous conditions at pH 3 has been previously reported [55]. Previous studies reported the stability of conjugates of aldehyde-chitosan at different pH depended of chemical structure of aldehyde and pH of medium [56].
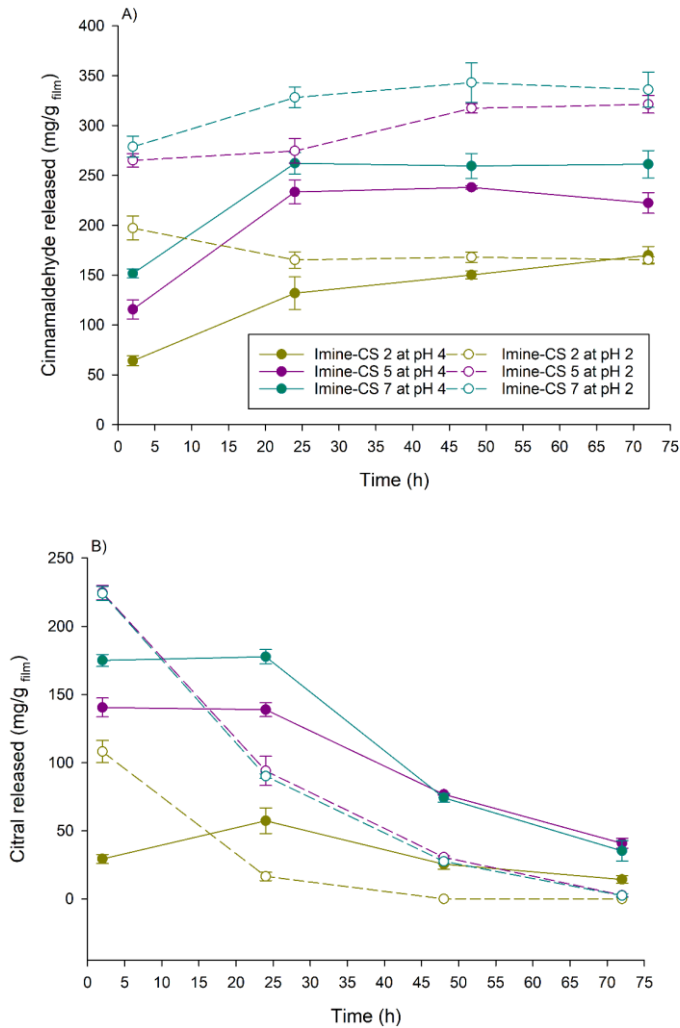
**Figure 7.** Cinnamaldehyde (A) and citral (B) released (mg/g film) from imine-chitosan films at 2, 5 and 7 subjected at hydrolytic solution at pH 4 and pH 2 at 23 °C during 72 h.
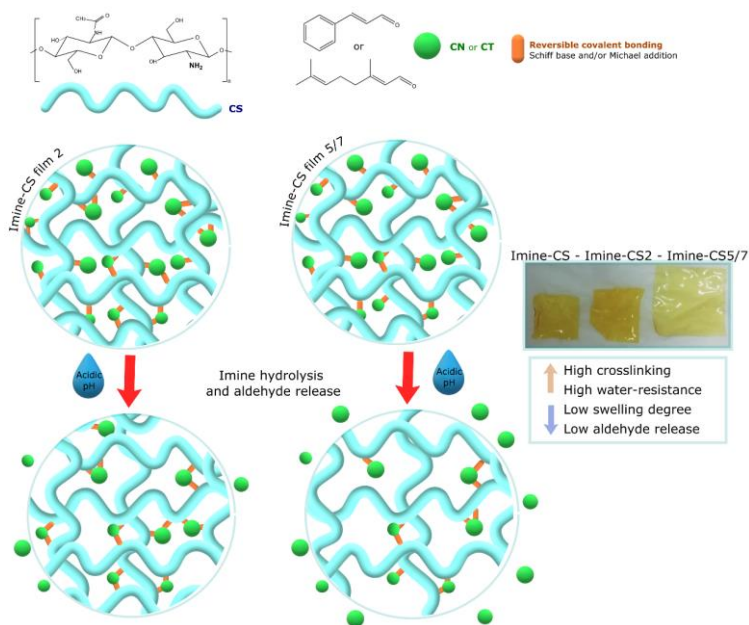
**Figure 8.** Schematic representation of the CS reacted matrix at pH 2 and pH 5/7 and its swelling and volatile release behaviour.

In view of the obtained results, the influence of the catalysis pH on the reaction between chitosan and α,β-unsaturated aldehydes is evident. The modification of reaction pH allowed the modulation of the function for these aldehydes that can not only act as antimicrobial agents when released but can also give structural stability to the polymeric matrix, acting as natural crosslinking agents. These results evidence the dual role of the naturally-occurring α,β-unsaturated aldehydes, and can be used to replace the usual crosslinking agents that present some toxicity, such as glutaraldehyde or formaldehyde. Although, crosslinking effect of the matrix can be interesting for some applications where greater stability is required, the crosslinking of the films significantly reduces the release of volatile active compounds as in active packaging.

*3.4. Effect of the reaction medium acidity on in vitro antimicrobial pH-response of synthetized films*

   *3.4.1. In vitro antimicrobial activity of free aldehydes*

  The antimicrobial effectiveness of aldehydes against *P. expansum* characterized by MIC and MFC values are described in **Table 2.** Micro-atmosphere generated by aldehydes vapour into plate headspace resulted in *P. expansum* inhibition. Both aldehydes exhibited strong antifungal activity against fungi growth, being CN most effective. CT and CN has been broadly used as antimicrobial compound against several pathogens [57,58], demonstrating its potential to be used as natural preservatives. Their antifungal mechanism can be related to lipophilic character [59]. Moreover, the ability of α,β-unsaturated aldehydes to form adducts with biological compound as proteins or DNA, could be also associated with their antimicrobial potential [60].

**Table 2.** Antimicrobial activity of aldehydes in vapour phase against *P. expansum*.

|  | *Penicillium expansum* | |
| :---: | :---: | :---: |
|  | **MIC (mg/plate)** | **MFC (mg/plate)** |
| CN | 1.6 | 3.2 |
| CT | 6.7 | 13.4 |

  *3.4.2. In vitro antimicrobial activity of modified chitosan films*

  The antimicrobial effectiveness of imine-chitosan films with CT or CN catalysed at several pH (2, 5, 7) was assessed by subjecting films at pH 4 and pH 2. The inhibition of fungal colony radial growth is presented in **Figure 9**. In addition, visual appearance of *P. expansum* colonies after 7 days of incubation is showed in **Figure 10**. The results showed clear differences when films were subjected at pH 2 or 4 with films modified with CN. Thus, a fungicidal effect resulted in the CSCN2, 5 and 7 when films were immersed at pH 2, while at pH 4 an inhibitory activity was obtained. In contrast, this effect was not observed in samples with chitosan modified with CT. In this case, similar fungal inhibition values were found, being slightly higher at pH 4. Thus, under the most acidic condition, effectiveness of CT decreased, especially in CSCT2, which is in agreement

with the release assay (**Figure 7**), and attributed to a rapid aldehyde degradation under acidic aqueous solution [61].
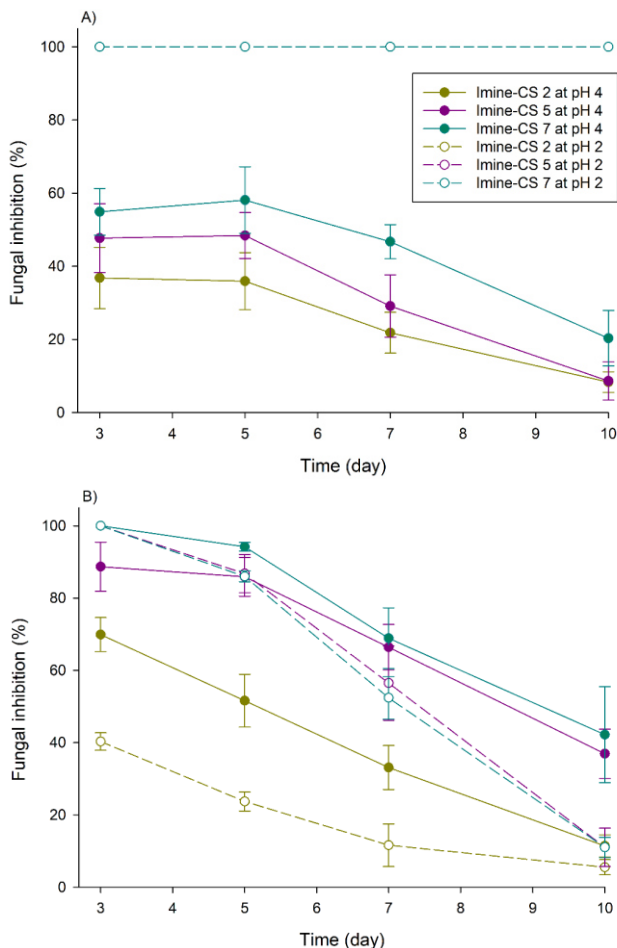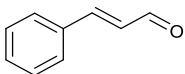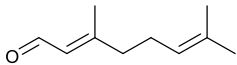


**Figure 9.** Inhibition of *P. expansum* growth colony (%) of CSCN (2,5 and 7) (A) and CSCT (2,5 and 7) (B) subjected at pH 4 and pH 2 during 10 days at 26 °C.

Interestingly, when comparing CSCN and CSCT whose hydrolysis was triggered at pH 4, more antimicrobial activity is observed in the CSCT and CSCN films, despite the free CN was most effective against *P. expansum*. This could be influenced by several factors, including the imine reversibility, which could be more stable for CN than for CT. As observed in the release assay, CT reached its maximum concentration after 2 h of

contact with the triggered medium, whereas CN required more time. Moreover, since the antimicrobial effectiveness is due to the presence of an enriched atmosphere with aldehyde released from the film, the properties of the volatile may influence its release, such as vapour pressure, volatility and lipophilicity [62,63]. The physicochemical parameters of these α, β-unsaturated aldehydes are showed in **Table 3**. CT present a higher volatility and a higher lipophilic character than CN, which could explain the easier release into the headspace from film and from triggered medium, and hence showing a higher activity than CSCN.

**Table 3**. Physicochemical parameters of cinnamaldehyde (CN) and citral (CT).

| Aldehyde | CAS number and structure | MW (g/mol) | Log P (o/w) | Vapour Pressure at 25 °C (mmHg) |
|---|---|---|---|---|
| CN | 14371-10-9  | 132.16 | 1.90 | 0.029 |
| CT | 5392-40-5  | 152.23 | 3.45 | 0.091 |

Regarding the synthesis pH of Schiff bases, the imine-chitosan films catalysed at pH 2 obtained the lowest ratios of inhibition. According to the above results, imine-CS films at pH 2 showed a more cross-linked structure, hindering the release of aldehyde from the matrix, and hence, reducing its effectiveness. This is in agreement with the lower release data at pH 2.
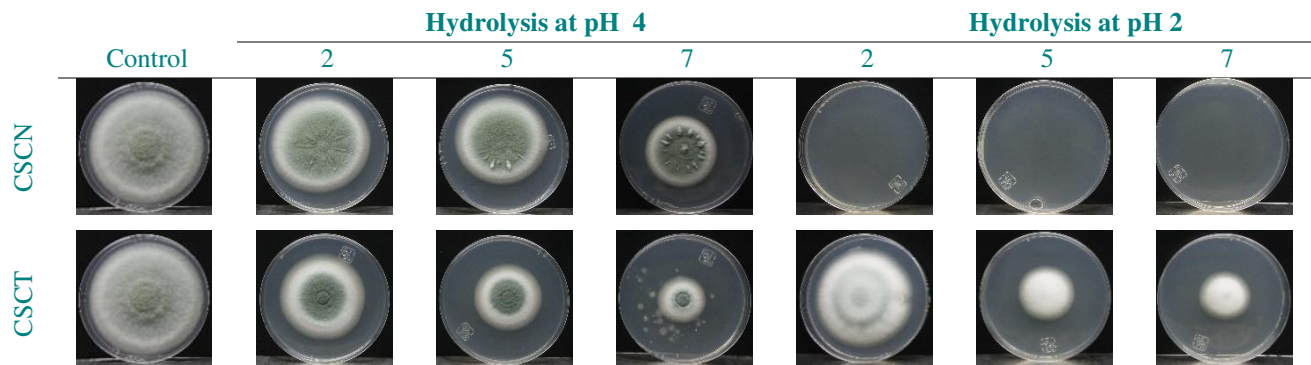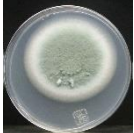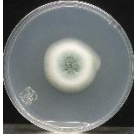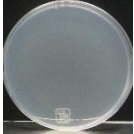
**Figure 10.** Antifungal effect of aldehyde release from imine-chitosan films subjected at different hydrolytic media (pH 4 and pH 2) against *P. expansum* after 7 days of incubation at 26 °C.

To observe differences between the CSCN films catalysed at different pH when is triggered at pH 2, it is necessary to decrease the amount of film to 0.05 g. In **Table 4** shows the effectiveness of 0.05 g CSCN2, 5 and 7 immersed at pH 2 against *P. expansum* is shown. In this case, the films maintained a great antimicrobial activity, resulting fungicide for CSCN7 and inhibitory for CSCN5 and CSCN2. Following a similar trend as when the films were exposed to pH 4 (**Figure 9**). The antimicrobial activity of CSCN2 and CSCT2, and hence, the release of CN and CT was more limited due to the fact that some aldehydes molecules can be involved in Michael addition hindering its reversibility. Nevertheless, these molecules, especially those involved in the double reaction, maintained the film structure [64] even when they were immersed at the most acid pH. It is clear that the reactivity of α,β-unsaturated aldehydes allowed the modulation of aldehyde linkage to amino group, generating films with different properties as a function of pH.

**Table 4**. Inhibition of *P. expansum* growth colony (%) of 0.05 g of CSCN (2, 5 and 7) at pH 2.

| | **Time (day)** | | | | **Visual appearance at 7 day** |
|---|---|---|---|---|---|
| pH | 3 | 5 | 7 | 10 | |
| 2 | 24.1±7.9[aB] | 24.7±5.7[aB] | 17.2±4.1[aAB] | 10.1±5.4[aA] |  |
| 5 | 62±33.3[abA] | 57.4±37.8[abA] | 53.1±35.6[bA] | 69.8±40.6[bA] |  |
| 7 | 100[bA] | 100[bA] | 100[cA] | 100[bA] |  |

Different superscript letters in the same row[(A-B)] and column[(a-c)] indicate a statistically significant difference (P ≤ 0.05).

## 4. Conclusions

The results obtained by spectroscopic analysis support that CT and CN can be covalently anchored to the amino group of CS efficiently. The pH of reaction between the aldehydes and the biopolymer allowed the modulation of swelling properties and aldehyde release. The swelling analysis revealed that the modification of acidic catalysis of reaction of α,β-unsaturated aldehydes with chitosan may promote another reaction in addition to the well-known Schiff base formation. The double cross-linked bond based on Schiff base and Michael addition between aldehydes and amino group generated a more robust film structure, stable at acidic pH, though its formation reduced the release of the active compound. The modulation of the degree of cross-linking by reaction pH was revealed as key factor to match required functional properties of the film. This allows the generation of imine-chitosan films with a wide range of novel applications.

## References

1.   Wada-Hiraike, O. Chapter 7 - Nrf2 and Oxidative Stress. In; Preedy, V.R.B.T.-P., Ed.; Academic Press, **2020**; pp. 77–86 ISBN 978-0-12-815972-9.

2.   Preedy, V.R. *Essential oils in food preservation, flavor and safety*; Academic Press, **2015**; ISBN 012416644X.

3.   Sarkic, A.; Stappen, I. Essential oils and their single compounds in cosmetics-a critical review. *Cosmetics* **2018**, *5*, 1–21, doi:10.3390/cosmetics5010011.

4.   Wuryatmo, E.; Klieber, A.; Scott, E.S. Inhibition of citrus postharvest pathogens by vapor of citral and related compounds in culture. *J. Agric. Food Chem.* **2003**, *51*, 2637–2640, doi:10.1021/jf026183l.

5.   Shen, Y.; Kahramanoğlu, İ.; Chen, C.; Chen, J.; Okatan, V.; Wan, C. Application of cinnamaldehyde for the postharvest storage of fresh horticultural products.

*Hortic. Int. J.* **2021**, *5*, 103–105, doi:10.15406/hij.2021.05.00212.

6.  Adams, T.B.; Cohen, S.M.; Doull, J.; Feron, V.J.; Goodman, J.I.; Marnett, L.J.; Munro, I.C.; Portoghese, P.S.; Smith, R.L.; Waddell, W.J.; et al. The FEMA GRAS assessment of cinnamyl derivatives used as flavor ingredients. *Food Chem. Toxicol.* **2004**, *42*, 157–185, doi:10.1016/j.fct.2004.11.014.

7.  JECFA safety evaluation of certain food additives and contaminants prepared by the sixty-first meeting of the Joint FAO/WHO Expert Committee on Food Additives (JECFA). *World Heal. Organ. Geneva* **2004**, *Series 52*.

8.  JEFCA evaluation of certain food additives and contaminants: Fifty-fifth report of the Joint FAO/WHO Expert Committee on Food Additives. **2001**, *Series 901*.

9.  Ponce, A.; Roura, S.I.; Moreira, M. del R. Essential oils as biopreservatives: different methods for the technological application in lettuce Leaves. *J. Food Sci.* **2011**, *76*, 34–41, doi:10.1111/j.1750-3841.2010.01880.x.

10. Neri, F.; Mari, M.; Menniti, A.M.; Brigati, S.; Bertolini, P. Control of *Penicillium expansum* in pears and apples by trans-2-Hexenal vapours. *Postharvest Biol. Technol.* **2006**, *41*, 101–108, doi:10.1016/j.postharvbio.2006.02.005.

11. Turek, C.; Stintzing, F.C. Stability of essential oils: A review. *Compr. Rev. Food Sci. Food Saf.* **2013**, *12*, 40–53, doi:10.1111/1541-4337.12006.

12. Liu, Y.; Wang, Y.; Huang, J.; Zhou, Z.; Zhao, D.; Jiang, L.; Shen, Y. Encapsulation and controlled release of fragrances from functionalized porous metal–organic frameworks. *AIChE J.* **2019**, *65*, 491–499, doi:10.1002/aic.16461.

13. Lashkari, E.; Wang, H.; Liu, L.; Li, J.; Yam, K. Innovative application of metal-organic frameworks for encapsulation and controlled release of allyl isothiocyanate. *Food Chem.* **2017**, *221*, 926–935, doi:10.1016/j.foodchem.2016.11.072.

14. Wei, M.; Pan, X.; Rong, L.; Dong, A.; He, Y.; Song, X.; Li, J. Polymer carriers for controlled fragrance release. *Mater. Res. Express* **2020**, *7*, doi:10.1088/2053-1591/aba90d.

15. Perinelli, D.R.; Palmieri, G.F.; Cespi, M.; Bonacucina, G. Encapsulation of flavours and fragrances into polymeric capsules and cyclodextrins inclusion complexes: An update. *Molecules* **2020**, *25*, doi:10.3390/molecules25245878.

16. Nagarajan, V.; Kizhaeral S, S.; Subramanian, M.; Rajendran, S.; Ranjan, J. Encapsulation of a volatile biomolecule (hexanal) in cyclodextrin metal–organic frameworks for slow release and its effect on preservation of mangoes. *ACS Food Sci. Technol.* **2021**, doi:10.1021/acsfoodscitech.1c00205.

17. Heras-Mozos, R.; Hernández, R.; Gavara, R.; Hernández-Muñoz, P. Dynamic covalent chemistry of imines for the development of stimuli-responsive chitosan films as carriers of sustainable antifungal volatiles. *Food Hydrocoll.* **2022**, *125*, doi:10.1016/j.foodhyd.2021.107326.

18. Huang, S.; Kong, X.; Xiong, Y.; Zhang, X.; Chen, H.; Jiang, W.; Niu, Y.; Xu, W.; Ren, C. An overview of dynamic covalent bonds in polymer material and their applications. *Eur. Polym. J.* **2020**, *141*, 110094, doi:10.1016/j.eurpolymj.2020.110094.

19. Herrmann, A.; Ghiseppone, N.; Lehn, J.M. Electric-field triggered controlled release of bioactive volatiles from imine-based liquid crystalline phases. *Chem. -

*A Eur. J.* **2009**, *15*, 117–124, doi:10.1002/chem.200801782.

20. Levrand, B.; Ruff, Y.; Lehn, J.M.; Herrmann, A. Controlled release of volatile aldehydes and ketones by reversible hydrazone formation - "Classical" profragrances are getting dynamic. *Chem. Commun.* **2006**, 2965–2967, doi:10.1039/b602312f.

21. Tchakalova, V.; Lutz, E.; Lamboley, S.; Moulin, E.; Benczédi, D.; Giuseppone, N.; Herrmann, A. Design of stimuli-responsive dynamic covalent delivery systems for volatile compounds (Part 2): Fragrance-releasing cleavable surfactants in functional perfumery applications. *Chem. - A Eur. J.* **2021**, *27*, 13468–13476, doi:10.1002/chem.202102051.

22. Marin, L.; Popa, M.; Anisiei, A.; Irimiciuc, S.A.; Agop, M.; Petrescu, T.C.; Vasincu, D.; Himiniuc, L. A Theoretical model for release dynamics of an antifungal agent covalently bonded to the chitosan. *Molecules* **2021**, *26*, doi:10.3390/molecules26072089.

23. Fadida, T.; Selilat-Weiss, A.; Poverenov, E. N-Hexylimine-chitosan, a biodegradable and covalently stabilized source of volatile, antimicrobial hexanal. Next generation controlled-release system. *Food Hydrocoll.* **2015**, *48*, 213–219, doi:10.1016/j.foodhyd.2015.02.033.

24. Kaminskas, L.M.; Pyke, S.M.; Burcham, P.C. Differences in lysine adduction by acrolein and methyl vinyl ketone: Implications for cytotoxicity in cultured hepatocytes. *Chem. Res. Toxicol.* **2005**, *18*, 1627–1633, doi:10.1021/tx0502387.

25. Ishii, T.; Yamada, T.; Mori, T.; Kumazawa, S.; Uchida, K.; Nakayama, T. Characterization of acrolein-induced protein cross-links. *Free Radic. Res.* **2007**, *41*, 1253–1260, doi:10.1080/10715760701678652.

26. Wang, H.T.; Hu, Y.; Tong, D.; Huang, J.; Gu, L.; Wu, X.R.; Chung, F.L.; Li, G.M.; Tang, M.S. Effect of carcinogenic acrolein on DNA repair and mutagenic susceptibility. *J. Biol. Chem.* **2012**, *287*, 12379–12386, doi:10.1074/jbc.M111.329623.

27. Azeredo, H.M.C.; Waldron, K.W. Crosslinking in Polysaccharide and Protein Films and Coatings for Food Contact - A Review. *Trends Food Sci. Technol.* **2016**, *52*, 109–122, doi:10.1016/j.tifs.2016.04.008.

28. Balaguer, M.P.; Gómez-Estaca, J.; Gavara, R.; Hernandez-Munoz, P. Biochemical properties of bioplastics made from wheat gliadins cross-linked with cinnamaldehyde. *J. Agric. Food Chem.* **2011**, *59*, 13212–13220, doi:10.1021/jf203055s.

29. Inukai, Y.; Chinen, T.; Matsuda, T.; Kaida, Y.; Yasuda, S. Selective separation of germanium(IV) by 2,3-dihydroxypropyl chitosan resin. *Anal. Chim. Acta* **1998**, *371*, 187–193, doi:10.1016/S0003-2670(98)00313-4.

30. Kasaai, M.R.; Arul, J.; Chin, S.L.; Charlet, G. The use of intense femtosecond laser pulses for the fragmentation of chitosan. *J. Photochem. Photobiol. A Chem.* **1999**, *120*, 201–205, doi:10.1016/S1010-6030(98)00432-8.

31. Heras-Mozos, R.; Gavara, R.; Hernández-Muñoz, P. Development of antifungal biopolymers based on dynamic imines as responsive release systems for the postharvest preservation of blackberry fruit. *Food Chem.* **2021**, *357*, doi:10.1016/j.foodchem.2021.129838.

32.     Chen, J.Y.; Jiang, H.; Chen, S.J.; Cullen, C.; Sabbir Ahmed, C.M.; Lin, Y.H. Characterization of electrophilicity and oxidative potential of atmospheric carbonyls. *Environ. Sci. Process. Impacts* **2019**, *21*, 856–866, doi:10.1039/c9em00033j.

33.     Dizdarević, A.; Marić, M.; Shahzadi, I.; Ari Efiana, N.; Matuszczak, B.; Bernkop-Schnürch, A. Imine bond formation as a tool for incorporation of amikacin in self-emulsifying drug delivery systems (SEDDS). *Eur. J. Pharm. Biopharm.* **2021**, *162*, 82–91, doi:10.1016/j.ejpb.2021.03.001.

34.     Erdtman, E.; Bushnell, E.A.C.; Gauld, J.W.; Eriksson, L.A. Computational studies on Schiff-base formation: Implications for the catalytic mechanism of porphobilinogen synthase. *Comput. Theor. Chem.* **2011**, *963*, 479–489, doi:10.1016/j.comptc.2010.11.015.

35.     Delmar, K.; Bianco-Peled, H. The dramatic effect of small pH changes on the properties of chitosan hydrogels crosslinked with genipin. *Carbohydr. Polym.* **2015**, *127*, 28–37, doi:10.1016/j.carbpol.2015.03.039.

36.     Di Giovannantonio, M.; Kosmala, T.; Bonanni, B.; Serrano, G.; Zema, N.; Turchini, S.; Catone, D.; Wandelt, K.; Pasini, D.; Contini, G.; et al. Surface enhanced polymerization via Schiff-base coupling at the solid-water interface under pH control. *J. Phys. Chem. C* **2015**, *119*, 19228–19235, doi:10.1021/acs.jpcc.5b05547.

37.     Barbosa, H.F.G.; Francisco, D.S.; Ferreira, A.P.G.; Cavalheiro, É.T.G. A new Look towards the thermal decomposition of chitins and chitosans with different degrees of deacetylation by coupled TG-FTIR. *Carbohydr. Polym.* **2019**, *225*, 115232, doi:10.1016/j.carbpol.2019.115232.

38.     Guaresti, O.; Basasoro, S.; González, K.; Eceiza, A.; Gabilondo, N. *In situ* cross–linked chitosan hydrogels via Michael addition reaction based on water–soluble thiol–maleimide precursors. *Eur. Polym. J.* **2019**, *119*, 376–384, doi:10.1016/j.eurpolymj.2019.08.009.

39.     Gadkari, R.R.; Suwalka, S.; Yogi, M.R.; Ali, W.; Das, A.; Alagirusamy, R. Green synthesis of chitosan-cinnamaldehyde cross-linked nanoparticles: Characterization and antibacterial activity. *Carbohydr. Polym.* **2019**, *226*, 115298, doi:10.1016/j.carbpol.2019.115298.

40.     Ailincai, D.; Porzio, W.; Marin, L. Hydrogels based on imino-chitosan amphiphiles as a matrix for drug delivery systems. *Polymers (Basel).* **2020**, *12*, 1–16, doi:10.3390/polym12112687.

41.     Agatonovic-Kustrin, S.; Ristivojevic, P.; Gegechkori, V.; Litvinova, T.M.; Morton, D.W. Essential oil quality and purity evaluation via FT-IT spectroscopy and pattern recognition techniques. *Appl. Sci.* **2020**, *10*, 1–12, doi:10.3390/app10207294.

42.     Higueras, L.; López-Carballo, G.; Gavara, R.; Hernández-Muñoz, P. Reversible covalent immobilization of cinnamaldehyde on chitosan films via Schiff base formation and their application in active food packaging. *Food Bioprocess Technol.* **2015**, *8*, 526–538, doi:10.1007/s11947-014-1421-8.

43.     Marin, L.; Moraru, S.; Popescu, M.C.; Nicolescu, A.; Zgardan, C.; Simionescu, B.C.; Barboiu, M. Out-of-water constitutional self-organization of chitosan-

cinnamaldehyde dynagels. *Chem. - A Eur. J.* **2014**, *20*, 4814–4821, doi:10.1002/chem.201304714.

44. Silva, P.J. New Insights into the mechanism of Schiff base synthesis from aromatic amines in the absence of acid catalyst or polar solvents. *PeerJ Org. Chem.* **2020**, *2*, e4, doi:10.7717/peerj-ochem.4.

45. Lopachin, R.M.; Gavin, T. Molecular mechanisms of aldehyde toxicity: A chemical perspective. *Chem. Res. Toxicol.* **2014**, *27*, 1081–1091, doi:10.1021/tx5001046.

46. Schiffman, J.D.; Schauer, C.L. Cross-linking chitosan nanofibers. *Biomacromolecules* **2007**, *8*, 594–601, doi:10.1021/bm060804s.

47. Rao, M.R.; Fang, Y.; De Feyter, S.; Perepichka, D.F. Conjugated covalent organic frameworks via Michael addition-elimination. *J. Am. Chem. Soc.* **2017**, *139*, 2421–2427, doi:10.1021/jacs.6b12005.

48. Gao, X.; Zhou, Y.; Ma, G.; Shi, S.; Yang, D.; Lu, F.; Nie, J. A Water-soluble photocrosslinkable chitosan derivative prepared by Michael-addition reaction as a precursor for injectable hydrogel. *Carbohydr. Polym.* **2010**, *79*, 507–512, doi:10.1016/j.carbpol.2009.08.033.

49. Li, R.; Zhao, J.; Gan, Z.; Jia, W.; Wu, C.; Han, D. Gold promotion of MCM-41 supported ruthenium catalysts for selective hydrogenation of α,β-unsaturated aldehydes and ketones. *Catal. Letters* **2018**, *148*, 267–276, doi:10.1007/s10562-017-2218-y.

50. Wegrzynowska-Drzymalska, K.; Grebicka, P.; Mlynarczyk, D.T.; Chelminiak-Dudkiewicz, D.; Kaczmarek, H.; Goslinski, T.; Ziegler-Borowska, M. Crosslinking of chitosan with dialdehyde chitosan as a new approach for biomedical applications. *Materials (Basel).* **2020**, *13*, 1–27, doi:10.3390/ma13153413.

51. Zhang, Y.; Thomas, Y.; Kim, E.; Payne, G.F. pH- and voltage-responsive chitosan hydrogel through covalent cross-linking with catechol. *J. Phys. Chem. B* **2012**, *116*, 1579–1585, doi:10.1021/jp210043w.

52. Zhang, Y.; Wang, Q.; Wang, Z.; Zhang, D.; Gu, J.; Ye, K.; Su, D.; Zhang, Y.; Chen, J.; Barboiu, M. Strong, self-healing gelatin hydrogels cross-linked by double dynamic covalent chemistry. *Chempluschem* **2021**, *86*, 1524–1529, doi:10.1002/cplu.202100474.

53. Gómez-Estaca, J.; Montero, P.; Gómez-Guillén, M.C. Shrimp (*Litopenaeus Vannamei*) muscle proteins as source to develop edible films. *Food Hydrocoll.* **2014**, *41*, 86–94, doi:10.1016/j.foodhyd.2014.03.032.

54. Bao, J.; Zhang, H.; Zhao, X.; Deng, J. Biomass polymeric microspheres containing aldehyde groups: Immobilizing and controlled-releasing amino acids as green metal corrosion inhibitor. *Chem. Eng. J.* **2018**, *341*, 146–156, doi:10.1016/j.cej.2018.02.047.

55. Ay, E.; Gérard, V.; Graff, B.; Morlet-Savary, F.; Mutilangi, W.; Galopin, C.; Lalevée, J. Citral photodegradation in solution: Highlighting of a radical pathway in parallel to cyclization pathway. *J. Agric. Food Chem.* **2019**, *67*, 3752–3760, doi:10.1021/acs.jafc.8b07034.

56. Chen, H.; Zhao, R.; Hu, J.; Wei, Z.; Mcclements, D.J.; Liu, S.; Li, B.; Li, Y. One-

step dynamic imine chemistry for preparation of chitosan-stabilized emulsions using a natural aldehyde: Acid trigger mechanism and regulation and gastric delivery. *J. Agric. Food Chem.* **2020**, *68*, 5412–5425, doi:10.1021/acs.jafc.9b08301.

57. Wang, H.; Yang, Z.; Ying, G.; Yang, M.; Nian, Y.; Wei, F.; Kong, W. Antifungal evaluation of plant essential oils and their major components against toxigenic fungi. *Ind. Crops Prod.* **2018**, *120*, 180–186, doi:10.1016/j.indcrop.2018.04.053.

58. Friedman, M.; Henika, P.R.; Mandrell, R.E. Bactericidal activities of plant essential oils and some of their isolated constituents against C*ampylobacter jejuni, Escherichia coli, Listeria monocytogenes,* and *Salmonella enterica*. *J. Food Prot.* **2002**, *65*, 1545–1560, doi:12380738.

59. Wang, Y.; Feng, K.; Yang, H.; Yuan, Y.; Yue, T. Antifungal mechanism of cinnamaldehyde and citral combination against: *Penicillium expansum* based on FT-IR fingerprint, plasma membrane, oxidative stress and volatile profile. *RSC Adv.* **2018**, *8*, 5806–5815, doi:10.1039/c7ra12191a.

60. Friedman, M. Chemistry, antimicrobial mechanisms, and antibiotic activities of cinnamaldehyde against pathogenic bacteria in animal feeds and human foods. *J. Agric. Food Chem.* **2017**, *65*, 10406–10423, doi:10.1021/acs.jafc.7b04344.

61. Ueno, T.; Masuda, H.; Ho, C.T. Formation mechanism of P-methylacetophenone from citral via a tert-alkoxy radical intermediate. *J. Agric. Food Chem.* **2004**, *52*, 5677–5684, doi:10.1021/jf035517j.

62. Muller, J.; Casado Quesada, A.; González-Martínez, C.; Chiralt, A. Antimicrobial properties and release of cinnamaldehyde in bilayer films based on Polylactic Acid (PLA) and starch. *Eur. Polym. J.* **2017**, *96*, 316–325, doi:10.1016/j.eurpolymj.2017.09.009.

63. Lian, H.; Peng, Y.; Shi, J.; Wang, Q. Effect of emulsifier Hydrophilic-Lipophilic Balance (HLB) on the release of thyme essential oil from chitosan films. *Food Hydrocoll.* **2019**, *97*, doi:10.1016/j.foodhyd.2019.105213.

64. Balaguer, M.P.; Borne, M.; Chalier, P.; Gontard, N.; Morel, M.H.; Peyron, S.; Gavara, R.; Hernandez-Munoz, P. Retention and release of cinnamaldehyde from wheat protein matrices. *Biomacromolecules* **2013**, *14*, 1493–1502, doi:10.1021/bm400158t

# CAPÍTULO II.

# Aplicación tecnológica de películas antimicrobianas que responden a estímulos externos en el envasado de alimentos

## Artículo 4

**Development of antifungal biopolymers based on dynamic imines as responsive release system for the postharvest preservation of blackberry fruit**

## Artículo 5

**Responsive packaging for extending the shelf-life of refrigerated fresh-cut pineapple**

## Artículo 6

**pH modulates antibacterial activity of hydroxybenzaldehyde derivates immobilized in chitosan films via reversible Schiff bases and their application to preserve freshly-squeezed juice**

# Artículo 4

**Development of antifungal biopolymers based on dynamic imines as responsive release systems for the postharvest preservation of blackberry fruit**

Raquel Heras-Mozos, Rafael Gavara, Pilar Hernández-Muñoz

Instituto de Agroquímica y Tecnología de Alimentos (IATA-CSIC),

Av, Agustín Escardino, 7, 46980, Paterna, Valencia, Spain.

**ABSTRACT**

This study describes the synthesis and reversibility of Schiff bases from chitosan and bioactive compounds, and their application in the antifungal packaging of fruit. Imine bonds between primary amine groups of chitosan and carbonyl groups of antifungal aldehydes were synthesised and their reversibility was assayed in an aqueous medium under different acidic conditions. The mechanism of action of the imine-chitosan films is based on the hydrolysis of imine bond and the release of the active agent. The new films were effective at inhibiting the growth of *Penicillium expansum* and *Botrytis cinerea*, and their effectivity depended on the degree of hydrolysis achieved which was greater when the bonds were hydrolysed in a mild acidic medium. A double bottom cylindrical tray was used for the responsive antimicrobial packaging of blackberries. The package extended the shelf-life of berries from 3 to 12 days without causing phytotoxic effects on the fruit being safe for human consumption.

**Keywords:** trans-2-hexenal, perillaldehyde, chitosan, reversible covalent bond, Schiff base, imine hydrolysis, antifungal packaging, blackberries

## 1. Introduction

Food loss is a major concern in the world giving rise to a significant waste of resources, and causing negative impact on economic development, food security and environment. In general, food loss refers to the decrease in edible food mass for human consumption throughout all the stages of the supply chain from production to final consumption [1]. Regarding postharvest loss of fruits and vegetables, it accounts for 52-55% in developing countries, and between 37 and 52% in industrialized countries [2]. Whereas in industrialized regions postharvest losses are associated with quality standards and consumer dissatisfaction, in developing countries main losses are due to agricultural production, being those associated to postharvest and distribution are also considerable [3].

Worldwide, microbial infection of harvested fruit and vegetables is a critical issue throughout the postharvest supply chain, from harvesting contamination to transformation, trade, and the final sale [4] regardless of the country. The direct consequences are considerable food losses limiting the storage time of fruit and vegetables and their self-life in the market.

Classically, synthetic chemicals have been mostly used to manage postharvest diseases of fruits and vegetables. However, environmental, and health issues with fungal resistance have favoured the search of new safer and natural strategies to mitigate postharvest fungal diseases. Many natural molecules existing in plants are secondary metabolites produced for signalling and defence purposes. As a defence mechanism, when plants suffer tissue damage, they stress and produce large quantities of molecules with antimicrobial properties to prevent invasion by harmful microorganisms [5]. Among natural molecules with antifungal activity produced by plants they are volatile compounds. Commonly, they are present as components of essential oils and plant extracts. Moreover, they are recognised as safe and mostly used as flavouring agents in the food and beverage industry and as fragrances in perfumery and household industrial uses [6]. Most of these molecules have a considerable vapour pressure and an adequate volatility which makes them appropriate to be applied in cold storage chambers and in active food packaging. Therefore, due to their antifungal capacity and safety, they are being extensively studied as an

alternative to synthetic fungicides to prevent fungal rotting of fruit and vegetables [7].

Although there is a lot of research on applying natural antifungal volatiles on postharvest disease of fruits and vegetables [5,8,9], there is a lack of studies on creating appropriate controlled release devices to efficiently applying these volatile compounds [10]. To date, most of the studies regarding applying naturally occurring antifungal volatiles are conducted spraying directly the volatile or embedding it in a paper disc, whereas a more sophisticated alternative, consists on incorporating the antifungal in the walls of the package for the design of active packaging [11]. However, this technology presents several drawbacks. Mainly, there is not a triggering mechanism for the release of the volatile from the polymer besides the accounting losses of the volatile during the polymer processing, this also is lost after polymer processing and storage before the food is packaged. Moreover, often the extent and kinetics of the volatile release is not adequate to reach a constant concentration to be active in the head space of the package.

Therefore, the aim of this study was to develop a new device capable of carrying the antifungal volatile covalently grafted to the polymer backbone with a reversible Schiff base or imine. The molecule will be stabilised in the polymer and liberated under acid hydrolysis of the imine bond. Thus, α, β-unsaturated aldehydes *trans*-2-hexenal, and perillaldehyde (*p*-mentha-1,8-dien-7-al) were chosen as naturally occurring antifungal volatiles for grafting in the primary amino functional groups of a chitosan biopolymer.

Trans-2-Hexenal is an α, β-unsaturated aldehyde which belongs to the group comprised by six-carbon aldehydes and their corresponding alcohol and ester derivatives, and known as green leaf volatiles (GLVs) since are responsible for the green odour of plants [12].

Trans-2-hexenal with other GLVs are emitted by stressed or wounded plants to protect them against fungi and insects due to pathological properties [13]. Trans-2-hexenal has been evaluated as safe for human consumption by the FAO/WHO Expert Committee on Food Additives (*JECFA*) [14]. The ability of this compound to fight microbial infection has been assayed in different fruits [15].

Perillaldehyde is a monocyclic terpene α, β-unsaturated aldehyde found in perilla herb; this is allowed by the FAO/WHO Expert

Committee on Food Additives (*JECFA*) as a flavouring agent for human consumption. There are some studies regarding the antifungal activity of this molecule in cherry tomatoes [9]. Recently, under a request of the European Commission, the EFSA has elaborated a study on the genotoxicity of perillaldehyde and has changed the status of this flavouring agent to tentative [16]. However, *in vivo* studies on the genotoxicity of perillaldehyde are controversial [17].

In this study, these aldehydes were covalently grafted to primary amino groups of chitosan films with a Schiff base or imine (C=N) formation. The effect of the pH on the reversibility of the bond and subsequent release of the volatile was studied measuring the antifungal effectivity of the system *in vitro* against common fruit spoilage fungi *Penicillium expansum* and *Botrytis cinerea*. The effectiveness of the synthesised biodynamers was assayed to prevent the fungal spoilage of blackberry fruit. Finally, the new active material was incorporated in the design of a package to extend the shelf-life of the fruit. Blackberry fruits have a delicate structure and presents a thin fragile skin, and a great susceptibility to fungal decay by *B. cinerea* which give the fruit a short postharvest shelf-life and its time in the market very limited [18].

## 2. Materials and methods
### 2.1. Materials

Low molecular weight chitosan with a degree of deacetylation (DD) of 75-85%, acetic acid glacial, *trans*-2-hexenal 98% (HX) and (S)-(-)-perillaldehyde 92% (PL) was purchased from Sigma-Aldrich (Barcelona-Spain). Ethanol 96%, hydrochloric acid 37%, di-phosphorus pentoxide and granulated sodium hydroxide of synthesis grade were supplied by Scharlab (Barcelona, Spain).

### 2.2. Chitosan film formation

Chitosan film forming solution was prepared dissolving 1.5 g of chitosan in 100 ml of 0.5% (w/w) acetic acid aqueous solution under stirring for 1 hour at 50 °C, after that the solution was filtered with a cheesecloth to eliminate impurities. Chitosan acetate solution was cast on polystyrene plates and dried at 37 °C for 24 h with 30-40 % relative humidity. Chitosan acetate films were peeled from the trays, and the resulting average thickness was $35 \pm 5$ μm, measured with a digital

Mitutoyo micrometer (Metrotec, San Sebastian, Spain). Chitosan films were cut into $2 \times 2$ cm samples and neutralised with 0.1 M sodium hydroxide for 24 h. After neutralisation, the films were washed with distilled water and dried at 37 °C. The dry chitosan films were stored in glass desiccators until usage.

## 2.3. Synthesis of dynamic chitosan

Chitosan (CS) films attached with an aldehyde-Schiff base were achieved at the solid/liquid interface via a solvent method using ethanol 96% (v/v) as the reaction medium. For that, 2 g of neutralised CS films were immersed in an Erlenmeyer flask containing 75 ml of 96% ethanol (v/v) and 4 g of the corresponding aldehyde. The flask was placed in a shaking bath at 60 °C for 24 h. After, the films were washed to remove the excess of aldehyde by immersing and shaking them three times in 96% ethanol (v/v) for 24 h at 60 °C. Finally, reacted CS films were dried and stored in a glass desiccator with $P_2O_5$ prior to use.

## 2.4. Evidence of Schiff base formation

Formation of carbon–nitrogen double *bonds* (C=N) between the primary amino groups of 2-amino-2-deoxy-d-glucopyranose (*GlcN*) units of chitosan and aldehydes was shown using Attenuated Total Reflectance-Fourier Transform Infrared Spectroscopy (ATR-FTIR). The extent of the Schiff base formation in relation to the unreacted amino groups, named degree of substitution (DS), was calculated by Elemental Analysis.

### 2.4.1. ATR-FTIR

Formation of the IR band of the imine group in neutralised CS films was recorded with a Bruker Tensor 27 FTIR spectrometer (Bruker Española S.A., Barcelona, Spain). The spectrum was obtained by accumulating of at least 32 scans per test at a resolution of 4 $cm^{-1}$ between 4000 to 600 $cm^{-1}$. Results were analysed in triplicate and treated with the OPUS v. 5.0 software.

### 2.4.2. Elemental Analysis

Elemental analysis was used to quantify the percentage of amine groups that reacted with the aldehyde. The DS was calculated using the C/N ratio of dry modified films. The analysis was performed with a CHNS-O elemental analyser FlashSmart (Thermo Fisher Scientific, Waltham, MA, USA). Elemental composition was used to estimate the degree of acetylation (DA) of neutralised CS films according to the methodology proposed by Kasaai, Arul, Chin, & Charlet, (1999). In addition, the DS was calculated following the method suggested by Inukai, Chinen, Matsuda, Kaida, & Yasuda, (1998). A relation between C/N ratio of imine-chitosan film and ratio of the neutralised CS were applied to estimate both parameters. Samples were analysed in triplicate.

### 2.5. Antifungal pH-response of synthetized Schiff bases

Dynamic chitosan was assayed at pH 4 and 7 to test the reversibility of the imine bond and release of the aldehyde. For that, the films were tested *in vitro* against *B. cinerea* and *P. expansum.* The device with better antifungal response was incorporated in a package for blackberries.

#### 2.5.1. Preparation of fungal cultures

Fungal strains were supplied by the Spanish Type Culture Collection (CECT). *B. cinerea* (CECT 2100) and *P. expansum* (CECT 2278) were grown and maintained in potato dextrose agar (PDA) for at least 7 days at 26 °C. Conidial suspensions of each fungi strain were obtained from the fungal surface of the petri dishes with sterile peptone water and Tween 80 (0.05% v/v). Mould aliquots were transferred to a sterile Eppendorf and several dilutions were conducted until obtaining $10^6$ spores/mL. The spore concentration was adjusted using the improved Neubauer method (Bright-Line Hemacytometer, Hausser Scientific, Horsham, PA).

#### 2.5.2. Antifungal activity of aldehydes

The antifungal activity of both aldehydes, HX and PL, was evaluated in vapour phase against *P. expansum* and *B. cinerea* determining the minimum inhibitory and the fungicidal concentrations.

The minimum inhibitory concentration (MIC) of the active agent was defined as the smallest volume of aldehyde that causes at least 50% of inhibition respect to the control growth after 7 days of incubation. The minimum fungicidal concentration (MFC) was defined as the aldehyde concentration in the vapour phase, after 7 days of contact with the mould and without observable fungal growth; after the paper is removed and no more fungal growth is observed over the next 3 days of incubation. To evaluate the MIC and MFC, petri plates of 90 mm were filled with 15 mL of PDA, allowing a headspace volume of 80 $cm^3$, and were then inoculated with 3 μL of the spore solution at three equidistant points. Different amounts of each aldehyde, between 1 to 10 μL, were added on 50 mm sterile paper filter and placed on the cover inside of the petri plate. The plates were sealed with Parafilm® to decrease the volatile agent loss and incubated at 26 °C for 9 days. Controls were prepared without a volatile and all the test were conducted in triplicate. The values of MIC and MFC were expressed as concentration (μL/$cm^3$) based on the volume (μL) of each aldehyde added to the paper and the headspace volume (80 $cm^3$) of the petri dish. Fungal growth was evaluated measuring fungal growth diameter (cm) and expressed as inhibition degree. All analyses were conducted in triplicate.

### 2.5.3. In vitro antifungal assay based on pH-response of dynamic aldehyde-imine-chitosan films

The antifungal activity of peryllaldehyde-imine-chitosan films (CSPL) and trans-2-hexenal-imine-chitosan films (CSHX) was tested against *P. expansum* and *B. cinerea*. A double plate system was used to conduct the assay (**Figure 1**). For that, a petri dish of 58 mm with PDA medium was inoculated with 3 μL of the conidial suspension at one middle point and was placed in a larger petri dish of 90 mm of diameter containing 0.10 g of film. The films were covered with a buffer solution at different pH (pH 7 or 4) to evaluate the reversibility of the formed imine bonds and the release of the aldehyde. Then, the larger petri dishes were lidded and incubated at 26 °C for 7 days. A control with CS film and another, without film, also were tested. After the incubation period, the films were removed and incubated 3 days more to observe fungicidal or fungistatic activity of the aldehyde released. Fungal

growth was checked on days 3, 5, 7, and 9 of incubation and the diameter of fungal growth was measured. All experiments were performed in triplicate.
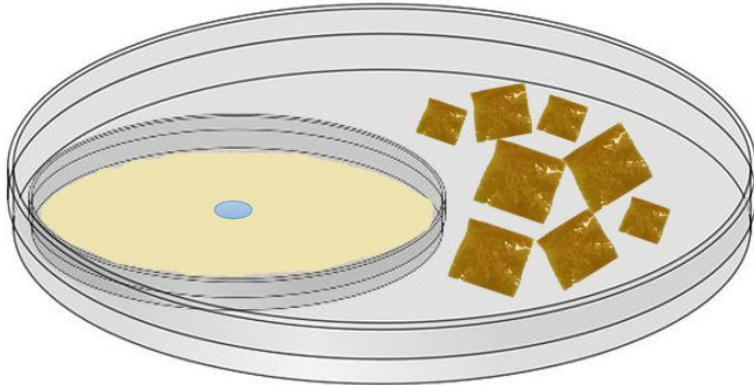


**Figure 1.** Double plate system used to test *in vitro* antifungal properties of aldehyde-imine-chitosan films.

*2.5.4. Antifungal effectiveness of dynamic films on packaged blackberries*

The antifungal activity of CSHX films was evaluated in blackberries (*Rubus fruticosus*), a variety called Driscoll's Victoria, purchased in a local supermarket. For that, 0.5 g of responsive film was placed inside a petri dish of 58 mm and was activated with a pH 4 buffer solution to promote hydrolysis of imine bonds. Then, the plate with the active system was placed inside 500 cm$^3$ trays made of PP/EVOH/PP containing 50 g of blackberries (between five and six units) which were located inside the tray without contact. Finally, the trays were sealed with PP film of 30 μm using a heat sealer SMART 300 traysealer (ULMA. Embalaje S.C., Spain) at 175 °C for 2 s to allow natural respiration processes of the fruit, the PP film was perforated with a needle with a diameter of 0.7 mm along the PP film. A control without the biodynamer also was tested. A schematic of the system used to test the effectivity of the biodynamer on blackberries can be found in **Figure 2A**. The trays were stored at room temperature (22 °C) and at refrigeration temperature (4 °C). The fungal growth was evaluated over

time by visual inspection of each fruit until the complete decay of the berries.

After testing the antifungal effectiveness of biodynamers on blackberries, a prototype package on a cylindrical tray of 220 cm$^3$ equipped with a double bottom was used to evaluate the microbiological shelf-life of blackberries. Two amounts of film were assayed, 0.15 g and 0.5 g. The double bottom packaging system was developed to avoid direct contact between the active film and the fruit. The responsive film was placed at the bottom of the package and covered with pH 4 buffer as the antifungal trigger. Then, a perforated plastic pad was placed upon the films, simulating the double bottom. The perforated double bottom allowed the access of the released aldehyde to the headspace of the package. Finally, the blackberries were placed on the top of the plastic pad allowing contact among them; the package was sealed with perforated PP and stored at 4 °C for 15 days. A schematic of the prototype package used to test the shelf-life of fruit is depicted in **Figure 2B**.
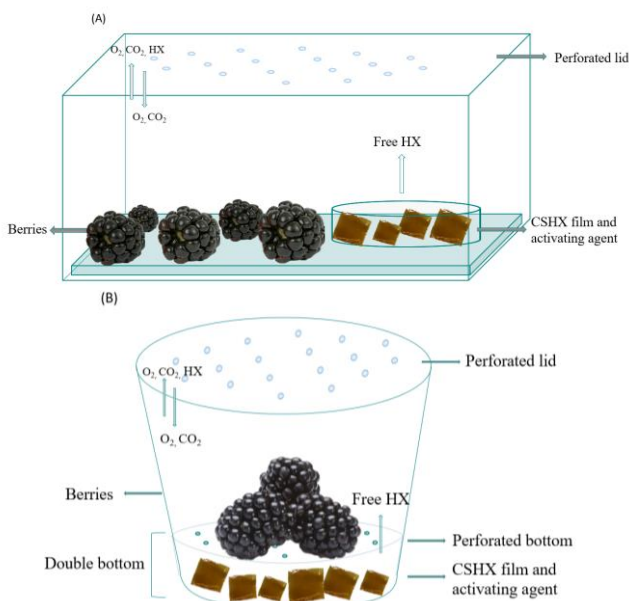


**Figure 2.** Packaging system employed to evaluate antifungal effectiveness of biodynamer films on blackberries (A); and double bottom package incorporated with biodynamer film used to study shelf-life of blackberries (B).

Fungal infection of the berries was monitored at days 1, 3, 6, 9, 12, and 15 by visual inspection. In this developed packaging, the mean number of contaminated berries was obtained, and the infection percentage of berries was calculated. Blackberries with visible fungal growth were considered infected but level of infection was not estimated. All the tests were conducted in triplicate.

*2.5.5. Evolution of the concentration of trans-2-hexenal in the headspace of the double bottom package*

The concentration of HX in the headspace of the double bottom package containing blackberries and stored at 4 °C was monitored using gas chromatography (GC) after 6 h of packaging and at days 1, 3, 6, 9, 12, and 15. The monitoring was conducted in packages with 0.15 and 0.5 g of CSHX films, and in the control package without film. For that, samples of 500 μL were manually collected from the headspace of each package and injected in a gas chromatograph (GC) mod. 6850 Series II Network GC System (Agilent Technologies, Palo Alto, CA, USA). The GC was equipped with a flame ionisation detector (FID) and a Restek RTX1 capillary column (30 m of length, 0.53 mm internal diameter, and 5 μL thickness) with a flow rate 14.6 mL/min of helium as carrier gas. Injector temperature and FID temperature was fixed at 220 °C. Temperature of oven was from 35 to 220 °C, with an initial hold time of 5 min, after that, a temperature increase of 10 ºC/min until 120 °C, and then at 30 °C/min until 220 °C, with 5 min of hold temperature. Thus, measurement time was 21.8 min. Samples were run in the splitless mode. The obtained values were quantified according to a previous calibration curve. Results were expressed as μg of trans-2-hexenal per $L_{air}$ of headspace. All analyses were conducted in triplicate.

*2.5.6. Evolution trans-2-hexenal and its metabolites in packaged blackberries*

The concentration of HX retained in blackberries packaged in the double bottom trays alone containing 0.5 g of CSHX film was monitored through the storage time at days 1, 3, 6, and 12. The analysis was performed using the solid phase micro-extraction (SPME) technique coupled with GC based on the method created by Almenar, Catala, Hernandez-Muñoz, & Gavara, (2009). For compound analysis,

50 g of blackberries were mixed with the same amount of distilled water and homogenised for 3 min with a Ultraturrax IKA T18 Basic (IKA, Staufen, Germany) until obtaining a purée. After that, 15 g of blackberries purée was placed in a 20 mL crimp-sealed vial. The extraction of the volatile compounds was conducted with a 50/30 µm DVB/CAR/PDMS fibre (Supelco Inc., Barcelona, Spain), which was exposed to the vial content during 20 min at 23 °C. After, the fibre was removed, and was immediately thermally desorbed into the GC injector at 220 °C for 10 min. The samples were analysed using the same chromatographic conditions specified for evaluating the volatile in the package's headspace. A calibration of known amounts of trans-2-hexenal in this fruit matrix was performed following the same methodology as explained in section 2.5.5. Three replicates were prepared for each treatment and storage day.

Besides the quantification of HX in berries, the identification and evolution of the volatile, through the storage time and the presence of volatiles associated to the metabolism of HX by blackberries, was studied using GC-MS. For that, SPME fibre was also desorbed in Agilent 7809B GC coupled to an Agilent 5977B MSD detector (Agilent Technologies, Palo Alto, CA, USA) equipped with a HP-5MS column (30 m x 0.25 mm of internal diameter and 0.25 µm thickness). The fibre was introduced into the GC inlet in with a 5:1 split mode at 250 °C for a 10 min of thermal desorption. The oven conditions were an initial temperature of 40 °C with a hold time of 4 min, rising at 10 °C/min until reach 220 °C, and then a hold time of 10 min. The detector temperature was held at 250 °C. MS detection was performed in full scan mode from 33 to 500 m/z at 3.1 scan/s. Detected compounds were identified with the National Institute of Standards and Technology (NIST) spectral library v.2.3 (Agilent Technologies, Palo Alto, CA, USA). The control obtained mass spectra were compared to the mass spectra of samples packaged with biodynamers to identify compound differences.

## 2.6. Statistical analysis

All the tests were conducted at least in triplicate. Statistical analysis of the results was performed with the SPSS® computer program, v.24 (SPSS commercial software, SPSS Inc., Chicago, IL, USA). Results were analysed by applying a one-way analysis of

variance (ANOVA). Means were separated using the Tukey *b* test with a level of significance of $P \leq 0.05$.

## 3. Results and discussion

### 3.1. Characterisation of Schiff base formation

ATR-FTIR was used to show the synthesis of Schiff bases in films. The IR spectra of neutralised chitosan films and imine-chitosan films are represented in **Figure 3**. All the spectra were represented from 1950 to 600 cm$^{-1}$ and were maximised at 1025 cm$^{-1}$, a peak characteristic of chitosan, which corresponds to stretching of C$_6$-OH of the polymer. Chitosan distinctive absorption bands appeared at 1643 cm$^{-1}$ corresponding to the C=O stretching of amide I, and at 1581 cm$^{-1}$ assigned to the N-H bending of the primary amine [22]. The formation of the imine bond (C=N) by the nucleophilic addition of trans-2-hexenal to primary amino groups of 2-amino-2-deoxy-d-glucopyranose (*GlcN*) units of chitosan gave rise to a new and strong absorption band at 1650 cm$^{-1}$, whereas this band appeared at 1640 cm$^{-1}$ when the imine bond was formed with perillaldehyde. Moreover, the distinctive band related to carbonyl group (C=O) of free aldehydes which could appear around 1685-1740 cm$^{-1}$ [23], was not observed, thus free aldehyde was not occluded in the film.

Due to the transformation of primary amine groups to imines, the intensity of the band at 1580 cm$^{-1}$ associated to primary amine group of chitosan, experienced a decrease after formation of Schiff bases with both aldehydes. Identification by FTIR analyses of Schiff base between chitosan and several aldehydes was reported. For instance, the strong peak corresponding to imine formation between the amino group of chitosan and cinnamaldehyde was reported at 1633 cm$^{-1}$ [24]. However, when the Schiff base was synthesised using vanillin, the imine group appeared around 1646 cm$^{-1}$ [25]. Other authors have reported the Schiff base around 1630 and 1640 cm$^{-1}$ with salicylaldehyde and its derivates [26]. According to the data obtained in this study, and the reported information by other authors, the imine band (-C=N-) appears in the range 1630–1660 cm$^{-1}$ depending on the chemical structure of the aldehyde used for synthesis.
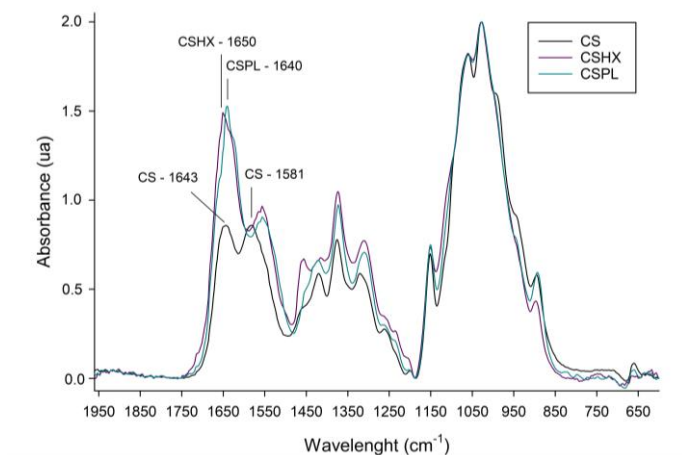
**Figure 3.** ATR-FTIR spectra of chitosan neutralised films and synthetised Schiff bases with trans-2-hexenal (CSHX) and perillaldehyde (CSPL).

The degree of substitution of free amino groups of CS film due to the attachment of aldehydes was quantified using elemental analysis and given as the percentage of primary amine groups transformed into imines in relation to available primary amino groups. The deacetylation degree of neutralised CS films was previously evaluated, being around 75% and in accordance with the value given by the commercial supplier. **Table 1** shows that the DS varied with the aldehyde grafted to the chitosan matrix. The greater DS was obtained with trans-2-hexenal, being above 70% of primary amino groups of chitosan grafted to the aldehyde. However, only 35% of DS was obtained with perillaldehyde.

The difference between the rates of conversion of both aldehydes could be related with the aldehyde reactivity. Aldehydes are electrophilic compounds, which can easily react with primary amino groups of a chitosan polymer. Different studies have reported on the reactivity of aldehydes and their relationship with electronegativity potential [27], and its structure, long chain or substituent [26,28]. Great DS in chitosan has been also reported for other α, β-unsaturated aldehyde [24].

**Table 1.** Elemental analysis and substitution degree (%) of Schiff bases derived from chitosan films.

| Films | N (%) | C (%) | (C/N) | DS (%) |
|-------|-------|-------|-------|--------|
| CS | $7.70 \pm 0.03^b$ | $43.60 \pm 0.12^a$ | $5.66 \pm 0.01^a$ | - |
| CSHX | $5.62 \pm 0.08^a$ | $50.59 \pm 0.07^c$ | $9.01 \pm 0.13^c$ | $73.97 \pm 2.97^b$ |
| CSPL | $5.58 \pm 0.10^a$ | $46.38 \pm 0.05^b$ | $8.31 \pm 0.16^b$ | $35.16 \pm 2.08^a$ |

[a-c] Different letters in the same column indicate a statistically significant difference (P ≤0.05)

### 3.2. Antifungal pH-response of synthetised Schiff bases

#### 3.2.1. Antifungal activity of aldehydes

The MIC and MFC of free trans-2-hexenal (HX) and perillaldehyde (PL) was studied in vapour phase against *P. expansum* and *B. cinerea*, and the results are showed in **Table 2**. HX presented greater antifungal activity than PL against both fungi. HX was more active against *P. expansum,* as the MIC was double for *B. cinerea*; whereas the MIC of PL against both fungi was similar. However, MFC of HX was slightly higher against *B. cinerea* than *P. expansum*. In contrast, *B. cinerea* was more sensitive to PL than *P. expansum* and a greater concentration was necessary to kill the fungi. Unsaturated aliphatic aldehydes have been reported to have antimicrobial activity greater than their saturated homologous, exhibiting a broad spectrum of antibacterial and antifungal activity [28]. Their mechanism of action is believed to involve the electrophilic nature of carbonyl groups and its ability to form Schiff Bases or Michael additions [29]. Thus, these compounds can react with molecules like proteins or DNA, and obstruct the successful growth of the pathogen [30]. The slight differences between both aldehydes observed in **Table 2** could be linked to several factors. The quantitative structure-activity relationship (QSAR) approach is a valuable tool used to find relationships between structural-related properties and biological activity of molecules [27,30]. Different properties of several aldehydes have been related with their antifungal properties, such as electronegativity [30], position of substituent [31], lipophilic character [32], and the volatility of the compound [8].

**Table 2.** Antifungal properties of *trans*-2-hexenal (HX) and perillaldehyde (PL).

| | *Penicillium expansum* | | *Botrytis cinerea* | |
|---|---|---|---|---|
| | **Concentration of aldehyde (µL/cm$^3$) per plate** | | | |
| | **MIC** | **MFC** | **MIC** | **MFC** |
| HX | 0.012 | 0.025 | 0.025 | 0.038 |
| PL | 0.044 | 0.125 | 0.050 | 0.094 |

The antifungal activity of both aldehydes was evaluated by other authors and showed similar results. Neri et al. [8] showed that HX in the vapour phase had a greater antifungal activity against *P. expansum* than other α,β-unsaturated aldehydes such as citral and cinnamaldehyde. The susceptibility of *B. cinerea* to HX has also been reported, this aldehyde damages the membranes of conidia, hence resulting in the deterioration of the fungi's hyphae [33]. A considerable inhibition of spore germination and mycelial growth of *B. cinerea* by HX has also been reported by Hamilton-Kemp et al. [34].

The PL antimicrobial activity has not been as well documented as HX. However, some researchers have reported its antifungal activity in the vapour phase against fungi [9]. Both aldehydes have potential as antimicrobial agents in antifungal packaging.

### 3.2.2. Antifungal pH-response of synthetised Schiff bases

The antifungal response of imine-chitosan films was studied *in vitro* against *P. expansum* and *B. cinerea*. The mechanism of activation of the films consisted on the hydrolysis of the dynamic imine bond formed between the aldehyde and the CS film, and the release of the aldehyde to the headspace of the petri dish. The assay was conducted at pH 7 and 4 to test the effect of the pH on the activity of the films. The hydrolysis of the imine bond is favoured at mildly acidic conditions and thus, greater antifungal activity is expected when the film is in acidic medium. The double plate system developed to test the antifungal properties of the responsive films was designed to avoided direct contact between the film together with the acid medium and the plate with the inoculated mould. Therefore, the antifungal effect was only due to the aldehyde released from the acidic medium to the headspace

of the system. **Figure 4** shows the antifungal activity of CSHX and CSPL activated films at pH 4 and 7 against *P. expansum* and *B. cinerea* measured at 26 °C for 7 days. After that time the films were removed, and the petri dishes were incubated for 3 more days at the same temperature to evaluate the fungicide effect of the films. No differences were found between the control neutralised CS films and the experiments conducted without the control film (data not shown). CS films did not show antimicrobial activity against the two fungi tested which fully colonised the petri dish after 7 days of incubation.

Films previously modified with Schiff bases (CSHX and CSPL) exerted antifungal activity when subjected at pH 4 and 7. However considerable differences were observed depending on the pH. The activity of CSPL films against both fungi increased when were activated at pH 4 compared with pH 7. Shown by a greater release of PL from the film in the acidic medium, therefore a greater extension of the hydrolysis than films subjected at neutral pH. As shown in **Figure 4A**, total inhibition of the growth of *B. cinerea* was obtained for 7 days, when films were subjected at pH 4. However, after removing CSPL films, a slight fungal growth was observed on day 9. Therefore, CSPL films exerted fungistatic activity, but it was not fungicidal. CSPL films activated at pH 7 showed some antifungal activity of *B. cinerea* when compared with the control, although was very limited and the fungi rapidly expanded through the petri dish after the third day of storage. When CSPL films were tested against *P. expansum* (**Figure 4B**), the growth of the fungi was slowed down. Moreover, fungal growth was very limited when exposed to films activated at pH 4. After 7 days of storage, the diameter of the fungi colony did not reach 1 cm for films activated at pH 4, and the fungi colonies were over 2.5 cm for films activated at pH 7.

The effectiveness of CSHX films against *B. cinerea* was fungicidal at pH 4 and inhibitory at pH 7 (**Figure 4A**). For films activated at pH 7 the growth of *B. cinerea* was remarkably similar to when the fungi were exposed to CSPL films. When CSHX films were tested against *P. expansum* (**Figure 4B**), no fungal growth was observed. Thus, CSHX films showed fungicidal activity against *P. expansum* at both pH. These findings may be related to the greater toxicity of HX against *P. expansum* regarding its effect against *B. cinerea* (**Table 2**).
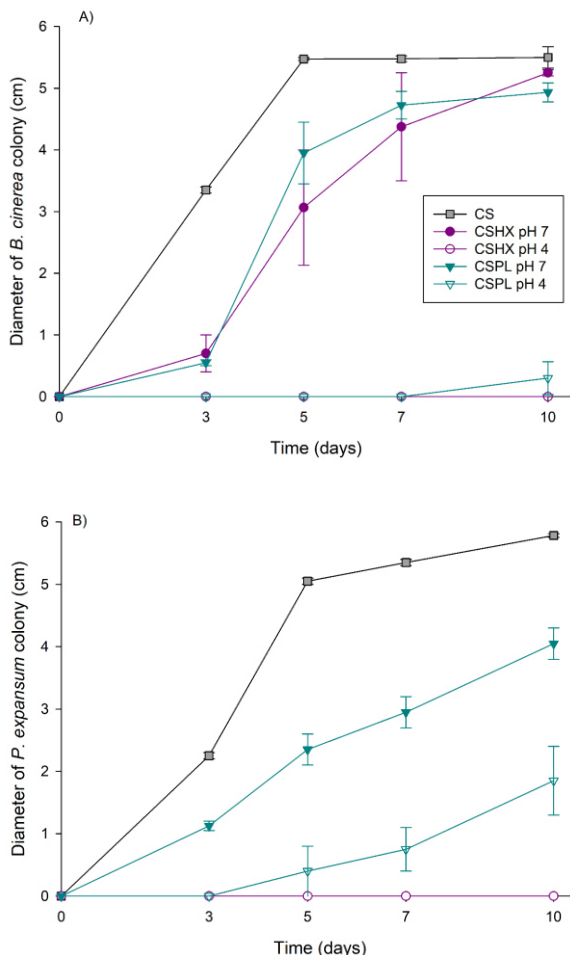
**Figure 4.** Diameter of colony growth of *B. cinerea* (A) and *P. expansum* (B) exposed to 0.1 g of aldehyde-imino-chitosan biodynamer films activated at pH 4 and 7.

Photographs of the visual aspects of both fungi after 7 days of incubation at 26 °C without films and co-incubated with pH-responsive films activated at pH 7 or 4 are found in **Figure 5**. Greater activity of CSHX and CSPL films against both fungi at pH 4 can be seen. *P. expansum* did not grow when using 0.1 g of CSHX films activated at pH 7, showing the greater antifungal activity of trans-2-hexenal against *P. expansum* compared with their activity against *B. cinerea*. Whereas, both fungi grew when exposed to CSPL at pH 7, which also denotes the

higher antifungal activity of trans-2-hexenal than perillaldehyde. Although, previous experiments showed complete inhibition of fungal growth of both fungi with just 0.05 g of CSHX films activated at pH 4 (data not shown).

Morphological differences can also be observed in the growth of both fungi when exposed to the films, a colourless growth of the mycelia happened for *B. cin*erea exposed to CSHX films activated at pH 7, and for *P. expansum* exposed to CSPL films activated at pH 4. This can be due to the inhibition of the sporulation because the aldehyde is at a low concentration [35].
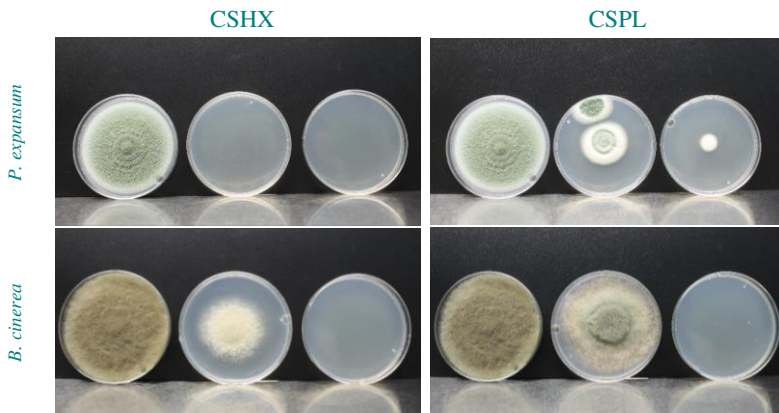


**Figure 5.** Antifungal activity of 0.1 g of activated CSHX and CSPL films against *P. expansum* and *B. cinerea* after 7 days of incubation at 26 °C. From left to right: control, biodynamers activated at pH 7, and biodynamers activated at pH 4.

### 3.3.3. Antifungal effectiveness of dynamic films in packaged blackberries

Due to the higher antifungal activity and substitution degree of trans-2-hexenal in chitosan, CSHX films were selected to evaluate their effectivity against fungal growth in blackberry fruit. Trays containing 50 g of blackberries and incorporating 0.5 g of film placed on a plate with a buffered solution at pH 4, as the triggering agent, were stored at 4 °C for 12 days or at 22 °C for 6 days. Fungal contamination was evaluated by direct visual inspection of each fruit.

Photographs displaying berries packaged in trays, without the biodynamer and incorporating the activated biodynamer, after 6 days of storage at 22 °C and after 12 days of storage at 4 °C are shown in **Figure 6**. Regarding the test run at 22 °C, fungal growth started after 2 days of storage in the control tray and rapidly extended through the entire surface of the fruit. Fungal contamination was delayed by 3 days in the tray with CSHX film, and the fungal growth expanded slower than in the control. As seen in **Figure 6**, at the end of the storage, control samples were fully colonised; however, although all the berries packaged with CSHX films were contaminated after 6 days, the films notably reduced the mycelium growth.

As expected, and as observed in **Figure 6**, when berries were stored at 4 °C fungal spoilage occurred more slowly. Fungi was visible in the control tray after 3 days of storage and infected about 80% of samples after 9 days (results not shown). After 12 days of storage, control trays showed full contamination of all the berries but the mycelium growth was less than observed at room temperature. In contrast, after 12 days of refrigerated storage, only around 30% of the berries were infected using the synthesised biodynamer. Therefore, biodynamers made from trans-2-hexenal and chitosan film revealed a great inhibition of mycelium growth at both temperatures. Blackberries are highly perishable and susceptible to decay, and clearly the temperature of storage plays an important role to prevent fungal growth. Temperature is considered during harvest, transporting and storing until the consumption of berries, where fungal spoilage could rapidly growth [36]. Unwanted changes of temperature during the marketing stages could reduce and a loss of fruit due to fungal decay [37]. Thus, fungal decay due to temperature fluctuations could be minimised using these dynamers.
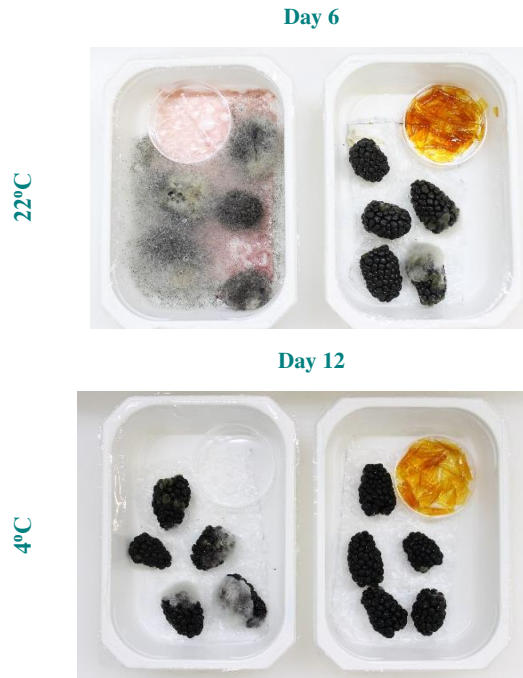
**Day 6**



**Day 12**



**Figure 6.** Fungal decay of blackberries after storage at 22 °C for six days or at 4 °C for twelve days in control trays and in trays incorporated with trans-2-hexenal-imine-chitosan biodynamer films activated at pH 4.

After evaluating the antifungal effectiveness of pH-responsive films on blackberries, a commercial package prototype, consisting of a cylindrical tray provided with a double bottom, was assayed to extent the shelf-life of the fruit. The shape of the tray allows berries to be in contact and the pH activated CSHX film was placed in the bottom of the tray avoiding contact with the berries. The test was run at 4 °C and visual inspection of the berries, looking for fungal infection, was monitored after 1, 3, 6, 9, 12, and 15 days of storage. Two amounts of film were tested, 0.5 g and 0.15 g.

**Figure 7** shows the percentage of infected berries in the control trays and fruit packaged with different amounts of active film; the evolution of trans-2-hexenal in the headspace of the trays has also been represented in the graph. Photographs of control berries packaged using a double bottom tray and those packaged incorporating 0.15 and 0.5 g of responsive film at days 6, 9, and 15 are displayed in **Figure 8**. The percentage of infected berries was around 15% after three days of

storage in the passive package and increased to 60% after 6 days. Contact between blackberries implies the fastest spread of fungal infection, thus, after 9 days of storage all the berries were contaminated. Incorporating the package of 0.15 g of pH-responsive film delayed the presence of moulds until the sixth day of storage, being 20% of berries infected. However, infection spread rapidly and at the end of the storage 100% of berries were colonised by fungi. When 0.5 g of the responsive film was incorporated in the double bottom tray, the presence of fungal infection was delayed due to a greater amount of aldehyde released to the headspace of the package. No fungal growth was observed after 9 days of storage, on day 12, fungal growth infected over 50% of the berries as shown in **Figure 7**. Although, after 12 days of storage a slight fungal growth was observed in some berries packaged incorporating 0.5 g of CSHX film, hyphal length was lower in berries packaged without biodynamers (**Figure 8**).
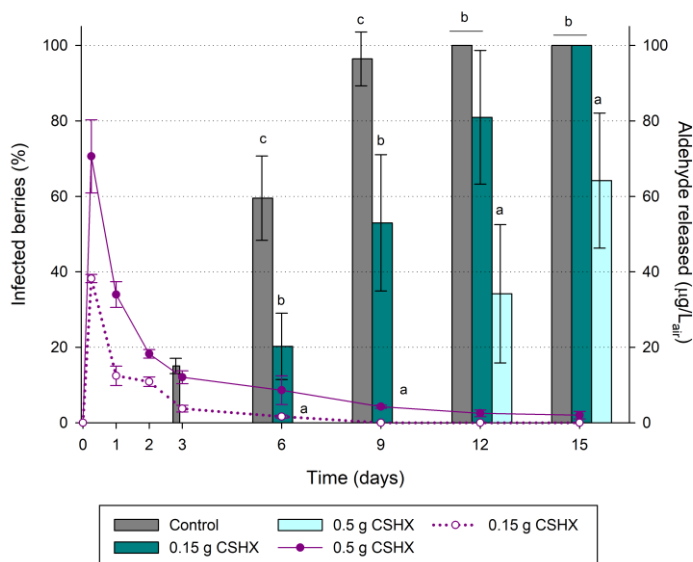


**Figure 7.** Percentage of infected blackberries (bars) packaged in double bottom trays without biodynamer and incorporating 0.15 g or 0.5 g of trans-2-hexenal-imine-chitosan biodynamer film activated at pH 4. The concentration of trans-2-hexenal in the headspace of the packages is also displayed (lines). Bars with same letters are not significantly different (P≤0.05).

Using naturally occurring volatiles as postharvest fungicides to manage the grow of moulds in packaged fruit is an alternative to using synthetic chemicals, however their use should not cause fruit damage related with phytotoxic effects such us blemishes, oleosis, pitting, or staining. Those will depend on the fruit, cultivar, and the concentration of the antifungal applied [38]. Thus, the optimisation of the active volatile in the package's headspace is crucial to maintain its antimicrobial efficacy during the storage of the fruit without compromising fruit quality.
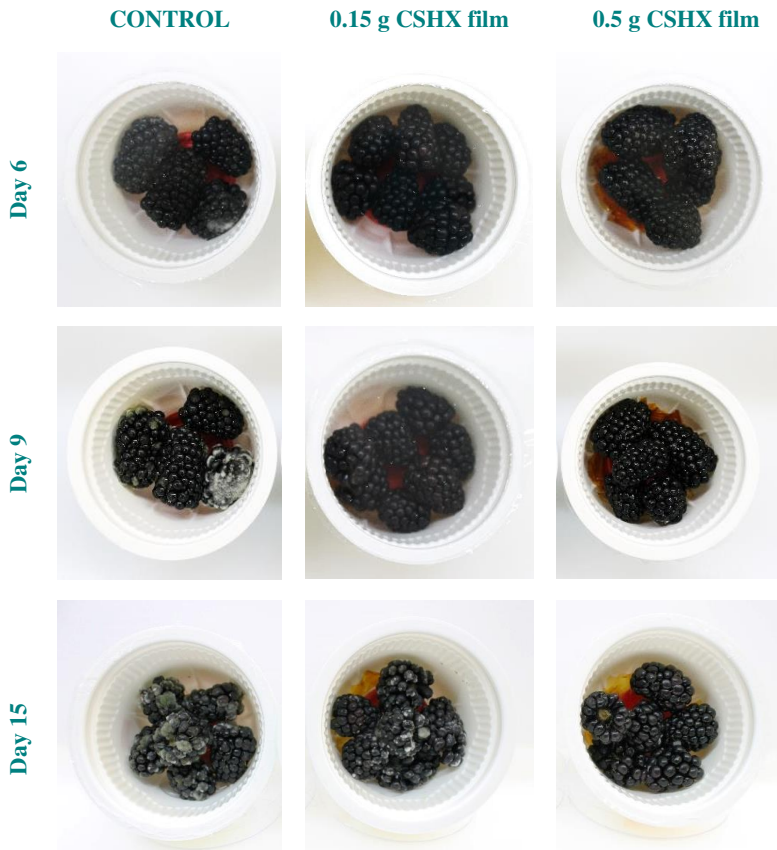


**Figure 8.** Blackberries packaged in double bottom trays without a biodynamer film (control) and with 0.15 and 0.5 g of CSHX film activated in acidic medium. Images show the effect of packaging on fungal growth at days 6, 9 and 15 in berries stored at 4 °C.

Archbold et al. [39] studied symptoms of phytotoxicity including discoloration, loss of tissue turgidity and shape, and exudate appearance on the fruit surface in strawberries, grapes, and blackberries after fruit treatment with several concentrations of trans-2-hexenal and other aldehyde green-leaf volatiles. They concluded that only strawberry fruit was damaged at specific concentrations of the volatile. These authors also stated that the damage could be associated to the higher accumulation and metabolism of HX in strawberry fruit.

In this study, HX release from 0.5 g of CSHX films activated at pH 4 avoided fungal growth and extended the shelf-life of packaged blackberries without observing signs of phytotoxic damage on the fruit.

*3.3.4. Evolution of the concentration of trans-2-hexenal in berries and in the headspace of the double bottom package*

The concentration of trans-2-hexenal in the package's headspace was monitored through the storage of the fruit and is represented in **Figure 7**. The volatile was not detected in the headspace of the control packages. As expected, a greater release of trans-2-hexenal was observed when incorporating a higher amount of CSHX film in the package as both curves have the same release profile. The maximum concentration of aldehyde detected in the headspace of the trays was after activating the film, being 70 and 40 µg/L for 0.50 and 0.15 g of CSHX film, respectively. This behaviour denotes a rapid hydrolysis of the imine bond in the films and the release of the volatile. After reaching the maximum concentration of the volatile in the package headspace, which happened a few hours after activating the responsive film, the concentration of the volatile was gradually depleted and could be detected at the end of the storage. When packaging with 0.15 g of CSHX film, fungal detection was observed after 6 days of storage and the concentration of HX in the headspace was 1.63 µg/$L_{air}$. After the sixth day, and although fungal activity was observed, the length of the mycelium was lower than in the control, indicating that the concentration of aldehyde despite being low, exerted some activity.

The aldehyde detection using GC was not seen after 9 days of storage, where a rapid spread of the mould in the entire fruit was observed. In contrast, when 0.5 g of CSHX film was incorporated in the package, HX was detected during all the days of storage. Additionally,

fungicidal activity was observed until the ninth day of storage corresponding to a concentration of aldehyde of 4.25 μg/L. Notably, in previous studies conducted in our laboratory, the direct incorporation of 50 μL of free aldehyde per packaging caused a high amount of volatile availability in the headspace at the beginning of the storage, around 300 μg/L. However, it decreased quickly to 2 μg/L on the sixth day of storage, where a slight fungal growth was observed with 10% of berries infected. Thus, a huge amount of free trans-2-hexenal was necessary to be injected in the package to delay fungal growth, still blackberries showed phytotoxic damage. In contrast, the developed dynamic films showed an extended and gradual release of the active compound during all the storage period, being effective at controlling fungal growth for a longer period and not damaging the fruit. The films extended the shelf-life of blackberries from 3 to 6 or 9 days when using 0.15 or 0.5 g of film, respectively.

Besides providing an appropriate level of protection against moulds, without causing phytotoxic damage to the fruit, the levels of the antimicrobial absorbed by the food should not be a health risk to the consumer. Concerning the toxicity of trans-2-hexenal, the EFSA Panel on Additives and Products or Substances used in Animal Feed (FEEDAP), following a request from the European Commission, produced in an inform [40], agrees with the "no observed adverse effect level" (NOAEL) of 80 mg/kg body weight per day identified for this compound by [41]. The oral $LD_{50}$ values found by these authors were 780–1130 and 1550–1750 mg/kg in rats and mice, respectively. Therefore, the concentration of trans-2-hexenal was evaluated in packaged berries and monitored through the storage time. The content of the volatile was 4.53 ± 1.04 and 4.89 ± 1.22 mg/kg of fruit at the first and third day of storage, respectively. The concentration of the aldehyde in berries decreased to 2.39 ± 0.19 and 2.73 ± 0.79 mg/kg of fruit after 6 and 9 days of storage, respectively; at the end of 12 days of storage the volatile concentration was 1.9 ± 0.29 mg/kg of berries. All the concentrations of trans-2-hexenal found in berries are very low to have toxicity concerns according to the NOAEL.

Finally, since some compounds can be metabolised to other products, GC-MS was used to detect new compounds formed from HX. Two new volatiles, trans-2-hexen-1-ol and 1-hexanol, were

qualitatively detected in berries after being packaged incorporating CSHX films. The formation of these compounds do not imply a toxicological problem, as they are recognised as "generally recognized as safe" compounds. Archbold et al. [39] has also reported these compounds due to the metabolism of HX by blackberries.

## 4. Conclusions

Naturally occurring volatile aldehydes perillaldehyde and trans-2-hexenal with proved antifungal activity were grafted to CS films through reversible imine bonds. The films based their activity on the hydrolysis of the imine bond and the release of the active volatile. The developed responsive films were tested *in vitro* against *B. cinerea* and *P. expansum.* Films grafted with trans-2-hexenal were more effective against both fungi and thus, were used for the packaging of blackberries. Thus, these films were incorporated in the design of a double-bottom package extending microbiological shelf-life of berries from 3 to 12 days without causing phytotoxic effect to the fruit which is safe for human consumption.

The new dynamer films are an example of the evolution of active antimicrobial packaging to responsive packaging. It has been demonstrated that the active volatile can be stabilized in the film forming a Schiff base, and mild acidic medium can trigger the hydrolysis of the imine bond and the release of the antifungal aldehyde for an extended period of time. The new antifungal system can be used for the postharvest preservation of different fruits just matching the appropriate antifungal aldehyde to each fruit.

## References

1.  Porat, R.; Lichter, A.; Terry, L.A.; Harker, R.; Buzby, J. Postharvest losses of fruit and vegetables during retail and in consumers' homes: Quantifications, causes, and means of prevention. *Postharvest Biol. Technol.* **2018**, *139*, 135–149, doi:10.1016/j.postharvbio.2017.11.019.
2.  FAO *Global food losses and food waste – Extent, causes and prevention.*

*Rome*; Rome, Italy, **2011**; ISBN 9789251072059.

3. Hodges, R.J.; Buzby, J.C.; Bennett, B. Postharvest losses and waste in developed and less developed countries: Opportunities to improve resource use. *J. Agric. Sci.* **2011**, *149*, 37–45, doi:10.1017/S0021859610000936.

4. FAO Post-harvest losses along value and supply chains in the Pacific Island Countries. **2015**.

5. Tripathi, P.; Dubey, N.K. Exploitation of natural products as an alternative strategy to control postharvest fungal rotting of fruit and vegetables. *Postharvest Biol. Technol.* **2004**, *32*, 235–245, doi:10.1016/j.postharvbio.2003.11.005.

6. Patrignani, F.; Siroli, L.; Serrazanetti, D.I.; Gardini, F.; Lanciotti, R. Innovative strategies based on the use of essential oils and their components to improve safety, shelf-life and quality of minimally processed fruits and vegetables. *Trends Food Sci. Technol.* **2015**, *46*, 311–319, doi:10.1016/j.tifs.2015.03.009.

7. Romanazzi, G.; Lichter, A.; Gabler, F.M.; Smilanick, J.L. Recent advances on the use of natural and safe alternatives to conventional methods to control postharvest gray mold of table grapes. *Postharvest Biol. Technol.* **2012**, *63*, 141–147, doi:10.1016/j.postharvbio.2011.06.013.

8. Neri, F.; Mari, M.; Brigati, S. Control of *Penicillium expansum* by plant volatile compounds. *Plant Pathol.* **2006**, *55*, 100–105, doi:10.1111/j.1365-3059.2005.01312.x.

9. Tian, J.; Zeng, X.; Lü, A.; Zhu, A.; Peng, X.; Wang, Y. Perillaldehyde, a potential preservative agent in foods: Assessment of antifungal activity against microbial spoilage of cherry tomatoes. *LWT - Food Sci. Technol.* **2015**, *60*, 63–70, doi:10.1016/j.lwt.2014.08.014.

10. Brockgreitens, J.; Abbas, A. Responsive Food Packaging: Recent Progress and Technological Prospects. *Compr. Rev. Food Sci. Food Saf.* **2016**, *15*, 3–15, doi:10.1111/1541-4337.12174.

11. Nguyen Van Long, N.; Joly, C.; Dantigny, P. Active packaging with antifungal activities. *Int. J. Food Microbiol.* **2016**, *220*, 73–90, doi:10.1016/j.ijfoodmicro.2016.01.001.

12. Tanaka, T.; Ikeda, A.; Shiojiri, K.; Ozawa, R.; Shiki, K.; Nagai-Kunihiro, N.; Fujita, K.; Sugimoto, K.; Yamato, K.T.; Dohra, H.; et al. Identification of a Hexenal Reductase That Modulates the Composition of Green Leaf Volatiles. *Plant Physiol.* **2018**, *178*, 552–564, doi:10.1104/pp.18.00632.

13. Kunishima, M.; Yamauchi, Y.; Mizutani, M.; Kuse, M.; Takikawa, H.; Sugimoto, Y. Identification of (Z)-3:(E)-2-Hexenal isomerases essential to the production of the leaf aldehyde in plants. *J. Biol. Chem.* **2016**, *291*, 14023–14033, doi:10.1074/jbc.M116.726687.

14. FAO/WHO Evaluation of certain food additives. Prepared by the sixty-third meeting of the Joint FAO/WHO Expert Committee on Food Additives (JEFCA). *World Health Organ. Tech. Rep. Ser.* **2006**, *934*.

15. Taghavi, T.; Kim, C.; Rahemi, A. Role of Natural Volatiles and Essential Oils in Extending Shelf Life and Controlling Postharvest Microorganisms of Small

Fruits. *Microorganisms* **2018**, *6*, 104, doi:10.3390/microorganisms6040104.

16. Organization, W.H.; on Food Additives, J.F.E.C. *Evaluation of certain food additives: eighty-seventh report of the Joint FAO/WHO Expert Committee on Food Additives*; WHO technical report series;1020; World Health Organization, 2019;

17. Hobbs, C.A.; Taylor, S. V.; Beevers, C.; Lloyd, M.; Bowen, R.; Lillford, L.; Maronpot, R.; Hayashi, S. mo Genotoxicity assessment of the flavouring agent, perillaldehyde. *Food Chem. Toxicol.* **2016**, *97*, 232–242, doi:10.1016/j.fct.2016.08.029.

18. Joo, M.; Lewandowski, N.; Auras, R.; Harte, J.; Almenar, E. Comparative shelf life study of blackberry fruit in bio-based and petroleum-based containers under retail storage conditions. *Food Chem.* **2011**, *126*, 1734–1740, doi:10.1016/j.foodchem.2010.12.071.

19. Kasaai, M.R.; Arul, J.; Chin, S.L.; Charlet, G. The use of intense femtosecond laser pulses for the fragmentation of chitosan. *J. Photochem. Photobiol. A Chem.* **1999**, *120*, 201–205, doi:10.1016/S1010-6030(98)00432-8.

20. Inukai, Y.; Chinen, T.; Matsuda, T.; Kaida, Y.; Yasuda, S. Selective separation of germanium(IV) by 2,3-dihydroxypropyl chitosan resin. *Anal. Chim. Acta* **1998**, *371*, 187–193, doi:10.1016/S0003-2670(98)00313-4.

21. Almenar, E.; Catala, R.; Hernandez-Muñoz, P.; Gavara, R. Optimization of an active package for wild strawberries based on the release of 2-nonanone. *LWT - Food Sci. Technol.* **2009**, *42*, 587–593, doi:10.1016/j.lwt.2008.09.009.

22. Mauricio-Sánchez, R.A.; Salazar, R.; Luna-Bárcenas, J.G.; Mendoza-Galván, A. FTIR spectroscopy studies on the spontaneous neutralization of chitosan acetate films by moisture conditioning. *Vib. Spectrosc.* **2018**, *94*, 1–6, doi:10.1016/j.vibspec.2017.10.005.

23. Smith, B.C. *Infrared spectral interpretation: a systematic approach*; CRC press: Boca Raton, Florida, **1999**; ISBN 0203750845.

24. Higueras, L.; López-Carballo, G.; Gavara, R.; Hernández-Muñoz, P. Reversible covalent immobilization of cinnamaldehyde on chitosan films via Schiff base formation and their application in active food packaging. *Food Bioprocess Technol.* **2015**, *8*, 526–538, doi:10.1007/s11947-014-1421-8.

25. Peng, H.; Xiong, H.; Li, J.; Xie, M.; Liu, Y.; Bai, C.; Chen, L. Vanillin cross-linked chitosan microspheres for controlled release of resveratrol. *Food Chem.* **2010**, *121*, 23–28, doi:10.1016/j.foodchem.2009.11.085.

26. Dos Santos, J.E.; Dockal, E.R.; Cavalheiro, É.T.G. Synthesis and characterization of Schiff bases from chitosan and salicylaldehyde derivatives. *Carbohydr. Polym.* **2005**, *60*, 277–282, doi:10.1016/j.carbpol.2004.12.008.

27. Andrade-Ochoa, S.; Nevárez-Moorillón, G.V.; Sánchez-Torres, L.E.; Villanueva-García, M.; Sánchez-Ramírez, B.E.; Rodríguez-Valdez, L.M.; Rivera-Chavira, B.E. Quantitative structure-activity relationship of molecules constituent of different essential oils with antimycobacterial activity against *Mycobacterium tuberculosis* and *Mycobacterium bovis*. *BMC Complement. Altern. Med.* **2015**, *15*, 1–11, doi:10.1186/s12906-015-0858-2.

28. Bisignano, G.; Laganà, M.G.; Trombetta, D.; Arena, S.; Nostro, A.; Uccella,

N.; Mazzanti, G.; Saija, A. In vitro antibacterial activity of some aliphatic aldehydes from *Olea europaea* L. *FEMS Microbiol. Lett.* **2001**, *198*, 9–13, doi:10.1016/S0378-1097(01)00089-1.

29.    Witz, G. Biological interacitions of alpha,beta-unsaturated aldehydes. *Free Radic. Biol. Med.* **1989**, *7*, 333–349.

30.    Ramos-Nino, M.E.; Ramirez-Rodriguez, C.A.; Clifford, M.N.; Adams, M.R. QSARs for the effect of benzaldehydes on foodborne bacteria and the role of sulfhydryl groups as targets of their antibacterial activity. *J. Appl. Microbiol.* **1998**, *84*, 207–212, doi:10.1046/j.1365-2672.1998.00324.x.

31.    Friedman, M.; Henika, P.R.; Mandrell, R.E. Antibacterial activities of phenolic benzaldehydes and benzoic acids against *Campylobacter jejuni, Escherichia coli, Listeria monocytogenes,* and *Salmonella enterica*. *J. Food Prot.* **2003**, *66*, 1811–1821, doi:10.4315/0362-028X-66.10.1811.

32.    Sikkema, J.; de Bont, J.A.M.; Poolman, B. Mechanisms of membrane toxicity of hydrocarbons. *Microbiol. Rev.* **1995**, *59*, 201–222.

33.    Fallik, E.; Archbold, D.D.; Hamilton-Kemp, T.R.; Clements, A.M.; Collins, R.W.; Barth, M.M. (E)-2-Hexenal can stimulate *Botrytis cinerea* growth *in vitro* and on strawberries *in vivo* during storage. *J. Am. Soc. Hortic. Sci.* **1998**, *123*, 875–881, doi:10.21273/jashs.123.5.875.

34.    Hamilton-Kemp, T.R.; McCracken, C.T.; Loughrin, J.H.; Andersen, R.A.; Hildebrand, D.F. Effects of some natural volatile compounds on the pathogenic fungi *Alternaria alternata* and *Botrytis cinerea*. *J. Chem. Ecol.* **1992**, *18*, 1083–1091, doi:10.1007/BF00980064.

35.    Ma, W.; Zhao, L.; Zhao, W.; Xie, Y. (E)-2-Hexenal, as a potential natural antifungal compound, inhibits *Aspergillus flavus* spore germination by disrupting mitochondrial energy metabolism. *J. Agric. Food Chem.* **2019**, *67*, 1138–1145, doi:10.1021/acs.jafc.8b06367.

36.    Perkins-Veazie, P. *Postharvest storage and transport of blackberries*; CABI, Ed.; **2017**; Vol. 26; ISBN 1780646682.

37.    Bower, C. Postharvest handling, storage, and treatment of fresh market berries. In *FOOD SCIENCE AND TECHNOLOGY-NEW YORK-MARCEL DEKKER-*; MARCEL DEKKER AG, **2007**; Vol. 168, p. 261.

38.    Munhuweyi, K.; Caleb, O.J.; Lennox, C.L.; van Reenen, A.J.; Opara, U.L. In vitro and in vivo antifungal activity of chitosan-essential oils against pomegranate fruit pathogens. *Postharvest Biol. Technol.* **2017**, *129*, 9–22, doi:10.1016/j.postharvbio.2017.03.002.

39.    Archbold, D.D.; Hamilton-Kemp, T.R.; Barth, M.M.; Langlois, B.E. Identifying natural volatile compounds that control gray mold (*Botrytis cinerea*) during postharvest storage of strawberry, blackberry, and grape. *J. Agric. Food Chem.* **1997**, *45*, 4032–4037, doi:10.1021/jf970332w.

40.    Bampidis, V.; Azimonti, G.; Bastos, M. de L.; Christensen, H.; Kouba, M.; Kos Durjava, M.; López-Alonso, M.; López Puente, S.; Marcon, F.; Mayo, B.; et al. Safety and efficacy of 26 compounds belonging to chemical group 3 (α,β-unsaturated straight-chain and branched-chain aliphatic primary alcohols, aldehydes, acids and esters) when used as flavourings for all animal species

and categories. *EFSA J.* **2019**, *17*, doi:10.2903/j.efsa.2019.5654.

41.    Gaunt, I. F., Colley, J., Creasey, M. W. M., Grasso, P., & Gangolli, S.D. Acute and short-term toxicity studies on trans-2-Hexenal. *Food Cosmet. Toxicol.* **1971**, *9*, 775–786.

# Artículo 5

**Responsive packaging based on imine-chitosan films for extending the shelf-life of refrigerated fresh-cut pineapple**

Raquel Heras-Mozos, Rafael Gavara, Pilar Hernández-Muñoz

Instituto de Agroquímica y Tecnología de Alimentos (IATA-CSIC),

Av, Agustín Escardino, 7, 46980, Paterna, Valencia, Spain.

*Food Hydrocolloids* (2022), 133, 107968

**ABSTRACT**

Reversible imine chemistry has been employed to stabilize antimicrobial liquid volatiles trans-2-hexenal (HX) and salicylaldehyde (SL) to the surface of chitosan films. The reactivity of both aldehydes to amine groups of chitosan was high and the synthesis of imine bonds was assessed by ATR-FTIR. The hydrolysis of the bonds and the release of the aldehydes depended on the pH of the medium. Films exerted *in vitro* microbiocidal effect against *E. coli, S. cerevisae* and pineapple wild yeast when were immersed at pH 3.6. Finally, films were incorporated in the double-bottom of plastic containers filled with fresh-cut pineapple maintained at 4 °C for 18 days. Juice leakage from pineapple pieces triggered the release of aldehydes to the headspace of the package. Both aldehydes extended microbiological shelf-life of fruit and slowed down browning. SL increased juice leakage from fruit and affected firmness negatively.

**Keywords:** Chitosan, pH-responsive films, imine bond, antimicrobial packaging, pineapple, fresh-cut, trans-2-hexenal, salicylaldehyde.

## 1. Introduction

Pineapple is one of the most popular tropical fruits and is often found cut and ready-to-eat in markets. Fresh-cut fruit is a minimally processed product, which provide consumers convenient, nutritious, healthy, and fresh tasting food. Despite its benefits, fruit processing makes the product very perishable and susceptible to rapid deterioration and quality loss due to microbial growth and oxidative process on the product surface [1,2]. Pineapple presents an endogenous microbial population mainly consisting on yeasts [3] which together with browning and leaking due to minimally processing operations limits its shelf-life. Acid pH of pineapple allows the growth of lactic and acetic bacteria, moulds, and yeasts, whereas the high acidity is expected to hinder the proliferation of foodborne pathogen bacteria. However, there are several works reporting the survival of these pathogens in different varieties of fresh-cut pineapple [4,5]. Moreover, pineapples have been associated with outbreaks of *Escherichia coli* and *Salmonella* spp. [6].

There is a huge amount of studies regarding the use of naturally-occurring antimicrobial compounds in fresh-cut produce. In most of them the antimicrobial is applied by dipping or incorporated in an edible coating. These techniques together with refrigeration and packaging with passive or active MAP are the main tools to avoid or delay deterioration processes of fresh-cut produce [7].

Advanced packaging technologies are based on the development of active packages which, among other designs, use encapsulating materials as carriers and release systems of antimicrobial volatiles. In this regard, active packaging technologies based on the sustained release of antimicrobials combine with other hurdle technologies are promising for extending the shelf life and improving the safety of fresh-cut fruit [8].

Most of the studies regarding the use of antimicrobial compounds in fresh-cut pineapple are based on their application by dipping/spraying or, by incorporating them into edible coatings; only a few studies have explored the application of the active compound in the headspace of the package. Thus, methyl jasmonate was embedded in cotton and applied in fresh-cut pineapple stored in jars [9].

In this work, a new sophisticated approach consisting on the chemical immobilization of antimicrobial volatiles in the surface of a

polymer film through reversible covalent bonds has been developed with the aim to stabilize the volatile molecules. The antimicrobial activity of the films is due to the reversibility of the synthetized bonds and the subsequent release of the active molecules to the surrounding environment when necessary. Currently, the use of reversible covalent bonds is being explored in different fields for multiple purposes [10] including the design of smart release systems of bioactives [11–15]. However, their application in the design of antimicrobial responsive food packaging is practically unexplored. Therefore, the novelty of this work relies on the synthesis of pH-reversible imines to create responsive materials with antimicrobial properties that can be applied to the design of responsive packaging to extend the shelf-life of minimally processed fruit.  The synthesis of imine bonds has been chosen due to their capability of breaking apart under mild acid hydrolysis.

A series of naturally-occurring aldehydes proceeding from essential oils and classified as Generally Recognized as Safe (GRAS) compounds were evaluated for antimicrobial properties against pathogen and spoilage microorganism capable of growing in fresh-cut pineapple. Those having the greatest antimicrobial activity against these microorganisms were chosen to be chemically immobilized on the surface of chitosan films through the formation of imines. Chitosan was chosen as the polymer to stabilize the active volatiles because it has a large number of free amino groups that can be converted into imines. The modified chitosan films were characterised to verify the formation of imine bonds, and pH-reversibility of imines was also tested. The release of grafted aldehydes is based on the hydrolytic breakage of the imine bond catalysed by mild acids. In that sense, fresh-cut pineapple exudates could be the trigger to release the antimicrobial volatiles from the films. The antimicrobial effectivity of synthetized imine-chitosan films was evaluated *in vitro* against *E. coli*, *S. cerevisae* and pineapple wild yeast. Later on, the responsive films developed were tested *in vivo* on fresh-cut pineapple. For that, the films were incorporated in the design of a double-bottom package containing the fresh-cut produce. This kind of package avoids the direct contact between the fruit and the active film, whereas the double perforated bottom collects the exudate from the processed fruit and triggers the hydrolysis of imine bonds on

chitosan films and the release of the antifungal volatile to the package headspace creating a biocidal atmosphere around the fruit surface. The evolution of several shelf-life parameters (firmness, pH and colour) and microbiological growth was monitored on passive and responsive packaged fresh-cut pineapple stored at 4 °C for 18 days.

## 2. Materials and methods

### 2.1. Materials

Low molecular weight (LMW) chitosan (75 – 85% deacetylation degree), glacial acetic acid and all aldehydes used in this work were provided by Sigma-Aldrich (Barcelona-Spain). Citric acid monohydrate, and disodium phosphate to carry out buffer medium at pH 7 and pH 4 was also purchased from Sigma-Aldrich (Barcelona-Spain). Hydrochloric acid 37%, ethanol 96%, di-phosphorus pentoxide and granulated sodium hydroxide of synthesis grade were supplied by Scharlab (Barcelona, Spain). Milli-Q water was obtained by Milli-Q Plus purification system (Millipore, Molsheim, France). *Escherichia coli* (CECT 434) and *Listeria innocua* (CECT 910) was supplied by the Spanish Type Culture Collection (CECT, Valencia, Spain). The yeast *Sacharomyces cerevisae var. ellipsoideys* (NCYC 2959) was supplied by National Collection of Yeasts Cultures (NCYC). All culture medium employed were supplied by Scharlab (Barcelona, Spain).

### 2.2. Antimicrobial assays

#### 2.2.1. Microorganisms and preparation of inoculums

Bacterial strains, *E. coli* (CECT 434) and *L. innocua* (CECT 910) were grown and maintained on tryptone soy broth (TSA) and incubated for 24 h at 37 °C. The yeast *Sacharomyces cerevisae var. ellipsoideys* (NCYC 2959) was used as reference. In addition, a wild yeast was isolated from a chunk of pineapple following the method reported by Amorim, Piccoli, & Duarte, [16] and was labelled as PWY (Pineapple Wild Yeast). The PWY was used to assess the effectiveness of the active compounds on pineapple yeast population. Yeasts were grown on malt extract agar (MEA) for 72 h at 26 °C. All microorganisms were stored at 4 °C on agar medium and transferred monthly. Previous to experiments, an overnight culture was obtained. For that, a loopful of the microorganism cultured in agar was transferred to sterile broth

medium and incubated for 72 h at 26 °C for yeasts and 24 h at 37 °C for bacterial strain to obtain early stationary phase of cells.

### 2.2.2. Antimicrobial activity of aldehydes

Previous to grafting aldehydes to the surface of chitosan films, a screening on the antimicrobial activity of several food grade aldehydes was carried out, and those with the greatest activity were later on used for developing responsive films. Thus, the antimicrobial properties of citral (CT), citronellal (CO), trans-2-hexenal (HX), benzaldehyde (BZ), cuminaldehyde (CU), p-anisaldehyde (AN), salycilaldehyde (SL), trans-cinnamaldehyde (CN), hydrocinnamaldehyde (HC) and (S)-(-)-perillaldehyde (PL), all supplied by Sigma-Aldrich (Barcelona-Spain), were evaluated in vitro against *E. coli*, *L. innocua*, *S. cerevisae* and pineapple wild yeast. The micro atmosphere test was used to evaluate the antibacterial activities of the aldehydes in the vapour phase [17]. For this purpose, each overnight was diluted until obtain an inoculum with $10^7$ CFU/mL. Then, 100 µL of each inoculum was spread on MEA when working with yeasts, and TSA for *E. coli* and *L. innocua*. A sterile paper disk of 25 mm was placed and fixed in the lid cover of a Petri dish and 10 µL of each aldehyde were added. The plates were sealed using parafilm to reduce losses of the aldehyde evaporated from the paper. Finally, bacterial strains were incubated at 37 °C for 24 h and *S. cerevisae* and PWY at 26 °C for 72 h. After that time, the inhibition halo was measured and a percentage of inhibition (%) calculated.

The most effective aldehydes were tested against bacterial and yeast strains to determine minimal inhibition concentration (MIC) and minimal microbicidal concentration (MMC). Following the previously described method, an antimicrobial test of vapour phase of aldehydes was carried out. Different volumes of aldehydes were dossed in a disk of paper attached on the lid of plates containing 15 mL of agar medium. A range between 0.5 to 10 µL of aldehyde per plate was assessed. Controls without volatile were also analysed. After incubation time, the diameter of the inhibition zone was measured to determinate MIC and MMC. The MIC is described as the minimal amount of volatile causing growth inhibition or retraction zone. MMC is defined as the minimal amount of volatile that completely inhibits microorganism growth. All analyses were conducted in triplicate.

FlashSmart (Thermo Fisher Scientific, Waltham, MA, USA). The degree of acetylation of chitosan was also determined by using elemental analysis and according to the methodology proposed by [19]. All test was carried out in triplicate.

## 2.6. Release of aldehydes grafted to chitosan films: effect of the pH

The effect of the pH on the hydrolysis of formed imine bonds, and subsequent release of the aldehyde molecules previously grafted to chitosan films was evaluated by gas chromatography (GC). For this purpose, 0.1 g of responsive films were placed in a glass jar with a volume of 250 mL. Films were covered with 10 mL of aqueous solution buffered at several pH (3, 4, 5, 6 and 7). Glass jars were hermetically sealed with a twist off lid, previously perforated (Ø = 1 cm) to place a septum for gas samples withdrawal from the jar headspace. Samples of 0.5 mL were manually collected after 24 h of jar storage at 23 °C, and injected into a gas chromatograph mod. 6850 Series II Network GC System (Agilent Technologies, Palo Alto, CA, USA) equipped with a flame ionization detector (FID) and a Restek RTX1 capillary column (30 m of length, 0.53 mm internal diameter, and 5 μL thickness) with a flow rate 14.6 mL/min of helium as carrier gas. Injector temperature and FID temperature was fixed at 220 °C. Temperature of the oven was from 35 to 220 °C in 21.8 min. Injected samples were run in the splitless mode. The obtained values were quantified according to a previous calibration curve with known amounts of aldehyde. Results were represented as concentration of aldehyde (mg per $L_{air}$ of headspace per g of film). All analyses were performed in triplicate.

## 2.7. In vitro antimicrobial activity of responsive films

The antimicrobial activity of developed responsive films was tested against the same microorganisms tested for free aldehydes. A double plate system was used to carry out the *in vitro* assays as described in a previous study [20]. Briefly, a Petri dish (58 mm) with agar medium was placed into an empty Petri dish (90 mm). A volume of 60 μL of the aliquot with $10^7$ CFU/mL was deposited and extended with a Digralsky handle on different agar medium depending on the microorganism as mentioned above.

### 2.3. Grafting aldehydes to chitosan films

Those aldehydes more active against all tested microorganisms were selected to be immobilized in chitosan films through reversible imine bonds. For that, 1.5% (w/w) of LMW chitosan with a molecular weight range of 50-190 kDa was dissolved in 0.5% (w/w) of acetic acid under continuous stirring at 50 °C until chitosan was completely dissolved. Chitosan acetate films were obtained by solvent casting method. For that, 90 g of film forming solution was poured in polystyrene plates (25 x 16 cm) and dried at 37 °C for 24 h. Then, the films with a thickness of 35±5 μm were neutralized by immersion in 0.1 M sodium hydroxide aqueous solution at room temperature for 24 h. After that, neutralized chitosan films (CS) were washed with deionized water and dried at 37 °C and stored in glass desiccators.

Aldehyde immobilization in chitosan film was carried out by a reaction between neutralized CS films and aldehydes in 96% (v/v) ethanol and hydrochloric acid was used as catalyst. CS films and aldehyde were added in a weight ratio 1:2 and the reaction took place at 60 °C during 24 h using a shaking bath. After that, reaction medium was removed, and films were washed with ethanol for 24 h to remove free aldehyde from films. This operation was carried out three times. Finally, responsive chitosan films were dried and kept in a desiccator.

### 2.4. Spectroscopic characterization of imine bonds

Fourier transform infrared spectrophotometer with Attenuated Total Reflectance accessory (ATR-FTIR) was used to characterize the imine bonds formed in chitosan film. Infrared spectra were recorded with a Bruker Tensor 27 FTIR spectrometer (Bruker Española S.A., Barcelona, Spain). At least 32 scans were recorded in the range of 4000 to 600 cm$^{-1}$ for each sample and with a resolution of 4 cm$^{-1}$. Infrared spectrum was treated with the OPUS v. 5.0 software.

### 2.5. Quantification of aldehydes grafted to chitosan films

The amount of aldehydes respect to glucosamine units of chitosan films was measured as degree of substitution (DS, %) according to the equation proposed by [18]. For that C/N ratio of the films was determined by elemental analysis with a CHNS-O elemental analyser

The responsive films (0.25 g) were placed in the empty plate and activated by embedding it with aqueous buffer solution (pH 7 and 3.6). The system was covered with a lid and sealed with parafilm. Using double Petri dish avoids direct contact between films and culture medium. Two systems, one having untreated CS film and the other one without film were used as controls. The test for *L. innocua* and *E. coli* were incubated incubated at 37 °C for 24 h, whereas yeasts were incubated at 26 °C for 72 h. After that time, the inhibition was evaluated by visual inspection of growth surface and comparison with the control. All analyses were performed in triplicate.

## 2.8. Shelf-life studies of fresh-cut pineapple packaged with responsive films

### 2.8.1. Packaging and storage of fruit

Costa Rican 'Tropical Gold´ type fresh pineapples (*Ananas comosus*) were purchased in a local market and were stored at 7 °C until its processing. Pineapple fruit was processed at room temperature. To minimize possible cross contamination, the whole pineapple was sanitized by immersion in a sodium hypochlorite solution (1%) for 5 min and then, pineapple was dried. Peeling and cutting of the fruit took place aseptically on a sterile surface and sharp knives. Pineapple's core was removed and cut into triangular pieces with a thickness of 25 mm and weight in the 10 - 12 g range. Polypropylene (PP)/ethylene-vinyl alcohol copolymer (EVOH)/PP containers of 220 cm$^3$ were used to package pineapple pieces. The containers were provided of a double bottom to avoid direct contact between responsive films and fruit. The films (0.5 g) were placed at the bottom of the container, and a perforated plastic pad was placed between the film and 60 g of fruit. A cross-section view of the package is showed in **Figure 1**. The perforated double bottom system, besides to avoid direct contact between the film and the fruit, allows pineapple exudate to contact the films and thus, and triggers the release of anchored aldehyde during the storage of the fruit. A package without films was used as control.
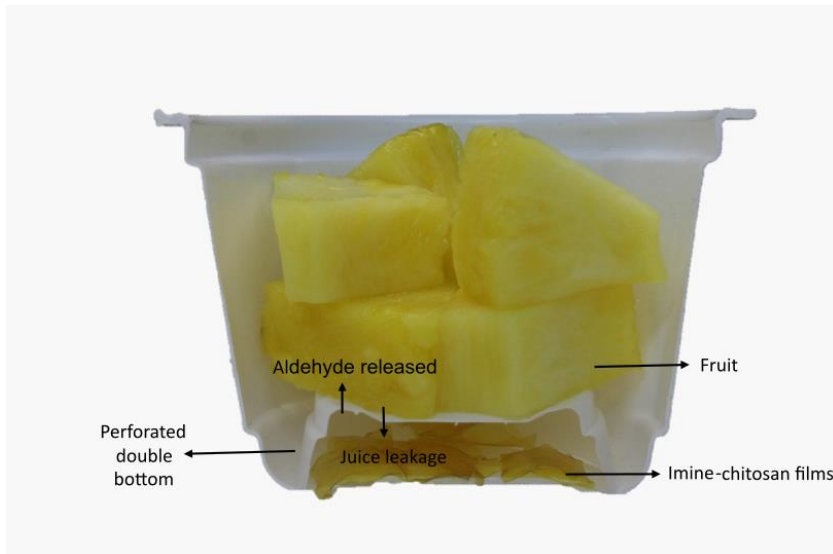
**Figure 1.** Antifungal responsive package for fresh-cut pineapple.

Finally, the containers were thermo-sealed with PP film (30 μm) using a SMART 300 heat sealer for trays (ULMA. Embalaje S.C., Spain). The samples were stored at 4 °C for 18 days. Analyses of packaged pineapple were conducted at days 3, 6, 9, 12, 15 and 18 after packaging. The packaged samples were performed in triplicate.

*2.8.2. Quality parameters of packaged fresh-cut pineapple*
Packaged fresh-cut pineapple was evaluated for main quality parameters such as colour, pH, juice leakage and firmness.

Colour of individual chunks of pineapple was determined using a CR-300 Minolta Chroma meter® (Minolta Camera Co. Ltd., Osaka, Japan). CIELAB colour coordinates were measured, and hue angle (h⁰) and Chroma (C*) determined. Total colour difference values (ΔE) were evaluated according to the equation:

$$\Delta E = \sqrt{(L - L_0)^2 + (a - a_0)^2 + (b - b_0)^2}$$

where $L_0$, $a_0$, and $b_0$ refer to the colour values at 0 day. The results of colour were expressed as the average ± standard deviation of the values of at least 5 chunks of pineapple in both sides.

Measurements of pH were performed using a portable pH meter (Consort C830, Belgium) with a penetration pH electrode for solids (PHEL-PB5-001, Metria, Spain) to measure the pH directly in the fruit. Juice leakage was recollected from the bottom of all packages and reported as mg of exudate per g of pineapple.

Texture was evaluated with a TA.XT.plus Texture Analyzer (Stable Micro Systems, Godalming, UK). A 15-mm penetration was made with a 0.1-inch diameter cylindrical probe with a flat base (TA/0.1) at a speed of 1 mm/s. The test was carried out to determine the work to penetrate and values were expressed as N x mm.

### 2.8.3. Microbiological analysis of packaged fruit
#### 2.8.3.1. Natural microbiota

The microbiological quality of refrigerated fresh-cut pineapple packaged using responsive films was evaluated through monitoring the growth of moulds and yeast, mesophilic and psychrophilic microorganisms. The microbiological load was measured every 3 days during 18 days of storage. For this propose, around 30 g of fruit were aseptically transferred to a sterile Stomacher bag and blended with 30 mL of 0.1% sterile peptone water. It was homogenized for 3 min in a stomacher bag using a Stomacher Blender (IUL S.L., Barcelona). Subsequently, serial dilutions were made in sterile peptone water and aliquots of each dilution were plated in Petri dishes containing several agar culture media through spread plate method. The media employed was plate count agar (PCA) to determinate the mesophilic and psychrophilic microorganism. The plates of psychrophilic were incubated at 4 °C for 10 days, whereas the mesophilic were incubated at 30 °C for 48 h. For determination of moulds and yeast counts, the dilutions were spread in Malt Extract Agar (MEA) and incubated at 26 °C for 4 days. The colonies were enumerated, and results were reported as logarithm of colony forming units (CFU) per grams of fruit (log CFU/$g_{fruit}$). All microbiological analysis was carried out in triplicate.

*2.8.3.2. Inoculation and survival of pathogens in packaged fruit*

Antimicrobial response of imine-chitosan films against *E. coli* and *L. innocua* on pineapple fruit was carried out. Containers of 60 cm$^3$ were filled with 20 g of inoculated fruit and 0.17 g of films were placed in the bottom of the packages. Prior to the assays, inoculum of *E. coli* was prepared. For that, an aliquot of 100 µL of overnight culture was transferred to 10 mL of sterile TSB tube and incubated at 37 °C until reach exponential phase with 10$^6$ CFU/mL. Inoculation of fresh-cut fruit pieces with pathogenic bacteria was carried out by depositing 0.1 mL of inoculum with 10$^6$ CFU/mL on the surface of 20 g of fresh-cut pineapple per each package. The bacterial suspension was distributed uniformly over the surface of pineapple pieces. Inoculated samples were maintained under sterile atmosphere for 10 min to allow the inoculum to dry. Packaged fruit without responsive films was used as control. After that, the packages were closed and stored at 4 °C for 9 days. The microbial load in fruit was evaluated at 0, 1, 3, 6 and 9 days of storage. For that, the same process as described above was followed. The selective medium for *E. coli* enumeration was Violet Red Bile Dextrose (VRDB agar) and Polymyxin Acriflavine Lithium Chloride Ceftazidime Aesculin Mannitol agar (PALCAM agar) was used to enumerate *L. innocua*. The plates were incubated for 24 h at 37 °C and the data were expressed as log CFU/g$_{fruit}$. All test was carried out in triplicate.

*2.9. Statistical analyses*

All the tests were conducted at least in triplicate and represented as the average ± standard deviation. Statistical analysis of the results was performed with SPSS® computer program, v.27 (SPSS commercial software, SPSS Inc., Chicago, IL). Results were analysed applying a one-way analysis of variance (ANOVA). Means were separated using the Tukey *b* test with a level of significance of $P \leq 0.05$.

## 3. Results and discussion
*3.1. In vitro antimicrobial activity of aldehydes*

**Table 1** shows antimicrobial properties of the aldehydes assayed against *E. coli*, *L. innocua*, *S. cerevisae* and PWY (Pineapple Wild Yeast). No inhibitory effect was observed against the microorganisms

assayed when exposed to 10 µL in vapour phase of benzaldehyde (BZ), cuminaldehyde (CU) and p-anisaldehyde (AN). *S. cerevisae* and PWY were susceptible to citronellal (CO) and perillaldehyde (PL), whereas these aldehydes did not show any inhibition on the growth of the bacteria strains tested. Citral (CT), hydrocinnamaldehyde (HC) and cinamaldehyde (CN) showed a considerable antimicrobial activity against all the microorganisms tested, with an inhibition ca. 40-50%. However, the most effective aldehydes were trans-2-hexenal (HX) and salicylaldehyde (SL). HX inhibited 100% the growth of the microorganisms assayed and SL showed the same behaviour except for *L. innocua*, which caused a 58% of inhibition. Antimicrobial activity of aldehydes has been widely studied against several microorganisms [21]. In particular, antimicrobial potential of trans-2-hexenal and salicylaldehyde have been previously evaluated against food pathogens [22,23]. Thus, SL and HX were selected based on this preliminary aldehyde screening for antimicrobial activity in vapour phase.

**Table 1.** Growth inhibition (%) of several microorganisms exposed to 10 µL of several naturally-occurring aldehydes.

| Active | Growth Inhibition (%) | | | |
|---|---|---|---|---|
| | *E. coli* | *L. innocua* | *S. cerivisae* | *PWY* |
| CT | 39.7 ± 0.8[bA] | 52 ± 3.3[cB] | 50 ± 5.6[cB] | 47.2 ± 2.8[bcAB] |
| CO | 0[aA] | 0[aA] | 87.8 ± 6.7[eB] | 89.4 ± 2[eB] |
| HX | 100 ± 0[cA] | 100 ± 0[eA] | 100 ± 0[fA] | 100 ± 0[fA] |
| BZ | 0[aA] | 0[aA] | 0[aA] | 0[aA] |
| CU | 0[aA] | 0[aA] | 0[aA] | 0[aA] |
| PL | 0[aA] | 0[aA] | 63.9 ± 2.8[dC] | 49.2 ± 0.8[cB] |
| AN | 0[a] | 0[a] | 0[a] | 0[a] |
| SL | 100 ± 0[cA] | 58 ± 2.2[dA] | 100 ± 0[fA] | 100 ± 0[fA] |
| CN | 43.1 ± 1.4[bA] | 100 ± 0[eD] | 67.5 ± 0.8[dC] | 53.6 ± 1.9[dB] |
| HC | 42 + 4.4[bAB] | 33 ±5 .6[bA] | 40.6 ± 1.7[bA] | 45.6 ± 0.6[bB] |

Different letters (a-f) in the same column indicate a statistically significant difference between different aldehydes. Different letters (A-C) in the same row indicate a statistically difference of same aldehyde against different microorganism ($P \leq 0.05$).

The antimicrobial effectiveness of SL and HX against tested microorganism was assessed by determining MIC and MMC. **Table 2** shows the MIC and MMC values of both aldehydes for each microorganism. The aldehydes were more active against yeasts than bacteria strains, being MIC in the 0.5 – 1 and 2.5 μL/plate ranges, respectively.

**Table 2.** Antimicrobial activity of trans-2-hexenal (HX) and salicylaldehyde (SL) tested as vapour phase against *E. coli* and *L. innocua* incubated at 37 ºC for 24 h and *S. cerevisae* and PWY incubated at 26 °C for 48 h.

|  | **Trans-2-Hexenal (HX)** | | **Salicylaldehyde (SL)** | |
| --- | --- | --- | --- | --- |
|  | **MIC (μL/plate)** | **MMC (μL/plate)** | **MIC (μL/plate)** | **MMC (μL/plate)** |
| *E. coli* | 2.5 | 7.5 | 2.5 | 7.5 |
| *L. innocua* | 2.5 | 10 | 5 | 15 |
| *S. cerevisae* | 1 | 2.5 | 0.5 | 3 |
| PWY | 1 | 2.5 | 0.5 | 3 |

*3.2. Spectroscopic characterization of imine bonds*

The formation of new imine bonds obtained by the condensation between primary amine groups of chitosan and carbonyl groups of salicylaldehyde (SL) and 2-trans-hexenal (HX) was evaluated by ATR-FTIR analysis of the new films. The IR spectra of control chitosan films, and films modified with aldehydes are represented in **Figure 2**. The spectra show a characteristic peak of chitosan, corresponding to the stretching of $C_6$-OH corresponding to the glycosidic ring of the polymer. An overlapping and wide absorption band corresponding to O-H and N-H vibrations was observed from 3600 to 3000 cm$^{-1}$, and around 2900 cm$^{-1}$ appears other band which is assigned for stretching vibration of C-H of chitosan. The bands allocated to C=O stretching of amide I, and N-H bending of the primary amine were observed at 1644 and 1582 cm$^{-1}$, respectively [24].
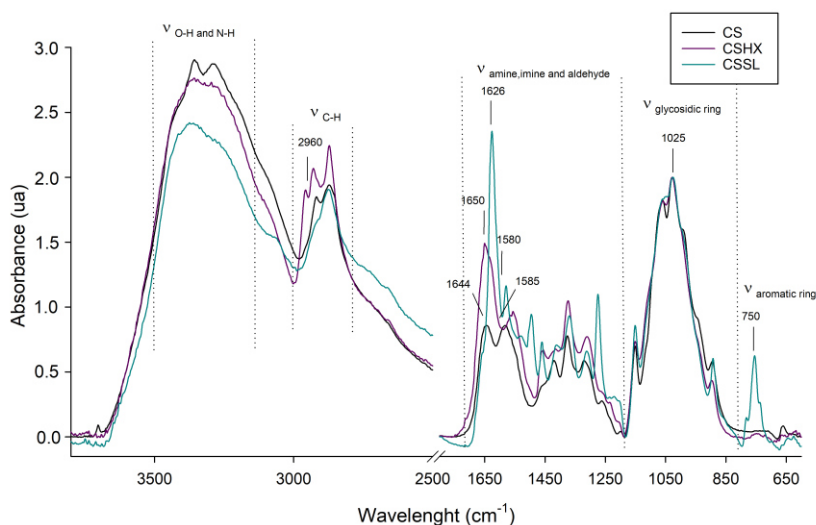
**Figure 2.** ATR-FTIR spectra in the range of 4000 to 600 cm$^{-1}$ of chitosan and imine-chitosan films.

Zoom IR spectra of films in the range of 1750 to 700 cm$^{-1}$ is shown in **Figure 3**. The modification of chitosan with SL and HX gave rise to novel absorption bands at 1626 and 1650 cm$^{-1}$, respectively, which correspond to the formation of imine bonds (C=N) by the nucleophilic addition of aldehydes to primary amino groups of chitosan. In addition, other peaks were altered after Schiff base formation, the involvement of primary amine groups to form imines caused a reduction of the intensity of the band associated to primary amine group at 1585 cm$^{-1}$ [25].

New peaks are observed in the spectra of imine-chitosan films, which are associated to the immobilization of the aldehydes in chitosan films. Also, a new band is observed around 2900 cm$^{-1}$, especially notable in CSHX films, which is due to vibration of C-H of aliphatic chain of trans-2-hexenal [12,26]. After modification with salicylaldehyde, some peaks corresponding to aromatic ring of salicylaldehyde can be observed at 1580 and 750 cm$^{-1}$ [27]. Also, CSSL films showed a decrease of the broadband around 3300 cm$^{-1}$, which could be due to an interaction between hydroxyl group of aldehyde in *ortho* position with N-H and O-H groups of chitosan backbone [25].
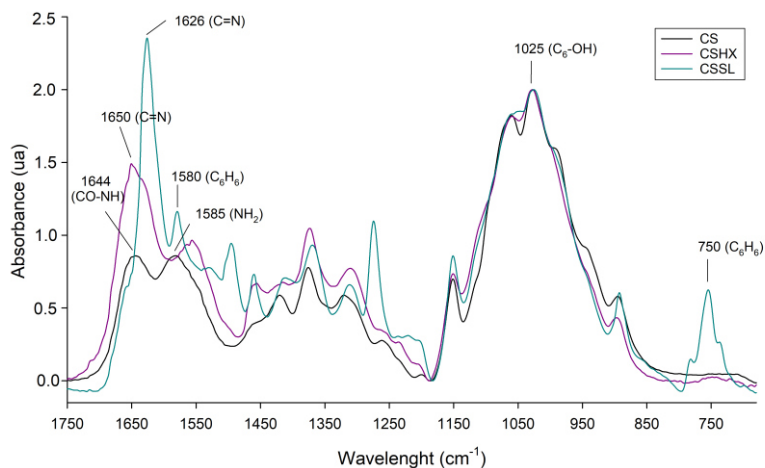
**Figure 3.** ATR-FTIR spectra of chitosan films and responsive films synthetized with trans-2-hexenal (CSHX) and salicylaldehyde (CSSL) in the range of 1750-700 cm$^{-1}$.

### 3.3. Quantification of aldehydes grafted to chitosan films

Elemental composition, C/N ratio and degree of substitution (% DS) of chitosan films and those modified with salicylaldehyde (SL) and trans-2-hexenal (HX) is presented in **Table 3**. Previously, the degree of acetylation of untreated CS films was calculated, being around 16%, this involves a large amount of free amino groups where aldehydes can be anchored to form imines. Chitosan films modified with aldehydes showed an increase of C/N ratio due to the incorporation of the compound, being 5.4 for untreated chitosan films and over 9.0 for modified chitosan films. DS values of modified films showed a great degree of conversion of amino groups of chitosan films to imines, reaching values above 50% in both films, and being slightly higher for CSHX films (71.6%) compared with CSSL films (64.3%). Trans-2-hexenal is a lineal α,β-unsaturated aldehyde, contrary to saturated aldehydes, the carbonyl group is conjugated with an alkene which makes it electrophilic at both the carbonyl carbon as well as the β-carbon. Thus, either site can be attacked by nucleophiles. The conjugated double bond makes this aldehyde more reactive, whereas its

lineal structure favours a more reduced steric hindrance when it is grafted to chitosan compared with aromatic aldehydes.

**Table 3.** Elemental analysis of chitosan and imine-chitosan films.

| Films | N (%) | C (%) | C/N | Substitution degree (%) |
|-------|-------|-------|-----|-------------------------|
| CS | $7.8 \pm 0.2^b$ | $42.1 \pm 0.4^a$ | $5.4 \pm 0.1^a$ | - |
| CSHX | $5.6 \pm 0.1^a$ | $50.6 \pm 0.1^b$ | $9 \pm 0.1^b$ | $71.6 \pm 2.7$ |
| CSSL | $5.6 \pm 0.1^a$ | $51.6 \pm 0.1^c$ | $9.2 \pm 0.2^b$ | $64.3 \pm 2.6$ |

Different letters (a-c) in the same column indicate a statistically significant difference between samples ($P \leq 0.05$).

### 3.3.1. Effect of the pH on the release of aldehydes grafted to chitosan films

The acidity of hydrolytic environments has been identified as a primary factor influencing the reversibility of imines [28]. Thus, the effect of the pH on the reversibility of the imine bonds created in chitosan films, and subsequent release of salicylaldehyde (SL) and trans-2-hexenal (HX) was evaluated by gas chromatography. The amount of aldehyde released to the headspace of closed hermetic jars after 24 h of immersing the films in buffered solutions of different pH is depicted in **Figure 4**. The results show that regardless of the aldehyde, an increasing amount is recovered in the headspace of the jars as the pH of the hydrolytic solution decreases. Thus, the greater aldehyde concentration was obtained at pH 3, reaching $5 \pm 0.1$ mg/L·$g_{film}$ of HX, and $9.3 \pm 0.2$ mg/L·$g_{film}$ of SL, whereas at pH 7 these values were $0.3 \pm 0.1$ and $1.1 \pm 0.1$ mg/L·$g_{film}$, for HX and SL respectively. The latter values represent 12 and 6 % of the amount measured when the films were activated in acid medium (pH 3). Thus, the films developed are considerably stable in neutral hydrolytic environments. In this line, different acidic environments have been used to reverse imine formation and subsequently trigger the release of the active molecule. Thus, the acid microenvironment of tumour tissues [29,30], the organic acids produced by microorganisms [31], or gastric juices [12] are examples of bioactive triggers. In the current work, it is expected that pineapple juice rich in organic acids triggers the

hydrolysis of imine bond and the release of volatile aldehydes to exert its antimicrobial action on the fruit.

Regarding the amount of aldehyde released to the medium, it was observed that, in spite of the greater amount of HX incorporated into the films (DS ~ 72% and 64% for HX and SL, respectively), the amount of HX released was lower compared with that for SL (**Figure 4**). Thus, besides the pH of the media, the structural features of the aldehyde anchored to chitosan plays a role on the release of the molecule to the headspace of the package. Chen et al. [12] have recently studied the stability of aldehyde-chitosan conjugates in acid medium. The authors reported that cinnamaldehyde and citral form more stable imines than citronellal and vanillin. Similar to cinnamaldehyde and citral, trans-2-hexenal is a polyfunctional substrate, containing a double bond conjugated with a carbonyl group. This feature makes the molecule more reactive than saturated aldehydes. Thus, besides nucleophilic addition of primary amines of chitosan to carbonyl group, α, β-unsaturated aldehydes can undergo Michael addition, that is, nucleophilic attack to the electrophilic β-alkene carbon and the formation of a covalent bond which is not easily hydrolysable. Therefore, trans-2-hexenal could be also grafted to chitosan in a different way to the formation of a reversible Schiff base. The consequence would be that aldehyde molecules attached via Michael addition could not be available for release in acidic media. This rational could explain the lower release of HX from the films. Other important point to consider is that when the imine bond is hydrolysed, the aldehyde molecules migrate from the film to the water solution, and then evaporates to the surrounding atmosphere. Therefore, some physico-chemical parameters such as log P and vapour pressure at saturation of the aldehyde affect the equilibrium liquid-vapour and thus, to the amount of aldehyde determined in the headspace.
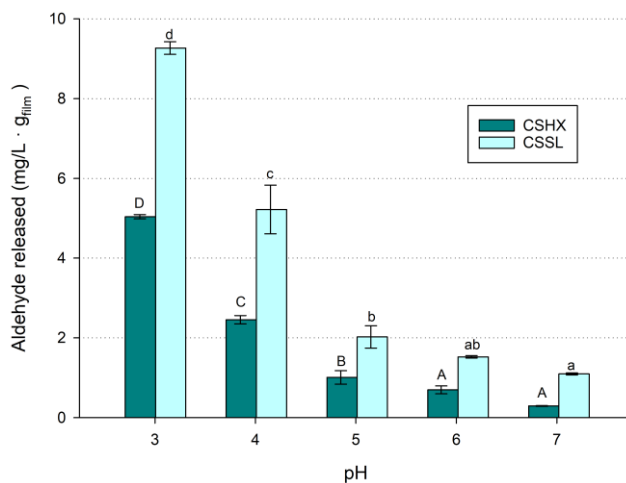
**Figure 4.** Concentration of aldehyde (mg/L·$g_{film}$) released to the vapour phase from imine-chitosan films immersed at different pH during 24 h at 23 °C. Different letter in capital (A-D) and lower case (a-d) indicate significant differences for CSHX and CSSL films, respectively.

### 3.3.2. In vitro antimicrobial activity of responsive films

The antimicrobial activity of CSHX and CSSL was tested *in vitro* against *E. coli*, *S. cerevisae* and PWY (Pineapple Wild Yeast). The hydrolysis of the imine bonds was studied at pH 3.6 and 7 to evaluate the effect of the triggering solution pH on the antimicrobial activity of the films. **Figure 5** shows pictures of the growth of the tested microorganisms on the agar surface in Petri dishes exposed to the vapours of HX and SL released from films after being activated at two pH values. The control that appears in the picture refers to the surface growth of microorganisms in a Petri dish that was not exposed neither to plain chitosan films nor to new films developed. It is important to point out that no differences were observed between control without film or with plain chitosan films because in the *in vitro* antimicrobial system assayed there was no direct contact with the growth medium. A visible decrease of microbial density on agar surface of Petri dish corresponding to CSSL films activated at pH 7 is observed and is related to the antimicrobial effect exerted by the low amount of aldehyde released at this pH. CSSL films exerted microbicidal activity when were activated at pH 3.6, except for *L. innocua*, which is in

accordance the highest values of MMC. According to the data obtained by gas chromatography, which showed that acid pH promotes the highest release of aldehyde, a greater antimicrobial activity is expected when the trigger is a buffer solution at pH 3.6.

Films modified with HX (CSHX) also exerted microbicidal activity at pH 3.6, for *E. coli*, PWY and *S. cerevisae*, whereas the growth of *L. innocua* was inhibited, observing a reduction of bacterial density on surface agar. The HX release at pH 7 was fungicidal but not bactericidal. The results showed a higher susceptibility of both yeasts to the presence of aldehydes, while bacterial strains were more resistant, especially *L. innocua* as observed in the MIC and MMC data. Although the amount of HX released is lower than that for SL as discussed in the above section, HX has a potent fungicidal activity (as reflected by the low MIC values, see **Table 2**) which explains the results obtained.
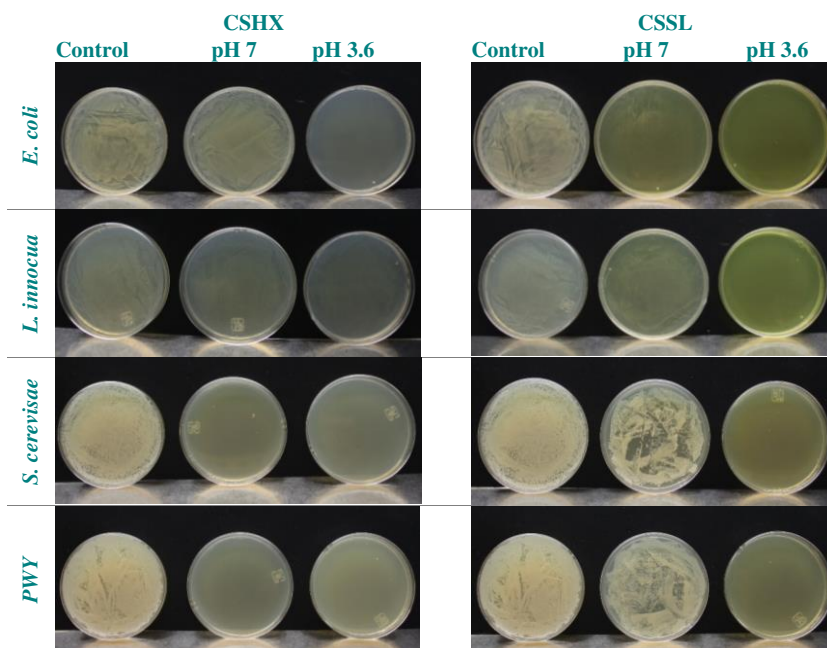


**Figure 5.** Antimicrobial effect of untreated chitosan and imine-chitosan films of trans-2-hexenal (CSHX) and salicylaldehyde (CSSL) at several pH against *E. coli, L. innocua, S. cerevisae* and *isolated yeast* (PWY) after incubation time.

### 3.4. Shelf-life studies of fresh-cut pineapple packaged with responsive films

#### 3.4.1. Quality parameters of packaged fruit

Fresh-cut pineapple is a ready-to-eat product packaged for direct consumption. When it is cut into portions, its shelf-life is compromised as a consequence of broken vegetable tissue. **Figure 6** shows the visual aspect at different storage time of pineapple chunks packaged with and without responsive films. As can be appreciated, responsive films contributed to preserve the original aspect of the fruit.
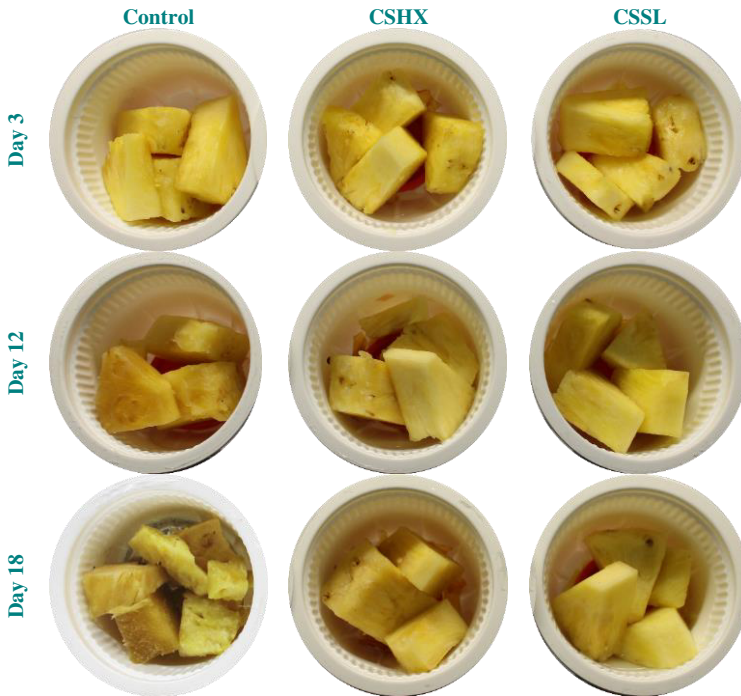


**Figure 6.** Effect of responsive packaging on the visual aspect of pineapple pieces after 3, 12 and 18 days of storage at 4 °C. (CSHX: trans-2-hexenal-imine-chitosan films, CSSL: salicylaldehyde-imine-chitosan films).

The colour of the ready-to-eat cut pineapple is a quality parameter that affects consumer acceptance. Changes in the colour of pineapple chunks during storage was monitored through $\Delta E^*$, lightness ($L^*$), Chroma ($C^*$) and hue angle ($h°$) parameters. **Figure 7** shows $\Delta E^*$ evolution of pineapple chunks stored under passive and responsive

packages incorporating CSHX and CSSL films. In general, ΔE* increased progressively through the storage period but this increase was more pronounced for fruit stored in a passive package, and differences in colour between passive and responsive package were significant after nine days of storage.
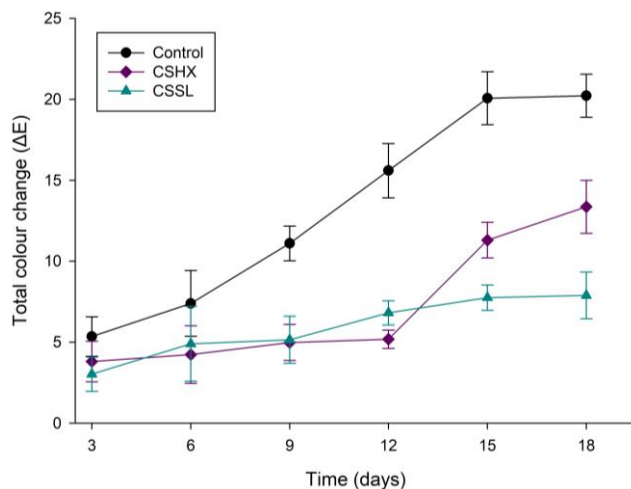


**Figure 7.** Evolution of the total colour difference (ΔE*) of pineapple pieces packaged without and with imine-chitosan films of trans-2-hexenal (CSHX) and salicylaldehyde (CSSL) for 18 days at 4 °C.

The evolution of L*, Chroma and hue angle of pineapple chunks packaged in passive and responsive packages is shown in **Figure 8.** In all the samples, L* tended to decreased through storage which is indicative of fruit darkening. However, L* dropped from 63.9 to 46.7 after 18 days of storage in fruit packaged without responsive films. The darkening of samples packed with the active system was less accused, and only a slight decrease of L* from 63.9 to 58.4 for CSHX and to 57.0 for CSSL was observed. Decompartmentalisation and bruising of tissue lead to oxidative reactions such as enzymatic browning reaction and consequent generation of dark pigments [32]. Several authors have also reported the beneficial effect of essential oils delaying browning [7,33,34]. Over time, chroma values of the samples tended to diminish indicating that the colour intensity of pineapple chunks decreased with storage, this tendency being significantly less accused in fruit that was stored in responsive packages. Hue angle of fruit was maintained

through storage without finding significant changes between passive and responsive packaging carrying CSHX films, whereas h° of fruit pieces packaged with CSSL slightly increased.
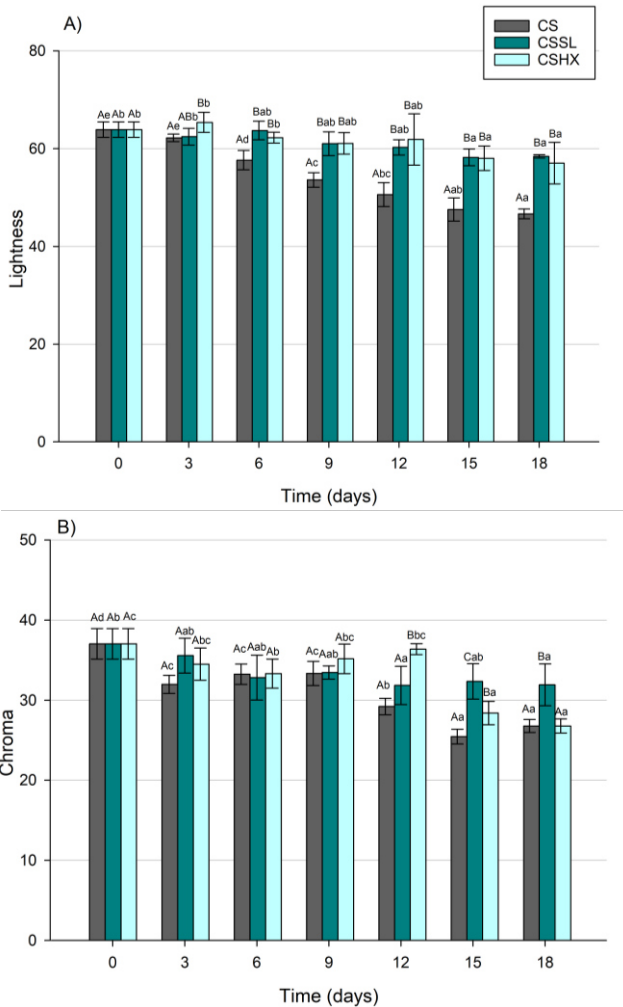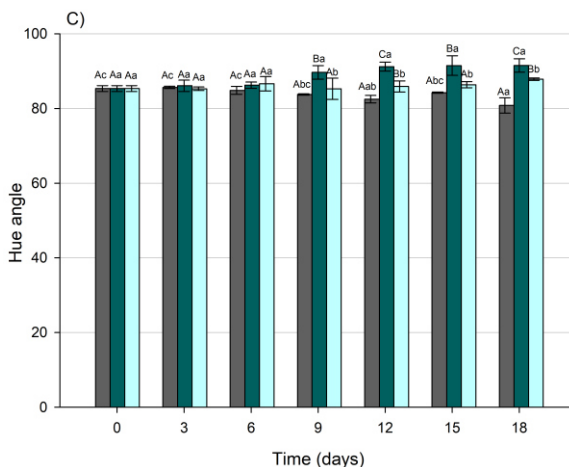
**Figure 8.** Colour parameters of pineapple pieces packaged without and with imine-chitosan films for 18 days at 4ºC. (CSHX: trans-2-hexenal-imine-chitosan films, CSSL: salicylaldehyde-imine-chitosan films). Bars with different letters in lower (a-d) show significant differences between days for each treatment and capital letters (A-C) between films at same time ($P \leq 0.05$).

The evolution of acidity of pineapple pieces was monitored through pH and is shown in **Table 4**. The pH of control fresh-cut pineapple slightly increased through storage, whereas changes were less accused in the samples packaged with responsive films. During fruit ripening, acidity decreases and pH increases due to conversion of organic acids into sugars [35]. A delay in the consumption of organic acids could explain these results. Since polyphenol oxidase (PPO) activity depends on the pH, and PPOs from pineapple are more active around neutral pH [33], pH evolution results are in agreement with the retention of L* values of fruit packaged using responsive films.

**Table 4.** pH of pineapple packaged for 18 days at 4 °C without and with imine-chitosan films of trans-2-hexenal (CSHX) and saliciylaldehyde (CSSL).

| | Time (days) | | | | | |
|---|---|---|---|---|---|---|
| | 3 | 6 | 9 | 12 | 15 | 18 |
| Control | 3.7±0.1$^{aA}$ | 3.8±0.2$^{aAB}$ | 4.1±0.2$^{cBC}$ | 4.3±0.2$^{bCD}$ | 4.2±0.1$^{bCD}$ | 4.4±0.1$^{bD}$ |
| CSHX | 3.8±0.1$^{aB}$ | 3.8±0.2$^{aB}$ | 3.5±0.1$^{aA}$ | 3.8±0.1$^{aB}$ | 3.9±0.1$^{aBC}$ | 4.1±0.1$^{aC}$ |
| CSSL | 3.8±0.1$^{aA}$ | 3.8±0.2$^{aA}$ | 3.8±0.2$^{bA}$ | 3.9±0.1$^{aA}$ | 4.0±0.1$^{aA}$ | 4.0±0.2$^{aA}$ |

Different letters (a-c) in the same column indicate a statistically significant difference between packaged samples per day. Different letters (A-C) in the same row indicate a statistically difference of same treatment at different days.

Juice leakage is together with brown discoloration, microbial and visible fungal growth the main factor limiting the shelf-life of fresh-cut pineapple [7]. Pineapple cultivar and the fresh-cut shape have been reported to affect juice leakage whereas neither temperature nor atmosphere modification have effect on juice leakage incidence [36–38]. **Figure 9** shows firmness and juice leakage of pineapple chunks packaged in passive containers and those employing responsive films. The amount of juice that leaked from fruit pieces increased following a linear trend line, however the slope was much greater for fruit packaged using CSSL films. No differences were found in the juice leaked from pieces packaged in passive containers and using CSHX. Salicylaldehyde released into the headspace of the package could be more absorbed by the fruit than trans-2-hexenal, interacting with cell wall components of pineapple causing fruit leakage.
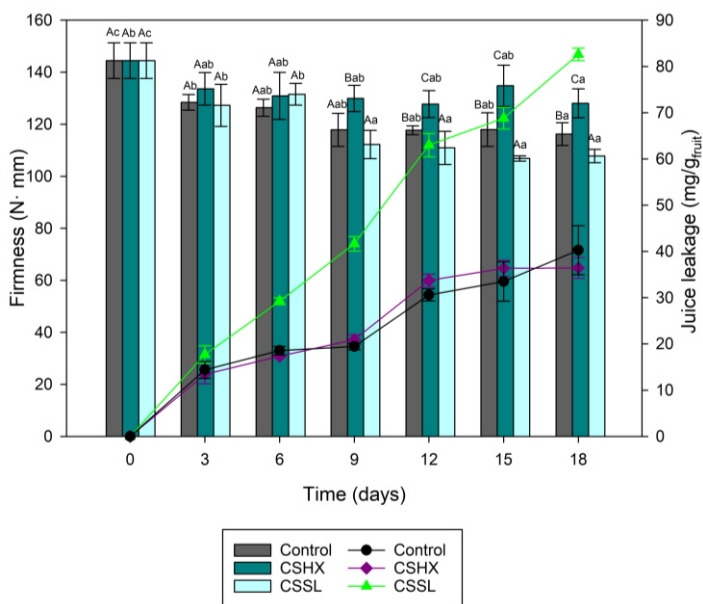


**Figure 9.** Firmness (bars) and juice leakage (lines) of pineapple pieces stored for 18 days at 4 °C under passive and responsive packaging (CSHX, CSSL). Bars with different letters in lower (a-d) show significant differences between days for each package and capital letters (A-C) between treatment at same time ($P \le 0.05$).

Firmness evolution of pineapple chunks stored at 4 °C for 18 days using passive and responsive packaging is displayed in **Figure 9**. Firmness of fresh-cut pineapple slightly decreased during the storage period, but the decrease was greater for fruit packaged with CSSL films, especially after ninth days of storage. Thus, at the end of the storage, firmness of control fruit was reduced by 19 % respect to the initial value, whereas the firmness of fruit packaged with CSHX suffered a reduction of 11%, and the decrease was around 25% for fruit packaged incorporating CSSL films. In general, essential oils or their components do not alter or exert some beneficial effect on fruit firmness and other quality parameters. However, some of them can cause adverse effects on fruit, with occurrence of phytotoxicity and acceleration of the physico-chemical and physiological changes related to ripening and senescence [37,39]. In other cases, adverse effects of natural volatiles or essential oils depend on the concentration applied on the fruit [26,40]. In the present study, the amount of SL released from CSSL films to the headspace of the package increased juice leakage and had an adverse effect on fruit firmness.

### 3.4.2. Microbiological assays
### 3.4.2.1. Microbiological analysis of packaged fruit

Besides biochemical and physiological changes associated to processing operations such as peeling and cutting, the shelf life of fresh-cut pineapple is limited mainly by microbial and visible fungal growth [7]. In the current study, the natural microbial load of pineapple including the growth of moulds and yeasts, mesophilic and psychrophilic microorganisms was monitored in pineapple chunks stored for 18 days under refrigeration in passive containers without or incorporating CSHX and CSSL films. **Figure 10** shows microbial counts evolution of the natural microorganisms of pineapple. The results showed a great difference on the evolution of microorganisms in passive and responsive packaged fresh-cut pineapple. The differences were more marked for the growth evolution of moulds and yeasts since these microorganisms capable of growing at low pH, are the predominant population in fresh-cut pineapple.

Just prepared fresh-cut pineapple presented a total count of around 3.5, 2.6 and 3.6 log CFU/$g_{fruit}$ of mesophiles, psychrophiles, and moulds and yeasts, respectively. These data are in accordance with those reported by other authors [41,42]. Similar to other countries of the European Union, Spanish legislation stablishes for fresh-cut produce a range of aerobic mesophilic counts from 5-6 log CFU/$g_{fruit}$ on the day of processing and packaging, to 6-7 log CFU/$g_{fruit}$ on the expiration date of the product, but it does not specify limits on moulds and yeasts count for ready-to-eat fruits [43]. However visible fungal growth is one of the main causes limiting the shelf-life of fresh-cut pineapple [44]. Moreover, in accordance with the microbiological standards for food not thermally processed of IFTS [45], around 6 log CFU/$g_{fruit}$ is considered the limit of acceptance of moulds and yeasts in fresh-cut fruit. Besides the ability of fungi to spoil minimally-processed pineapple, Leneveu-jenvrin et al. [41] reported the ability of some fungal isolates from pineapple to produce mycotoxins.

In this study, microbial flora of fruit stored without or with responsive films was maintained inside the quantitative levels of microbiological quality until the 6th day of storage, although responsive packaged fruit had lower microbiological load. At day 9, considerable differences were found in moulds and yeasts population between passive and responsive packaged fruit. Control fruit reached a population around 6 log CFU/$g_{fruit}$ which is in the limit recommended by IFST, whereas this value was 4.5 and 4 log CFU/$g_{fruit}$ in pineapple packaged with CSHX and CSSL films, respectively. Regarding mesophilic population, it was maintained below legislation levels of 6-7 log CFU/$g_{fruit}$, although mesophilic counts were much lower for fruit packaged with responsive films.

At 12th day of storage, mesophilic counts of control fruit were in the up limit allowed by the legislation, whereas fruit packaged with CSSL and CSHX films has count of 4 and 5 log CFU/$g_{fruit}$, respectively. Psychrophilic counts were 6.8 log and around 4-5 log CFU/$g_{fruit}$ for control and fruit packaged with responsive films. Regarding moulds and yeasts counts, they were around 7 log for fruit packaged in passive system, whereas 5.3 and 4.2 log CFU/ $g_{fruit}$ were enumerated when fruit was packaged with CSHX and CSSL films. These data correspond with the strong visual deterioration of passive packaged fresh-cut pineapple

at day 12, while the other samples maintained a better appearance (**Figure 6**). Typically, ready-to-eat fruit become spoiled once microbial flora levels are in the range $10^7$-$10^8$ CFU/$g_{fruit}$, the growth of moulds and yeasts, and bacteria produce a wide variety of enzymes and processes responsible of limiting shelf-life of foods, with changes in colour, odour and texture. At the end of the storage, moulds and yeasts enumerated in fruit packaged with responsive films did not exceed the limit recommended by IFST, whereas mesophilic and psychrophilic counts were around 5 log CFU/$g_{fruit}$.

Comparing responsive films, the best microbiological results were obtained employing CSSL films. However, SL caused a loss of firmness and an excess of juice leakage respect to control and fruit packaged with CSHX films (as described earlier, **Figure 9**). Similar results of microbial inhibition were observed when a nanoemulsion containing citral was incorporated in a coating for fresh-cut pineapple [26]. The authors reported that although the best microbiological results were obtained with the higher amount of citral tested, it affected negatively to quality parameters of pineapple. Therefore, it should be interesting to study if it is possible to find the optimal salicylaldehyde concentration necessary to retard microbial proliferation without damaging fruit texture.
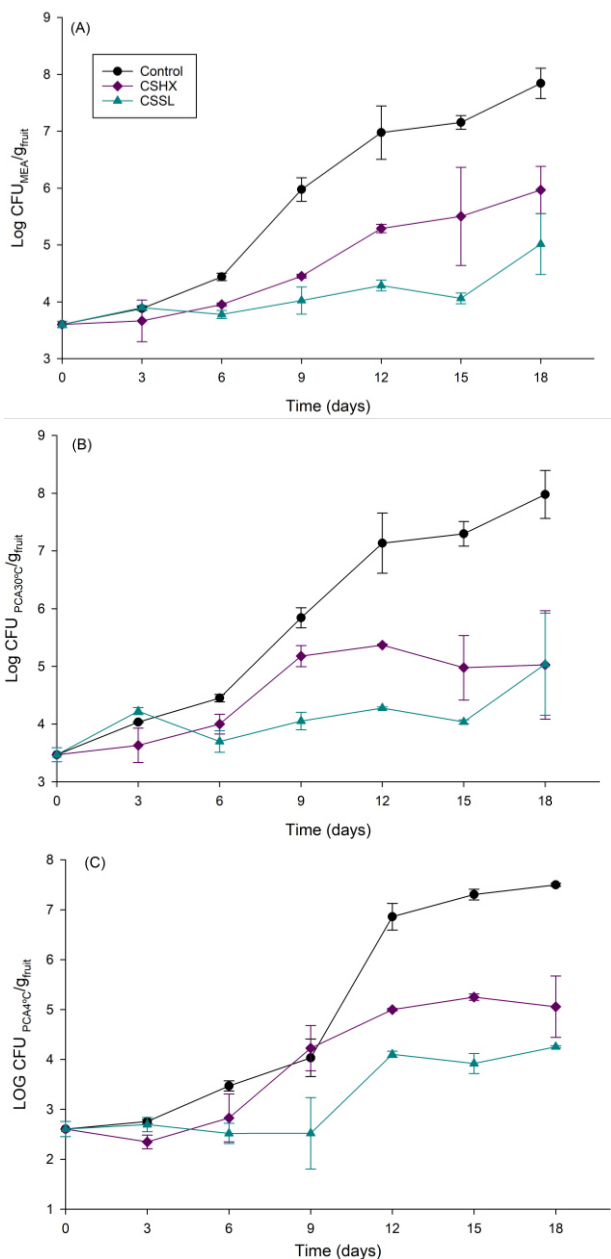
**Figure 10.** Evolution of moulds and yeasts (A), mesophilic (B) and psychrophilic (C) counts in pineapple pieces stored for 18 days at 4 °C under passive and responsive packaging (CSHX: trans-2-hexenal-imine-chitosan films, CSSL: salicylaldehyde-imine-chitosan films).

*3.4.2.2. Growth and survival of pathogens inoculated in fresh-cut pineapple after packaging*

The evolution of *E. coli* and *L. innocua* previously inoculated on the surface of pineapple pieces is presented in **Figure 11** and **Figure 12**, respectively. Passive packaged pineapple showed a slow and gradual decrease in *E. coli* population. After nine days of storage pathogen population was reduced 50 and 70 % for *E. coli* and *L. innocua* in control packages. Similarly, others studies reported a reduction of population of *E. coli* on fresh-cut pineapple [46]. Previous studies also reported that pineapple resulted largely unsuitable for *Listeria monocytogenes* growth [47]. The low pH of pineapple could avoid the growth of the pathogens. Depending on pineapple variety, fruit acidity, nutrient composition and pH are different, and these parameters affect the growth of microorganisms [4]. Responsive packages incorporating CSHX and CSSL films showed antimicrobial activity after 6 days of storage, and they exerted bactericidal activity on *E. coli* inoculated in pineapple pieces after nine days of refrigerated storage. However, no significant reduction in the *L. innocua* growth was observed, which could be related to the greater MIC and MMC values measured for *L. innocua* than *E. coli.*
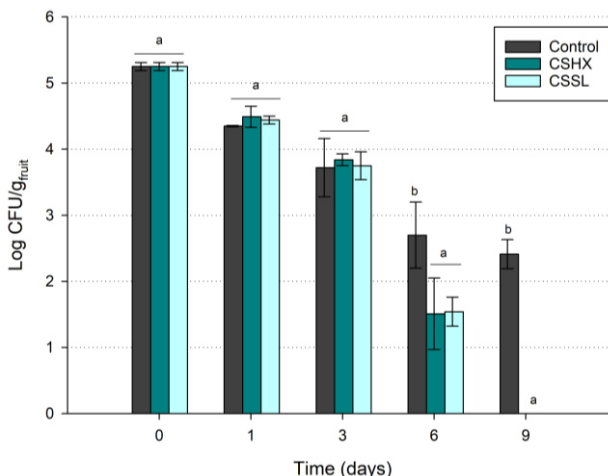


**Figure 11.** Evolution of *E. coli* inoculated in pineapple pieces stored at 4 °C for 9 days under passive and responsive packaging. Bars with different letters in lower (a-b) show significant differences between days for each package (*P*≤ 0.05).
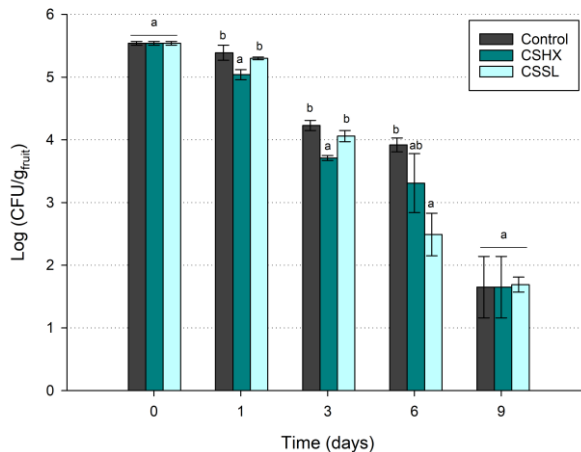
**Figure 12.** Evolution of *L. innocua* inoculated in pineapple pieces stored at 4 °C for 9 days under passive and responsive packaging. Bars with different letters in lower (a-b) show significant differences between days for each package ($P \leq 0.05$).

## 4. Conclusions

Trans-2-hexenal and salicylaldehyde were successfully grafted to the surface of chitosan films by means of imine bonds. The films were pH-responsive and after immersion in aqueous solution buffered at pH ranging 3-7, imines suffered hydrolysis and consequently, the aldehydes were released to the surrounding atmosphere. The amount of aldehyde liberated depended on the pH of the medium and the physico-chemical features of the molecule. *In vitro* assays showed films that presented microbicidal effect against tested microorganisms when they were activated at pH 3.6. The responsive films were incorporated in a double-bottom tray used to package refrigerated fresh-cut pineapple. Juice leaked from pineapple pieces entered in contact with the responsive films placed in the bottom of the container, and thus, triggered the release of the aldehydes to the surrounding atmosphere. CSHX and CSSL films considerably reduced microbial load in packaged fruit, and also delayed browning. However, CSSL films led to a marked decrease in fruit firmness and an increase in juice leakage, that could be due to an excessive release of SL from the films at the pH

of pineapple exudate. Moreover, responsive packages showed bactericidal activity against inoculated *E. coli.* Future studies are needed to optimize the amount of CSSL film incorporated into the double-bottom package in order to avoid the observed negative effects of SL on the texture of pineapple pieces without compromising antimicrobial effectiveness. Moreover, a sensory evaluation should be also conducted to determine how the aldehydes affect the flavour of pineapple pieces.

## *Acknowledgments*

## References

1.  Lante, A.; Tinello, F.; Nicoletto, M. UV-A light treatment for controlling enzymatic browning of fresh-cut fruits. *Innov. Food Sci. Emerg. Technol.* **2016**, *34*, 141–147, doi:https://doi.org/10.1016/j.ifset.2015.12.029.

2.  Barth, M.; Hankinson, T.R.; Zhuang, H.; Breidt, F. *Compendium of the Microbiological Spoilage of Foods and Beverages*; **2009**; ISBN 9781441908261.

3.  Tournas, V.H.; Heeres, J.; Burgess, L. Moulds and yeasts in fruit salads and fruit juices. *Food Microbiol.* **2006**, *23*, 684–688, doi:10.1016/j.fm.2006.01.003.

4.  Abadias, M.; Alegre, I.; Oliveira, M.; Altisent, R.; Viñas, I. Growth potential of *Escherichia coli* O157: H7 on fresh-cut fruits (melon and pineapple) and vegetables (carrot and escarole) stored under different conditions. *Food Control* **2012**, *27*, 37–44, doi:10.1016/j.foodcont.2012.02.032.

5.  Feng, K.; Hu, W.; Jiang, A.; Saren, G.; Xu, Y.; Ji, Y.; Shao, W. Growth of *Salmonella* spp. and *Escherichia coli* O157:H7 on Fresh-Cut Fruits Stored at Different Temperatures. *Foodborne Pathog. Dis.* **2017**, *14*, 510–517, doi:10.1089/fpd.2016.2255.

6.  Strawn, L.K.; Schneider, K.R.; Danyluk, M.D. Microbial safety of tropical

fruits. *Crit. Rev. Food Sci. Nutr.* **2011**, *51*, 132–145, doi:10.1080/10408390903502864.

7. Çandır, E. Fresh-Cut Fruits. In *Minimally processed refrigerated fruits and vegetables*; Yildiz, F., Wiley, R.C., Eds.; Boston, MA, **2017**; pp. 327–384.

8. da Rocha Neto, A.C.; Beaudry, R.; Maraschin, M.; Di Piero, R.M.; Almenar, E. Double-bottom antimicrobial packaging for apple shelf-life extension. *Food Chem.* **2019**, *279*, 379–388, doi:10.1016/j.foodchem.2018.12.021.

9. Martínez-Ferrer, M.; Harper, C. Reduction in microbial growth and improvement of storage quality in fresh-cut pineapple after methyl jasmonate treatment. *J. Food Qual.* **2005**, *28*, 3–12, doi:10.1111/j.1745-4557.2005.00007.x.

10. Huang, S.; Kong, X.; Xiong, Y.; Zhang, X.; Chen, H.; Jiang, W.; Niu, Y.; Xu, W.; Ren, C. An overview of dynamic covalent bonds in polymer material and their applications. *Eur. Polym. J.* **2020**, *141*, 110094, doi:10.1016/j.eurpolymj.2020.110094.

11. Zentner, C.A.; Anson, F.; Thayumanavan, S.; Swager, T.M. Dynamic imine chemistry at complex double emulsion interfaces. *J. Am. Chem. Soc.* **2019**, *141*, 18048–18055, doi:10.1021/jacs.9b06852.

12. Chen, H.; Zhao, R.; Hu, J.; Wei, Z.; Mcclements, D.J.; Liu, S.; Li, B.; Li, Y. One-step dynamic imine chemistry for preparation of chitosan-stabilized emulsions using a natural aldehyde: acid trigger mechanism and regulation and gastric delivery. *J. Agric. Food Chem.* **2020**, *68*, 5412–5425, doi:10.1021/acs.jafc.9b08301.

13. Tchakalova, V.; Lutz, E.; Lamboley, S.; Moulin, E.; Benczédi, D.; Giuseppone, N.; Herrmann, A. Design of stimuli-responsive dynamic covalent delivery systems for volatile compounds (Part 2): Fragrance-releasing cleavable surfactants in functional perfumery applications. *Chem. - A Eur. J.* **2021**, *27*, 13468–13476, doi:10.1002/chem.202102051.

14. Rizzo, F.; Kehr, N.S. Recent advances in injectable hydrogels for controlled and local drug delivery. *Adv. Healthc. Mater.* **2021**, *10*, doi:10.1002/adhm.202001341.

15. Fadida, T.; Selilat-Weiss, A.; Poverenov, E. N-hexylimine-chitosan, a biodegradable and covalently stabilized source of volatile, antimicrobial hexanal. Next generation controlled-release system. *Food Hydrocoll.* **2015**, *48*, 213–219, doi:10.1016/j.foodhyd.2015.02.033.

16. Amorim, J.C.; Piccoli, R.H.; Duarte, W.F. Probiotic potential of yeasts isolated from pineapple and their use in the elaboration of potentially functional fermented beverages. *Food Res. Int.* **2018**, *107*, 518–527, doi:10.1016/j.foodres.2018.02.054.

17. Wang, H.; Yang, Z.; Ying, G.; Yang, M.; Nian, Y.; Wei, F.; Kong, W. Antifungal evaluation of plant essential oils and their major components against toxigenic fungi. *Ind. Crops Prod.* **2018**, *120*, 180–186, doi:10.1016/j.indcrop.2018.04.053.

18. Takeshita, S.; Konishi, A.; Takebayashi, Y.; Yoda, S.; Otake, K. Aldehyde approach to hydrophobic modification of chitosan aerogels.

*Biomacromolecules* **2017**, *18*, 2172–2178, doi:10.1021/acs.biomac.7b00562.

19. Kasaai, M.R.; Arul, J.; Chin, S.L.; Charlet, G. The use of intense femtosecond laser pulses for the fragmentation of chitosan. *J. Photochem. Photobiol. A Chem.* **1999**, *120*, 201–205, doi:10.1016/S1010-6030(98)00432-8.

20. Heras-Mozos, R.; Gavara, R.; Hernández-Muñoz, P. Development of antifungal biopolymers based on dynamic imines as responsive release systems for the postharvest preservation of blackberry fruit. *Food Chem.* **2021**, *357*, doi:10.1016/j.foodchem.2021.129838.

21. Friedman, M.; Henika, P.R.; Mandrell, R.E. Antibacterial activities of phenolic benzaldehydes and benzoic acids against *Campylobacter jejuni, Escherichia coli, Listeria monocytogenes,* and *Salmonella enterica*. *J. Food Prot.* **2003**, *66*, 1811–1821, doi:10.4315/0362-028X-66.10.1811.

22. Ma, W.; Zhao, L.; Zhao, W.; Xie, Y. (E)-2-Hexenal, as a potential natural antifungal compound, inhibits *Aspergillus flavus* spore germination by disrupting mitochondrial energy metabolism. *J. Agric. Food Chem.* **2019**, *67*, 1138–1145, doi:10.1021/acs.jafc.8b06367.

23. Kawacka, I.; Olejnik-Schmidt, A.; Schmidt, M.; Sip, A. Natural plant-derived chemical compounds as *Listeria monocytogenes* inhibitors *in vitro* and in food model systems. *Pathogens* **2021**, *10*, 1–36, doi:10.3390/pathogens10010012.

24. Barbosa, H.F.G.; Attjioui, M.; Leitão, A.; Moerschbacher, B.M.; Cavalheiro, É.T.G. Characterization, solubility and biological activity of amphihilic biopolymeric Schiff bases synthesized using chitosans. *Carbohydr. Polym.* **2019**, *220*, 1–11, doi:10.1016/j.carbpol.2019.05.037.

25. Iftime, M.M.; Morariu, S.; Marin, L. Salicyl-imine-chitosan hydrogels: Supramolecular architecturing as a crosslinking method toward multifunctional hydrogels. *Carbohydr. Polym.* **2017**, *165*, 39–50, doi:10.1016/j.carbpol.2017.02.027.

26. Prakash, A.; Baskaran, R.; Vadivel, V. Citral nanoemulsion incorporated edible coating to extend the shelf life of fresh cut pineapples. *Lwt* **2020**, *118*, 108851, doi:10.1016/j.lwt.2019.108851.

27. Dos Santos, J.E.; Dockal, E.R.; Cavalheiro, É.T.G. Synthesis and characterization of Schiff bases from chitosan and salicylaldehyde derivatives. *Carbohydr. Polym.* **2005**, *60*, 277–282, doi:10.1016/j.carbpol.2004.12.008.

28. Xin, Y.; Yuan, J. Schiff's base as a stimuli-responsive linker in polymer chemistry. *Polym. Chem.* **2012**, *3*, 3045–3055, doi:10.1039/c2py20290e.

29. Tao, Y.; Liu, S.; Zhang, Y.; Chi, Z.; Xu, J. A pH-responsive polymer based on dynamic imine bonds as a drug delivery material with pseudo target release behavior. *Polym. Chem.* **2018**, *9*, 878–884, doi:10.1039/c7py02108a.

30. Peng, X.; Liu, P.; Pang, B.; Yao, Y.; Wang, J.; Zhang, K. Facile fabrication of pH-responsive nanoparticles from cellulose derivatives via Schiff base formation for controlled release. *Carbohydr. Polym.* **2019**, *216*, 113–118, doi:10.1016/j.carbpol.2019.04.029.

31. Neqal, M.; Fernandez, J.; Coma, V.; Gauthier, M.; Héroguez, V. pH-Triggered release of an antifungal agent from polyglycidol-based nanoparticles against fuel fungus *H. resinae*. *J. Colloid Interface Sci.* **2018**, *526*, 135–144,

doi:10.1016/j.jcis.2018.03.106.

32.  González-Aguilar, G.A.; Ruiz-Cruz, S.; Cruz-Valenzuela, R.; Rodríguez-Félix, A.; Wang, C.Y. Physiological and quality changes of fresh-cut pineapple treated with antibrowning agents. *LWT - Food Sci. Technol.* **2004**, *37*, 369–376, doi:10.1016/j.lwt.2003.10.007.

33.  Nogales-Delgado, S. Polyphenoloxidase (Ppo): Effect, current determination and inhibition treatments in fresh-cut produce. *Appl. Sci.* **2021**, *11*, doi:10.3390/app11177813.

34.  Zhou, W.; Sun, Y.; Zou, L.; Zhou, L.; Liu, W. Effect of galangal essential oil emulsion on quality attributes of cloudy pineapple juice. *Front. Nutr.* **2021**, *8*, 1–11, doi:10.3389/fnut.2021.751405.

35.  Benítez, S.; Soro, L.; Achaerandio, I.; Sepulcre, F.; Pujolá, M. Combined effect of a low permeable film and edible coatings or calcium dips on the quality of fresh-cut pineapple. *J. Food Process Eng.* **2014**, *37*, 91–99.

36.  Montero-Calderón, M.; Rojas-Graü, M.A.; Martín-Belloso, O. Effect of packaging conditions on quality and shelf-life of fresh-cut pineapple (*Ananas comosus*). *Postharvest Biol. Technol.* **2008**, *50*, 182–189, doi:10.1016/j.postharvbio.2008.03.014.

37.  Serrano, M.; Martínez-Romero, D.; Castillo, S.; Guillén, F.; Valero, D. The use of natural antifungal compounds improves the beneficial effect of MAP in sweet cherry storage. *Innov. Food Sci. Emerg. Technol.* **2005**, *6*, 115–123, doi:10.1016/j.ifset.2004.09.001.

38.  Marrero, A.; Kader, A.A. Optimal temperature and modified atmosphere for keeping quality of fresh-cut pineapples. *Postharvest Biol. Technol.* **2006**, *39*, 163–168, doi:10.1016/j.postharvbio.2005.10.017.

39.  Taghavi, T.; Kim, C.; Rahemi, A. Role of natural volatiles and essential oils in extending shelf life and controlling postharvest microorganisms of small fruits. *Microorganisms* **2018**, *6*, 104, doi:10.3390/microorganisms6040104.

40.  Basaglia, R.R.; Pizato, S.; Santiago, N.G.; Maciel de Almeida, M.M.; Pinedo, R.A.; Cortez-Vega, W.R. Effect of edible chitosan and cinnamon essential oil coatings on the shelf life of minimally processed pineapple (*Smooth cayenne*). *Food Biosci.* **2021**, *41*, doi:10.1016/j.fbio.2021.100966.

41.  Leneveu-jenvrin, C.; Quentin, B.; Assemat, S.; Hoarau, M.; Meile, J.C.; Remize, F. Changes of quality of minimally-processed pineapple (*Ananas comosu*s, var. 'queen victoria') during cold storage: Fungi in the leading role. *Microorganisms* **2020**, *8*, doi:10.3390/microorganisms8020185.

42.  Bierhals, V.S.; Chiumarelli, M.; Hubinger, M.D. Effect of cassava starch coating on quality and shelf life of fresh-cut pineapple (*Ananas Comosus L. Merril* cv "Pérola"). *J. Food Sci.* **2011**, *76*, doi:10.1111/j.1750-3841.2010.01951.x.

43.  BOE Real Decreto 3484/2000, de 29 de diciembre, por el que se establecen las normas de higiene para la elaboración, distribución y comercio de comidas preparadas. **2001**, 1435–1441.

44.  Chonhenchob, V.; Chantarasomboon, Y.; Singh, S.P. Quality changes of treated fresh-cut tropical fruits in rigid modified atmosphere packaging

containers. *Packag. Technol. Sci.* **2007**, *20*, 27–37, doi:10.1002/pts.740.

45. IFST *Development and use of microbiological criteria for foods: Institute of Food Science and Technology*; The Institute., **1999**; ISBN 0905367162.

46. Strawn, L.K.; Danyluk, M.D. Fate of *Escherichia coli* O157:H7 and *Salmonella* on fresh and frozen cut pineapples. *J. Food Prot.* **2010**, *73*, 418–424, doi:10.4315/0362-028X-73.3.418.

47. Ziegler, M.; Rüegg, S.; Stephan, R.; Guldimann, C. Growth potential of *Listeria monocytogenes* in six different RTE fruit products: Impact of food matrix, storage temperature and shelf life. *Ital. J. Food Saf.* **2018**, *7*, 142–147, doi:10.4081/ijfs.2018.7581.

# Artículo 6

**pH modulates antibacterial activity of hydroxybenzaldehyde derivates immobilized in chitosan films via reversible Schiff bases and their application to preserve freshly-squeezed juice**

Raquel Heras-Mozos, Gracia López Carballo[a], Rebeca Hernández[b], Rafael Gavara[a], Pilar Hernández-Muñoz[a]

[a] Instituto de Agroquímica y Tecnología de Alimentos (IATA-CSIC), Av, Agustín Escardino, 7, 46980, Paterna, Valencia, Spain.

[b] Instituto de Ciencia y Tecnología de Polímeros (ICTP-CSIC), C/Juan de la Cierva, 3, 28006, Madrid, Spain.

**ABSTRACT**

Antimicrobial food grade hydroxybenzaldehyde derivatives were immobilized on the surface of chitosan films by means of reversible Schiff bases. Spectroscopy and elemental analysis evidenced the different ability of the aldehydes to form Schiff bases with chitosan. Chitosan films modified with Schiff bases of aldehydes exerted antimicrobial properties against *E. coli* under mild acidic environments. The efficacy of the films lied on the reversibility of synthetized imine bonds and release of the aldehydes which was promoted in mildly acid aqueous solutions. Besides acidity, imine bond reversibility depended on the chemical structure of the aldehyde covalently bonded. Films carrying salicylaldehyde presented the highest *in vitro* antimicrobial performance and thus, they were chosen to evaluate their effectivity in inhibiting *E. coli* proliferation in freshly-squeezed carrot-orange juice. Films were successfully activated by the acid environment of the juice and reduced the population of the inoculated pathogen. Salicylaldehyde migrated to the juice did not exert toxic effects on Caco-*2* cells.

**Keywords:** chitosan, salicylaldehyde, reversible Schiff base, *Escherichia coli*, fruit juice, cytotoxicity.

## 1. Introduction

Plants and herbs are a significant source of naturally-occurring antimicrobial molecules that can be used as food preservatives [1]. An effective approach to carry and administrate them in packaged foods is their incorporation into polymer structures for their posterior sustained release into the food. The polymer structures can be in the form of particles, films or coatings integrated in the design of the food package. This alternative to traditional packaging has been widely studied in the last two decades [2]. In this way, several strategies have been employed for the use of polymers to entrap the bioactives, the most current ones are extrusion and solvent casting. However, some drawbacks appear when working with compounds of high volatility, mainly due to the loss of the bioactive during processing and storage of the packaging material. In these regard, many studies have been focused on the use of cyclodextrins, nanoclays and zeolites to stabilize labile and volatile molecules, and also to delay the prompt release of the bioactive and loss of polymer activity [3,4]. Commonly, the humidity accumulated in the food package or food water plasticizes the polymer and promotes the release of the bioactive physically immobilized in the polymer matrix. However, it lacks alternative mechanisms that stabilize the bioactive in the matrix and triggers its release in a most precise manner when working with volatiles. Stimuli responsive polymers, which respond to environmental factors other than humidity, are a valuable tool for the smart delivery of antimicrobials in active packaging technologies.

In the current work, responsive polymer films based on the pH dependent release of antimicrobial molecules are explored. Previously, the active molecules were stabilized in the polymer matrix anchoring them in the pendant groups of the polymer skeleton by means of reversible Schiff bases. Schiff bases are formed by the condensation of aldehyde and primary amine groups giving rise to imine bonds (C=N), which can be effectively reverted with mild acid hydrolysis. Thus, imine bonds are very attractive to work with since they are covalent bonds that can be rapidly hydrolysed in an acid environment. Recently, imines have been explored for the sustained release of bioactives in various fields such as agronomy, pharmacology, medicine and cosmetics [5–7].

Chitosan is a biopolymer with excellent film forming properties and great versatility of shapes. This biopolymer has been greatly explored as a carrier of active compounds in different fields including food packaging [8]. Normally, the active compound is physically immobilized in the polymer matrix and its release is triggered by the plasticization of the polymer by water. However, chitosan contains a high percentage of free amino groups capable of condensing with bioactive aldehydes for the synthesis of reversible Schiff bases. The concept of chitosan as a pH- dependent reversible carrier of bioactive compounds is little explored in the area of food packaging.

The antimicrobial properties of naturally-occurring compounds against a wide range of fungi and bacteria are well-known [9,10]. Moreover, some of these derivatives are recognized as food grade substances by the FDA and the EFSA, which makes them good candidates to be employed for the synthesis of pH-stimuli responsive antimicrobial films based on reversible Schiff bases intended for preserving foods.

In this work, three naturally-occurring hydroxybenzaldehyde derivatives with antibacterial activity against *E. coli*, 2-hydroxybenzaldehyde, 4-hydroxybenzaldehyde and 3,4-dihydroxybenzaldehyde, were chosen to form Schiff bases with primary amine groups of chitosan polymer shaped as film. The synthetized Schiff bases were characterized by ATR-FTIR, and the degree of grafting of aldehydes to primary amino groups of chitosan film quantified by elemental analysis and $^1$H-NMR. Next, the reversibility of the Schiff bases and the antimicrobial properties of chitosan-Schiff bases films against *E. coli* were studied as a function of pH of the buffered aqueous media. Then, chitosan-Schiff bases films with the greater performance to be applied in food preservation were chosen to study its pH-responsiveness in different liquid food simulants. Finally, the pH response and antimicrobial efficacy of developed films was tested in fresh-squeezed carrot-orange juice having a pH of 5.1. The amount of aldehyde migrated to the juice and its cytotoxicity was also evaluated. A fruit juice with mild acid pH was chosen due to the occurrence around the world of frequent outbreaks of foodborne illness associated with juices of fruits and vegetables contaminated with *E. coli* [11,12].

## 2. Materials and methods

### 2.1. Materials

Low molecular weight chitosan (LMWC, 75 – 85% deacetylation degree), salicylaldehyde (SL, 2-hydroxybenzaldehyde), 4-hydroxybenzaldehyde (HB), 3,4-dihydroxybenzaldehyde (DHB), Casein peptone, soy peptone, glacial acetic acid, citric acid monohydrate, potassium dihydrogen phosphate and disodium phosphate to carry out buffer medium at pH 5 and 7 were supplied by Sigma-Aldrich (Barcelona-Spain). Sodium chloride, dextrose, D(+)-glucose monohydrate, sodium hydroxide (NaOH), hydrochloric acid 37% (HCl) and ethanol 96% (v/v) were purchased from Scharlab (Barcelona, Spain). Milli-Q water was obtained by Milli-Q Plus purification system (Millipore, Molsheim, France). *Escherichia coli* was supplied by the Spanish Type Culture Collection (CECT 434). The bacteria strain was grown Tryptone Soy Agar (TSA), Tryptone Soy Broth (TSB) and Violet Red Bile Dextrose (VRDB agar), which were supplied by Scharlab (Barcelona, Spain).

### 2.2. Functionalization of chitosan films with Schiff bases of hydroxybenzaldehyde derivatives

#### 2.2.1. Chitosan film formation

Chitosan films were obtained by solvent casting method. For that, a polymeric solution of 1.5% (p/v) LMWC in an aqueous medium containing 0.5% (p/v) of acetic acid was carried out. The polymeric solution was stirred at 50 °C until LMWC was fully dissolved and filtered to remove impurities. After that, polymer solution was poured into polystyrene plates and dried for 24 h at 37 °C. Finally, films of 2 x 2 cm with thickness of $35 \pm 5$ μm were obtained. Prior to storage, chitosan films were neutralized by immersion in 0.1M NaOH for 24 h, then, the films were washed with distilled water and dried at 37 °C. The neutralized films were stored in desiccators with $P_2O_5$ prior to use.

#### 2.2.2. Schiff bases synthesis

Schiff base reaction was performed at the solid/liquid interface via solvent method using ethanol 96% (v/v) as the reaction liquid medium. The reaction was carried out in an Erlenmeyer, where 4 g of the selected aldehyde (SL, HB and DHB) was dissolved in 75 mL of 96% ethanol,

and 2 g of neutralized chitosan films and 100 μL of HCl were added. The reaction flask was kept under steadily agitation in a shaking water bath at 60 °C for 24 h. After that, the reaction medium was replaced with clean ethanol and maintained under agitation to eliminate unreacted aldehyde; this step was repeated three times for 24 h. A control reacted chitosan was carried out without aldehyde (CS). Finally, CS and imine-chitosan films modified with hydroxybenzaldehyde derivatives (CSSL, CSHB and CSDHB) were dried and stored in desiccators with $P_2O_5$ prior to use.

## 2.3. Characterization of Schiff bases

### 2.3.1. $^1$H-Nuclear Magnetic Resonance ($^1$H-NMR)

Control and Schiff base-functionalized chitosan films (CSSL, CSDHB and CSHB) were dissolved in 1 mL of deuterated water with 1% of deuterated acetic acid. Sample CSSL was dissolved in deuterated acetic acid. $^1$H-NMR spectra were obtained in a Varian System 500 MHz NMR equipment. Quantification of the amount of aldehyde grafted to chitosan films was given by the degree of substitution (DS, %) of aldehyde to chitosan and was calculated following the methodology proposed by Dos Santos, Dockal, & Cavalheiro, (2005). Thus, DS (%) was determined by using the ratio $I_{imine}/I_{GlcNac}$ which describes the intensity of the proton assigned of the Schiff base ($I_{imine}$) in relation to the intensity of the proton of N-acetylated glucosamine ($I_{GlcNac}$) of chitosan. The DS obtained by relation of both proton intensity was corrected by the deacetylation degree of CS. The NMR spectra were processed using MestreNova x64 software (v.14.2.1).

### 2.3.2. Elemental analysis

Quantification of the amount of aldehyde grafted to chitosan films was also calculated from the C/N ratio of control and modified films following methodology suggested by [14]. Elemental composition of the samples (C, H, N) was previously evaluated using an Elemental FlashSmart analyser (Thermo Fisher Scientific, Waltham, MA, USA). The C/N ratio was also used to determinate the degree of acetylation of neutralized chitosan films [15], which was found around 75%. The test was carried out in triplicate.

### 2.3.3. Attenuated Total Reflectance-Fourier Transform Infrared

Synthetized imine bonds (C=N) were qualitatively determined by means of Attenuated Total Reflectance-Fourier Transform Infrared (ATR-FTIR). Infrared spectra of chitosan films and those modified with aldehydes were acquired using an FTIR spectrometer JASCO 4100 FTIR (Jasco, Easton, MD) with a single reflection attenuated total reflectance (ATR) accessory (ZnSe crystal, PIKE Technologies, USA). At least 32 scans with a resolution of 4 cm$^{-1}$ was carried out. Infrared spectra were represented in the range from 1850 to 600 cm$^{-1}$.

## 2.4. Water uptake and dimensional stability of functionalized chitosan films

Prior to carry out the test, films were dried in a glass desiccator until constant weight was achieved. Then, dry film specimens of around 1.5 x 1.5 cm were immersed in 5 mL of buffer medium (potassium dihydrogen phosphate and disodium phosphate) at pH 5 and 7, and placed in an orbital shaker at room temperature for 24 h. After that time, the films were weighed, removing water excess on film surface with an absorbent paper. In addition, area of the films was also measured. Mass and dimensional increase was calculated and represented as water uptake (%) and dimensional stability (%). The tests were conduct at least in triplicate.

## 2.5. Antimicrobial activity of chitosan films functionalized with Schiff bases of hydroxybenzaldehyde derivatives

### 2.5.1. Bacterial culture

*Escherichia coli* (CECT 434) was thawed and transferred on TSA plates. The strain was grown and maintained at 4 °C, subculturing to fresh TSA monthly. For experimental use, a cell suspension of $10^5$ colony-forming unit (CFU)/mL was prepared. To obtain the inoculum, a colony from TSA surface with *E. coli* was collected and transferred to sterile TSB tubes with 10 mL and incubated overnight at 37 °C. Then, 10 mL of sterile TSB was inoculated with 100 μL of *E. coli* overnight culture. The tubes were incubated at 37 °C until reaching the exponential phase, determined by an absorbance at 595 nm of 0.18 – 0.2, which corresponding at $10^5$ CFU/mL.

### 2.5.2. Antimicrobial activity of hydroxybenzaldehyde derivatives

The antimicrobial effectiveness of aldehydes against *E. coli* was evaluated by estimation of minimum inhibitory concentration (MIC) and minimal bactericidal concentration (MBC) of aldehyde which produced a partial or complete inhibition of pathogen growth, respectively. For that, different amounts of aldehydes were added to 10 mL of sterile TSB tubes, which were inoculated with 100 µL of *E. coli* suspension at $10^5$ CFU/mL. Tubes without aldehydes were also prepared as control samples. The inoculated tubes were incubated at 37 °C for 24 h. After that time, 1:10 serial dilutions with sterile peptone water were carried out and plated in TSA plates. Enumeration of colonies forming units were performed after 24 h of incubation at 37 °C and expressed as logarithmic of CFU per mL. The tests were done in triplicate.

### 2.5.3. Effect of pH on the amount of aldehyde released from functionalized films

The effect of pH on the release of SL, HB and DHB from imine-chitosan films was studied in buffer solutions (potassium dihydrogen phosphate and disodium phosphate) at pH 5 and 7. For that, around 0.1 g of films were placed in a glass vial containing 5 mL of phosphate buffer, vials were stored at 37 °C for 24 h. The amount of aldehyde released was measured after 24 h of immersing the film in the buffered solution. For that, an aliquot of 0.5 mL was taken out from the medium and quantified by UV-Visible spectroscopy (Agilent Cary 60 UV-Vis, Spectrophotometer, Barcelona, Spain). Absorbance was measured in a conventional quartz cuvette with wavelength of maximum absorption (λmax) at 255, 284 and 279 nm for SL, HB and DHB, respectively. A calibration curve was previously made, and the results were expressed as mg of released aldehyde per mL. The tests were conducted in triplicate.

### 2.5.4. Effect of pH on the antimicrobial activity of functionalized films

Antimicrobial response of chitosan functionalized films against *E. coli* was tested in liquid culture medium at pH 7 and pH 5. The culture medium was previously prepared by mixing casein peptone (17 g/L),

soy peptone (3 g/L), sodium chloride (5 g/L), D(+)-glucose monohydrate (2.5 g/L) with buffer medium. The final pH of medium was around $7.2 \pm 0.2$ and $5.4 \pm 0.2$ at 25 °C. Then, 10 mL of culture medium was aliquoted in tubes and sterilised at 121 °C for 15 min. Regarding the antimicrobial assay, 0.25 g of each film was placed in contact with 10 mL of culture medium buffered at pH 5 and pH 7. A control was prepared with 0.25 g of neutralized chitosan films (CS) and a control without film was also run. Then, a volume of 100 µL of $10^5$ CFU/mL suspension was added to tubes and incubated for 24 h at 37 °C. After that time, enumeration of live bacteria was carried out by seeding of 1:10 serial dilutions of tubes on TSA plates, which were incubated at 37 °C for 24 h. The results were expressed in log of CFU per mL. The tests were done in triplicate.

## 2.6. Release behaviour of salicylaldehyde from functionalized chitosan films in different liquid food simulants

Based on the results of the first part of this work, CSSL films were selected due to their greater potential to be applied on the preservation of refrigerated liquid foods. Thus, the release kinetics of salicylaldehyde from CSSL was studied in several stablished food simulants which mimic the behaviour of liquid foods according to European law (EC Regulation 10/2011). Two food simulants were chosen, 10% (v/v) ethanol simulating hydrophilic foods and 50% (v/v) ethanol for lipophilic liquid foods or oil in water emulsions. Although 3% (w/v) acetic acid simulates hydrophilic foods with pH < 4.5, the pH of the solution is 2.5 and, in this solution, CSSL films dissolved. As an alternative, and besides carrying out the release studies with 10% and 50% (v/v) ethanol, release studies were also carried out using the chosen food simulants modified at pH 5 with citrate buffer to simulate the pH of a great variety of fruit and vegetal juices.

For obtaining the release profile of SA, around a 10-mg film was placed in a glass vial containing 15 mL of each food simulant. The vials were hermetically sealed and placed in an orbital shaker at 4 °C. Aliquots of 0.1 mL were taken with a 1 mL syringe at pre-established times and the aldehyde concentration was quantified. After the removal of each aliquot, fresh medium was added to maintain a constant volume. The amount of aldehyde release to the media was determined by UV-

visible spectroscopy measuring absorbance at 255 nm. The equipment was previously calibrated with known concentrations of SL. The results were expressed as mg of released aldehyde per mL of simulant.

## 2.7. Antimicrobial activity of films functionalized with salicylaldehyde in refrigerated freshly-squeezed juice

The *in vivo* antimicrobial effectivity of the developed films against *E. coli*, was tested in untreated just-made juice elaborated with orange and carrot and inoculated with the pathogen. For juice preparation, carrots and oranges were bought in a local market, they were washed, peeled and cut into pieces, and the juices obtained individually with a Philips Centrifugal juicer (Valencia, Spain). The juices were mixed aseptically by combining 150 g of carrot juice with 15 g of orange juice for reaching pH 5, measured using a pH-meter (Hach Sension plus PH3, Barcelona, Spain). Sterile tubes were filled with 10 ml of juice and 0.25 g of CSSL films were added to each tube. Then, the tubes were inoculated with 100 μL of *E. coli* suspension with $10^5$ CFU/mL and stored for 6 days at 4 °C. A control was performed without film and another one with unmodifed CS film. The enumeration of *E. coli* was carried out after 1, 3 and 6 days of storage. For that, an aliquot of 100 μL was taken from the juice and ten-fold dilution series with sterile peptone water were conduct. The dilutions were plated on a selective agar Violet Red Bile Dextrose (VRDB agar) and colonies of *E. coli* were counted after incubation at 37 °C for 24 h. The results were expressed in log of CFU per mL of juice. The tests were done in triplicate.

## 2.8. Quantification of salicylaldehyde in the juice

The concentration of SL released from 0.25 g of CSSL film to 10 ml of juice stored at 4 °C was monitored after 1, 3 and 6 days of storage. The SL quantification was conducted using the solid phase micro-extraction (SPME) technique coupled with gas chromatograph (GC) mod. 6850 Series II Network GC System (Agilent Technologies, Palo Alto, CA, USA). For that, 10 mL of juice was transferred to crimp-sealed vial of 20 mL. The fibre composed of 50/30 μm DVB/CAR/PDMS (Supelco Inc., Barcelona, Spain) was immersed in the juice during 20 min at room temperature. Then, the fibre was

thermally desorbed into the GC injector at 220 °C for 15 min. The chromatograph was equipped with a flame ionisation detector (FID) and a Restek RTX1 capillary column (30 m x 0.53 mm x 5 μm). The temperature of the injector and detector was set at 220 °C. The oven temperature was established between 100 to 220 °C. Helium was selected as carrier gas and samples were run without split. The aldehyde release in the juice was quantified according to a previous calibration curve. Results were expressed as mg of SL per mL of juice. The tests were done in triplicate.

### 2.9. In vitro cytotoxicity studies

The cytotoxicity of SL was studied using the resazurin (7-hydroxy-3H-phenoxazin-3-one-10-oxide sodium salt,Sigma-Aldrich, Barcelona, Spain) reduction assay. This test is based on the ability of only viable and metabolically active cells to reduce resazurin to resorufin and dihydroresorufin which can be measured by colorimetric methods [16]. Human colon carcinoma Caco-2 cell line (ECACC, number 86010202) was gently supplied by V. Devesa from the Toxicology Group at IATA-CSIC.

The Caco-2 cells were maintained in 75 $cm^2$ flasks with 10 mL of Dulbecco's Modified Eagle Medium (DMEM) supplemented with 10% (v/v) fetal bovine serum (FBS), 10 mM HEPES (N-2-hydroxyethylpiperazine-N′-2-ethanesulfonic acid), 1% (v/v) of non-essential amino acids, 1 mM sodium pyruvate, 100 U/mL of penicillin, 0.1 mg/mL of streptomycin, and 0.0025 mg/L of amphotericin B. Cells were incubated at 37 °C in an atmosphere with 95% relative humidity and a $CO_2$ flow of 5% and the medium was changed every 2–3 days. When the cell monolayer reached 80% confluence, the cells were detached with trypsin (0.5 g/L) and EDTA (ethylene diamine tetraacetic acid, 0.22 g/L) and subcultured. For cytotoxicity assay the medium employed was DMEM supplemented as described above without FBS.

Caco-2 cells were seeded at a density of $2.4 \times 10^4$ cells $cm^{-2}$ in 12-well plates for 5 days and subsequently exposed for 4 and 24 h to different SL concentrations prepared in DMSO (dimethyl sulfoxide) (Sigma-Aldrich, Barcelona, Spain). During the treatment, cells were incubated at 37 °C in an atmosphere with 95% relative humidity and a $CO_2$ flow of 5%. Control treatment with only DMSO was carried out

simultaneously. After each treatment, the medium was removed and 500 μL resazurin solution (10 μg/mL in Eagle's minimal essential medium MEM) was added and incubated for 2 h at the same conditions. Then, 100 μl from each reaction mixture was transferred to a 96-well plate, and resazurin reduction was measured colourimetrically (570 and 600 nm) using a microplate reader (POLARstar OMEGA, BMG LABTECH). The experiments were done with four replicates each one.

## 2.10. Statistical analysis

All assays were conducted at least in triplicate and the data was expressed as means of the data ± standard deviation. One-way analysis of variance (ANOVA) was performed with statistical software SPSS® Statistics computer program, v. 27.0 (SPSS Inc., Chicago, IL, USA). Average of data was tested using the Tukey *b* test with a significance degree of 95%.

## 3. Results and discussion

### 3.1. Characterization of Schiff bases

The schematic reaction of Schiff bases formation between chitosan and aldehydes is showed in **Figure 1**, and $^1$H-NMR spectra of chitosan (CS) and imine-chitosan films are depicted in **Figure 2**. The data obtained from analysis of NMR spectra is represented in **Table 1**. The proton of N-acetylated glucosamine (H-2 proton) of chitosan was allocated around 3 – 3.2 ppm, and around 9.8 – 10 ppm for proton of Schiff base (H-C=N), proton H-7. The DS (%) was obtained by relation of both proton intensity ($I_{imine}/I_{GlcNac}$).
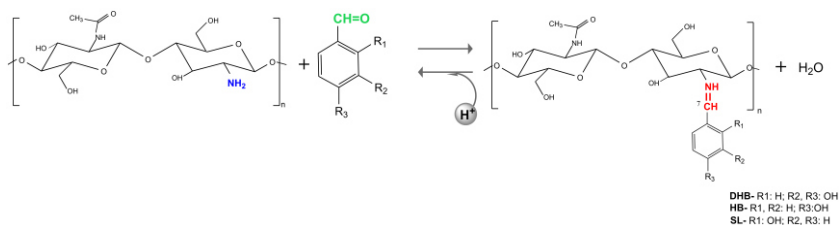


**Figure 1.** Schematic reaction of Schiff bases formation from chitosan and aldehydes.

The highest substitution degree was found for chitosan films modified with salicylaldehyde (CSSL) being around 64%. However, DS (%) did not surpassed 30% for CSHB and CSDHB, being 16% and 26%, respectively.
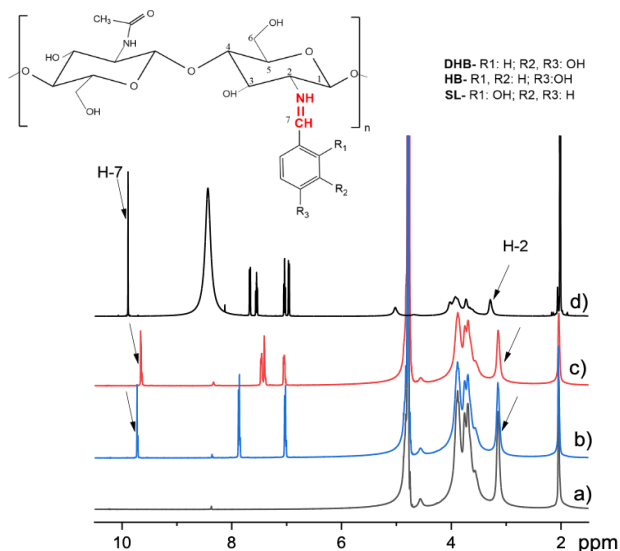


**Figure 2.** ^{1}H NMR spectrum for a) neutralized chitosan (control) and modified with b) DHB, c) HB and d) SL. The arrows indicate the bands employed for the imine quantification. The proton at C-2 position corresponding to the polysaccharide backbone of chitosan and the proton at C-7 position in the imine group.

The ability of HBD to form imines with chitosan could be attributed to differences in aldehyde reactivity. Comparatively, a higher efficiency to obtain imines was reported for 2-hydroxybenzaldehyde than for 4-hydroxybenzaldehyde or 3-hydroxybenzaldehyde when reacted with an excess of butylamine [17]. The ortho- position of the hydroxyl group in the benzene ring in SL makes the molecule more reactive to the nucleophilic attack of amine groups of chitosan, than hydroxyl group at para position in HB molecule or in meta and para-position in DHB. This is because the electrophilicity of carbonyl carbon in SL molecule can increased due to the interaction of hydrogen from hydroxyl group of benzene ring at ortho position with the oxygen of the protonated carbonyl group.

**Table 1.** Assignments of the ^{1}H NMR spectra peaks and substitution degree (DS (%)) calculated for the hydroxybenzaldehyde-Schiff bases films.

| | **Chemical shift (δ, ppm)** | | | |
|---|---|---|---|---|
| | **H-2** | **H-7** | **H-aromatic** | **DS (%)** |
| CS | 3.2 | Absent | Absent | - |
| CSHB | 3.0 | 9.5 | 7.5 – 6.9 | 16 |
| CSDHB | 2.9 | 9.5 | 8.0 – 6.9 | 26.7 |
| CSSL | 3.1 | 9.9 | 7.5 – 6.9 | 64 |

DS (%) of imine-chitosan films was also calculated by elemental analysis and the results are shown in **Table 2**. The calculated values showed that the substitution of primary amino groups was around 64.5%, 16.4% and 18.9%, for CSSL, CSHB and CSDHB, respectively. The DS (%) are similar to those obtained by elemental analysis, with the order of substitution CSSL > CSDHB > CSHB, corroborating that the aldehyde most reactive was SL.

**Table 2.** Elemental analysis and substitution degree of imine-chitosan films.

| | **N (%)** | **C (%)** | **H (%)** | **C/N** | **DS (%)** |
|---|---|---|---|---|---|
| CS | $7.1 \pm 0.1^d$ | $40.2 \pm 0.1^a$ | $6.7 \pm 0.1^b$ | $5.7 \pm 0.1^a$ | |
| CSHB | $6.4 \pm 0.1^c$ | $41.2 \pm 0.1^b$ | $6.5 \pm 0.02^b$ | $6.4 \pm 0.04^b$ | $16.4 \pm 0.8^a$ |
| CSDHB | $6.2 \pm 0.1^b$ | $40.9 \pm 0.2^b$ | $6.4 \pm 0.1^b$ | $6.6 \pm 0.03^b$ | $18.9 \pm 0.6^a$ |
| CSSL | $5.5 \pm 0.1^a$ | $49.2 \pm 0.1^c$ | $5.7 \pm 0.2^a$ | $8.9 \pm 0.2^c$ | $64.5 \pm 3.5^b$ |

Different letters in the same column indicate a statistically significant difference ($P \leq 0.05$).

ATR-FTIR spectra corresponding to the chitosan neutralized film (CS) and films reacted with aldehydes are represented in **Figure 3**. CS spectrum showed characteristics peaks for amide I and amine groups, which are allocated at 1650 and 1578 cm$^{-1}$, respectively. In addition, other peaks associated to the polysaccharide structure of chitosan are also observed in the range from 1150 to 850 cm$^{-1}$ [18]. After reaction with aldehydes, the infrared spectra of chitosan films were modified with respect to the control and the formation of the Schiff base was confirmed. Thus, a shift band appeared around 1635 cm$^{-1}$ in all the spectra that can be assigned to the imine bond (C=N) formed by

condensation of carbonyl group of aldehydes with primary amino group of chitosan films. The imine band in CSHB and CSDHB films was observed at 1638 cm^{-1}, whereas in CSSL the band appeared at 1633 cm^{-1} [13,19]. The condensation of primary amino groups of chitosan films with carbonyl groups gave rise to a decrease of the amino band at 1578 cm^{-1} [20]. After the grafting of aldehydes to chitosan films, other bands associated to structural features of aldehydes were observed in the spectra such as the phenolic hydroxyl group shown around 1290-1250 cm^{-1} [21] and new bands at 1585 and 750 cm^{-1} assigned to the aromatic structure of the aldehydes.
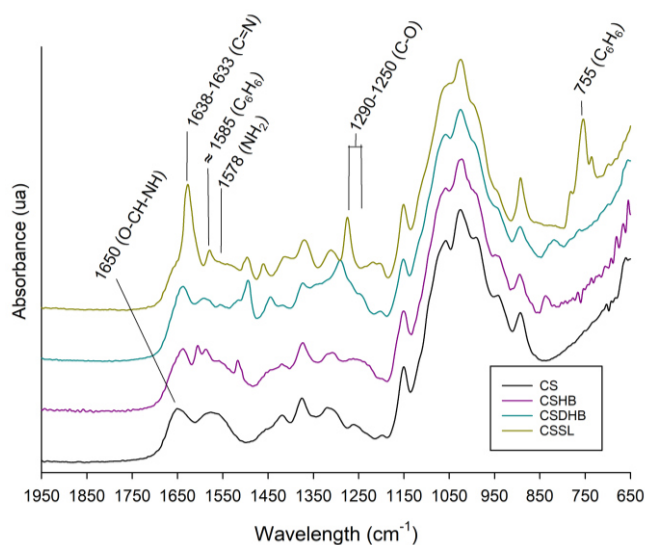


**Figure 3.** Infrared spectra of chitosan films and those modified with 4-hydroxybenzaldehyde (CSHB), 3,4-dihydroxybenzaldehyde (CSDHB) and salicylaldehyde (CSSL).

*3.2. Water uptake and dimensional stability of functionalized chitosan films*

**Table 3** shows the values of film water uptake (%) and also film area increase (%) which is a measure of the dimensional stability of the films after 24 h of immersion in buffered aqueous solutions at pH 7 and 5. Chitosan possesses numerous hydroxyl and amino group through its backbone structure, which confers it an excellent ability to absorb water, in addition due to the presence of amine groups, the capability to

257

absorb water of chitosan changes with the acidity of the medium. In acidic medium, primary amino groups of chitosan are protonated and the repulsion between chain favours the water increase [22]. Thus, water uptake of CS was considerably greater at pH 5 compared with it at pH 7 (**Table 3**).

After formation of Schiff bases with aldehydes, free amino groups in CS were reduced and also the capacity of the films to retain water. CSSL films showed a drastic reduction in water absorption capacity, while that for CSDHB films was slightly lower than for control films. However, this parameter increased for CSHB films. CSSL films present a high DS of amino groups by the imine of salicylaldehyde which is stabilized through resonance-assisted hydrogen bonding and enamine/imine tautomerism [23], which explains the low water uptake of the films even at pH 5, and consequently the higher dimensional stability observed. In spite of the low DS and also the high solubility in water of DHB compared with SL and HB, imines of DHB can form intermolecular hydroxy–hydroxy O—H⋯O hydrogen bonds which explains the slightly lower water uptake and greater dimensional stability of the Schiff-base films compared with control chitosan films. The greater water uptake and area increment of films substituted with HB compared with chitosan films, even with a low DS, can be explained by the presence of new hydroxyl groups in the film.

**Table 3.** Water uptake and dimensional stability of Schiff base-functionalized chitosan films after 24 h of immersion in aqueous buffered medium at pH 7 and 5.

|  | Water uptake (%) | | Area increase (%) | |
|---|---|---|---|---|
|  | pH 7 | pH 5 | pH 7 | pH 5 |
| CS | $179.9 \pm 3.5^b$ | $308.4 \pm 9.6^c$ | $118 \pm 7.1^c$ | $124.9 \pm 7.6^c$ |
| CSHB | $205.9 \pm 6.4^c$ | $348.8 \pm 5.5^d$ | $97.9 \pm 8.6^b$ | $141 \pm 8.3^d$ |
| CSDHB | $175.2 \pm 8.9^b$ | $258.2 \pm 4.7^b$ | $99.2 \pm 6.8^b$ | $89 \pm 6.7^b$ |
| CSSL | $50.5 \pm 7.8^a$ | $76.4 \pm 7.7^a$ | $27 \pm 7.6^a$ | $41.5 \pm 6.3^a$ |

Different letters in the same column indicate a statistically significant difference ($P \leq 0.05$).

### 3.3. Antimicrobial assays

#### 3.3.1. Antimicrobial activity of free aldehydes

All assessed aldehydes showed a great efficacy against *Escherichia coli* as it is shown in **Table 4**. Salicylaldehyde was the most effective compound, showing the lowest values to reduce or inhibit bacterial growth. The MIC for SL was 0.25 mg/mL, whereas the values for HB and DHB were around 1.5 and 1.75 mg/mL, respectively. Likewise, the MBC for SL was 0.75 mg/mL, however, 6 and 5 mg/mL were necessary to obtain a bactericide effect with HB and DHB, respectively. According with previous studies, *ortho*-phenolic substituent enhanced antimicrobial potential of hydroxybenzaldehydes [24]. Similar results were showed against fungal strains [25], reporting that the closer the –OH groups were to the aldehyde moiety a greater antifungal activity was exerted.

**Table 4.** Minimal inhibitory and bactericidal concentrations of the selected hydroxybenzaldehydes when tested in liquid medium against *E. coli* incubated at 37 ºC for 24 h.

|  | MIC (mg/mL) | MBC (mg/mL) |
|---|---|---|
| HB | 1.5 | 6 |
| DHB | 1.75 | 5 |
| SL | 0.25 | 0.75 |

#### 3.3.2. Effect of the pH on the amount of aldehyde released and antimicrobial response of functionalized films

The release of hydroxybenzaldehyde derivatives due to the hydrolysis of imine bond was evident as **Figure 4A** shows. Acid pH promoted a greater release of the aldehydes. In spite of the high DS of chitosan films with SL, its release was limited compared with the other derivatives. As discussed above, imines formed with salicylaldehyde are very stable even in acidified hydrolytic medium. **Figure 4B** shows the antimicrobial response of functionalized films against *E. coli* at 37 °C.

Films exerted antimicrobial properties at pH 5 whereas at pH 7 only a slight inhibition was noted when compared with the controls

(unmodified chitosan films and control sample without films). At pH 5, a bactericidal activity was found for CSSL, whereas CSDHB and CSHB reduced bacterial growth by 3.5 to 2.3 logs, respectively. The reversible nature of the imine bond at acidic pH promotes a higher aldehyde release and hence, a greater antimicrobial activity. These results are in agreement with the amount of aldehyde released to the medium under the same pH and temperature conditions and previously showed in **Figure 4A**.
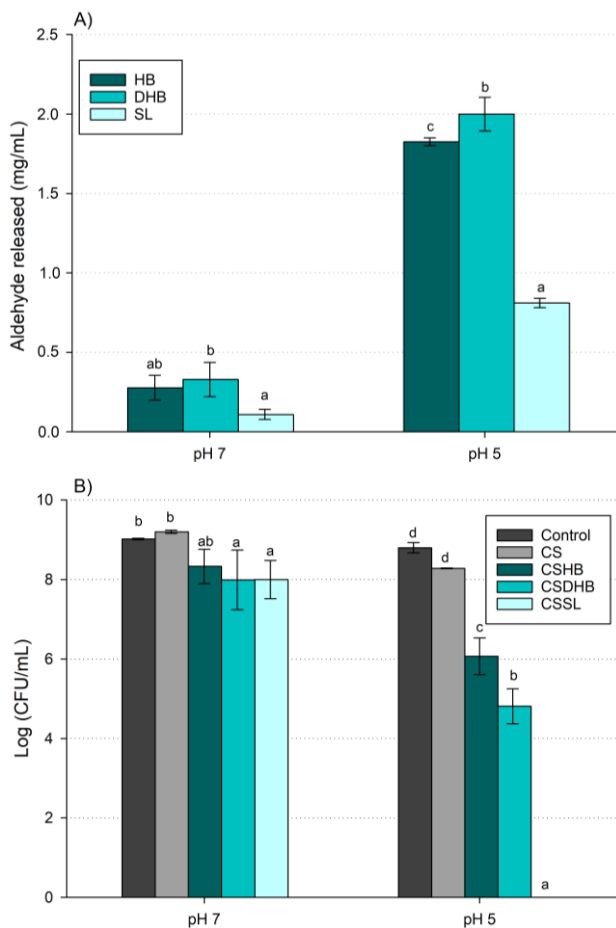


**Figure 4.** Aldehyde released after film immersion in buffer media at pH 5 and 7 at 37 °C after 24 h (A), and antimicrobial response of imine chitosan films against *E. coli* incubated at 37 °C for 24 h at pH 7 and 5 (B). Bars with same letters between samples of same group (pH 5 or 7) are not significantly different ($P \leq 0.05$).

Thus, the amount of SL released at pH 5 was above its MBC against the pathogen, exerting bactericidal effect, whereas at pH 7 the amount of SL released was below its MIC and the antimicrobial effect was not noticed. Imine-chitosan films formed with HB and DHB exerted limited antimicrobial activity at pH 7 since under this condition the concentration of aldehyde released was below their MIC of 1.5 and 1.75 mg/mL for HB and DHB, respectively. Under acidic conditions, the concentration of aldehydes in the medium increased above the MIC and exerted some antimicrobial activity. Antimicrobial response of imine-chitosan films, as well as the quantification of aldehyde released, proved the potential of these functionalized films to be applied in the development of responsive food packaging.

### 3.4. Release behaviour of salicylaldehyde from functionalized films in different liquid food simulants at 4 °C

Understanding the release behaviour of antimicrobials from polymer matrices to foods is necessary for an effective design of the active package. Due to the greater antimicrobial response of CSSL films against *E. coli*, they were chosen to study the release behaviour of SL in 10 and 50% (v/v) aqueous ethanol as liquid food simulants of hydrophilic and lipophilic foods, respectively. The release was studied in neutral and acid conditions and under refrigerated storage, and the results are depicted in **Figure 5**. A higher SL concentration was detected in the two food simulants acidified at pH 5, evidencing that protons from acid catalyst triggered the hydrolysis of imine bonds and the subsequent release of SL. Contrary, in neutral food simulants, the release of SL was greatly limited, reaching a concentration of 0.01 mg/mL. Moreover, although acid media triggered the release of SL in both liquid food simulants, the release of SL was more rapid when the amount of ethanol in the simulant was lower, that is, in 10% (v/v) ethanol. In the current study, SL was covalently immobilized in the chitosan matrix through imine bonds. The cleavage of these bonds requires the presence of water molecules and thus the swelling of the matrix which is favoured in a media reach in water such as 10% aqueous ethanol. This can explain the more rapid release of SL in 10% ethanol. Release of SL in different simulants shows that the synthetized responsive films could be effective in liquid food matrices mildly acid.
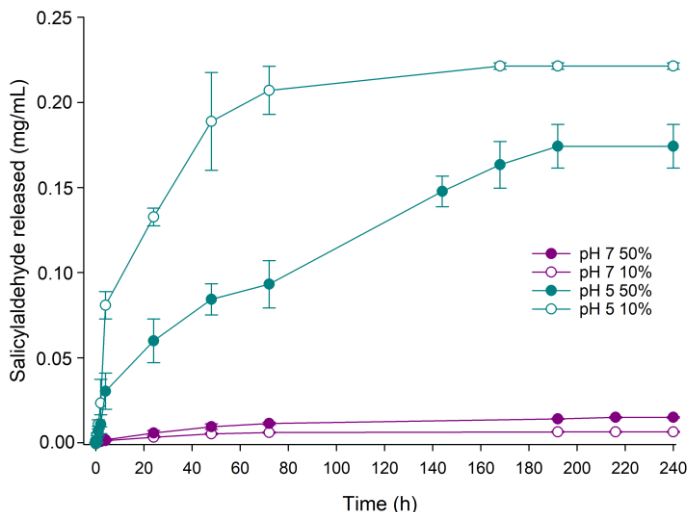
**Figure 5.** Release kinetics of salicylaldehyde from CSSL films in different hydrolytic media (food simulants) at 4 °C.

### 3.5. *Antimicrobial activity of films functionalized with salicylaldehyde in refrigerated freshly-squeezed juice* and *quantification of aldehyde released*

The antimicrobial effectiveness of CSSL films against *E. coli* inoculated in untreated just made carrot-orange juice stored for six days at 4 °C is shown in **Figure 6**. The pH of the juice was slightly acid, being around pH 5.1, which promoted SL release, and hence, the inhibition of *E. coli* during storage. An inhibition of 1.8, 3 and 2.9 logs was observed in the juice in contact with CSSL films after 1, 3, and 6 days of storage, respectively. The use of essential oils or their active components has been previously evaluated to reduce bacterial growth in fruit juices [26]. Moreover, CSSL films could be combined with other preservation techniques to improve its antimicrobial efficacy [27].

The quantification of SL released in the juice is also shown in **Figure 6**. The concentration of SL after 1 day of storage was 0.3 mg/mL, and slightly changed in the next days. The concentration detected was higher than the MIC value (0.25 mg/mL) and lower than the MBC (0.75 mg/mL), which is in accordance with the inhibitory response of the films. However, the *in vitro* effectivity of SL was

reduced in the juice. Juices are rich in sugars, which could provide a protective effect on bacterial cell damage [28], reducing its antimicrobial capacity.
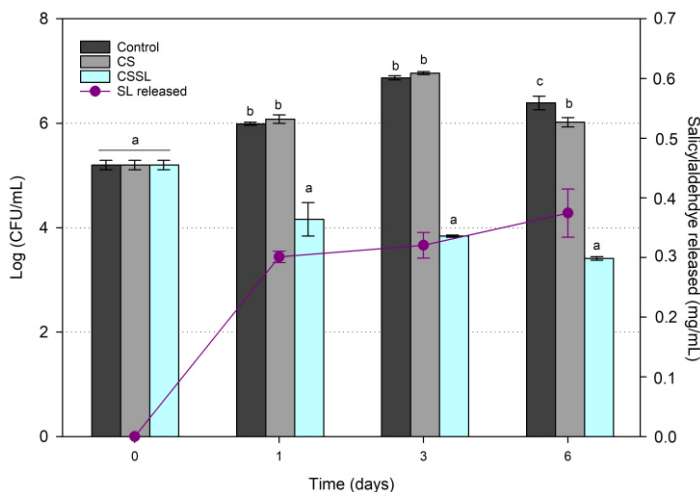


**Figure 6.** Antimicrobial effectivity of salicylaldehyde-imine-chitosan films against *E. coli* inoculated in carrot-orange juice stored at 4 °C for 6 days, and salicylaldehyde released from the films. Bars with same letters between samples at the same time are not significantly different ($P \leq 0.05$).

### 3.6. In vitro cytotoxicity studies

Salicylaldehyde release from imine-chitosan films exerted antimicrobial properties against *E. coli* inoculated in a carrot-orange juice. The *oral lethal* dose *50%* (LD*50*) of this compound has been reported as 520 and 504 mg/Kg in rats and mousses, respectively [29], being considerably high. However, cyotoxicity studies evaluating the viability of Caco-2 cells exposed to different concentrations of SL have been carried out. These concentrations were chosen according to the values obtained for MBC and MIC (0.75 and 0.25 mg/mL, respectively) and the amount of the aldehyde migrated to the juice (0.35 mg/mL).

Viability of Caco-2 cells cultured with these concentrations of SL is shown in **Figure 7**. Concentrations related to MIC and aldehyde migrated to the juice kept the viability of the cells similar to control cell population. However, the concentration related to MBC decrease cell viability after 24 h of exposure. Other studies have showed toxicity and

irritation of human skin produced by using a high content of antimicrobial aldehydes such as cinnamaldehyde [30]. In this work it has been probed that the amount of SL released to the juice is innocuous to Caco-2 cells.
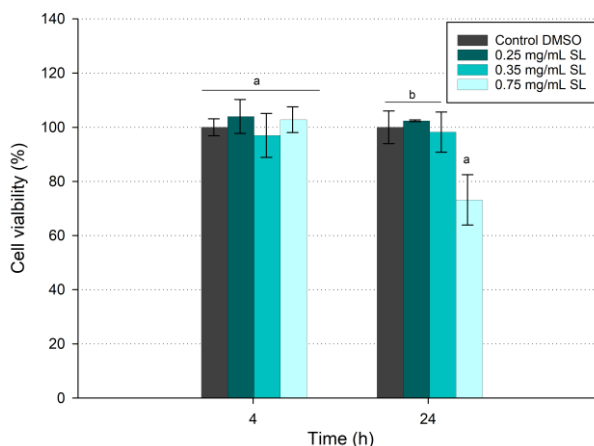


**Figure 7.** Citotoxicity evaluation of Caco-2 cells after treatment with different salicyladehyde concentrations. Bars with same letters between samples of same group are not significantly different (P ≤ 0.05).

## 4. Conclusions

Antimicrobial films which activity is based on the pH-responsive release of the active molecule were synthetized. For that, food grade hydroxybenzaldehyde derivatives with antimicrobial properties against *E. coli* were covalently attached to chitosan films forming reversible Schiff bases. The amount of aldehyde incorporated depended on its chemical structure, and the greatest incorporation was achieved with salicylaldehyde. The reversibility of imine bonds and release of the aldehyde depended on the acidity of assayed buffered aqueous medium, and also the chemical structure of the imine formed. All the films exerted antimicrobial properties in mildly acidic buffered aqueous medium whereas at neutral pH their activity was irrelevant. The antimicrobial activity of CSSL films was tested *in vivo* in freshly-squeezed carrot-orange juice having a pH of 5.1 and previously inoculated with *E. coli.* Films were activated by the acid environment of the juice and reduced the population of the inoculated pathogen. The

release of salicylaldehyde in the juice was evaluated having no cytotoxic effect.

This work presents Schiff bases as a successful way of incorporating antimicrobials in chitosan films and introduces a pH-responsive mechanism for activating their release. The synthetized films were validated with a real food matrix and their application could be extended to other aqueous mildly acid liquid foods.

**References**

1. Falleh, H.; Ben Jemaa, M.; Saada, M.; Ksouri, R. Essential oils: A promising eco-friendly food preservative. *Food Chem.* **2020**, *330*, 127268, doi:10.1016/j.foodchem.2020.127268.

2. Almasi, H.; Jahanbakhsh Oskouie, M.; Saleh, A. A review on techniques utilized for design of controlled release food active packaging. *Crit. Rev. Food Sci. Nutr.* **2020**, *0*, 1–21, doi:10.1080/10408398.2020.1783199.

3. Sanahuja, A.B.; García, A.V. New trends in the use of volatile compounds in food packaging. *Polymers (Basel).* **2021**, *13*, doi:10.3390/polym13071053.

4. Ho, T.M.; Howes, T.; Bhandari, B.R. Encapsulation of gases in powder solid matrices and their applications: A review. *Powder Technol.* **2014**, *259*, 87–108, doi:10.1016/j.powtec.2014.03.054.

5. Bao, J.; Zhang, H.; Zhao, X.; Deng, J. Biomass polymeric microspheres containing aldehyde groups: Immobilizing and controlled-releasing amino acids as green metal corrosion inhibitor. *Chem. Eng. J.* **2018**, *341*, 146–156, doi:10.1016/j.cej.2018.02.047.

6.      Peng, X.; Liu, P.; Pang, B.; Yao, Y.; Wang, J.; Zhang, K. Facile fabrication of pH-responsive nanoparticles from cellulose derivatives via Schiff base formation for controlled release. *Carbohydr. Polym.* **2019**, *216*, 113–118, doi:10.1016/j.carbpol.2019.04.029.

7.      Tchakalova, V.; Lutz, E.; Lamboley, S.; Moulin, E.; Benczédi, D.; Giuseppone, N.; Herrmann, A. Design of Stimuli-responsive dynamic covalent delivery systems for volatile compounds (part 2): Fragrance-releasing cleavable surfactants in functional perfumery applications. *Chem. - A Eur. J.* **2021**, *27*, 13468–13476, doi:10.1002/chem.202102051.

8.      Flórez, M.; Guerra-Rodríguez, E.; Cazón, P.; Vázquez, M. Chitosan for food packaging: Recent advances in active and intelligent films. *Food Hydrocoll.* **2022**, *124*, doi:10.1016/j.foodhyd.2021.107328.

9.      Burt, S.A. *Antibacterial activity of essential oils : potential applications in food*; **2004**; Vol. 94; ISBN 9789039346617.

10.     Mari, M.; Bautista-Baños, S.; Sivakumar, D. Decay control in the postharvest system: Role of microbial and plant volatile organic compounds. *Postharvest Biol. Technol.* **2016**, *122*, 70–81, doi:10.1016/j.postharvbio.2016.04.014.

11.     Krug, M.; Chapin, T.; Danyluk, M.; Goodrich-Schneider, R.; Schneider, K.; Harris, L.; Worobo, R. Outbreaks of foodborne disease associated with fruit and vegetable juices, 1922–2019. *Edis* **2020**, *2020*, doi:10.32473/edis-fs188-2020.

12.     Luna-Guevara, J.J.; Arenas-Hernandez, M.M.P.; Martínez De La Peña, C.; Silva, J.L.; Luna-Guevara, M.L. The role of pathogenic *E. coli* in fresh vegetables: Behavior, contamination factors, and preventive measures. *Int. J. Microbiol.* **2019**, *2019*, doi:10.1155/2019/2894328.

13.     Dos Santos, J.E.; Dockal, E.R.; Cavalheiro, É.T.G. Synthesis and characterization of Schiff bases from chitosan and salicylaldehyde derivatives. *Carbohydr. Polym.* **2005**, *60*, 277–282, doi:10.1016/j.carbpol.2004.12.008.

14.     Takeshita, S.; Konishi, A.; Takebayashi, Y.; Yoda, S.; Otake, K. Aldehyde approach to hydrophobic modification of chitosan aerogels. *Biomacromolecules* **2017**, *18*, 2172–2178, doi:10.1021/acs.biomac.7b00562.

15.     Kasaai, M.R.; Arul, J.; Chin, S.L.; Charlet, G. The use of intense femtosecond laser pulses for the fragmentation of chitosan. *J. Photochem. Photobiol. A Chem.* **1999**, *120*, 201–205, doi:10.1016/S1010-6030(98)00432-8.

16.     Musatti, A.; Devesa, V.; Calatayud, M.; Vélez, D.; Manzoni, M.; Rollini, M. Glutathione-enriched baker's yeast: Production, bioaccessibility and intestinal transport assays. *J. Appl. Microbiol.* **2014**, *116*, 304–313, doi:10.1111/jam.12363.

17.     Natsch, A.; Gfeller, H.; Haupt, T.; Brunner, G. Chemical reactivity and skin sensitization potential for benzaldehydes: Can Schiff base formation explain everything? *Chem. Res. Toxicol.* **2012**, *25*, 2203–2215, doi:10.1021/tx300278t.

18.     Kumirska, J.; Czerwicka, M.; Kaczyński, Z.; Bychowska, A.; Brzozowski, K.; Thöming, J.; Stepnowski, P. Application of spectroscopic methods for structural analysis of chitin and chitosan. *Mar. Drugs* **2010**, *8*, 1567–1636, doi:10.3390/md8051567.

19.     Iftime, M.M.; Morariu, S.; Marin, L. Salicyl-imine-chitosan hydrogels: Supramolecular architecturing as a crosslinking method toward multifunctional hydrogels. *Carbohydr. Polym.* **2017**, *165*, 39–50, doi:10.1016/j.carbpol.2017.02.027.

20.     Chen, H.; Zhao, R.; Hu, J.; Wei, Z.; Mcclements, D.J.; Liu, S.; Li, B.; Li, Y. One-step dynamic imine chemistry for preparation of chitosan-stabilized emulsions using a natural aldehyde: acid trigger mechanism and regulation and gastric delivery. *J. Agric. Food Chem.* **2020**, *68*, 5412–5425, doi:10.1021/acs.jafc.9b08301.

21.     Xu, C.; Zhan, W.; Tang, X.; Mo, F.; Fu, L.; Lin, B. Self-healing chitosan/vanillin hydrogels based on Schiff-base bond/hydrogen bond hybrid linkages. *Polym. Test.* **2018**, *66*, 155–163, doi:10.1016/j.polymertesting.2018.01.016.

22.     Nisar, S.; Pandit, A.H.; Wang, L.F.; Rattan, S. Strategy to design a smart photocleavable and pH sensitive chitosan based hydrogel through a novel crosslinker: A potential vehicle for controlled drug delivery. *RSC Adv.* **2020**, *10*, 14694–14704, doi:10.1039/c9ra10333c.

23.     Chen, H.; Ye, H.; Hai, Y.; Zhang, L.; You, L. N → π∗ interactions as a versatile tool for controlling dynamic imine chemistry in both organic and aqueous media. *Chem. Sci.* **2020**, *11*, 2707–2715, doi:10.1039/c9sc05698j.

24.     Friedman, M.; Henika, P.R.; Mandrell, R.E. Antibacterial Activities of Phenolic Benzaldehydes and Benzoic Acids against *Campylobacter jejuni, Escherichia coli, Listeria monocytogenes,* and *Salmonella enterica*. *J. Food Prot.* **2003**, *66*, 1811–1821, doi:10.4315/0362-028X-66.10.1811.

25.     Fitzgerald, D.J.; Stratford, M.; Gasson, M.J.; Narbad, A. Structure-function analysis of the vanillin molecule and its antifungal properties.

*J. Agric. Food Chem.* **2005**, *53*, 1769–1775, doi:10.1021/jf048575t.

26. Kim, J.; Kim, H.; Beuchat, L.R.; Ryu, J.H. Synergistic antimicrobial activities of plant essential oils against *Listeria monocytogenes* in organic tomato juice. *Food Control* **2021**, *125*, 108000, doi:10.1016/j.foodcont.2021.108000.

27. de Carvalho, R.J.; de Souza, G.T.; Pagán, E.; García-Gonzalo, D.; Magnani, M.; Pagán, R. Nanoemulsions of *Mentha piperita* L. essential oil in combination with mild heat, pulsed electric fields (PEF) and high hydrostatic pressure (HHP) as an alternative to inactivate *Escherichia coli* O157: H7 in fruit juices. *Innov. Food Sci. Emerg. Technol.* **2018**, *48*, 219–227, doi:10.1016/j.ifset.2018.07.004.

28. Molet-Rodríguez, A.; Turmo-Ibarz, A.; Salvia-Trujillo, L.; Martín-Belloso, O. Incorporation of antimicrobial nanoemulsions into complex foods: A case study in an apple juice-based beverage. *Lwt* **2021**, *141*, 110926, doi:10.1016/j.lwt.2021.110926.

29. EFSA Opinion of the Scientific Panel on food additives, flavourings, processing aids and materials in contact with Food (AFC) related to Flavouring Group Evaluation 20: Benzyl alcohols, benzaldehydes, a related acetal, esters from chemical group 23. *EFSA J.* **2005**, *296*, 1–117, doi:10.2903/j.efsa.2006.296.

30. Shreaz, S.; Wani, W.A.; Behbehani, J.M.; Raja, V.; Irshad, M.; Karched, M.; Ali, I.; Siddiqi, W.A.; Hun, L.T. Cinnamaldehyde and its derivatives, a novel class of antifungal agents. *Fitoterapia* **2016**, *112*, 116–131, doi:10.1016/j.fitote.2016.05.016.
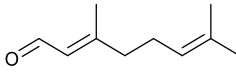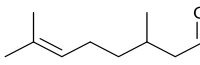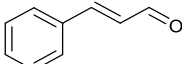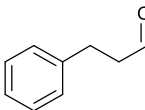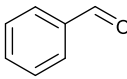
# 5. DISCUSIÓN GENERAL
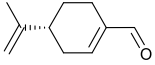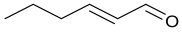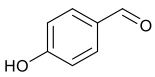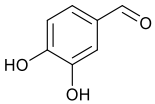
Una amplia variedad de compuestos volátiles naturales se ha empleado para mejorar la calidad y seguridad alimentaria por su excelente actividad antimicrobiana contra diferentes patógenos y alterantes alimentarios. Su uso plantea varios desafíos como son, la baja estabilidad de los agentes activos, las pérdidas durante el procesado y almacenamiento, así como la falta de mecanismos específicos de liberación controlada. Los avances en el desarrollo de envases activos antimicrobianos que incorporan volátiles se han enfocado principalmente en estabilizarlos en matrices poliméricas y controlar su liberación, con el objetivo de garantizar su efectividad antimicrobiana durante la comercialización del alimento. Entre los diferentes materiales portadores de activos, el quitosano resulta una alternativa sostenible, procedente de la revalorización de residuos de la industria alimentaria, y muy versátil, ya que su estructura química permite su modificación y adecuación a las necesidades de una aplicación concreta, especialmente a través del grupo amino de sus unidades de glucosamina, y específicamente, para la inmovilización covalente reversible de aldehídos de origen natural.

En este contexto, en la presente Tesis Doctoral se han desarrollado eficazmente películas activas de quitosano basadas en la química covalente reversible de volátiles antimicrobianos que pueden ser liberados de forma controlada como consecuencia de cambios de pH.

Esta memoria se ha estructurado en dos capítulos que comprenden por un lado el desarrollo y caracterización, y por otro, la aplicación en el diseño de envases activos antimicrobianos basados en películas de quitosano que han servido de sustrato para inmovilizar de forma covalente reversible aldehídos con propiedades antimicrobianas. En la **Tabla 1** se muestra un resumen de las películas desarrolladas.

**Tabla 1.** Desarrollo y caracterización de películas modificadas mediante el anclaje covalente reversible de aldehídos y su aplicación antimicrobiana. DS, grado de sustitución calculado mediante análisis elemental, $v_{C=N}$ (cm$^{-1}$) banda IR característico de la imina.

| Aldehído | DS (%) | Pico IR $v_{C=N}$ (cm$^{-1}$) | Microorganismo diana | Aplicación | Medio de hidrólisis | Alimento |
|---|---|---|---|---|---|---|
| Citral | 57 | 1645 | | Migración al espacio de cabeza | pH 4/pH 7 | - |
| Citronellal | 24 | 1659 | | Migración al espacio de cabeza | pH 4/pH 7 | - |
| Cinamaldehído | 64 | 1632 | *P. expansum* *B. cinerea* | Migración al espacio de cabeza | pH 4/pH 7 | - |
| Hidrocinamaldehído | 30 | 1634 | | Migración al espacio de cabeza | pH 4/pH 7 | - |
| Benzaldehído | 43 | 1639 | | Migración al espacio de cabeza | pH 4/pH 7 | - |

CAPÍTULO I

| | | | | | | |
|---|---|---|---|---|---|---|
| Perillaldehído | 35 | 1640 | *P. expansum* *B. cinerea* | Migración al espacio de cabeza | pH 4/pH 7 | - |
| Trans-2-Hexenal | 74 | 1650 | *P. expansum* *B. cinerea* | Migración al espacio de cabeza | pH 4/pH 7 | Moras frescas |
| | | | *S. cerevisae* *Levaduras aisladas de piña* *E. coli* | Migración al espacio de cabeza | pH 3.6/pH 7 Exudado de piña cortada a pH 3.6 | Piña fresca cortada |
| Salicilaldehído | 65 | 1626 | *S. cerevisae* *Levaduras aisladas de piña* *E. coli* | Migración al espacio de cabeza | pH 3.6/pH 7 Exudado de piña cortada a pH 3.6 | Piña fresca cortada |
| | | | *E. coli* | Migración al medio liquido | pH 5/pH 7 Zumo a pH 5 | Zumo de zanahoria y naranja |
| 4-hidroxibenzaldehído | 16 | 1638 | *E. coli* | Migración al medio liquido | pH 5/pH 7 | - |
| 3,4-dihidroxibenzaldehído | 19 | 1638 | *E. coli* | *In vitro* en contacto directo en medio líquido | pH 5/pH 7 | - |

Antes de la síntesis de las películas, en un estudio preliminar se determinó la actividad antimicrobiana de una serie de aldehídos de origen natural y permitidos para uso alimentario frente a diferentes patógenos y alterantes alimentarios, dos hongos fitopatógenos, *P. expansum* y *B. cinerea*, una bacteria Gram negativa*, E. coli* y una Gram positiva, *Listeria innocua*, cepa subrogada de *L. monocytogenes*. Para ello, se determinó la concentración mínima inhibitoria (MIC, por sus siglas en inglés) y la concentración mínima microbicida (MMC, por sus siglas en inglés) en fase vapor. La MIC y MMC se definieron como la cantidad de aldehído mínima dosificada por placa (μL de aldehído/placa) que inhibió un 50% y un 100% el crecimiento del microorganismo comparado con el control, respectivamente. Estos resultados se recogen en la **Tabla 2** y englobaron el primer objetivo específico sobre evaluación y determinación de la actividad antimicrobiana de compuestos naturales. Los resultados demostraron que los aldehídos poseen una elevada efectividad contra distintos microorganismos diana. En general, se observó que en fase vapor los hongos resultaron más susceptibles que las bacterias, ya que se requirieron menores dosis de aldehído para ejercer inhibición. Los valores obtenidos de MIC y MMC sugirieron que los aldehídos con estructura α,β-insaturada fueron más efectivos que sus homólogos saturados. Además, se observó que los sustituyentes del anillo aromático influyeron en su efectividad, así el salicialdehído fue más activo que el benzaldehído. Aunque otros parámetros como su volatilidad o lipofilicidad pueden influir en su actividad [1].

Los datos reflejados de aquel estudio demostraron el potencial de estos aldehídos para ser aplicados en el diseño de materiales antimicrobianos para el envasado activo de alimentos.

**Tabla 2.** Efectividad antimicrobiana de los aldehídos en fase vapor contra *Penicillium expansum*, *Botrytis cinerea*, *Escherichia coli* y *Listeria innocua* expresada como concentración mínima inhibitoria (MIC) y microbicida (MMC) (µL de aldehído/placa).

| Aldehído | MIC (µL/placa) | | | | MMC (µL/placa) | | | |
|---|---|---|---|---|---|---|---|---|
| | *P. expansum* | *B. cinerea* | *E. coli* | *L. innocua* | *P. expansum* | *B. cinerea* | *E. coli* | *L. innocua* |
| **Citral** | 7.5 | 5 | 5 | 2.5 | 15 | 10 | >150 | 50 |
| **Citronellal** | 25 | 20 | - | 10 | 75 | 50 | - | 75 |
| **Trans-2-hexenal** | 1 | 2 | 2.5 | 5 | 2 | 4 | 7.5 | 10 |
| **Perillaldehído** | 3.5 | 4 | 30 | 20 | 10 | 7.5 | >150 | 150 |
| **Benzaldehído** | 5 | 5 | 20 | 30 | 10 | 7.5 | 75 | 100 |
| **p-anisaldehído** | 20 | 10 | 10 | 50 | >150 | >150 | >150 | >150 |
| **Cuminaldehído** | 5 | 3.5 | 10 | 10 | 30 | 7.5 | >150 | 150 |
| **Salicilaldehído** | 1 | 1.5 | 2.5 | 5 | 2 | 2 | 7.5 | 15 |
| **Cinamaldehído** | 2 | 2.5 | 2.5 | 5 | 5 | 15 | 100 | 75 |
| **Hidrocinamaldehído** | 5 | 15 | 5 | 7.5 | 12.5 | 20 | 125 | 125 |

En el **capítulo I** de esta tesis se presentan los desarrollos y la caracterización de las películas de quitosano con aldehídos antifúngicos anclados reversiblemente para su liberación controlada. Durante el desarrollo de los diferentes estudios englobados en el capítulo I, se observó que la estructura del aldehído inmovilizado influyó notablemente en la formación y reversibilidad de las iminas cuando son sometidas a distintos pH. En la **Figura 1**, se muestran las diferentes partes en las que se divide este capítulo.
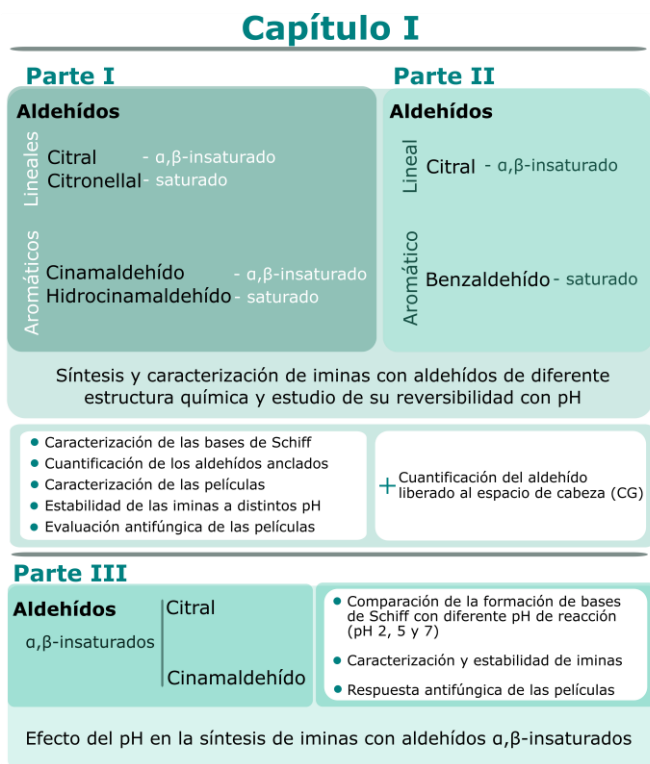


**Figura 1.** Esquema de las partes incluidas en el capítulo I.

En la **primera parte del capítulo I** y en base a los resultados obtenidos del estudio preliminar sobre la actividad antimicrobiana de los compuestos volátiles, se seleccionaron dos aldehídos α,β-insaturados con diferente estructura química y sus análogos saturados. Por una parte, se escogieron aldehídos con estructura lineal (citral y citronellal), y por otra, aldehídos con estructura aromática

(cinamaldehído e hidrocinamaldehído). Las películas activas obtenidas se caracterizaron por un notable cambio de color cuando los aldehídos α,β-insaturados fueron anclados, mientras que resultaron transparentes y sin color para los análogos saturados. Las bases de Schiff obtenidas con citral y cinamaldehído poseen un enlace conjugado entre la imina y el doble enlace insaturado -N=C-C=C-, lo que puede contribuir al cambio de color de las películas.

La caracterización de la presencia de bases de Schiff se realizó cualitativamente mediante ATR-FTIR, además, el grado de sustitución se cuantificó mediante análisis elemental. Ambas técnicas resultaron fundamentales durante el desarrollo de esta Tesis Doctoral. La posición de la banda característica del enlace imina en los espectros de infrarrojo, así como el grado de sustitución de los aldehídos en las películas de quitosano se muestran en la **Tabla 1**.

Tras la reacción, los espectros de infrarrojo de las películas modificadas evidenciaron un cambio significativo en el rango 1630 – 1659 cm$^{-1}$, correspondiente a la formación del nuevo enlace imina (C=N). Respecto a su cuantificación, el rendimiento fue mayor para citral y cinamaldehído (>55%), mientras que fue mucho más limitado para sus análogos saturados, citronellal e hidrocinamaldehído (25-30%) mostrando una diferencia significativa entre los diferentes tipos de estructuras, siendo menos reactivos los saturados que sus análogos α,β-insaturados. Otras propiedades funcionales, como propiedades térmicas u ópticas llevadas a cabo en este trabajo, evidenciaron la modificación de las películas de quitosano.

El enlace imina es fácilmente hidrolizable en contacto con agua. Se determinó que soluciones más ácidas promovían una mayor reversibilidad del enlace, observando una reducción de la banda asociada a la imina y una reducción del grado de sustitución cuando se sometieron a pH ácidos. La estructura química del aldehído junto con el pH del medio influyó en la reversibilidad de las iminas, hidrolizándose más en aquellas formadas con aldehídos saturados que α,β-insaturados, así, mientras que las películas con hidrocinamaldehído y citronellal disminuyeron su grado de sustitución drásticamente en contacto con el medio ácido, las modificadas con citral y cinamaldehído no redujeron más de 20-25% y mantuvieron un alto porcentaje de sustitución tras el tratamiento.

En la **segunda parte del capítulo I** se corroboró la susceptibilidad de la imina a pH ácido mediante cromatografía de gases, en la que se cuantificó el benzaldehído y citral liberado al espacio de cabeza tras someter a las películas a soluciones acuosas de pH 4 y pH 7. En el primer ensayo de cromatografía de gases basado en sistema estático o cerrado, se detectó el doble de concentración de aldehído en fase vapor a pH ácido respecto a la obtenida a pH neutro, además se observó un claro efecto de las diferentes estructuras de los aldehídos sobre la hidrólisis de la imina. Del mismo modo que se observó en el primer estudio, el enlace formado con el citral, resultó más estable que aquel obtenido con benzaldehído.

Además de la estabilidad estructural de la imina, la cantidad de aldehído detectada en fase vapor podría también estar influenciado por los parámetros físico-químicos de los mismos. Parámetros como la solubilidad o el logaritmo de partición octanol/agua, es decir su mayor o menor afinidad por el polímero y por el medio acuoso, así como la presión de vapor, podría favorecer en mayor o menor medida su migración al espacio de cabeza. De hecho, la presión de vapor del benzaldehído es mucho mayor (1.270 mm Hg a 25 °C) que la del citral (0.091 mm Hg a 25 °C), lo que podría explicar, en parte, la diferencia de compuesto detectado en el espacio de cabeza. No obstante, la cuantificación del grado de sustitución tras la hidrólisis a diferentes pH se mostró en consonancia con los datos obtenidos de liberación. El benzaldehído remanente en la película tras la hidrólisis a pH acido apenas alcanzó el 2%, mientras que para citral se mantuvo alrededor del 35%. Por lo tanto, se puede concluir que la estabilidad estructural de la imina formada con citral fue mucho mayor que la de benzaldehído bajo las mismas condiciones de hidrólisis.

Adicionalmente, la monitorización del estudio mediante el sistema dinámico permitió arrastrar el benzaldehído liberado y acumulado en el espacio de cabeza para evitar el equilibrio entre las fases película-agua-espacio de cabeza lo que posibilitó un mayor agotamiento de la película modificada con benzaldehído, alcanzando la liberación de elevadas cantidades de compuesto durante 6 días, siendo 29 y 65 mg/g film a pH 7 y pH 4, respectivamente.

En esta línea, el estudio de otras propiedades funcionales, como la sorción de agua a diferentes valores de pH, permitió determinar también

la estabilidad estructural de las iminas. Gracias a la naturaleza hidrofílica del quitosano, las películas absorbieron una gran cantidad agua, especialmente a pH más ácidos, sin embargo, tras su modificación a través del anclaje de los diferentes aldehídos, la absorción de agua se redujo notablemente. Esto puede explicarse por la incorporación de moléculas hidrofóbicas al biopolímero, además, por el alto grado de sustitución de los grupos amino. Este ensayo mostró nuevamente diferencias entre la estabilidad estructural de las iminas, especialmente a pH ácidos. Cuanto menos estables son las iminas obtenidas, mayor es su capacidad de absorber agua, puesto que parte de los enlaces imino se revierten liberando el aldehído al entorno y regenerando el grupo amino del quitosano, favoreciendo la absorción de agua por parte del polímero. De hecho, aquellas películas modificadas con aldehídos saturados, como benzaldehído, citronellal e hidrocinamaldehído, se disolvieron rápidamente en contacto con el medio a pH 3 al igual que las películas de quitosano no modificadas. Sin embargo, aquellas películas reaccionadas con aldehídos α,β-insaturados mantuvieron su integridad estructural. Estos resultados sugirieron que la reacción con citral y cinamaldehído podrían entrecruzar la matriz de quitosano.

En relación a la actividad antimicrobiana de las películas activas se observó una inhibición significativa del crecimiento de los hongos *P. expansum* y *B. cinerea* cuando se sometieron las películas a pH ácido. En la **Figura 2** se muestra un resumen de los estudios antifúngicos más relevantes desarrollados durante la Tesis Doctoral. La respuesta antifúngica de las películas cuando fueron sometidas a diferentes pH permitió confirmar de forma indirecta la reversibilidad de la imina, ya que un aumento de la actividad antimicrobiana en consecuencia de una mayor migración del volátil al espacio de cabeza.

De estos estudios se deduce que mientras que a pH neutro el aldehído permanece anclado, la presencia de pH ácido permite la liberación del aldehído a demanda y en consecuencia un aumento de su actividad antimicrobiana, proveyendo al quitosano de un mecanismo específico de liberación del aldehído anclado.
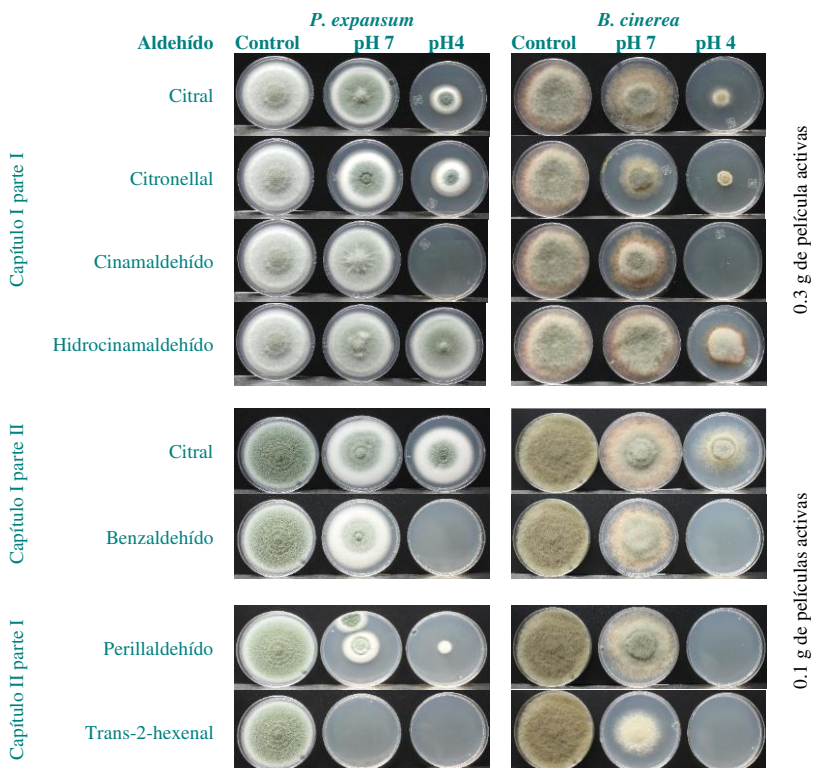
**Figura 2.** Respuesta antifúngica de dos cantidades diferentes de películas de quitosano con aldehídos inmovilizados contra *P. expansum* y *B. cinerea* tras 7 días de incubación.

En base a los resultados obtenidos se propuso un mecanismo de reacción para las distintas estructuras químicas de los aldehídos, que se encuentra resumido en la **Figura 3**. La inmovilización de aldehídos saturados como el benzaldehído, citronellal o el hidrocinamaldehído, en el grupo amino de las películas de quitosano solo puede ocurrir mediante la adición 1,2 o formación de iminas. Sin embargo, los aldehídos α,β-insaturados podrían presentar otros mecanismos de reacción, debido a la presencia del doble enlace carbono-carbono entre las posiciones α y β del aldehído (CHO-C=C-R), el cual puede formar nuevos enlaces mediante la adición de Michael con las aminas primarias (**Figura 3**) [2]. La presencia de un alto porcentaje de aminas primarias a lo largo del material (75-85%) podría favorecer la formación de una estructura conjugada con iminas y adiciones de

Michael, lo que explicaría la mayor estabilidad de estos aldehídos en las películas de quitosano modificadas, generando una estructura más estable. Este entrecruzamiento afectó directamente a la elevada estabilidad de la imina formada con citral y cinamaldehído en soluciones acuosas, lo que influyó a su vez en sus propiedades funcionales, liberación del compuesto anclado, así como en su respuesta antimicrobiana.
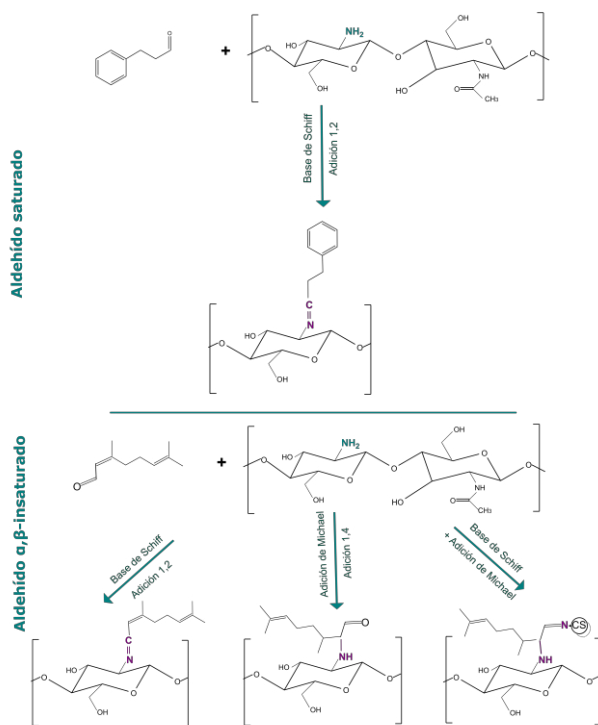


**Figura 3.** Mecanismos propuestos de reacción para la inmovilización de aldehídos saturados, como por ejemplo hidrocinamaldehído, y α,β-insaturados, como citral, en los grupos amino primario de quitosano.

En relación a la formación de iminas con aldehídos α,β-insaturados, en la **tercera parte del capítulo I** se estudió el efecto de la acidez del medio durante la síntesis de las bases de Schiff como un factor clave para modular el grado de entrecruzamiento de estos

aldehídos en las matrices biopoliméricas. Se trabajó con los aldehídos, citral y cinamaldehído y se establecieron valores de pH de reacción de 2, 5 y 7. Las condiciones marcadas para la reacción a pH 2 fueron las empleadas para la obtención de las películas en los trabajos previos. Se observó que en todos los valores de pH ensayados se formaron bases de Schiff y con un grado de sustitución elevado. También se observó que a pH 5 y 7 las películas perdieron su integridad estructural al ser sumergidas en medio ácido (pH 3), similarmente a lo observado con los aldehídos saturados. Las películas sintetizadas a pH 2 mantuvieron su integridad a pH 3 evidenciando que habían sido entrecruzadas, tal y como se muestra en la **Figura 4A**. Por lo tanto, se pudo confirmar que una elevada acidez del medio de reacción promueve que los aldehídos α,β-insaturados actúan como entrecruzantes heterobifuncionales produciéndose de forma conjunta reacciones de adición 1,2 (formación de bases de Schiff) y 1,4 (adición de Michael). El entrecruzamiento no solo afectó al hinchamiento de las películas, sino también contribuyó negativamente a la reversibilidad de la imina, y por tanto a la liberación del aldehído y con ello a su actividad antimicrobiana, como se esquematiza en la **Figura 4B**. Así, un mayor grado de entrecruzamiento resultó inversamente proporcional al hinchamiento y liberación del aldehído anclado, por lo que las películas sintetizadas empleando un medio de reacción a pH 2 mostraron una menor retención de agua y una menor migración del volátil al espacio de cabeza que aquellas sintetizadas a pH 5 y 7, las cuales asemejaron su comportamiento al observado en las películas reaccionadas con aldehídos saturados empleados en los trabajos previos.

Este estudio abre la posibilidad de obtener materiales con diferente grado de entrecruzamiento y diversas funcionalidades, dependiendo de la aplicación deseada.
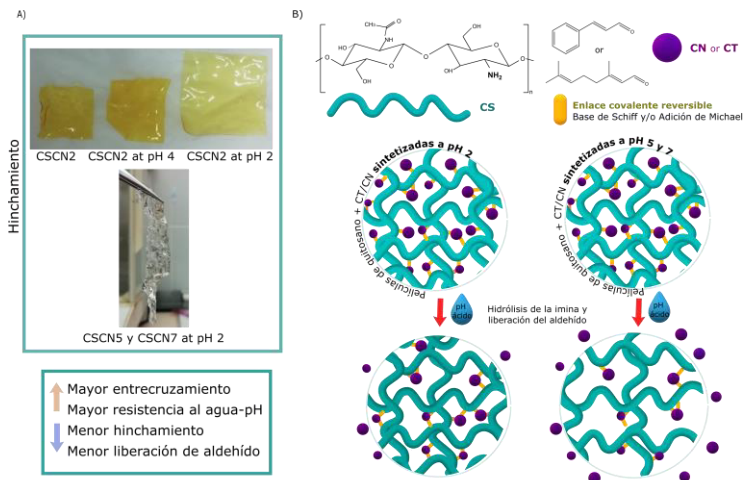
**Figura 4.** Hinchamiento tras la inmersión en una solución acuosa a pH 4 y 2 de las películas modificadas con cinamaldehído (CSCN) sintetizadas a pH 2, 5 y 7 (A); y representación esquemática sobre el hinchamiento de la matriz y liberación del activo tras el sumergir la matriz en una solución acuosa y (B).

Es evidente que la estructura química de los compuestos involucrados en la formación de la base de Schiff influyó en la estabilidad estructural de la imina cuando se sometieron a diferentes condiciones de hidrólisis. Este hecho, hace que dependiendo de la estructura del aldehído empleado en la formación de la base de Schiff con el quitosano, la estabilidad de la imina resultante pueda estar afectada en diferente medida, además de por la acidez del medio de hidrólisis, por la humedad ambiental, ya que el vapor de agua del medio podría producir la hidrólisis de las iminas. Este último factor es clave cuando se quiere conocer la estabilidad de las iminas formadas durante el almacenamiento de las películas. Por lo tanto, para obtener un mayor conocimiento de durante cuánto tiempo y bajo qué condiciones de almacenamiento puede permanecer el volátil estabilizado en la película, se realizó un estudio de estabilidad a largo plazo de películas de quitosano modificadas con dos aldehídos, benzaldehído y salicilaldehído, las cuales se almacenaron durante 12 meses en diferentes condiciones de humedad relativa. Aunque este estudio no se ha mostrado en los trabajos expuestos anteriormente se extrajeron datos interesantes, ya que se observó una elevada estabilidad de las iminas

tras un año de almacenamiento en distintas condiciones de humedad. En la **Figura 5**, se muestra la evolución del grado de sustitución de las películas de salicilaldehído y benzaldehído almacenadas durante 12 meses a diferentes humedades relativas (HR, %). Se observaron diferencias significativas entre los dos aldehídos empleados, puesto que las condiciones de elevada humedad afectaron negativamente a la estabilidad de la imina obtenida con benzaldehído, mientras que la imina sintetizada con salicilaldehído resultó más estable.
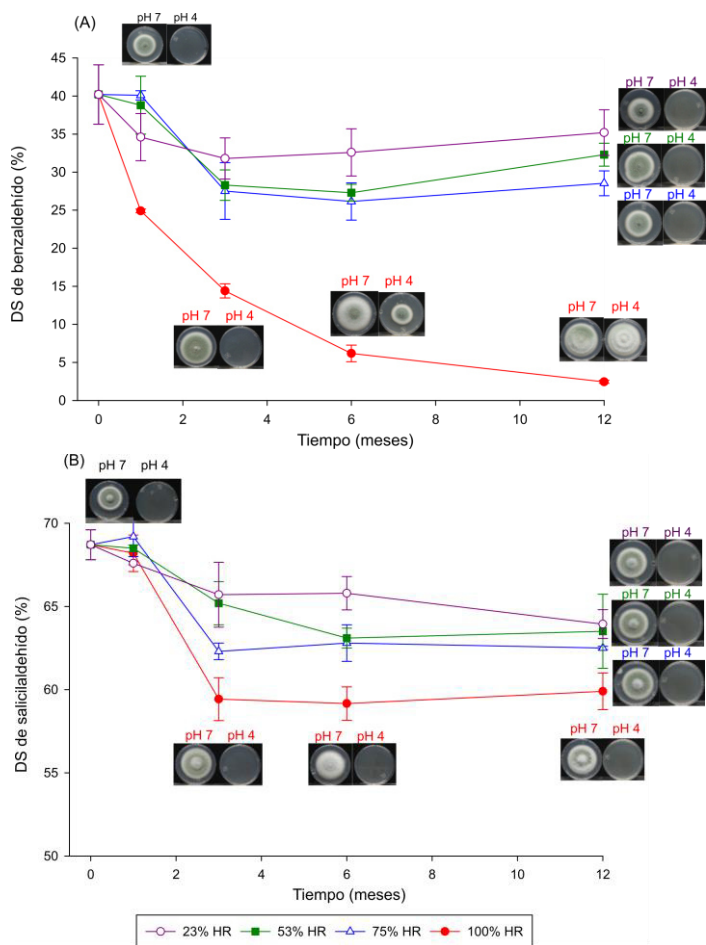


**Figura 5.** Evolución del grado de sustitución (DS, %) de las películas de quitosano modificadas con benzaldehído (A) y con salicilaldehído (B) almacenadas durante 12 meses a diferentes humedades relativas (%) a 23 °C.

El grado de sustitución de las películas de quitosano reaccionadas con benzaldehído y almacenadas con un 100% de HR descendió drásticamente hasta alcanzar un 6% tras 6 meses de almacenaje, afectando a su actividad antifúngica. Pero su efectividad se mantuvo en las películas almacenadas por debajo del 75% de HR (**Figura 5**). Por el contrario, las películas con salicilaldehído solo perdieron un 10% cuando se almacenó al 100% HR, sin comprometer su actividad antimicrobiana (**Figura 5**). Esto podría explicarse por el distinto grado de sustitución, así como por la estructura química de los aldehídos. La posición orto del grupo hidroxilo del salicilaldehído, además de favorecer altos rendimientos de reacción (>60%), podría incrementar la estabilidad estructural de las iminas por la formación de puentes de hidrogeno con grupos O-H adyacentes del quitosano [3].

Estos ensayos pusieron en evidencia que el anclaje covalente reversible de volátiles antifúngicos permite neutralizar la volatilidad del compuesto, mejora su manejabilidad y le proporciona estabilidad durante largos periodos de almacenamiento, incluso con altos porcentajes de HR. Además, ofrece un sistema de liberación específico, ya que la liberación del compuesto antimicrobiano es desencadenada a pH ácidos.

El **capítulo II** se ha centrado en las aplicaciones de las películas desarrolladas en el diseño de envases activos, las cuales se encuentran resumidas en la **Figura 6**. Por una parte, se evaluó la efectividad de las películas desarrolladas ejerciendo su acción en el espacio de cabeza del envase (parte I y II), y por otra, en contacto directo (parte III).

La **primera parte del capítulo II** consistió en la síntesis, caracterización y aplicación de películas de quitosano con trans-2-hexenal y perillaldehído. La formación de iminas en los grupos amino del quitosano se confirmó mediante técnicas espectroscópicas y se determinó, mediante análisis elemental, un menor contenido de perillaldehído que de trans-2-hexenal. Las películas que incorporaron este volátil resultaron altamente efectivas para inhibir el crecimiento del hongo (**Figura 2**).
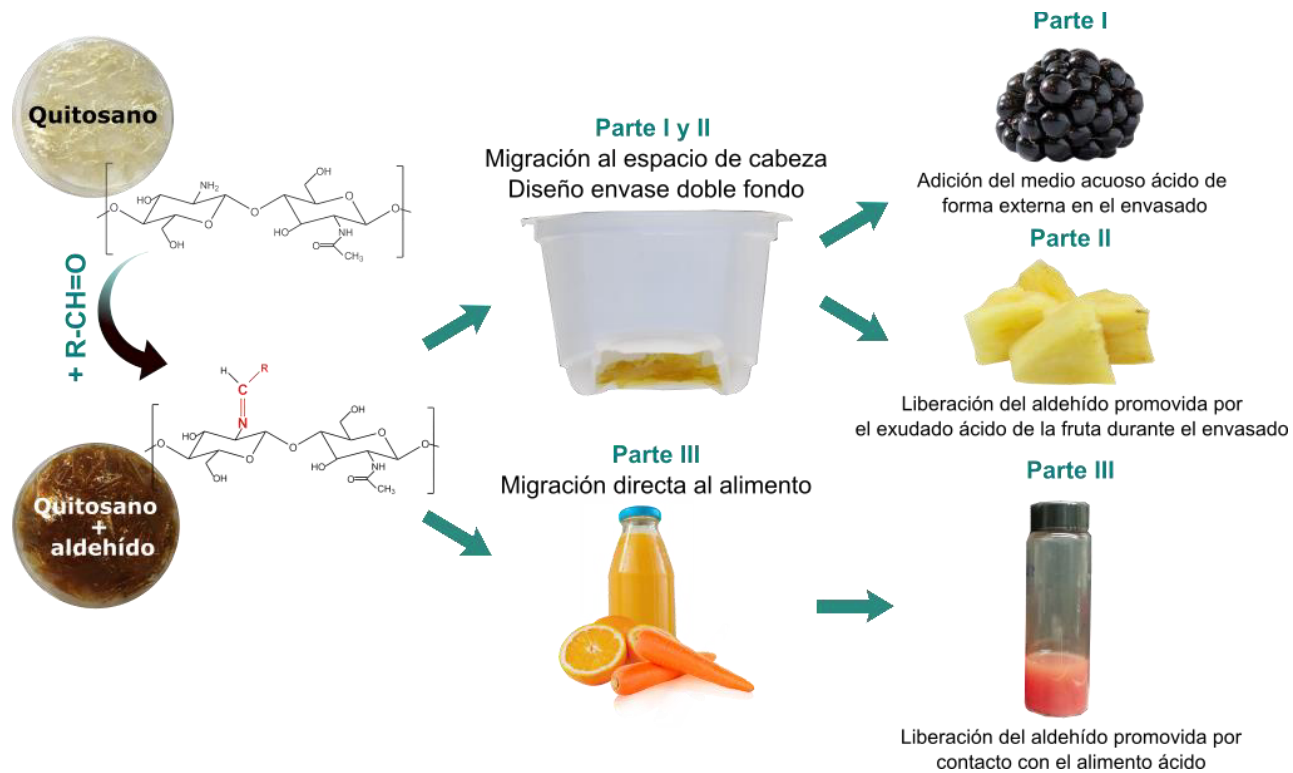
**Figura 6.** Esquema del contenido del capítulo II.

Como ya se ha detallado anteriormente, mediante el estudio *in vitro* de las películas activas se comprobó la reversibilidad de las iminas en contacto con soluciones acuosas ácidas. Por ello, se emplearon las películas con trans-2-hexenal anclado de forma covalente reversible junto con la solución activadora a pH 4 en el diseño del envasado activo de moras, un producto postcosecha altamente susceptible del crecimiento de hongos.

Se diseñó un envase de doble fondo para la incorporación de las películas antimicrobianas desarrolladas. La incorporación se realizó de de forma análoga a las bolsitas activas o almohadillas portadoras de compuestos activos descritas en la bibliografía y que se añaden en el interior del envase durante la etapa de envasado [4]. Previamente y como prueba de concepto, un primer estudio se llevó a cabo en bandejas, donde las moras fueron depositadas una por una junto con el sistema activo. Se observó una alta inhibición del crecimiento del hongo producida por la liberación del aldehído anclado al espacio de cabeza, incluso cuando se almacenó a 22 °C. Aunque a esa temperatura se favorece el crecimiento del hongo y la pérdida del volátil a través de las perforaciones, también se incrementa la volatilidad del compuesto lo que contribuye a un incremento de su efectividad (**Figura 7**).

La siguiente parte del trabajo consistió en el diseño de un envase de doble fondo, que permitiera depositar el sistema activo (película y medio activador) evitando el contacto directo con el alimento. Este doble fondo se separó del contenedor de la fruta mediante una membrana perforada para asegurar el acceso del aldehído liberado al espacio de cabeza del envase. Se consiguieron buenos resultados con el envase activo diseñado el cual inhibió el crecimiento de hongos sobre la superficie de las moras durante más de 10 días (**Figura 7**). Este sistema permitió aumentar el tiempo de vida útil de la fruta de 3 a 12 días. La migración del volátil al espacio de cabeza debido a la reversibilidad de la imina en contacto con la solución ácida fue monitorizada mediante cromatografía de gases. El contenido de trans-2-hexenal decreció gradualmente, aunque fue detectado durante todo el periodo de almacenamiento cuando se empleó 0.5 g de película.

El desarrollo de estas películas ha permitido emplear de forma eficiente un compuesto natural antimicrobiano, pero de gran volatilidad, de forma que se ha estabilizado en películas de quitosano y

se ha liberado de forma sostenida en el momento del envasado. Para verificar la aplicabilidad del sistema desarrollado frente a la inclusión del compuesto libre, se llevó a cabo un estudio en el que se incorporó trans-2-hexenal libre para el tratamiento de la contaminación fúngica de las moras y se observó que para alcanzar el mismo grado de inhibición era necesario incorporar grandes cantidades de activo al envase. El aldehído se encontraba altamente disponible al inicio del envasado y se perdía rápidamente durante siguientes días, pasando de 300 a 2 µg/L en seis días. Además, su actividad antifúngica fue limitada, observándose las primeras colonias tras los 6 días de almacenaje y provocando daños en el tejido de las frutas debido a la alta disponibilidad del compuesto al inicio del envasado. El uso de las películas de quitosano con trans-2-hexenal mejoró el tratamiento de las moras frescas y redujo la contaminación por hongos ya que retardó o inhibió su crecimiento de forma efectiva. Además, el diseño del envase de doble fondo permitió la incorporación del sistema activo al interior del envase evitando su contacto con la fruta.
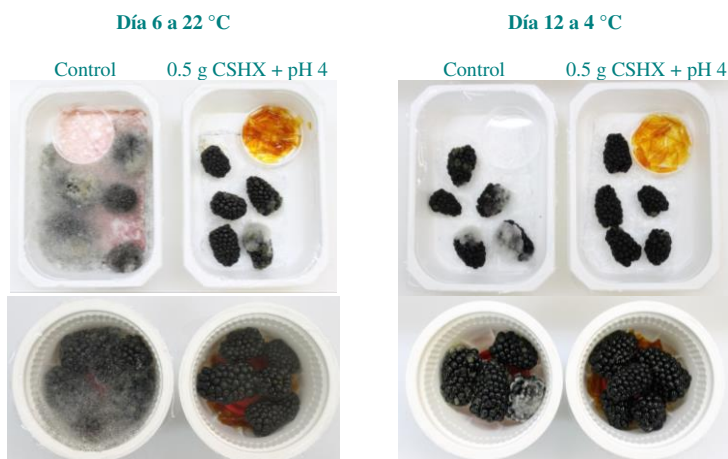


**Figura 7.** Apariencia visual de las moras envasadas en bandejas y con el envase de doble fondo almacenadas a 22 y 4 °C con las películas activas de quitosano modificadas mediante el anclaje covalente reversible de trans-2-hexenal.

En la **segunda parte del capítulo II**, se exploró la aplicación tecnológica de las películas activas en fase vapor para piña fresca cortada. Para ello, se sintetizaron películas activas de quitosano basadas

en el anclaje covalente reversible de salicilaldehído y trans-2-hexenal, ya que resultaron los compuestos más efectivos contra los principales microorganismos alterantes y patógenos de la fruta fresca cortada. Tras la reacción, se obtuvo un elevado grado de sustitución para ambos aldehídos (>60%). La liberación de los volátiles a la fase vapor se estudió *in vitro* en viales cerrados mediante cromatografía de gases, para ello se pusieron en contacto las películas de quitosano reaccionadas con salicilaldehído y trans-2-hexenal con soluciones acuosas a pH 3, 4, 5, 6 y 7. Se observó una respuesta al pH debido a la naturaleza reversible del enlace imina, siendo la liberación mayor a pH más ácidos. Por lo que el pH del jugo de la piña (3.6) podría favorecer la liberación del volátil. Además, se detectaron mayores cantidades de salicilaldehído que de trans-2-hexenal a todos los pH evaluados, pese a que este último aldehído presenta una mayor presión de vapor. Como se ha visto en el capítulo anterior, esto puede estar relacionado con la estructura α,β-insaturada del trans-2-hexenal, ya que puede formar una estructura entrecruzada basada en enlaces imina y adiciones de Michael con los grupos amino del quitosano (**Figura 3**).

Los estudios con piña cortada se realizaron envasándola en contenedores de doble fondo. El jugo de la piña se recolectó en el doble fondo del envase, donde entró en contacto con las películas. De acuerdo con los datos de liberación de volátiles por cromatografía de gases, el pH ácido del exudado de la piña cortada durante el almacenamiento resultó suficiente para producir una respuesta inhibitoria contra los microorganismos habituales de la piña testados *in vitro*, principalmente levaduras, aunque también se observó un efecto inhibitorio contra dos patógenos evaluados, y que fueron previamente inoculados en porciones de piña cortada, *L. innocua* y *E. coli*.

Con el sistema activo desarrollado se redujo eficazmente la carga microbiana de la fruta, principalmente formada por levaduras, manteniéndose por debajo de los 6 log UFC/$g_{fruta}$ cuando fue envasado con el sistema activo, mientras que superó los 8 log UFC/$g_{fruta}$ en las muestras envasadas sin incorporar películas activas en el doble fondo del envase. Además, su aplicación mejoró otros parámetros de calidad como el color, reduciendo el pardeamiento de la piña.

Se observó que las películas modificadas con salicialdehído tuvieron un marcado efecto sobre la firmeza y el exudado de la fruta.

La piña envasada con este aldehído redujo su firmeza y aumentó el exudado a partir del día 9 de almacenamiento, lo que podría estar asociado con una mayor liberación de este compuesto al espacio de cabeza del envase, y a la interacción del aldehído con la fruta.

La incorporación del sistema antimicrobiano desarrollado en un envase de doble fondo para fruta mínimamente procesada permitió la activación de éste mediante el exudado de la fruta y consecuentemente la liberación del antimicrobiano volátil al espacio de cabeza del envase ejerciendo su acción sobre la superficie del alimento. Puesto que la producción de exudado no es inmediata, el efecto antimicrobiano de estas películas podría retrasarse durante unos días, hasta alcanzar la concentración suficiente como para inhibir o retardar el crecimiento de los microorganismos. Por tanto, a partir de los 6 y 9 días de envasado el crecimiento de microorganismos totales parece estabilizarse para salicilaldehído y trans-2-hexenal, respectivamente.

Comúnmente, el principal mecanismo de migración de compuestos volátiles incorporados a matrices poliméricas se debe a su difusión en el polímero y evaporación desde su superficie directamente al espacio de cabeza del envase. Esta migración depende de la morfología del polímero, su polaridad, afinidad entre los componentes y por el coeficiente de reparto entre las fases polímero-espacio de cabeza [5,6]. Sin embargo, en las películas desarrolladas, el volátil anclado mediante el enlace imina con los grupos amino del quitosano debe hidrolizarse inicialmente. Su reversibilidad se desencadena por contacto con un medio acuoso, tras lo que el volátil liberado migra al agua ácida que actúa como activador, y de ésta a la fase vapor donde puede ejercer su función. En este sistema se incluyen dos fases nuevas, por una parte, el mecanismo de hidrólisis de la imina por contacto con la solución acuosa ácida, y por otra, la migración del volátil liberado del líquido al gas como se representa en la **Figura 8**.

Para simplificar la liberación del compuesto activo al entorno, en la **última parte del capítulo II** se investigó la aplicación de estas películas directamente en un alimento líquido ligeramente ácido, el cual promovía a su vez la hidrólisis de la imina.
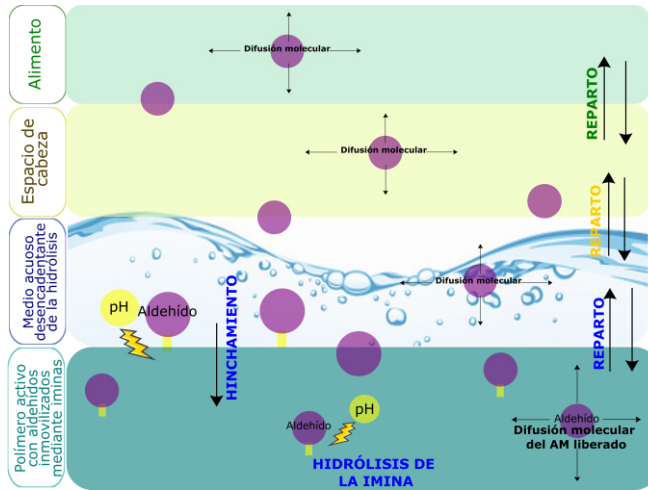
**Figura 8.** Liberación del volátil anclado mediante inmovilización covalente reversible desde la película de quitosano hasta el alimento.

En este trabajo se evaluaron tres aldehídos de estructura aromática con grupos hidroxilo adyacentes, siendo estos salicialdehído (2-hidroxibenzaldehído), 4-hidroxibenzaldehído, y 3,4-dihidroxi-benzaldehído. Como se comentaba anteriormente, la estructura del aldehído influyó notablemente en el grado de inmovilización conseguido y posteriormente en la reversibilidad de la imina formada. Se observó que la posición del grupo hidroxilo en la estructura del hidroxibenzaldehído es un factor determinante para la formación y estabilidad de las iminas. Los resultados de espectroscopia y análisis elemental demostraron que el salicilaldehído resultó mucho más reactivo que sus análogos (>60%). Por otro lado, la estructura de la imina sintetizada con salicilaldehído resultó ser más estable a la hidrólisis.

Según los datos surgidos de este estudio, el salicilaldehído resultó el más eficaz para inhibir el crecimiento de *E. coli* cuando se evaluó *in vitro*, por lo que, aunque la liberación fue menor en estas películas, resultó bactericida al ser aplicados en medios ligeramente ácidos (pH 5). Sin embargo, cuando las películas fueron sumergidas en medios neutros apenas se registró actividad antimicrobiana. Tampoco se observó inhibición cuando se añadieron películas de quitosano sin aldehído por lo que la actividad observada a pH ácido se debió exclusivamente a la liberación del aldehído al medio líquido.

La actividad antimicrobiana de las películas con salicilaldehído evaluadas en un zumo a base de zanahoria resultó inhibitoria durante los 6 días de envasado a 4 °C a pesar de que la composición de la matriz alimentaria y la temperatura de refrigeración podrían limitar la liberación del activo.

Durante el desarrollo de los diferentes estudios englobados en el capítulo I y II, se concluyó que la estructura química del aldehído inmovilizado influyó notablemente en la formación y reversibilidad del enlace imina. Los resultados obtenidos de esta investigación demostraron que el quitosano permite estabilizar aldehídos volátiles mediante enlaces covalentes reversibles, mejorando su manejabilidad y facilitando su incorporación en el diseño de envases activos, los cuales exhibieron un notable efecto antimicrobiano con diferentes patógenos y alterantes alimentarios en contacto con soluciones acuosas ligeramente ácidas, lo que permitió aumentar la seguridad y calidad de los alimentos.

## Referencias

1. Reyes-Jurado, F.; Navarro-Cruz, A.R.; Ochoa-Velasco, C.E.; Palou, E.; López-Malo, A.; Ávila-Sosa, R. Essential oils in vapor phase as alternative antimicrobials: A review. *Crit. Rev. Food Sci. Nutr.* **2020**, *60*, 1641–1650, doi:10.1080/10408398.2019.1586641.

2. Calow, A.D.J.; Carbó, J.J.; Cid, J.; Fernández, E.; Whiting, A. Understanding α,β-unsaturated imine formation from amine additions to α,β-unsaturated aldehydes and ketones: An analytical and theoretical investigation. *J. Org. Chem.* **2014**, *79*, 5163–5172, doi:10.1021/jo5007366.

3. Iftime, M.M.; Morariu, S.; Marin, L. Salicyl-imine-chitosan hydrogels: Supramolecular architecturing as a crosslinking method toward multifunctional hydrogels. *Carbohydr. Polym.* **2017**, *165*, 39–50, doi:10.1016/j.carbpol.2017.02.027.

4. Otoni, C.G.; Espitia, P.J.P.; Avena-Bustillos, R.J.; McHugh, T.H. Trends in antimicrobial food packaging systems: Emitting sachets and absorbent pads. *Food Res. Int.* **2016**, *83*, 60–73, doi:10.1016/j.foodres.2016.02.018.

5. Wu, Y.M.; Wang, Z.W.; Hu, C.Y.; Nerín, C. Influence of factors on release of antimicrobials from antimicrobial packaging materials. *Crit. Rev. Food Sci. Nutr.* **2018**, *58*, 1108–1121, doi:10.1080/10408398.2016.1241215.

6. Wang, L.; Dekker, M.; Heising, J.; Fogliano, V.; Berton-Carabin, C.C. Carvacrol release from PLA to a model food emulsion: Impact of oil droplet size. *Food Control* **2020**, *114*, 107247, doi:10.1016/j.foodcont.2020.107247.

# 6. CONCLUSIONES

De los resultados obtenidos durante el desarrollo de la presente Tesis Doctoral se pueden extraer las siguientes conclusiones:

- Se demostró el potencial antimicrobiano de un amplio abanico de aldehídos naturales permitidos para uso alimentario contra patógenos y alterantes presentes comúnmente en productos postcosecha frescos y mínimamente procesados.

- Se desarrolló un protocolo para la estabilización de los aldehídos en películas de quitosano mediante la síntesis de bases de Schiff.

- La acidez del medio de síntesis resultó ser un factor clave para modular la incorporación de aldehídos α,β-insaturados en estructuras de quitosano. Este tipo de aldehídos se comportan como agentes entrecruzantes heterobifuncionales en medios de reacción de elevada acidez.

- Se demostró la reversibilidad de las bases de Schiff formadas en medios ligeramente ácidos y la subsiguiente liberación de los aldehídos.

- La estructura química del aldehído inmovilizado influyó directamente en la estabilidad de la imina cuando fue sometida a las diferentes condiciones de hidrólisis.

- Las películas activas desarrolladas exhibieron una excelente actividad antimicrobiana *in vitro* cuando fueron activadas en soluciones acuosas ligeramente ácidas, mientras que a pH neutros la actividad fue limitada.

- Se diseñó un envase con doble fondo dónde depositar las películas desarrolladas evitando el contacto con el producto, y se aplicó al envasado de moras frescas y piña cortada desencadenándose la liberación del aldehído al espacio de cabeza por el contacto con una solución acuosa ácida, añadida en el momento del envasado o por el exudado de la fruta
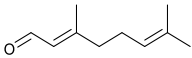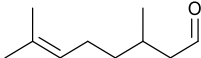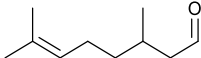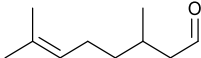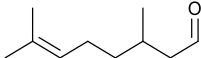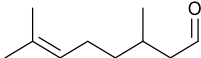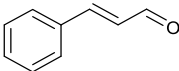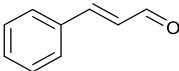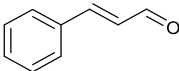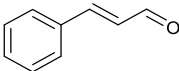
cortada, respectivamente. Su aplicación permitió aumentar el tiempo de vida útil de los productos postcosecha y mínimamente procesados.
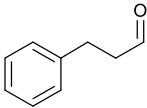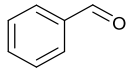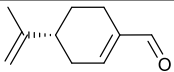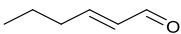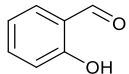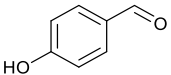
- Se estudió la actividad antimicrobiana de las películas de quitosano reaccionadas con salicilaldehído en un jugo de fruta refrigerado y previamente inoculado con *E. coli*. La acidez del alimento desencadenó la liberación del volátil, inhibiendo el crecimiento del patógeno.
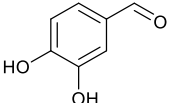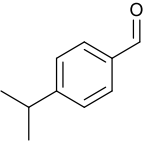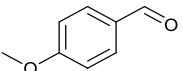
# 7. ANEXOS

# Anexo A

**Tabla 7.1.** Estructura química, parámetros físico-químicos actividad antimicrobiana contra microorganismos patógenos. Siendo $P_m$: Peso molecular (g/mol); $P_v$: Presión de vapor a 25 °C (mm de Hg); $T_b$: Temperatura de ebullición (°C), Log P (o/w): coeficiente de partición octanol/agua.

| Aldehídos | Estructura química | Propiedades | | | | Actividad antimicrobiana | Incorporación en polímeros |
|---|---|---|---|---|---|---|---|
| | | $P_m$ | $P_v$ | $T_b$ | Log P (o/w) | | |
| Citral | | 152.2 | 0.091 | 228 | 3.45 | *L. monocytogenes* [1] *E. coli* [2]  *S. enterica* [3] *Z. rouxii* [4] *P. expansum* [5] *P. digitatum* [6] *Penicillium* spp. *G. candidum* [7] | PBAT/PLA [8] EVOH [9] Ciclodextrinas [10] Quitosano/CMC [11] Quitosano [12] Alginato y pectina [13,14] Alginato [15] |
| Citronellal | | 154.3 | 0.250 | 205 | 3.29 | *P. grisea, C. musae* *A. flavus* [16] *P. digitatum* [17] *E. coli, S. aureus* [18] | - |
| Cinamaldehído | | 132.2 | 0.029 | 246 | 1.90 | *P. expansum* [5] *Aspergillus* spp.[19] *E. coli* *Salmonella* [20] *B. cereus* *Y. enterocolitica* *S. aureus* *E. coli* [21] | PBAT/PLA [22] PLA/Almidón [23] PLA/PCL[24] PLA [25] Gliadinas [26] Quitosano [27,28] Almidón de maíz [29] Celulosa [30] Ciclodextrinas [10] |

| | | | | | | | |
|---|---|---|---|---|---|---|---|
| **Hidrocinamaldehído** | | 134.2 | 0.130 | 224 | 1.78 | *E. coli*<br>*C. albicans*<br>*Penicillium* spp.<br>*A. flavus* [31]<br>*A. tumefaciens* [32] | PP [33] |
| **Benzaldehído** | | 106.1 | 1.270 | 179 | 1.48 | *C. jejuni*<br>*E. coli*<br>*L. monocytogenes*<br>*S. enterica* [34]<br>*Penicillium* spp. [35] | PAN [36]<br>Zeina [37]<br>Quitosano [38] |
| **Perillaldehído** | | 150.2 | 0.043 | 240 | 3.05 | *A. niger* [39] | Gelatina/Zeina [40] |
| ***Trans*-2-hexenal** | | 98.1 | 4.620 | 147 | 1.79 | *A. flavus* [41]<br>*P. expansum* [42]<br>*B. cinerea* [43] | PLA/Ciclodextrinas [44]<br>Almidón/Ciclodextrinas [45]<br>Almidón [46] |
| **Salicilaldehído** | | 122.1 | 0.590 | 197 | 1.81 | *C. jejuni*<br>*S. enterica*<br>*P. aeruginosa*<br>*E. coli* [34][47]<br>*Penicillium spp.* [35]<br>*A. niger*<br>*C. albicans* [48] | Quitosano [49–51]<br>Etilcelulosa-PEOX [52] |
| **4-hidroxibenzaldehído** | | 122.1 | 0.017 | 310 | 1.35 | *C. jejuni*<br>*E. coli*<br>*L monocytogenes*<br>*S. enterica* [34] | PAN [36]<br>Quitosano [53] |

| | | | | | | |
|---|---|---|---|---|---|---|
| **3-4-dihidroxibenzaldehído** | | 138.1 | 0.0001 | 323 | 1.09 | *C. jejuni*<br>*E. coli*<br>*L monocytogenes*<br>*S. enterica* [34] | - |
| **Cuminaldehído** | | 148.2 | 0.065 | 236 | 3.17 | *B. cereus*<br>*S. aureus*<br>*E. coli*<br>*S. Typhi* [54]<br>*A. flavus* [55] | Quitosano [56]<br>Ciclodextrina [57]<br>Zeína [58] |
| **p-anisaldehído** | | 136.2 | 0.030 | 248 | 1.76 | *C. jejuni*<br>*S. enterica*<br>*E. coli* [34]<br>*L. monocytogenes* [59] | Quitosano [60] |

*PBAT: poli(butilén adipato-co-tereftalato); PLA: ácido poliláctico; EVOH: etil-vinil-alcohol; CMC: carboximetilcelulosa; PCL: policaprolactona;

PP: polipropileno; PAN: poliacrilonitrilo; PEOX: poli(óxido de etileno).

## Referencias

1.  Silva-Angulo, A.B.; Zanini, S.F.; Rosenthal, A.; Rodrigo, D.; Klein, G.; Martínez, A. Combined effect of carvacrol and citral on the growth of *Listeria monocytogenes* and *Listeria innocua* and on the occurrence of damaged cells. *Food Control* **2015**, *53*, 156–162, doi:10.1016/j.foodcont.2015.01.028.

2.  Somolinos, M.; García, D.; Condón, S.; MacKey, B.; Pagán, R. Inactivation of *Escherichia coli* by citral. *J. Appl. Microbiol.* **2010**, *108*, 1928–1939, doi:10.1111/j.1365-2672.2009.04597.x.

3.  Muriel-Galet, V.; Cerisuelo, J.P.; López-Carballo, G.; Lara, M.; Gavara, R.; Hernández-Muñoz, P. Development of antimicrobial films for microbiological control of packaged salad. *Int. J. Food Microbiol.* **2012**, *157*, 195–201, doi:10.1016/j.ijfoodmicro.2012.05.002.

4.  Cai, R.; Hu, M.; Zhang, Y.; Niu, C.; Yue, T.; Yuan, Y.; Wang, Z. Antifungal activity and mechanism of citral, limonene and eugenol against *Zygosaccharomyces rouxii*. *Lwt* **2019**, *106*, 50–56, doi:10.1016/j.lwt.2019.02.059.

5.  Wang, Y.; Feng, K.; Yang, H.; Yuan, Y.; Yue, T. Antifungal mechanism of cinnamaldehyde and citral combination against: *Penicillium expansum* based on FT-IR fingerprint, plasma membrane, oxidative stress and volatile profile. *RSC Adv.* **2018**, *8*, 5806–5815, doi:10.1039/c7ra12191a.

6.  Zheng, S.; Jing, G.; Wang, X.; Ouyang, Q.; Jia, L.; Tao, N. Citral exerts its antifungal activity against *Penicillium digitatum* by affecting the mitochondrial morphology and function. *Food Chem.* **2015**, *178*, 76–81, doi:10.1016/j.foodchem.2015.01.077.

7.  Wuryatmo, E.; Klieber, A.; Scott, E.S. Inhibition of citrus postharvest pathogens by vapor of citral and related compounds in culture. *J. Agric. Food Chem.* **2003**, *51*, 2637–2640, doi:10.1021/jf026183l.

8.  Laorenza, Y.; Harnkarnsujarit, N. Carvacrol, citral and α-terpineol essential oil incorporated biodegradable films for functional active packaging of Pacific white shrimp. *Food Chem.* **2021**, *363*, 130252, doi:10.1016/j.foodchem.2021.130252.

9.  Muriel-Galet, V.; Cerisuelo, J.P.; López-Carballo, G.; Aucejo, S.; Gavara, R.; Hernández-Muñoz, P. Evaluation of EVOH-coated PP films with oregano essential oil and citral to improve the shelf-life of packaged salad. *Food Control* **2013**, *30*, 137–143, doi:10.1016/j.foodcont.2012.06.032.

10. Chen, H.; Li, L.; Ma, Y.; Mcdonald, T.P.; Wang, Y. Development of active packaging film containing bioactive components encapsulated in β-cyclodextrin and its application. *Food Hydrocoll.* **2019**, *90*, 360–366, doi:10.1016/j.foodhyd.2018.12.043.

11. Ma, H.; Zhao, Y.; Lu, Z.; Xing, R.; Yao, X.; Jin, Z.; Wang, Y.; Yu, F. Citral-loaded chitosan/carboxymethyl cellulose copolymer hydrogel microspheres with improved antimicrobial effects for plant protection. *Int. J. Biol. Macromol.* **2020**, *164*, 986–993, doi:https://doi.org/10.1016/j.ijbiomac.2020.07.164.

12. Arnon-Rips, H.; Cohen, Y.; Saidi, L.; Porat, R.; Poverenov, E. Covalent

linkage of bioactive volatiles to a polysaccharide support as a potential approach for preparing active edible coatings and delivery systems for food products. *Food Chem.* **2021**, *338*, 127822, doi:10.1016/j.foodchem.2020.127822.

13. Siracusa, V.; Romani, S.; Gigli, M.; Mannozzi, C.; Cecchini, J.P.; Tylewicz, U.; Lotti, N. Characterization of active edible films based on citral essential oil, alginate and pectin. *Materials (Basel).* **2018**, *11*, doi:10.3390/ma11101980.

14. Guerreiro, A.C.; Gago, C.M.L.; Miguel, M.G.C.; Faleiro, M.L.; Antunes, M.D.C. The influence of edible coatings enriched with citral and eugenol on the raspberry storage ability, nutritional and sensory quality. *Food Packag. Shelf Life* **2016**, *9*, 20–28, doi:10.1016/j.fpsl.2016.05.004.

15. Guerreiro, A.C.; Gago, C.M.L.; Faleiro, M.L.; Miguel, M.G.C.; Antunes, M.D.C. The effect of alginate-based edible coatings enriched with essential oils constituents on *Arbutus unedo L.* fresh fruit storage. *Postharvest Biol. Technol.* **2015**, *100*, 226–233, doi:10.1016/j.postharvbio.2014.09.002.

16. Aguiar, R.W.D.S.; Ootani, M.A.; Ascencio, S.D.; Ferreira, T.P.S.; Santos, M.M.D.; Santos, G.R.D. Fumigant antifungal activity of *Corymbia citriodora* and *Cymbopogon nardus* essential oils and citronellal against three fungal species. *Sci. World J.* **2014**, *2014*, doi:10.1155/2014/492138.

17. Wu, Y.; OuYang, Q.; Tao, N. Plasma membrane damage contributes to antifungal activity of citronellal against *Penicillium digitatum*. *J. Food Sci. Technol.* **2016**, *53*, 3853–3858, doi:10.1007/s13197-016-2358-x.

18. Lopez-Romero, J.C.; González-Ríos, H.; Borges, A.; Simões, M. Antibacterial Effects and Mode of Action of Selected Essential Oils Components against *Escherichia coli* and *Staphylococcus aureus*. *Evidence-based Complement. Altern. Med.* **2015**, *2015*, doi:10.1155/2015/795435.

19. Kim, J.H.; Chan, K.L.; Mahoney, N.; Campbell, B.C. Antifungal activity of redox-active benzaldehydes that target cellular antioxidation. *Ann. Clin. Microbiol. Antimicrob.* **2011**, *10*, doi:10.1186/1476-0711-10-23.

20. Yossa, N.; Patel, J.; Macarisin, D.; Millner, P.; Murphy, C.; Bauchan, G.; Lo, Y.M. Antibacterial Activity of Cinnamaldehyde and Sporan against *Escherichia coli* O157:H7 and *Salmonella*. *J. food Process. Preserv.* **2014**, *38*, 749–757.

21. Siddiqua, S.; Anusha, B.A.; Ashwini, L.S.; Negi, P.S. Antibacterial activity of cinnamaldehyde and clove oil: effect on selected foodborne pathogens in model food systems and watermelon juice. *J. Food Sci. Technol.* **2015**, *52*, 5834–5841, doi:10.1007/s13197-014-1642-x.

22. Srisa, A.; Harnkarnsujarit, N. Antifungal films from trans-cinnamaldehyde incorporated poly(lactic acid) and poly(butylene adipate-co-terephthalate) for bread packaging. *Food Chem.* **2020**, *333*, 127537, doi:10.1016/j.foodchem.2020.127537.

23. Muller, J.; Casado Quesada, A.; González-Martínez, C.; Chiralt, A. Antimicrobial properties and release of cinnamaldehyde in bilayer films based on polylactic acid (PLA) and starch. *Eur. Polym. J.* **2017**, *96*, 316–325,

doi:10.1016/j.eurpolymj.2017.09.009.

24.    Qin, Y.; Liu, D.; Wu, Y.; Yuan, M.; Li, L.; Yang, J. Effect of PLA/PCL/cinnamaldehyde antimicrobial packaging on physicochemical and microbial quality of button mushroom (*Agaricus bisporus*). *Postharvest Biol. Technol.* **2015**, *99*, 73–79.

25.    Makwana, S.; Choudhary, R.; Dogra, N.; Kohli, P.; Haddock, J. Nanoencapsulation and immobilization of cinnamaldehyde for developing antimicrobial food packaging material. *LWT-Food Sci. Technol.* **2014**, *57*, 470–476.

26.    Balaguer, M.P.; Lopez-Carballo, G.; Catala, R.; Gavara, R.; Hernandez-Munoz, P. Antifungal properties of gliadin films incorporating cinnamaldehyde and application in active food packaging of bread and cheese spread foodstuffs. *Int. J. Food Microbiol.* **2013**, *166*, 369–377, doi:10.1016/j.ijfoodmicro.2013.08.012.

27.    Higueras, L.; López-Carballo, G.; Gavara, R.; Hernández-Muñoz, P. Reversible Covalent Immobilization of Cinnamaldehyde on Chitosan Films via Schiff Base Formation and Their Application in Active Food Packaging. *Food Bioprocess Technol.* **2015**, *8*, 526–538, doi:10.1007/s11947-014-1421-8.

28.    Ghaderi-Ghahfarokhi, M.; Barzegar, M.; Sahari, M.A.; Ahmadi Gavlighi, H.; Gardini, F. Chitosan-cinnamon essential oil nano-formulation: Application as a novel additive for controlled release and shelf life extension of beef patties. *Int. J. Biol. Macromol.* **2017**, *102*, 19–28, doi:10.1016/j.ijbiomac.2017.04.002.

29.    Ke, J.; Xiao, L.; Yu, G.; Wu, H.; Shen, G.; Zhang, Z. The study of diffusion kinetics of cinnamaldehyde from corn starch-based film into food simulant and physical properties of antibacterial polymer film. *Int. J. Biol. Macromol.* **2019**, *125*, 642–650, doi:10.1016/j.ijbiomac.2018.12.094.

30.    Sanla-Ead, N.; Jangchud, A.; Chonhenchob, V.; Suppakul, P. Antimicrobial Activity of cinnamaldehyde and eugenol and their activity after incorporation into cellulose-based packaging films. *Packag. Technol. Sci.* **2012**, *25*, 7–17.

31.    López, P.; Sánchez, C.; Batlle, R.; Nerín, C. Vapor-phase activities of cinnamon, thyme, and oregano essential oils and key constituents against foodborne microorganisms. *J. Agric. Food Chem.* **2007**, *55*, 4348–4356, doi:10.1021/jf063295u.

32.    Lee, J.E.; Jung, M.; Lee, S.C.; Huh, M.J.; Seo, S.M.; Park, I.K. Antibacterial mode of action of trans-cinnamaldehyde derived from cinnamon bark (*Cinnamomum verum*) essential oil against *Agrobacterium tumefaciens*. *Pestic. Biochem. Physiol.* **2020**, *165*, 104546, doi:10.1016/j.pestbp.2020.02.012.

33.    Gutiérrez, L.; Escudero, A.; Batlle, R.; Nerín, C. Effect of mixed antimicrobial agents and flavors in active packaging films. *J. Agric. Food Chem.* **2009**, *57*, 8564–8571, doi:10.1021/jf901459e.

34.    Friedman, M.; Henika, P.R.; Mandrell, R.E. Antibacterial Activities of Phenolic Benzaldehydes and Benzoic Acids against *Campylobacter jejuni, Escherichia coli, Listeria monocytogenes,* and *Salmonella enteric*a. *J. Food*

*Prot.* **2003**, *66*, 1811–1821, doi:10.4315/0362-028X-66.10.1811.

35. Fitzgerald, D.J.; Stratford, M.; Gasson, M.J.; Narbad, A. Structure-function analysis of the vanillin molecule and its antifungal properties. *J. Agric. Food Chem.* **2005**, *53*, 1769–1775, doi:10.1021/jf048575t.

36. Alamri, A.; El-Newehy, M.H.; Al-Deyab, S.S. Biocidal polymers: Synthesis and antimicrobial properties of benzaldehyde derivatives immobilized onto amine-terminated polyacrylonitrile. *Chem. Cent. J.* **2012**, *6*, 1–13, doi:10.1186/1752-153X-6-111.

37. Soliman, E.A.; Khalil, A.A.; Deraz, S.F.; El-Fawal, G.; Elrahman, S.A. Synthesis, characterization and antibacterial activity of biodegradable films prepared from Schiff bases of zein. *J. Food Sci. Technol.* **2014**, *51*, 2425–2434, doi:10.1007/s13197-012-0792-y.

38. Damiri, F.; Bachra, Y.; Bounacir, C.; Laaraibi, A.; Berrada, M. Synthesis and Characterization of Lyophilized Chitosan-Based Hydrogels Cross-Linked with Benzaldehyde for Controlled Drug Release. *J. Chem.* **2020**, *2020*, doi:10.1155/2020/8747639.

39. Tian, J.; Wang, Y.; Zeng, H.; Li, Z.; Zhang, P.; Tessema, A.; Peng, X. Efficacy and possible mechanisms of perillaldehyde in control of *Aspergillus niger* causing grape decay. *Int. J. Food Microbiol.* **2015**, *202*, 27–34, doi:10.1016/j.ijfoodmicro.2015.02.022.

40. Wang, D.; Liu, Y.; Sun, J.; Sun, Z.; Liu, F.; Du, L.; Wang, D. Fabrication and characterization of gelatin/zein nanofiber films loading perillaldehyde for the preservation of chilled chicken. *Foods* **2021**, *10*, doi:10.3390/foods10061277.

41. Ma, W.; Zhao, L.; Zhao, W.; Xie, Y. (E)-2-Hexenal, as a Potential Natural Antifungal Compound, Inhibits *Aspergillus flavus* Spore Germination by Disrupting Mitochondrial Energy Metabolism. *J. Agric. Food Chem.* **2019**, *67*, 1138–1145, doi:10.1021/acs.jafc.8b06367.

42. Neri, F.; Mari, M.; Menniti, A.M.; Brigati, S.; Bertolini, P. Control of *Penicillium expansum* in pears and apples by trans-2-hexenal vapours. *Postharvest Biol. Technol.* **2006**, *41*, 101–108, doi:10.1016/j.postharvbio.2006.02.005.

43. Archbold, D.D.; Hamilton-Kemp, T.R.; Barth, M.M.; Langlois, B.E. Identifying Natural Volatile Compounds That Control Gray Mold (*Botrytis cinerea*) during Postharvest Storage of Strawberry, Blackberry, and Grape. *J. Agric. Food Chem.* **1997**, *45*, 4032–4037, doi:10.1021/jf970332w.

44. Joo, M.J.; Merkel, C.; Auras, R.; Almenar, E. Development and characterization of antimicrobial poly(l-lactic acid) containing trans-2-hexenal trapped in cyclodextrins. *Int. J. Food Microbiol.* **2012**, *153*, 297–305, doi:10.1016/j.ijfoodmicro.2011.11.015.

45. Wang, X.; Fu, M.; Qu, X.; Liu, J.; Bu, J.; Feng, S.; Zhao, H.; Jiao, W.; Sun, F. (E)-2-Hexenal-based coating induced acquired resistance in apple and its antifungal effects against *Penicillium expansum*. *Lwt* **2022**, *163*, 113536, doi:10.1016/j.lwt.2022.113536.

46. Abhari, N.; Madadlou, A.; Dini, A. Structure of starch aerogel as affected by crosslinking and feasibility assessment of the aerogel for an anti-fungal

volatile release. *Food Chem.* **2017**, *221*, 147–152, doi:10.1016/j.foodchem.2016.10.072.

47. Friedman, M.; Henika, P.R.; Mandrell, R.E. Bactericidal activities of plant essential oils and some of their isolated constituents against *Campylobacter jejuni, Escherichia coli, Listeria monocytogenes,* and *Salmonella enterica. J. Food Prot.* **2002**, *65*, 1545–1560, doi:12380738.

48. Radulović, N.; Mišić, M.; Aleksić, J.; Doković, D.; Palić, R.; Stojanović, G. Antimicrobial synergism and antagonism of salicylaldehyde in *Filipendula vulgaris* essential oil. *Fitoterapia* **2007**, *78*, 565–570, doi:10.1016/j.fitote.2007.03.022.

49. Dos Santos, J.E.; Dockal, E.R.; Cavalheiro, É.T.G. Synthesis and characterization of Schiff bases from chitosan and salicylaldehyde derivatives. *Carbohydr. Polym.* **2005**, *60*, 277–282, doi:10.1016/j.carbpol.2004.12.008.

50. Iftime, M.M.; Ailiesei, G.L.; Ungureanu, E.; Marin, L. Designing chitosan based eco-friendly multifunctional soil conditioner systems with urea controlled release and water retention. *Carbohydr. Polym.* **2019**, *223*, 115040, doi:10.1016/j.carbpol.2019.115040.

51. Barbosa, H.F.G.; Attjioui, M.; Leitão, A.; Moerschbacher, B.M.; Cavalheiro, É.T.G. Characterization, solubility and biological activity of amphihilic biopolymeric Schiff bases synthesized using chitosans. *Carbohydr. Polym.* **2019**, *220*, 1–11, doi:10.1016/j.carbpol.2019.05.037.

52. Shi, C.; Jash, A.; Lim, L.T. Activated release of hexanal and salicylaldehyde from imidazolidine precursors encapsulated in electrospun ethylcellulose-poly(ethylene oxide) fibers. *SN Appl. Sci.* **2021**, *3*, 1–13, doi:10.1007/s42452-021-04372-3.

53. Jagadish, R.S.; Divyashree, K.N.; Viswanath, P.; Srinivas, P.; Raj, B. Preparation of N-vanillyl chitosan and 4-hydroxybenzyl chitosan and their physico-mechanical, optical, barrier, and antimicrobial properties. *Carbohydr. Polym.* **2012**, *87*, 110–116, doi:10.1016/j.carbpol.2011.07.024.

54. Wongkattiya, N.; Sanguansermsri, P.; Fraser, I.H.; Sanguansermsri, D. Antibacterial activity of cuminaldehyde on food-borne pathogens, the bioactive component of essential oil from *Cuminum cyminum L.* collected in Thailand. *J. Complement. Integr. Med.* **2019**, *16*.

55. Xu, D.; Wei, M.; Peng, S.; Mo, H.; Huang, L.; Yao, L.; Hu, L. Cuminaldehyde in cumin essential oils prevents the growth and aflatoxin B1 biosynthesis of *Aspergillus flavus* in peanuts. *Food Control* **2021**, *125*, 107985, doi:https://doi.org/10.1016/j.foodcont.2021.107985.

56. Sharma, S.; Jain, P.; Tiwari, S. Dynamic imine bond based chitosan smart hydrogel with magnified mechanical strength for controlled drug delivery. *Int. J. Biol. Macromol.* **2020**, *160*, 489–495, doi:10.1016/j.ijbiomac.2020.05.221.

57. Sharif, N.; Golmakani, M.T.; Hajjari, M.M.; Aghaee, E.; Ghasemi, J.B. Antibacterial cuminaldehyde/hydroxypropyl-β-cyclodextrin inclusion complex electrospun fibers mat: Fabrication and characterization. *Food Packag. Shelf Life* **2021**, *29*, doi:10.1016/j.fpsl.2021.100738.

58. Hajjari, M.M.; Golmakani, M.-T.; Sharif, N.; Niakousari, M. *In-vitro* and *in-*

*silico* characterization of zein fiber incorporating cuminaldehyde. *Food Bioprod. Process.* **2021**, *128*, 166–176, doi:https://doi.org/10.1016/j.fbp.2021.05.003.

59. Chen, X.; Zhang, X.; Meng, R.; Zhao, Z.; Liu, Z.; Zhao, X.; Shi, C.; Guo, N. Efficacy of a combination of nisin and p-Anisaldehyde against *Listeria monocytogenes*. *Food Control* **2016**, *66*, 100–106, doi:10.1016/j.foodcont.2016.01.025.

60. Azmy, E.A.M.; Hashem, H.E.; Mohamed, E.A.; Negm, N.A. Synthesis, characterization, swelling and antimicrobial efficacies of chemically modified chitosan biopolymer. *J. Mol. Liq.* **2019**, *284*, 748–754, doi:10.1016/j.molliq.2019.04.054.

# Anexo B

**7.2. Resultados y publicaciones científicas asociadas a la Tesis Doctoral**

## Publicaciones internacionales

- Publicadas

**Development of antifungal biopolymers based on dynamic imines as responsive release systems for the postharvest preservation of blackberry fruit.** Heras-Mozos, R., Gavara, R., Hernández-Muñoz, P. *Food Chemistry* (2021), 357, 129838.

**Dynamic covalent chemistry of imines for the development of stimuli-responsive chitosan films as carriers of sustainable antifungal volatiles.** Heras-Mozos, R., Hernández, R., Gavara, R., Hernández-Muñoz, P. *Food Hydrocolloids* (2021), 125, 107326.

**Chitosan films as pH-responsive sustained release system of naturally occurring antifungal volatile compounds.** Heras-Mozos, R., Gavara, R., Hernández-Muñoz, P. *Carbohydrate Polymers* (2022), 283, 119137.

**Responsive packaging based on imine-chitosan films for extending the shelf-life of refrigerated fresh-cut pineapple.** Heras-Mozos, R., Gavara, R., Hernández-Muñoz, P. *Food Hydrocolloids* (2022), 133, 107968.

- Enviadas

**pH modulates antibacterial activity of hydroxybenzaldehyde derivates immobilized in chitosan films via reversible Schiff bases and their application to preserve freshly-squeezed juice.** Heras-Mozos, R., López-Carballo, G., Hernández, R., Gavara, R., Hernández-Muñoz, P. *Food Chemistry* (FOODCHEM-D-22-05164)

## Comunicaciones en congresos internacionales

**pH-responsive release of trans-2-hexenal from chitosan films based on dynamic imine linkages and their application in antifungal packaging**. Heras-Mozos, R., Gavara, R., Hernández-Muñoz, P. *20th Gums and Stabilisers for the Food Industry Conference*. San Sebastian, España (2019).

**Molecular biodynamers based on chitosan for the stimuli-responsive release of naturally ocurring antifungal volatiles.** Heras-Mozos, R., Gavara, R., Hernández-Muñoz, P. *7th International Conference on Biobased and Biodegradable Polymers (BIOPOL 2019).* Estocolmo, Suecia (2019).

**Chitosan derivatives based on dynamic imine chemistry for pH dependent release of antifungal volatiles.** Heras-Mozos, R., Gavara, R., Hernández-Muñoz, P. *XVI Reunión del Grupo Especializado de Polímeros – GEP y XVII Simposio Latinoamericano de Polímeros - SLAP (GEP-SLAP 2022)*. San Sebastián, España (2022).

**Antifungal responsive Schiff Bases based on reversible imine chemistry.** Heras-Mozos, R., Gavara, R., Hernández-Muñoz, P. *11th International Colloids Conference*. Lisboa, Portugal (2022)

## Otras comunicaciones

**Biopolímeros antimicrobianos basados en el anclaje de compuestos volátiles naturales.** Heras-Mozos, R., Gavara, R., Hernández-Muñoz, P. *V Jornadas estudiantes predoctorales del IATA-CSIC.* Valencia, España (2018).

**Development of antifungal food packaging based on pH-responsive chitosan films.** Heras-Mozos, R., Gavara, R., Hernández-Muñoz, P. *VII Jornadas estudiantes predoctorales del IATA-CSIC.* Valencia, España (2021).

## Co-supervisión de trabajos final de máster

**Anclaje de aldehídos naturales con actividad antimicrobiana a biopolímeros con grupos amino mediante enlaces covalentes reversibles o base de Schiff.** García González, Javier (2017). Máster Universitario en Química. Facultad de Química. Universidad de Valencia.

**Desarrollo y caracterización de películas antimicrobianas basadas en el anclaje reversible de aldehídos naturales en quitosano mediante bases de Schiff.** Franco Agurto, Gianella Lisbeth (2018). Máster Universitario en Calidad y Seguridad Alimentaria. Facultad de Farmacia. Universidad de Valencia.

**Development of antimicrobial films based on immobilization and release of trans-2-hexenal in chitosan polymer.** Santus, Eleanora (2018). Corso di Laurea Magistrale in Scienze e Tecnologie Alimentari. Facoltà di Scienze Agrarie e Alimentari. Università degli Studi di Milano.

**Determinación de la cinética de liberación de compuestos volátiles naturales incorporados en matrices poliméricas.** Semanate Esquivel, Marcela (2020). Máster Universitario de Ingeniería Química. Escuela Técnica Superior de Ingeniería. Universidad de Valencia.

**Estudio de la reversibilidad de las bases de Schiff y liberación de compuestos antimicrobianos en matrices de quitosano.** Ríos Mejía, Alejandro (2022). Máster Universitario de Ingeniería Química. Escuela Técnica Superior de Ingeniería. Universidad de Valencia.

# Anexo C

**7.3. Resultados y publicaciones científicas adicionales**

**Publicaciones internacionales:**

- Publicadas

**Active EVOH/PE bag for sliced pan loaf based on garlic as antifungal agent and bread aroma as aroma corrector.** Heras-Mozos, R., Muriel-Galet, V., López-Carballo, G., Catalá, R., Hernández-Muñoz, P., Gavara, R. *Food Packaging and Shelf Life* (2018) 18, 125-130.

**Development and optimization of antifungal packaging for sliced pan loaf based on garlic as active agent and bread aroma as aroma corrector.** Heras-Mozos, R., Muriel-Galet, V., López-Carballo, G., Catalá, R., Hernández-Muñoz, P., Gavara, R. *International Journal of Food Microbiology* (2019), 290, 42-18.

**Hot-Melt-Extruded Active Films Prepared from EVOH/Trans-Cinnamaldehyde Blends Intended for Food Packaging Applications.** Aragón-Gutiérrez, A., Heras-Mozos, R., Gallur, M., López, D., Gavara, R., Hernández-Muñoz, P. *Foods* (2021), 10, 1591.

**Trans-2-Hexenal Based Antifungal Packaging to Extend the Shelf Life of Strawberries.** Heras-Mozos, R., García-Moreno, A., Monedero-Prieto, M., Tone, A., Higueras-Contreras, L., Hernández-Muñoz, P., Gavara, R. *Foods* (2021), 10, 2166.

**Exploiting the Redox Activity of MIL-100(Fe) Carrier Enables Prolonged Carvacrol Antimicrobial Activity.** Caamaño, K., Heras-Mozos, R., Calbo, J., Cases Díaz, J., Waerenborgh, J.C., Vieira, B., Hernández-Muñoz, P., Gavara, R., Giménez-Marqués, M. *Applied Materials & Interfaces* (2022), 14, 8, 10758-10768.

## Publicaciones en revistas no indexadas

**Quitosano: un biopolímero multifunctional para el envasado activo de alimentos.** Heras-Mozos, R., Esteve-Redondo, P., López-Carballo, G., Gavara, R., Higueras-Contreras, L., Hernández-Muñoz, P. *Revista de plásticos modernos: Ciencia y tecnología de polímeros. (Ejemplar dedicado a: Polímeros naturales, biodegradables y de fuentes renovables)* (2021), 122, Nº. 772.

## Comunicaciones en congresos internacionales

**Antifungal packaging for extending the shelf life of sliced bread.** Heras-Mozos, R., López-Carballo, G., Gavara, R., Hernández-Muñoz, P. *V National and IV International student congress of food science and technology.* Valencia, España (2018).

**Antifungal coatings based on garlic essential oil to extend the shelf life of sliced bread packaged in PE bags.** Heras-Mozos, R., López-Carballo, G., Gavara, R., Hernández-Muñoz, P. *32nd EFFoST International Conference, European Federation of Food Science and Technology.* Nantes, Francia (2018).